SHYAM BALAJI

STELLAR LIMITS ON A LIGHT SCALAR

In collaboration with: P.S.B. Dev, Y. Zhang and J. Silk
[arxiv: 2205.01669] accepted for publication with JCAP

December 6, 2022

MOTIVATION

- Supernovae (SN) and stars provide a unique environment to copiously produce light hypothetical particles: axions/ALPs, dark photon, heavy neutrino, compact extra dimensions, CP-even scalar

- Raffelt criterion: the energy loss due to these exotic particles cannot exceed that from the measured neutrino emission as this would reduce the cooling time of the SN to less than what is observed

- Very limited SN limits in the literature on light CP-even scalar (compared to axion/ALP & dark photon)

- Motivation for a scalar singlet
    - Stabilise the SM vacuum
    - Address the hierarchy problem in relaxion models
    - Generate the baryon asymmetry via baryogenesis
    - Address the cosmological constant problem
    - Mediate the interaction between DM and the SM particles
    - S with mass at the keV scale, can also play the role of light DM


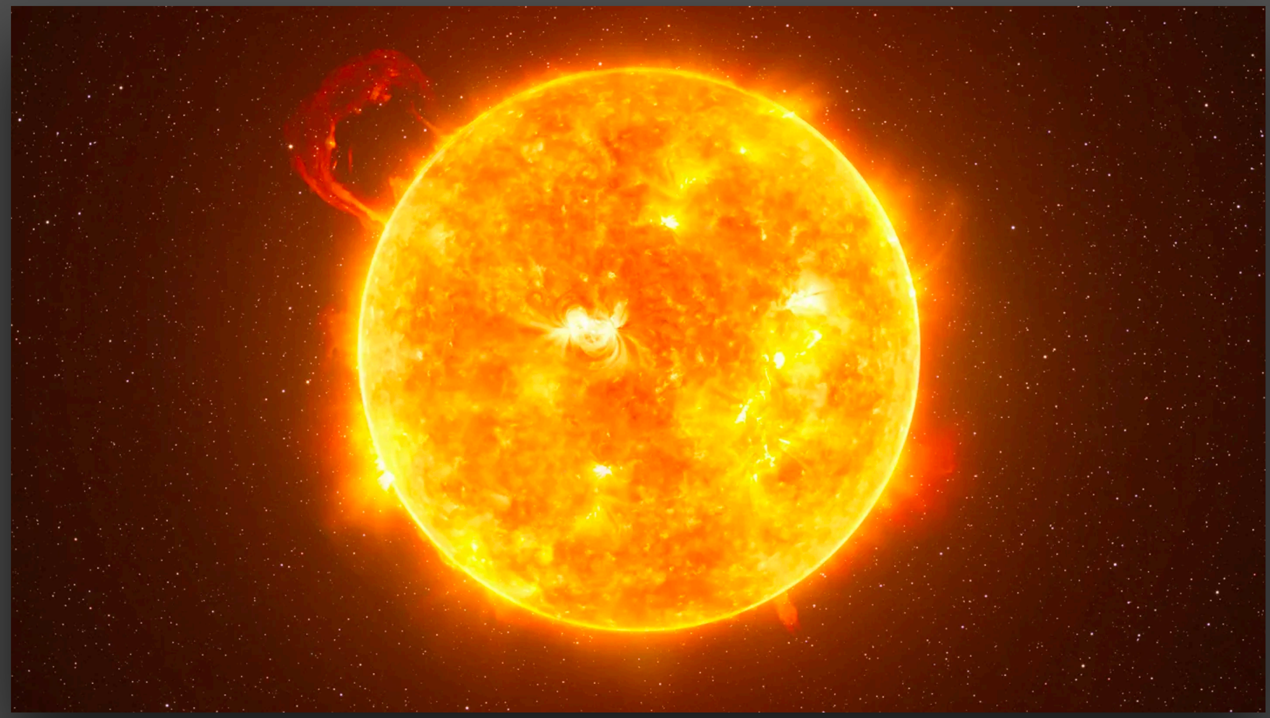

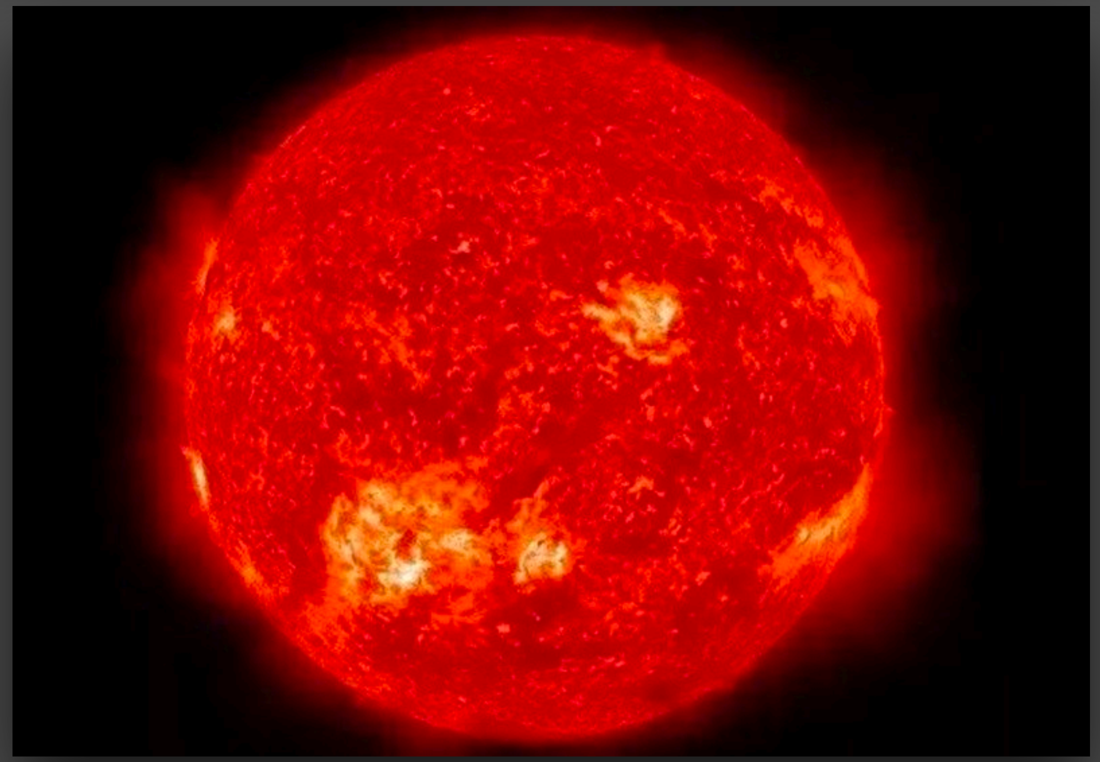

SN1987A

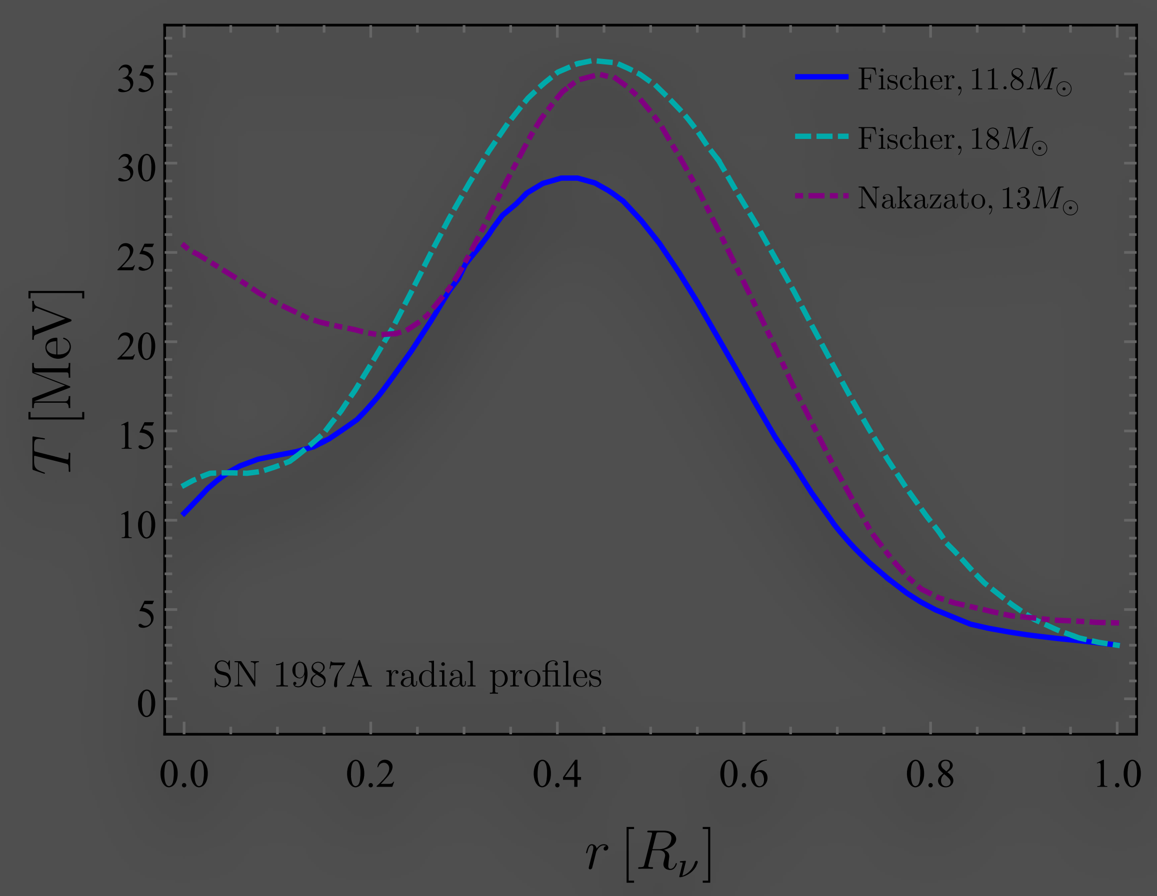

T [MeV]
r [R_ν]
Fischer, 11.8M_⊙
Fischer, 18M_⊙
Nakazato, 13M_⊙
SN 1987A radial profiles

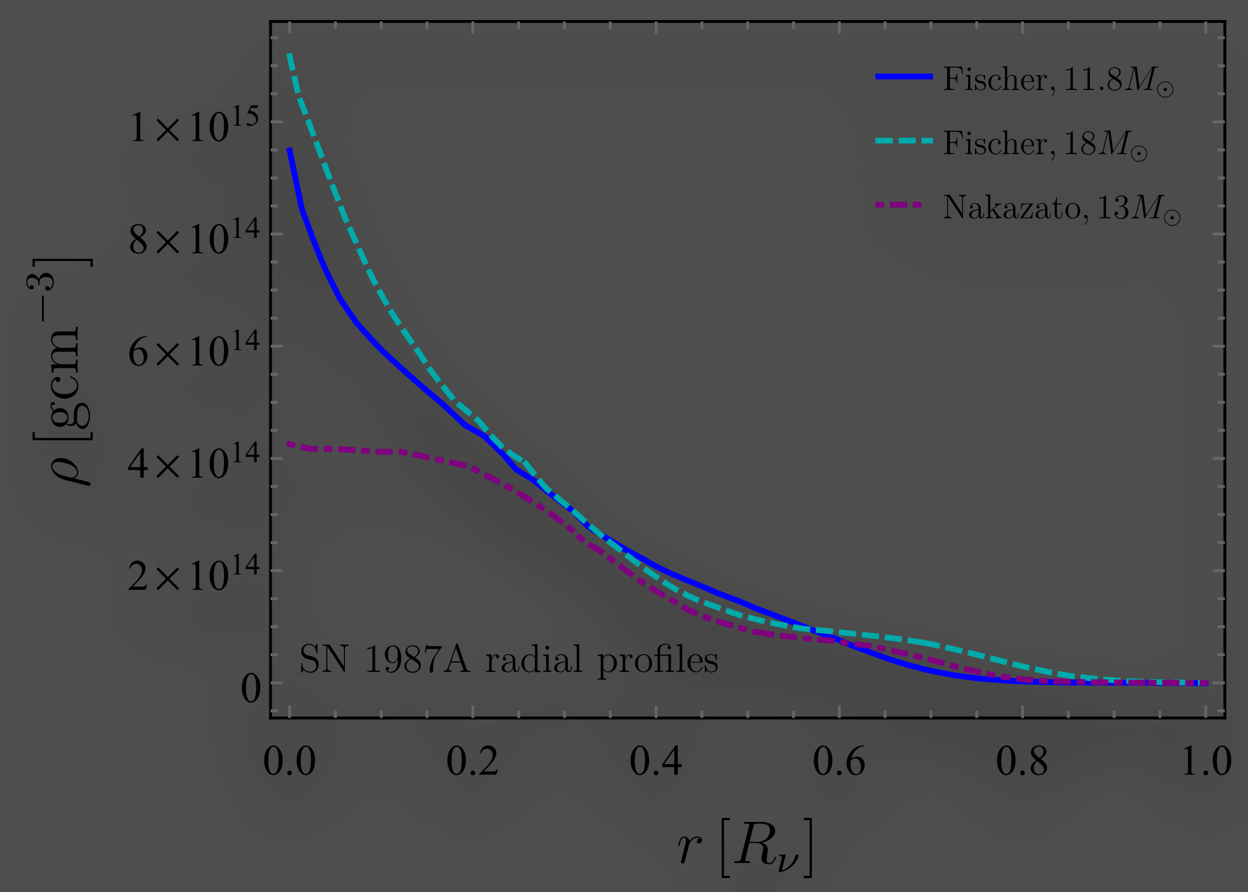

ρ [gcm^-3]
r [R_ν]
Fischer, 11.8M_⊙
Fischer, 18M_⊙
Nakazato, 13M_⊙
SN 1987A radial profiles

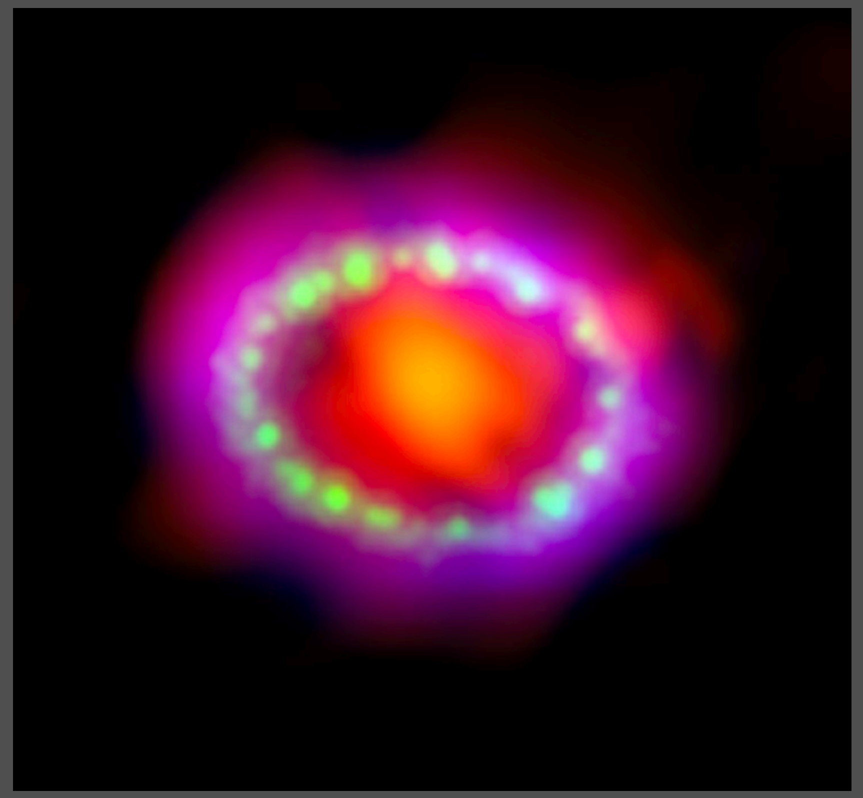

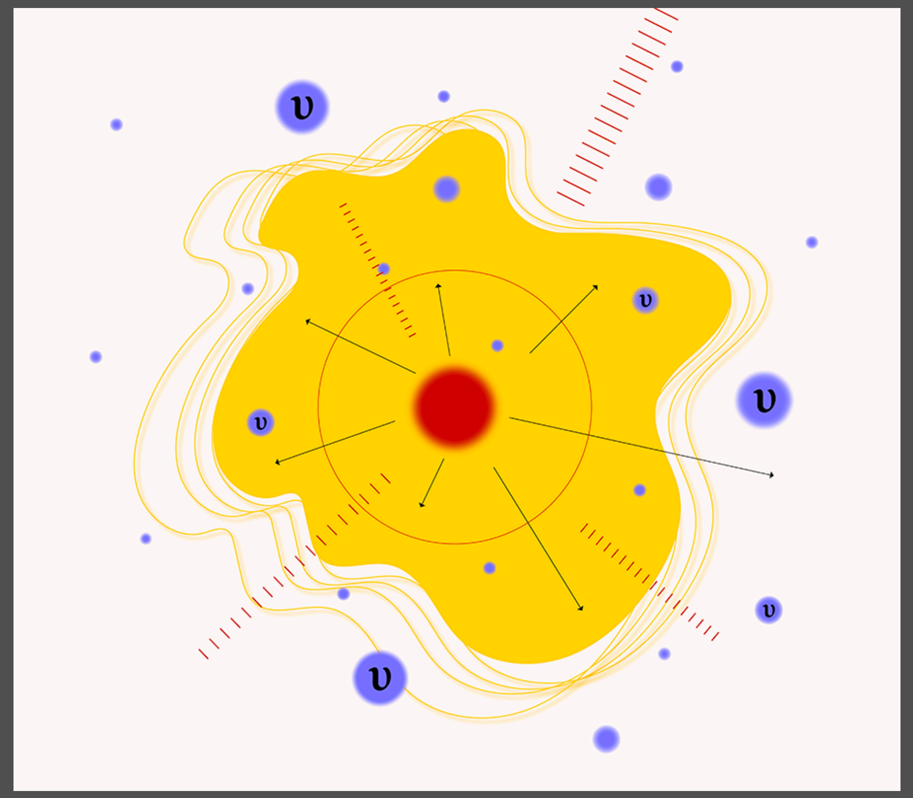

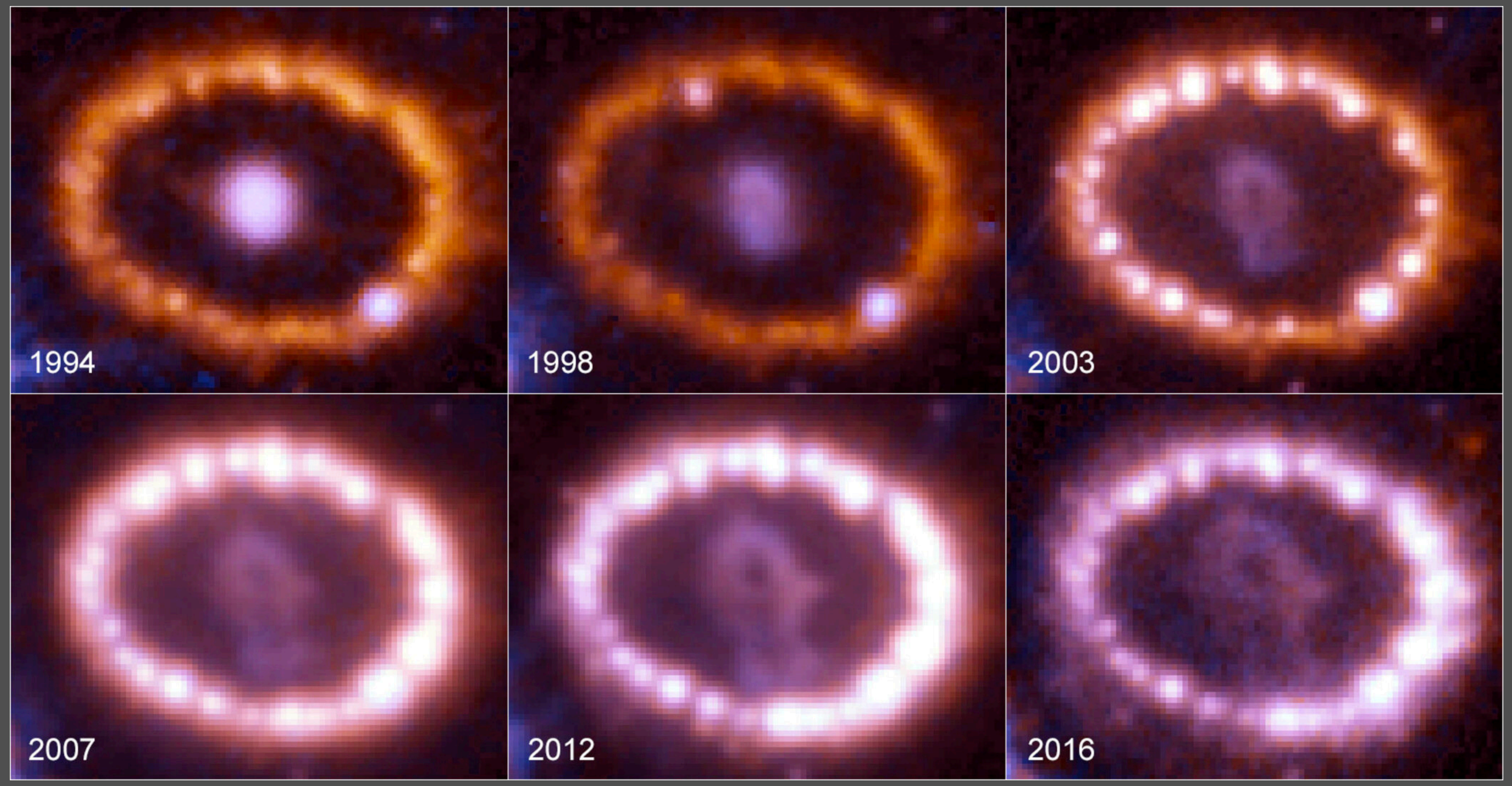

1994
1998
2003
2007
2012
2016

SN1987A

- We consider SN1987A, a type II supernova (SN) in the Large Magellanic Cloud

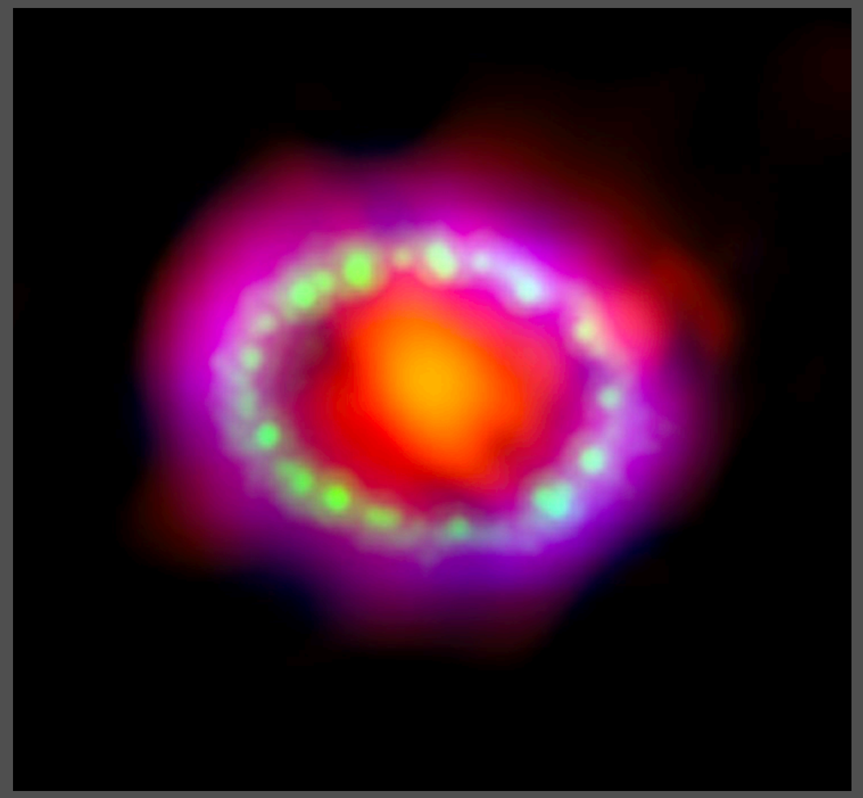

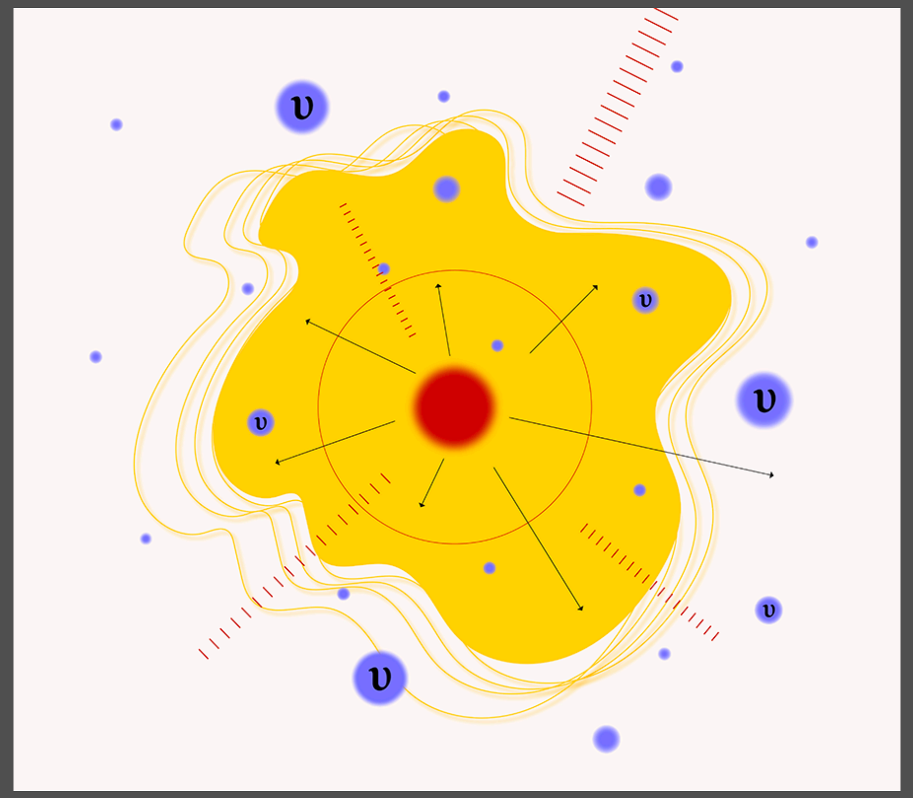

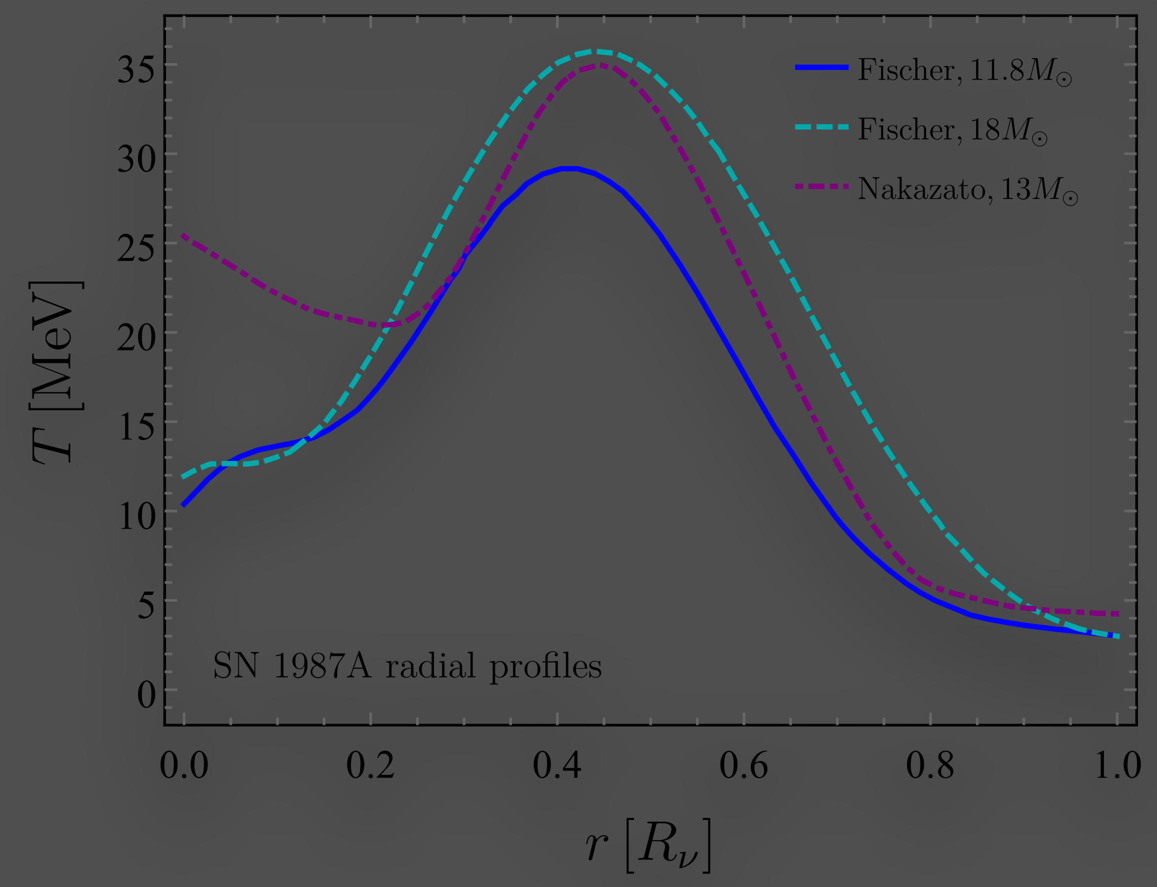

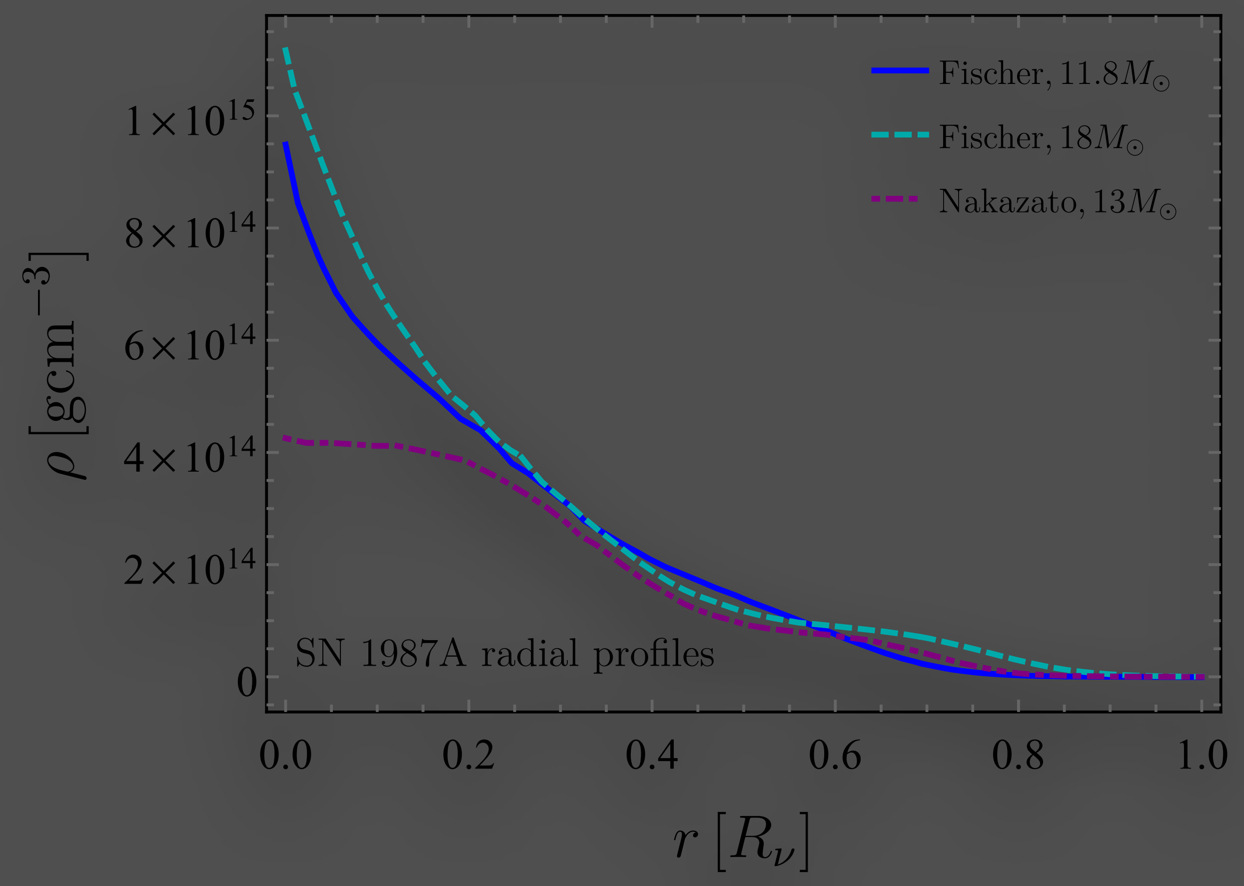

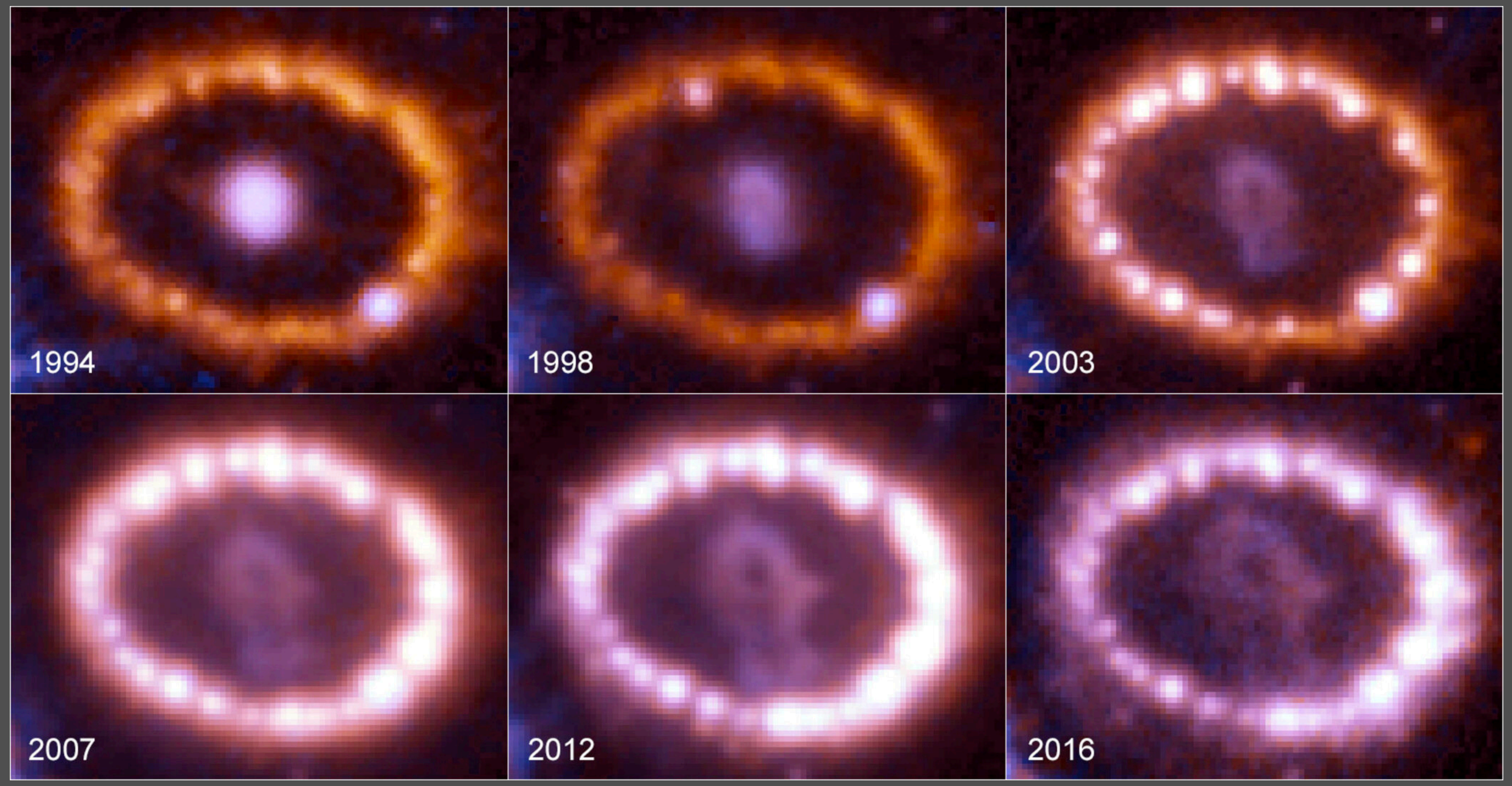

SN1987A

- We consider SN1987A, a type II supernova (SN) in the Large Magellanic Cloud
- Neutrino emission happens just before core collapse but before visible light is emitted

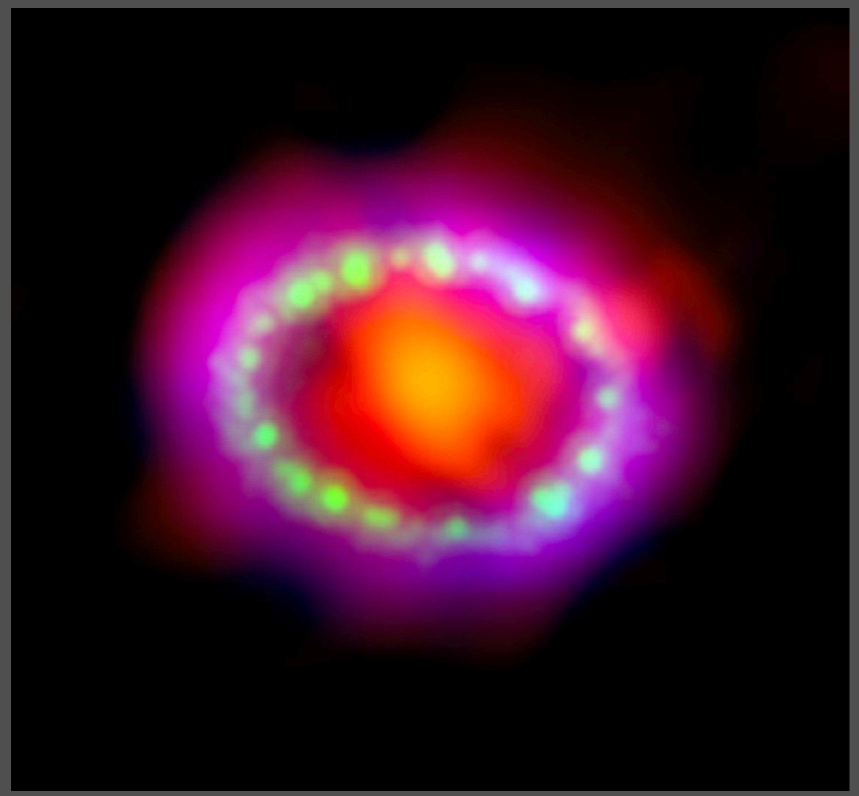

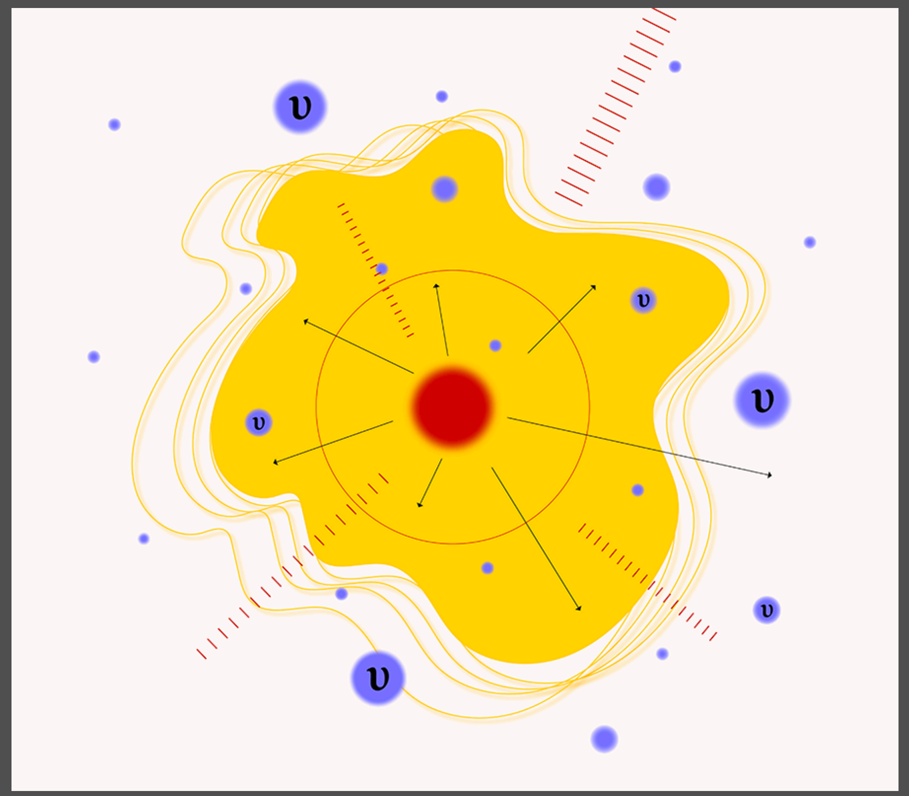

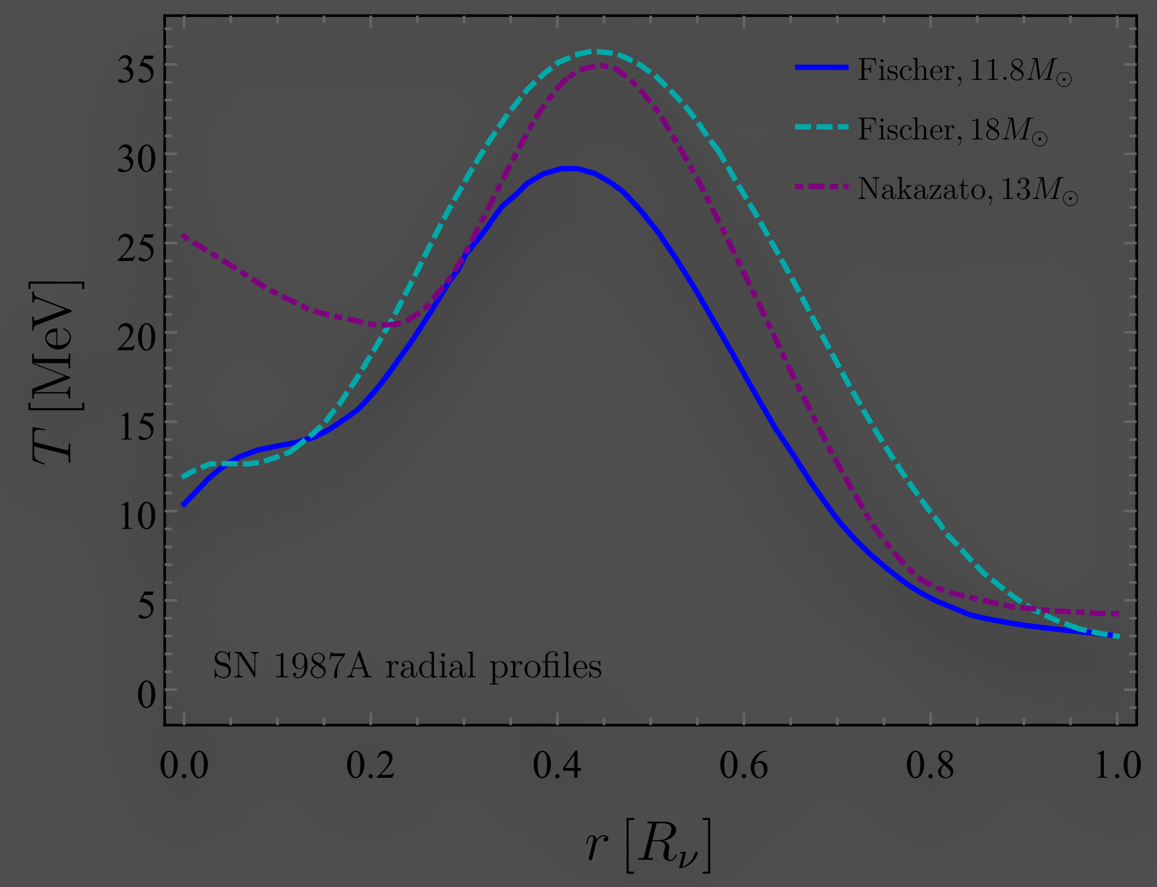

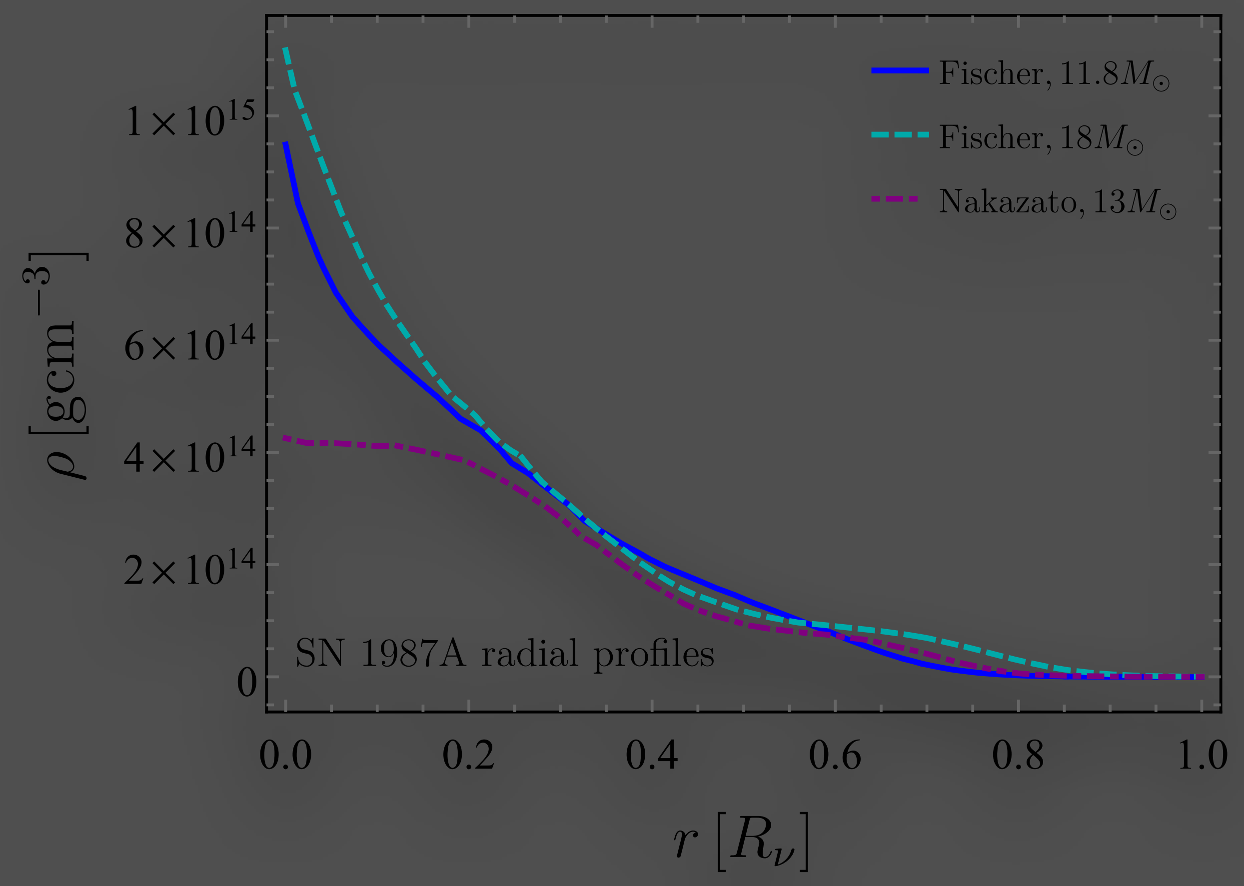

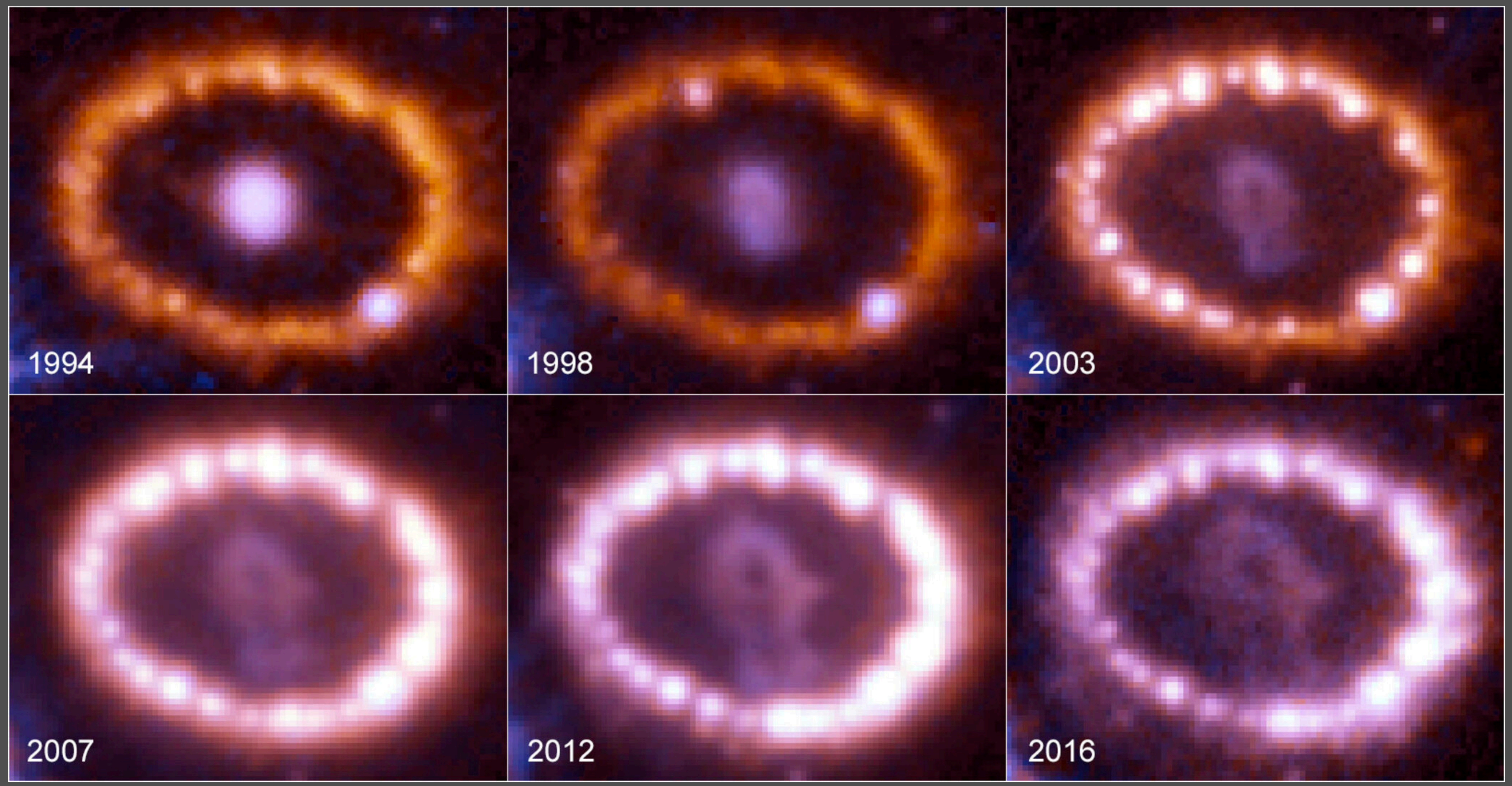

SN1987A

- We consider SN1987A, a type II supernova (SN) in the Large Magellanic Cloud
- Neutrino emission happens just before core collapse but before visible light is emitted
- We use SN1987A to set limits because it has well established neutrino luminosity measurements $\mathscr{L}_\nu = 3 \times 10^{53}\ \mathrm{erg/sec}$

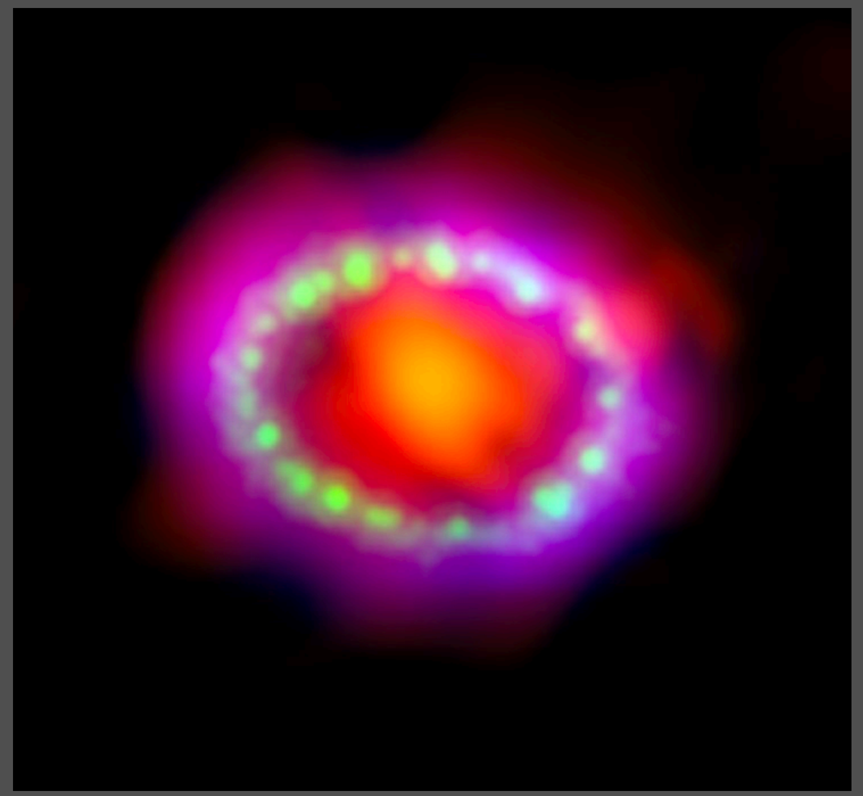

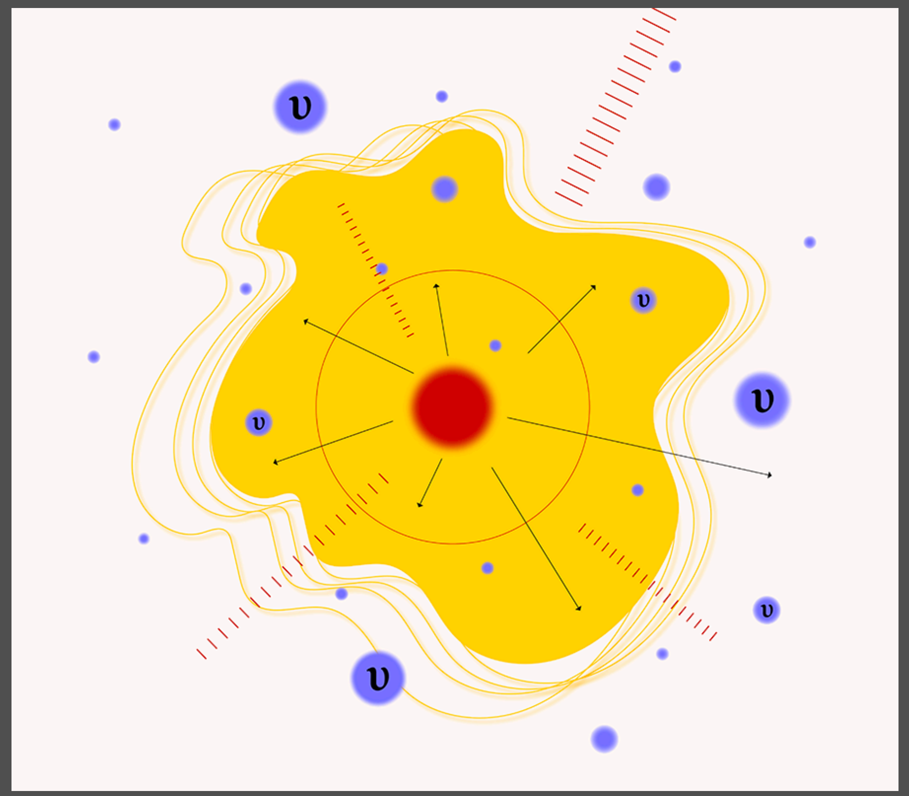

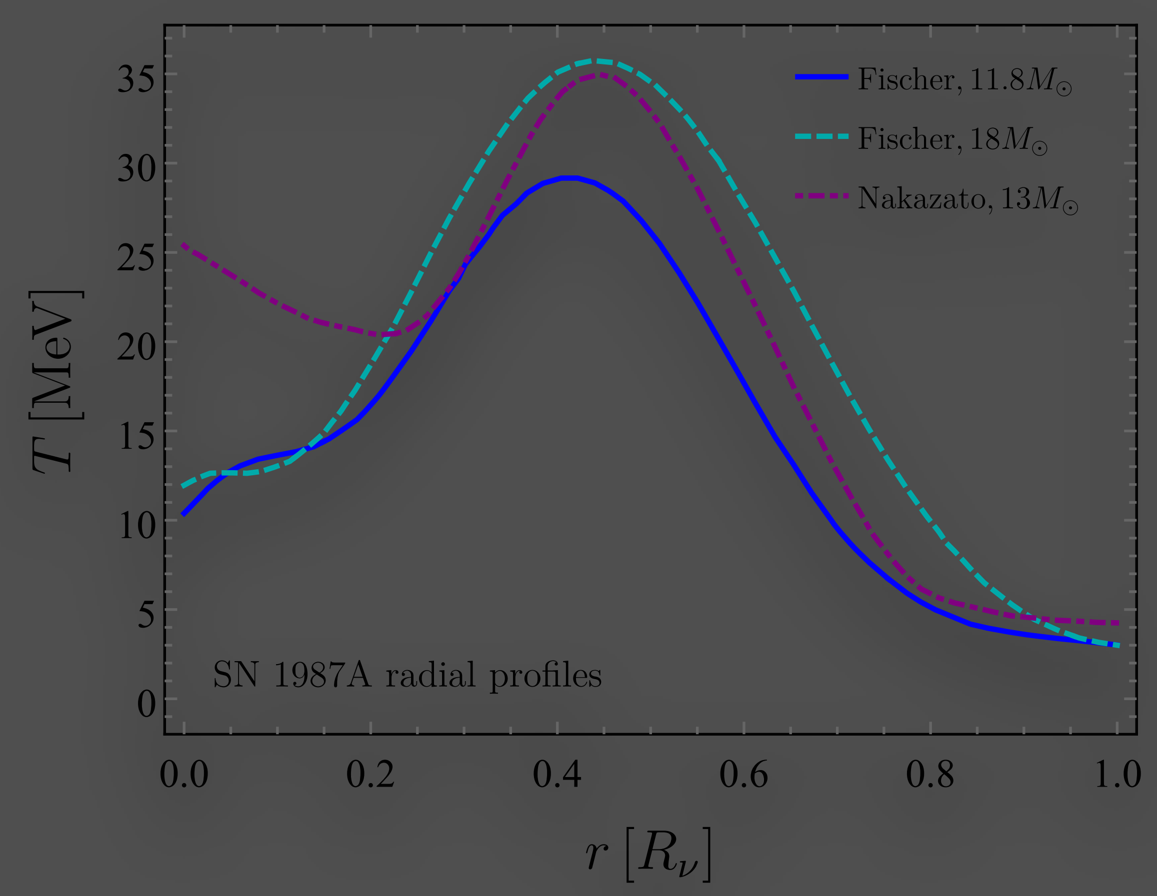

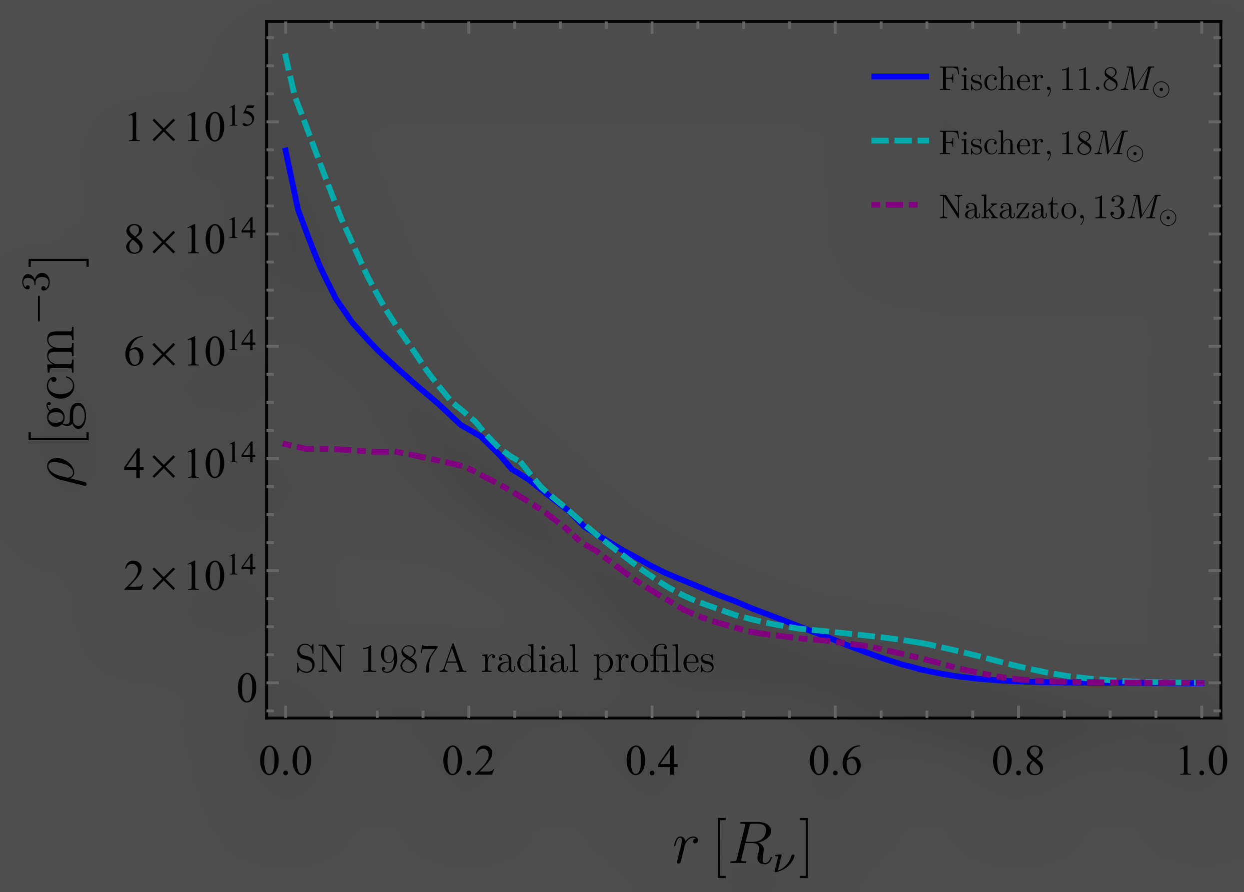

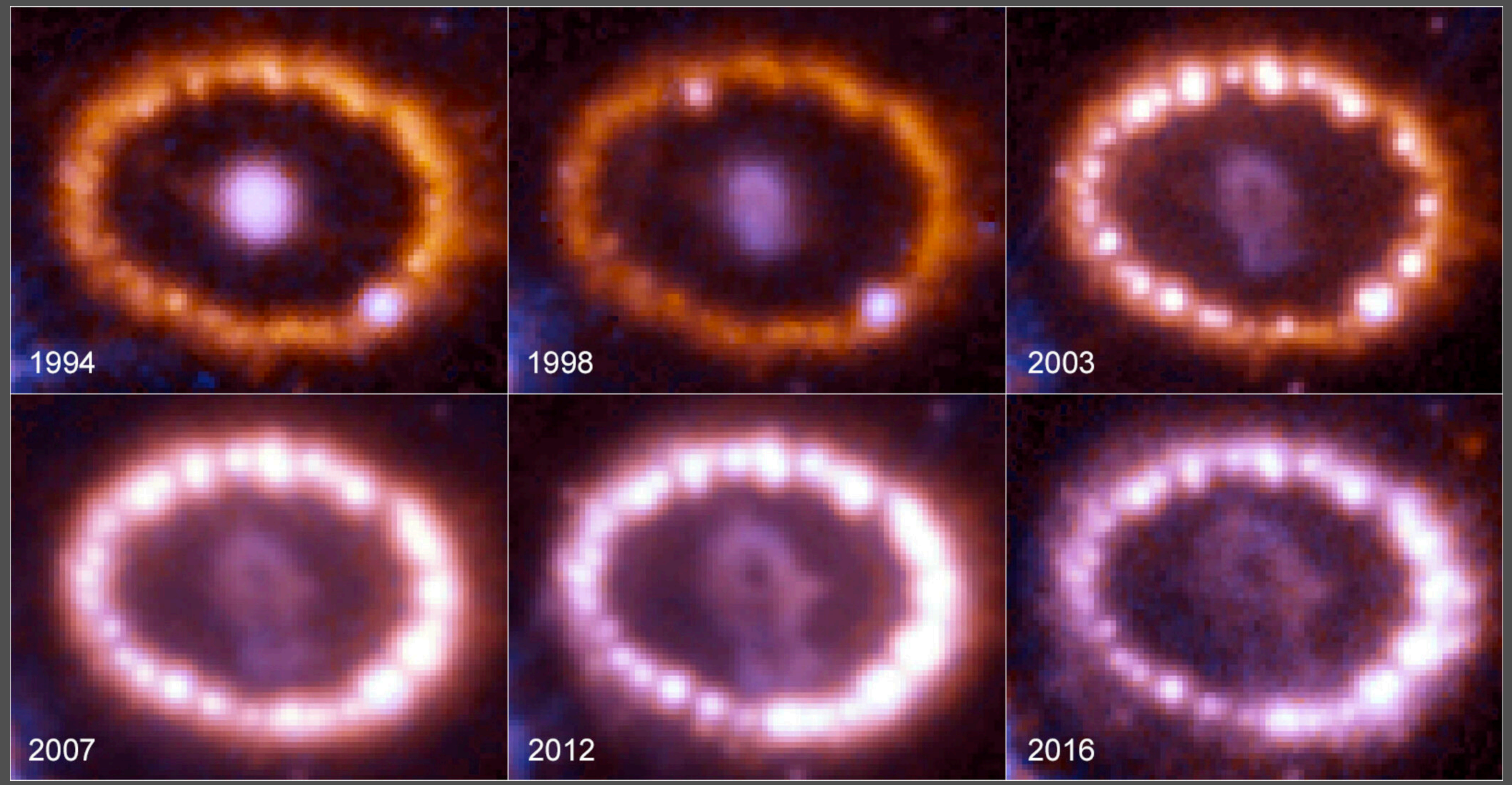

SN1987A RADIAL PROFILES

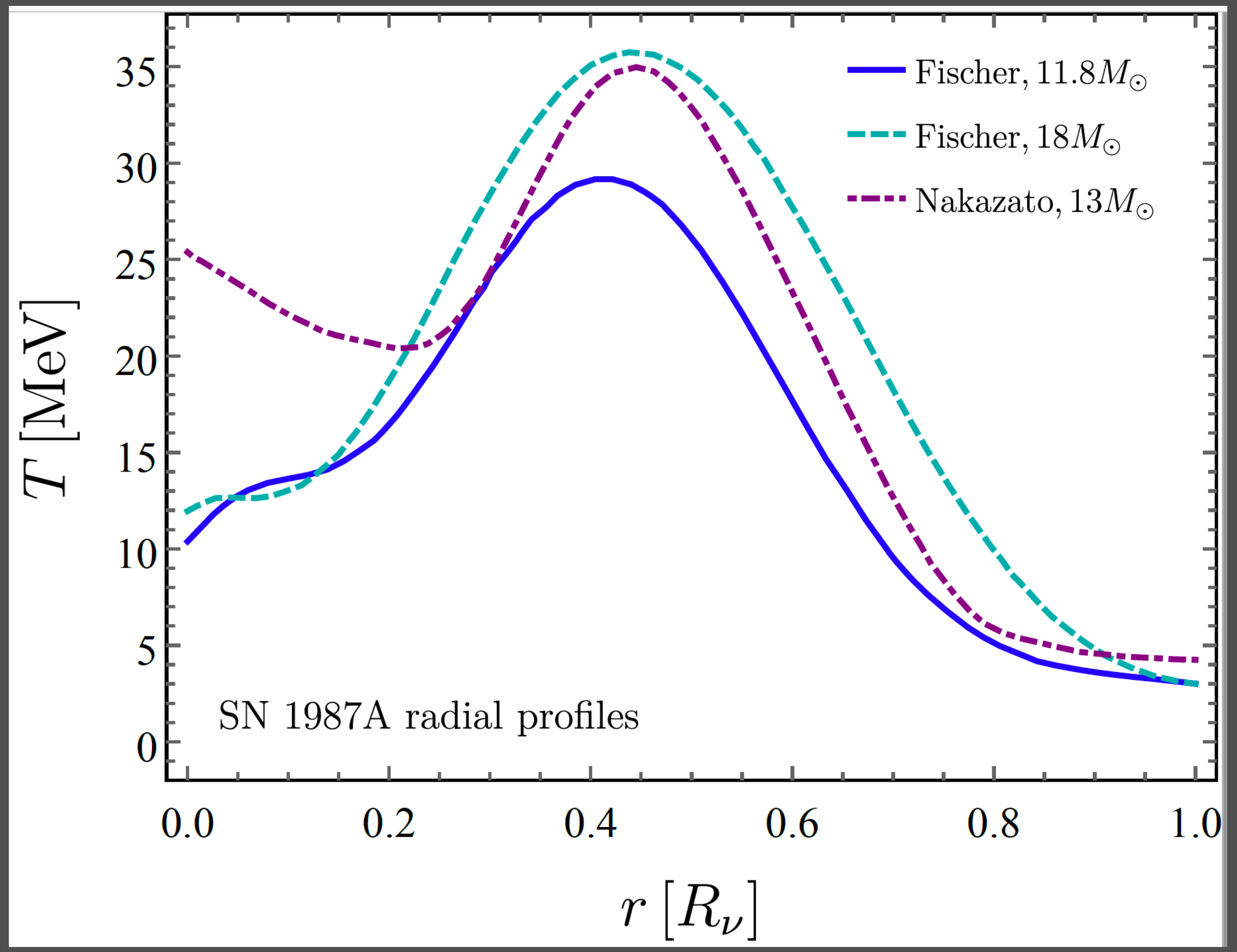

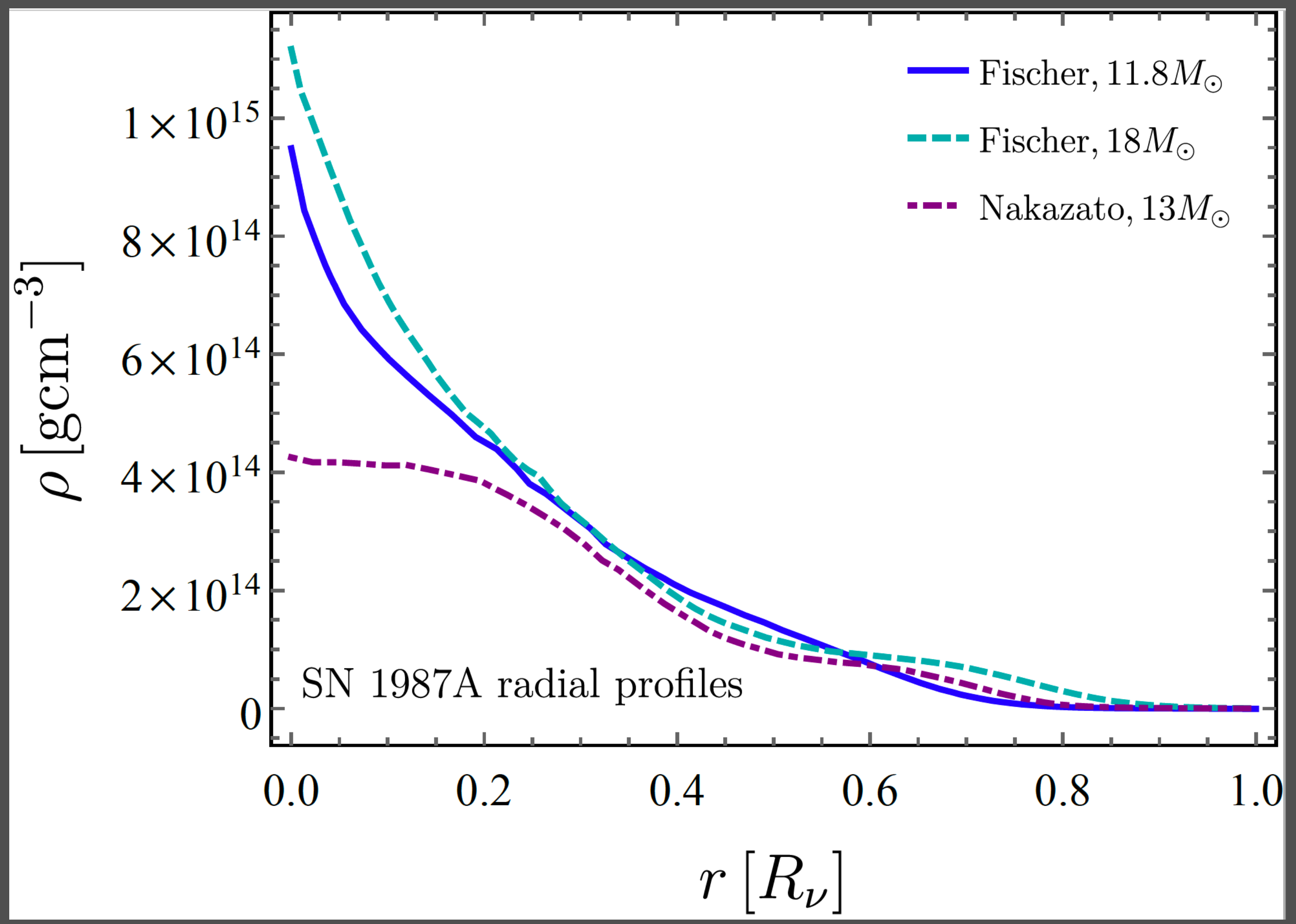

SN1987A RADIAL PROFILES

- SN1987A is an excellent candidate for examining new physics models because of the combination of the unique physical conditions attained in the star and the proximity of the explosion to our solar system.

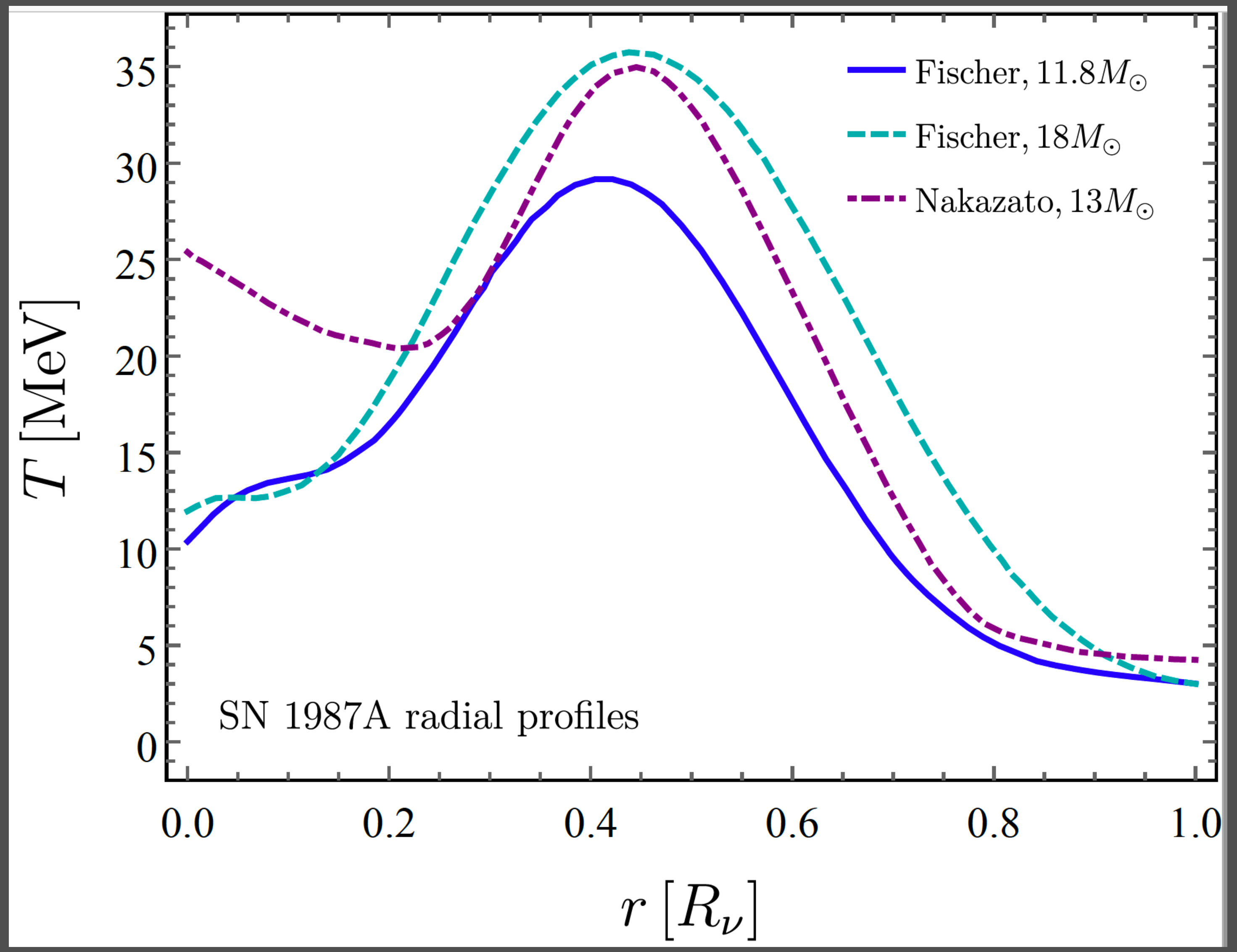

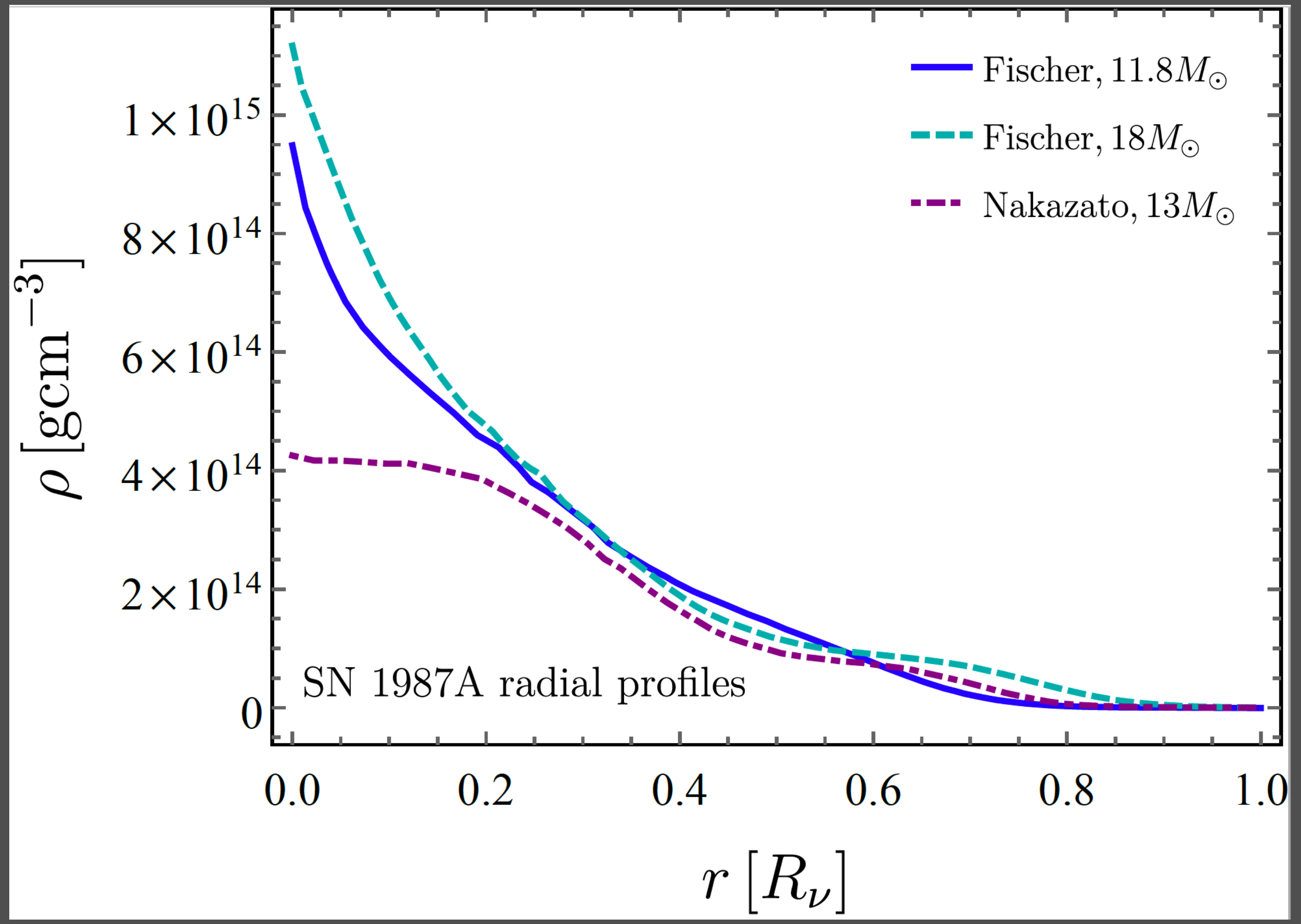

SN1987A RADIAL PROFILES

- SN1987A is an excellent candidate for examining new physics models because of the combination of the unique physical conditions attained in the star and the proximity of the explosion to our solar system.

- Despite this, constraints on new physics from SN1987A are inherently limited due to the difficulties associated with understanding the detailed physical processes of the supernova, even in the case without BSM physics.

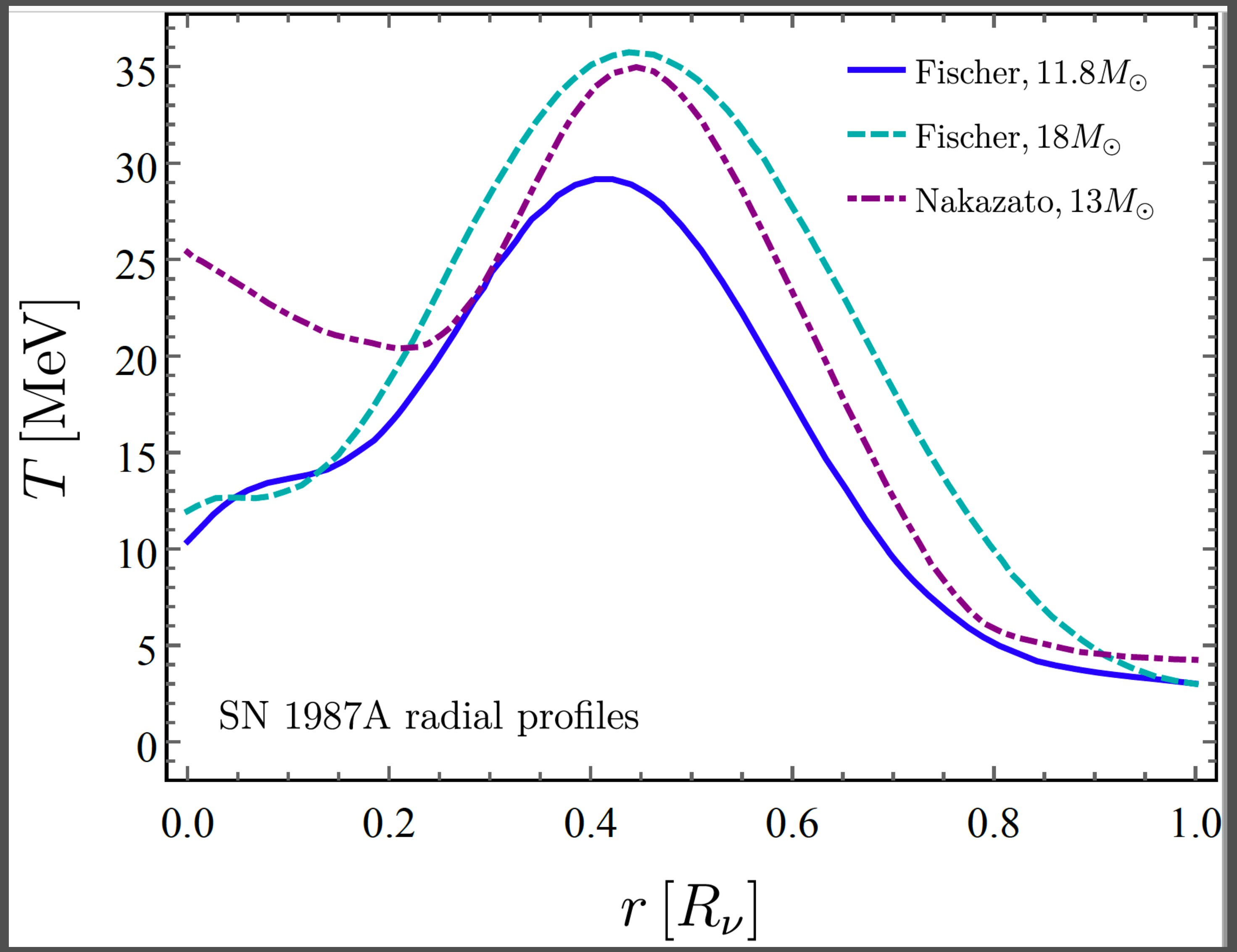

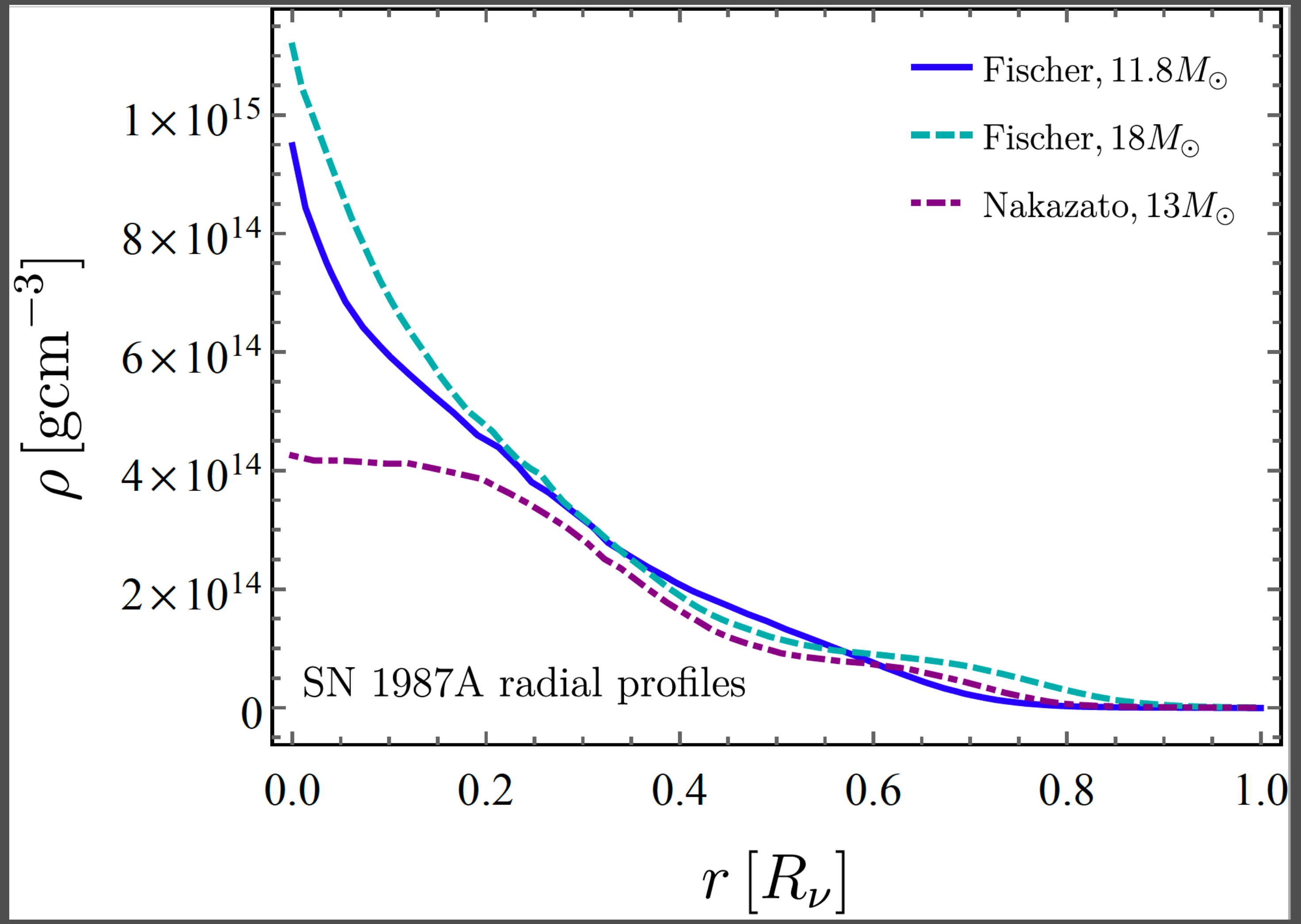

SN1987A RADIAL PROFILES

- SN1987A is an excellent candidate for examining new physics models because of the combination of the unique physical conditions attained in the star and the proximity of the explosion to our solar system.

- Despite this, constraints on new physics from SN1987A are inherently limited due to the difficulties associated with understanding the detailed physical processes of the supernova, even in the case without BSM physics.

- The main challenge in using SN1987A to constrain new physics is due to uncertainty surrounding the nature of the progenitor proto-neutron star which comprises the primary driver of the "shock revival" required to sustain the ultimate explosion.

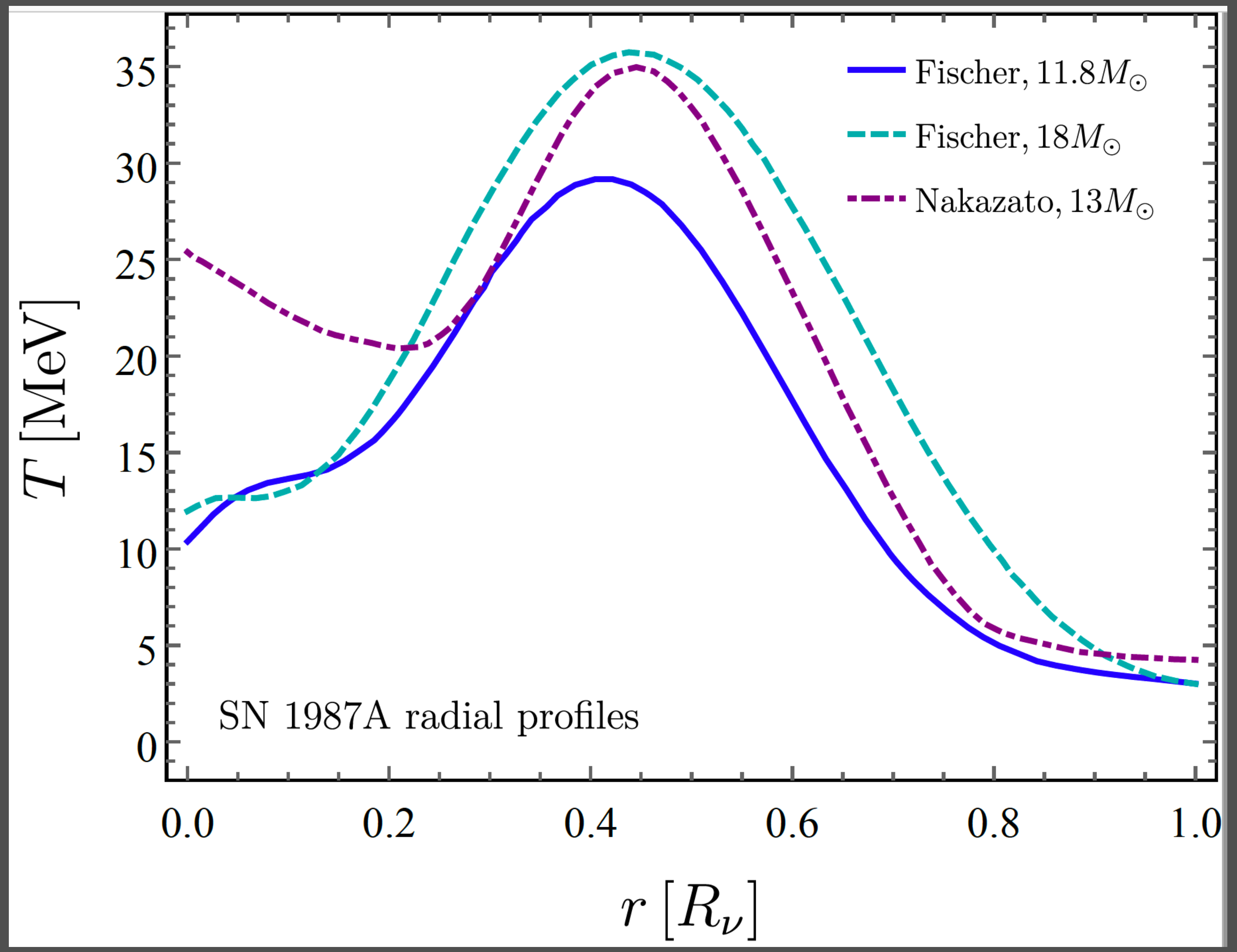

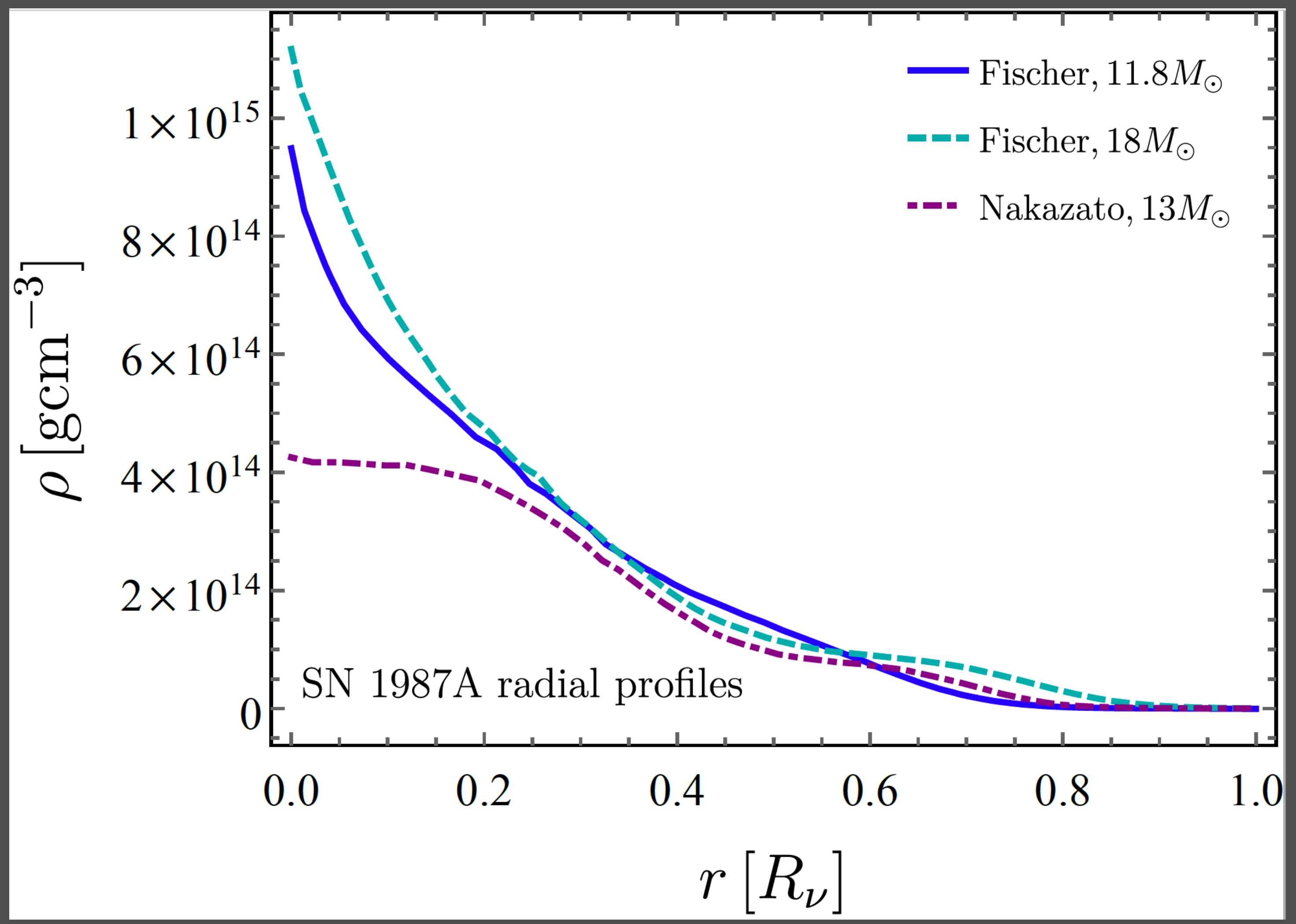

SN1987A RADIAL PROFILES

- SN1987A is an excellent candidate for examining new physics models because of the combination of the unique physical conditions attained in the star and the proximity of the explosion to our solar system.

- Despite this, constraints on new physics from SN1987A are inherently limited due to the difficulties associated with understanding the detailed physical processes of the supernova, even in the case without BSM physics.

- The main challenge in using SN1987A to constrain new physics is due to uncertainty surrounding the nature of the progenitor proto-neutron star which comprises the primary driver of the "shock revival" required to sustain the ultimate explosion.

- The mass of the progenitor star is uncertain up to a factor of two, and consequently the temperature and density profiles have large, qualitative uncertainties

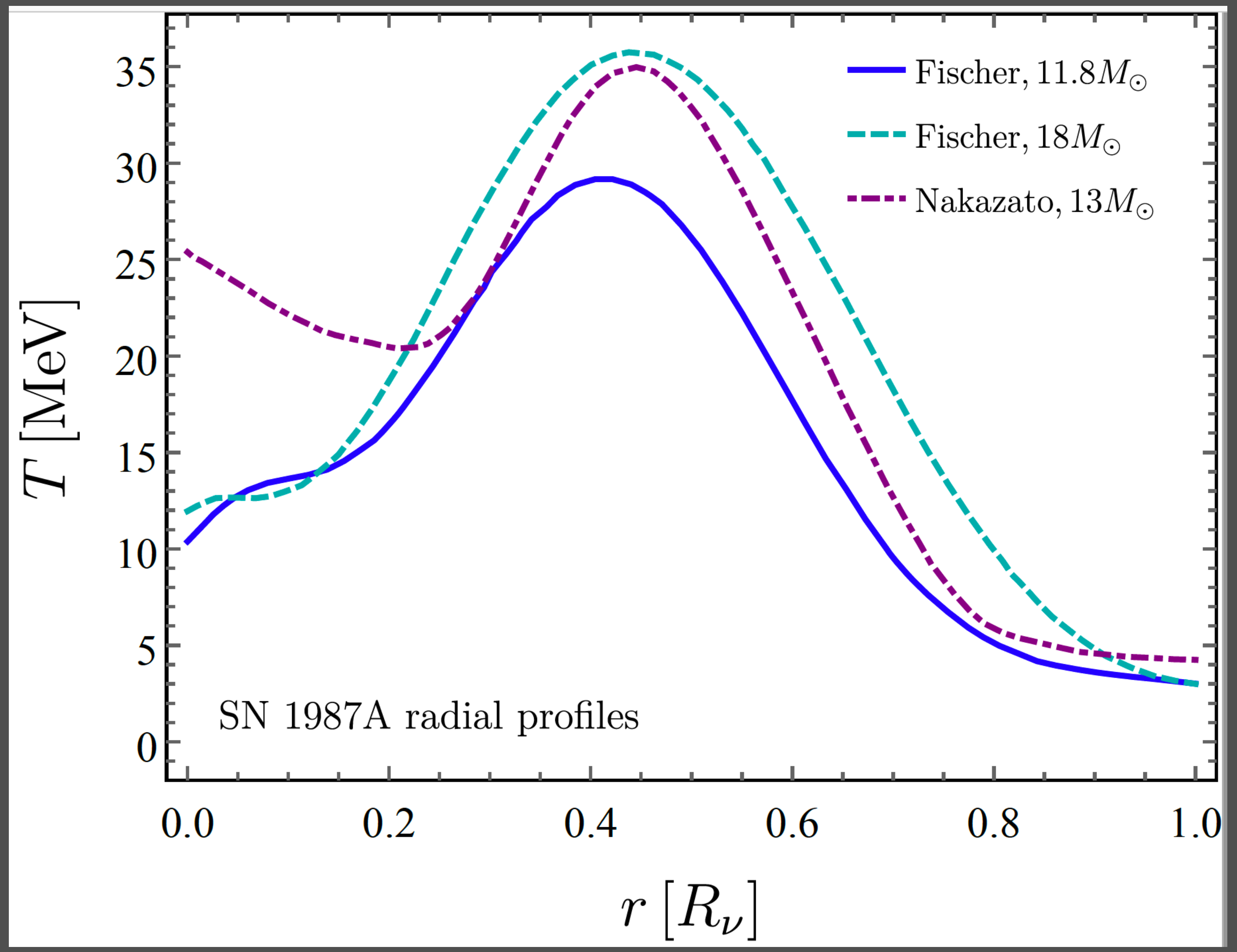

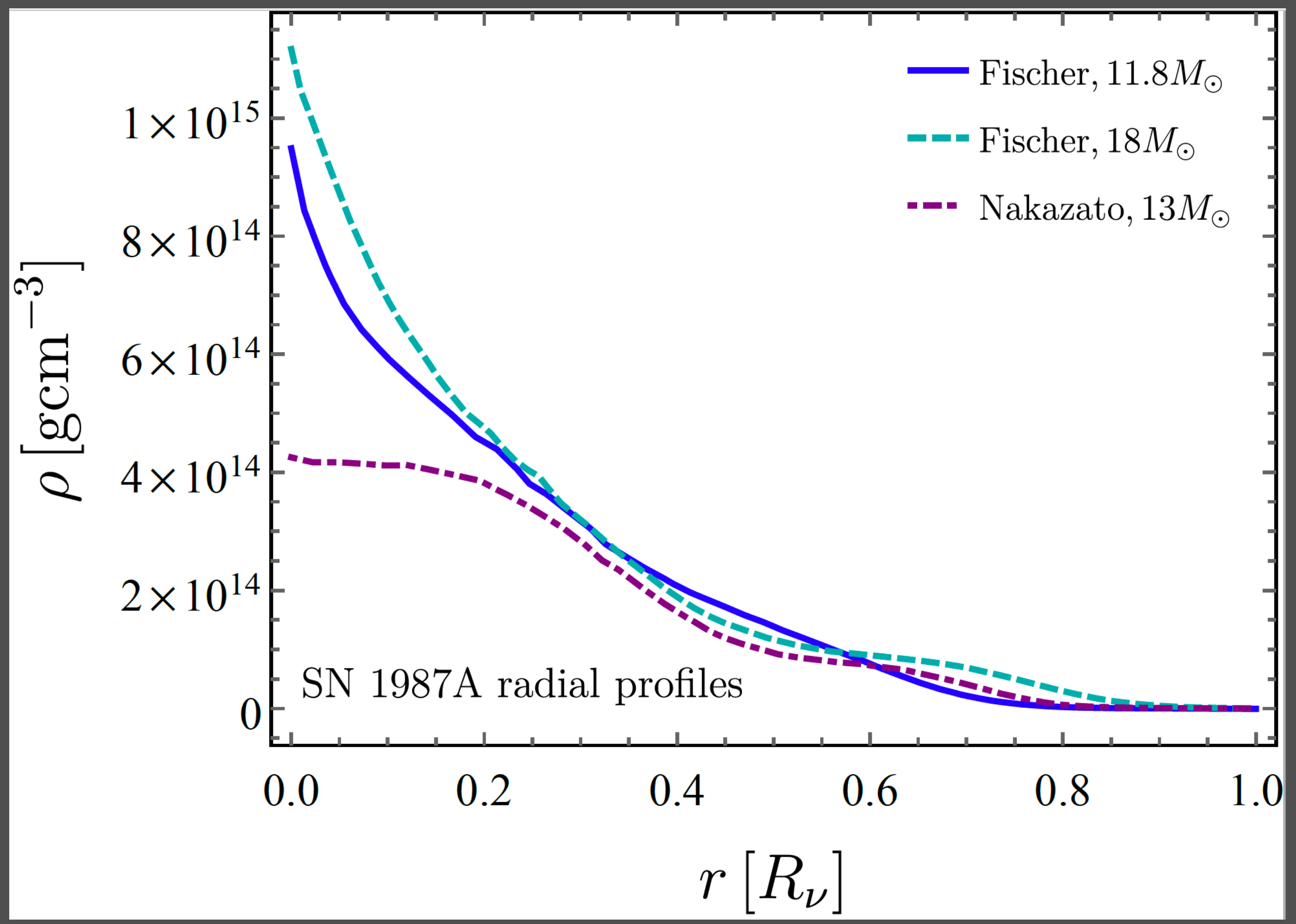

SN1987A RADIAL PROFILES

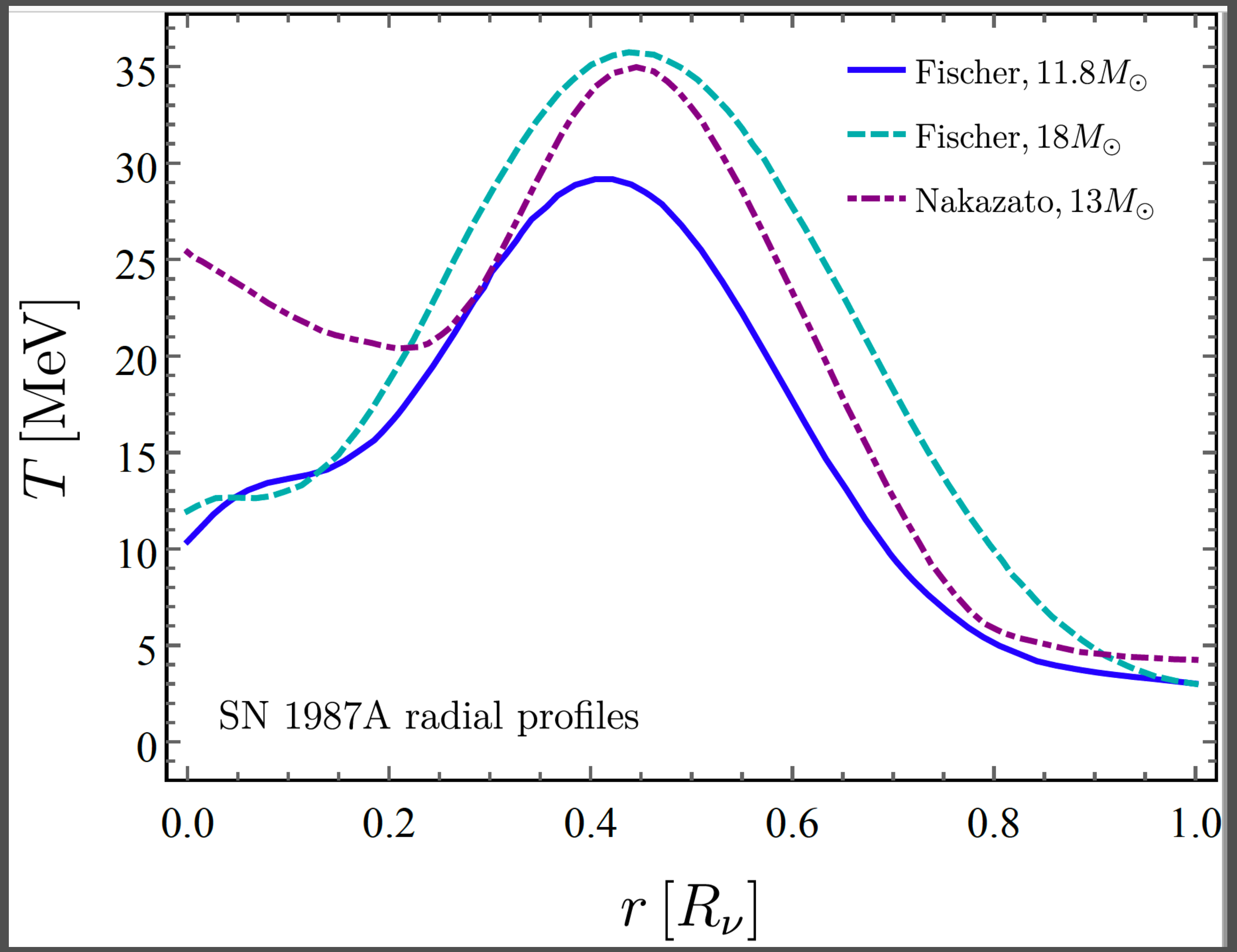

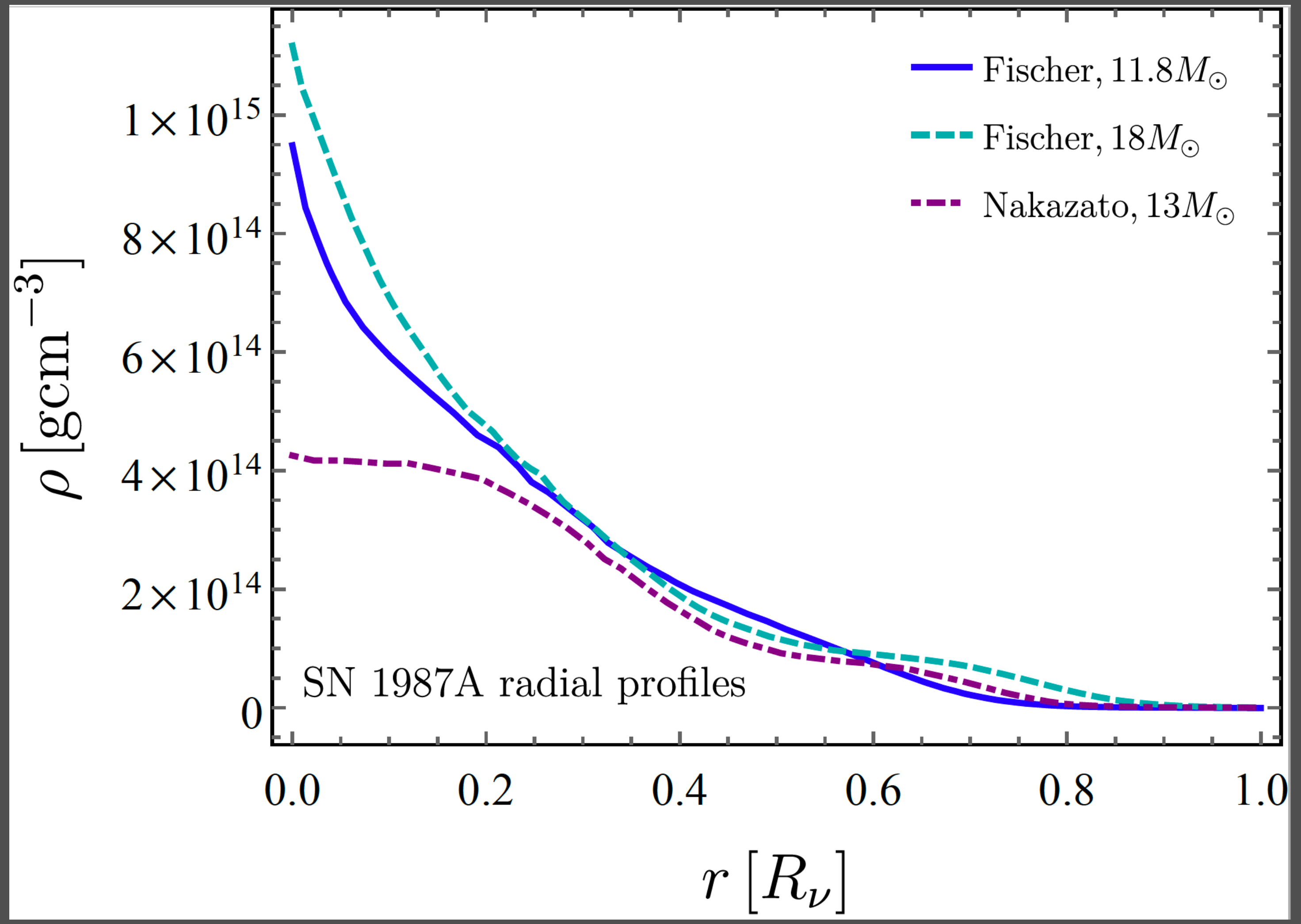

SN1987A RADIAL PROFILES

- We adopt the numerical profiles

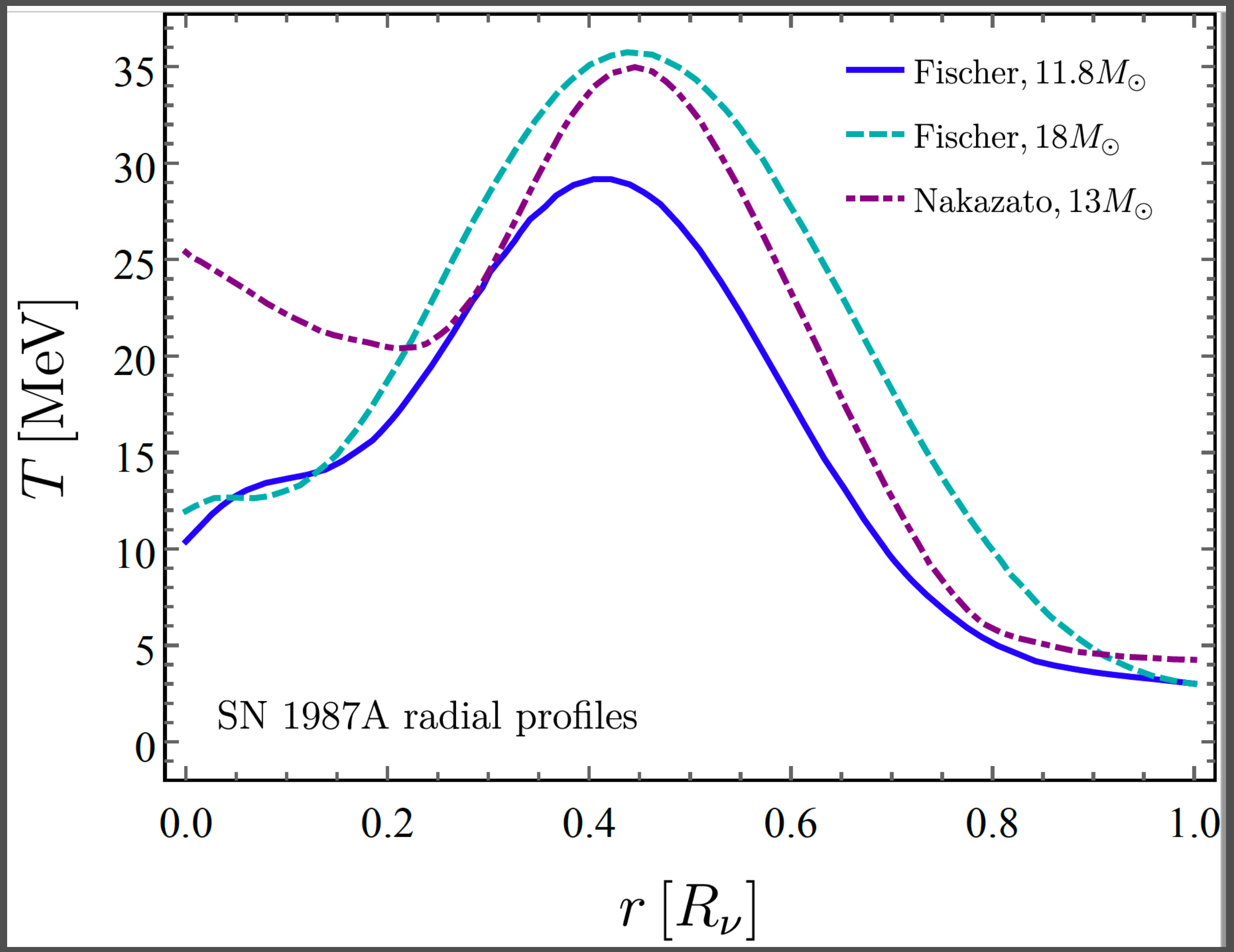

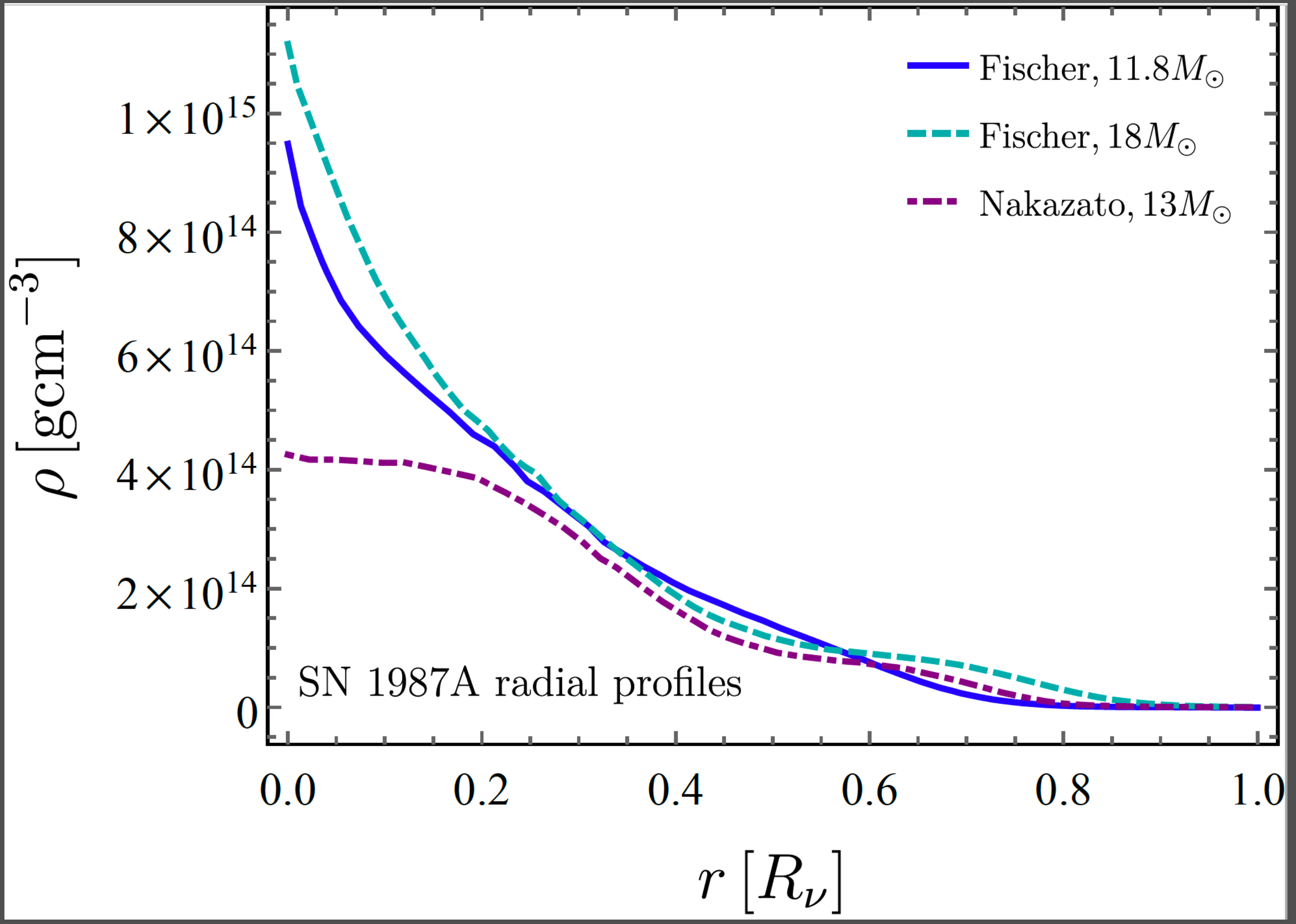

SN1987A RADIAL PROFILES

- We adopt the numerical profiles

  ➡ Fischer $11.8\,M_\odot$

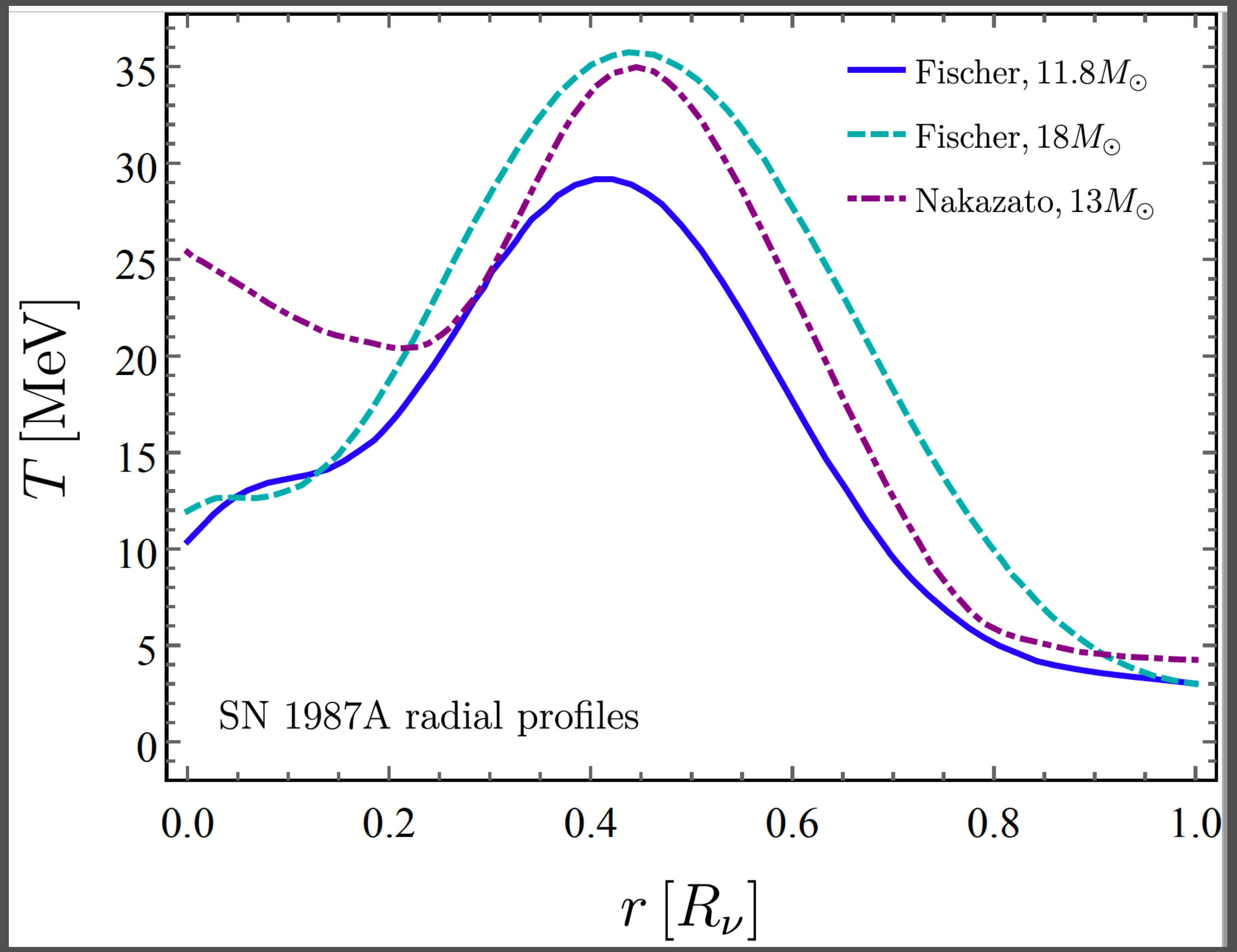

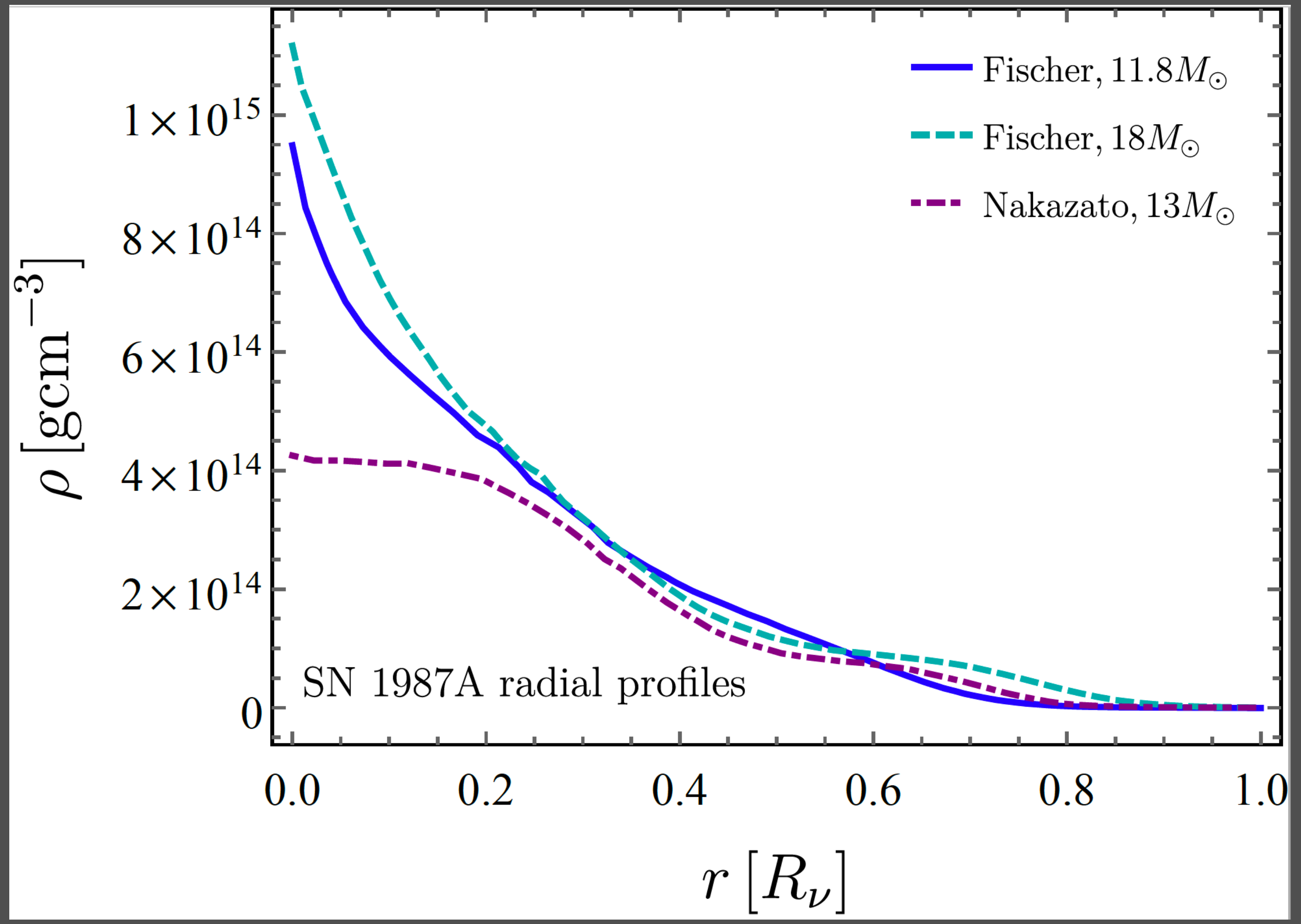

SN1987A RADIAL PROFILES

- We adopt the numerical profiles
  - ➡ Fischer $11.8\, M_{\odot}$
  - ➡ Fischer $18\, M_{\odot}$

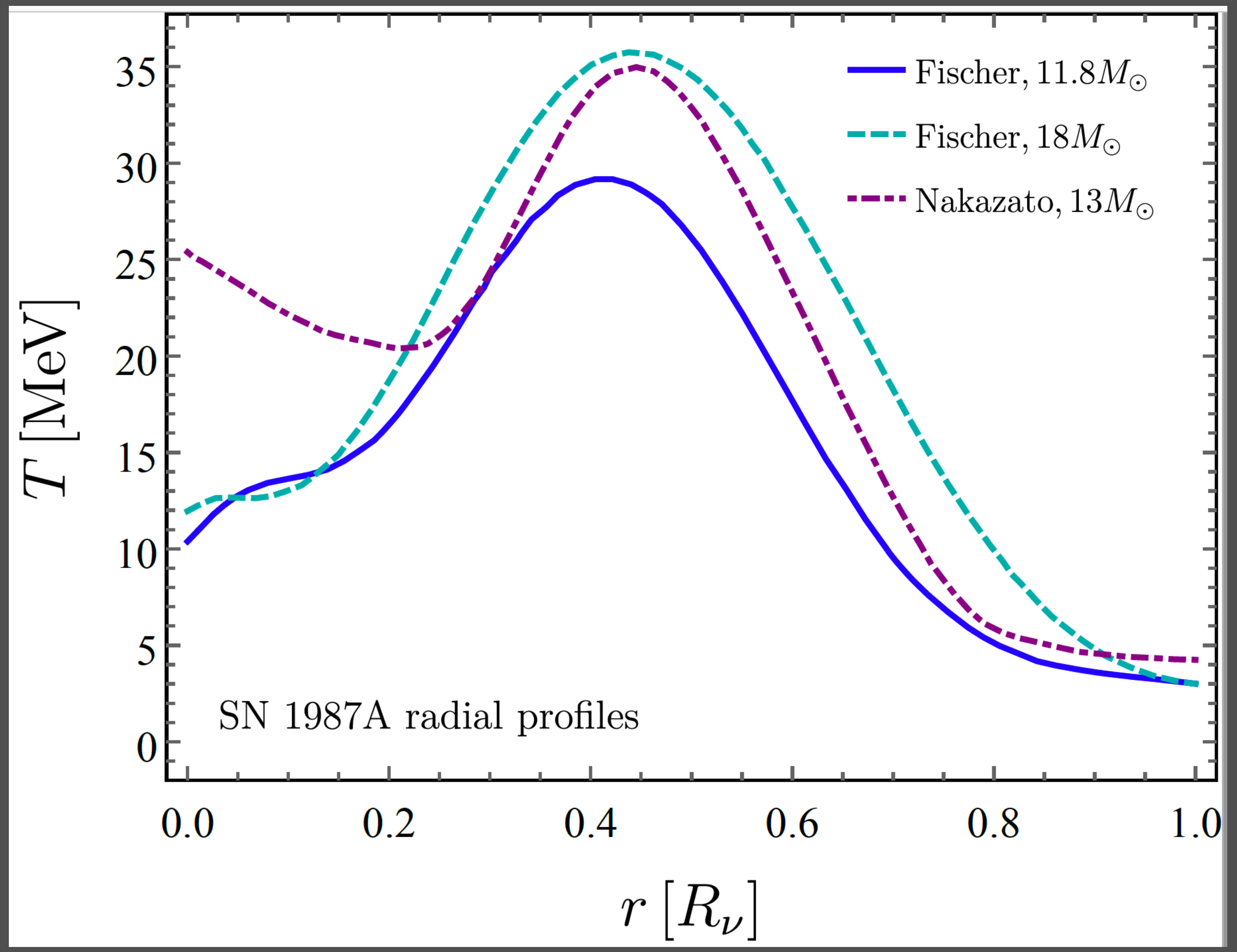

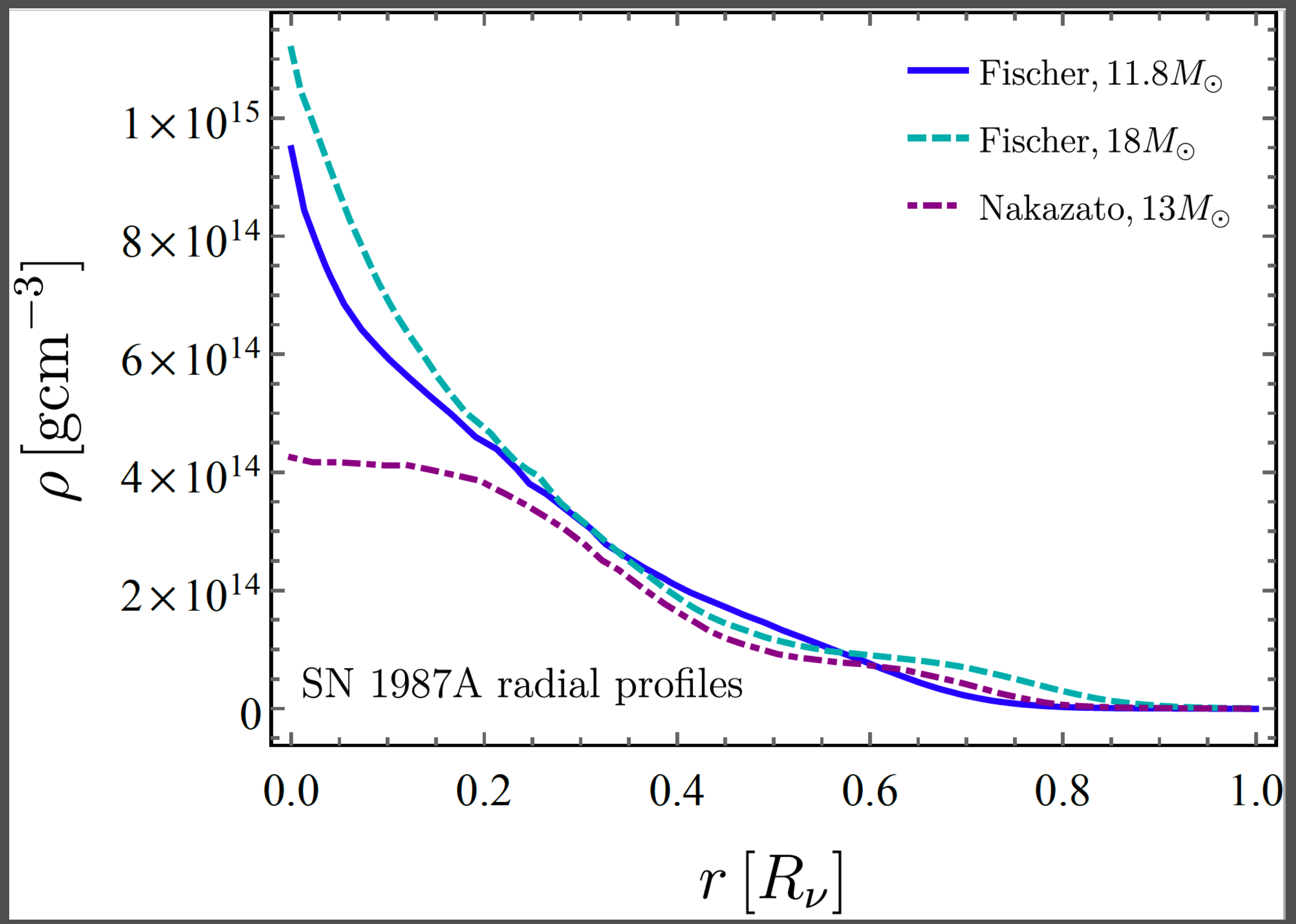

SN1987A RADIAL PROFILES

- We adopt the numerical profiles
  - ➡ Fischer $11.8\,M_\odot$
  - ➡ Fischer $18\,M_\odot$
  - ➡ Nakazato $13\,M_\odot$

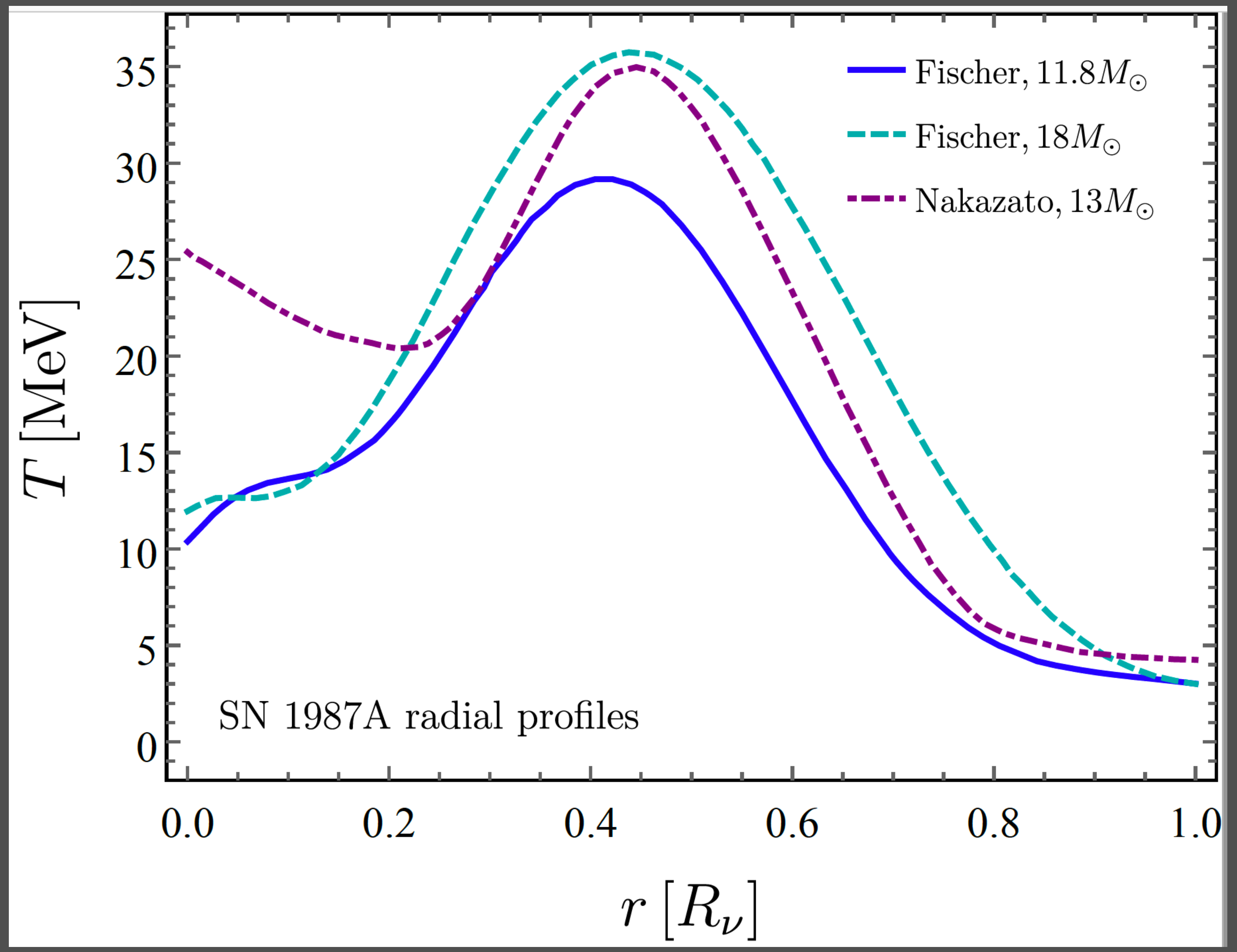

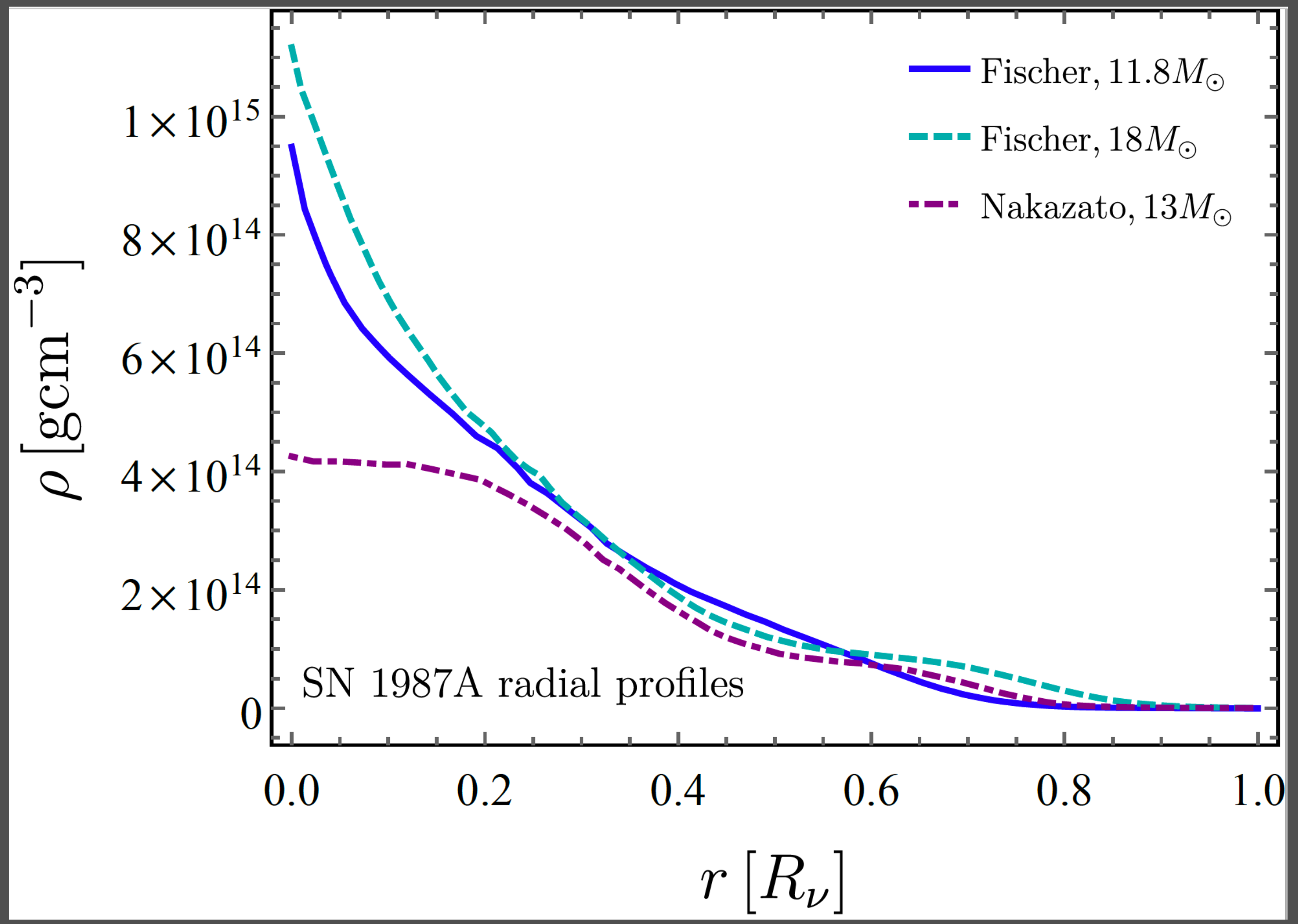

SN1987A RADIAL PROFILES

- We adopt the numerical profiles
  - ➡ Fischer $11.8\,M_{\odot}$
  - ➡ Fischer $18\,M_{\odot}$
  - ➡ Nakazato $13\,M_{\odot}$

Computed by solving the Boltzmann equation for neutrino transport with the AGILE-BOLTZTRAN code and an equation of state based on known nuclear isotopes and relativistic mean field models

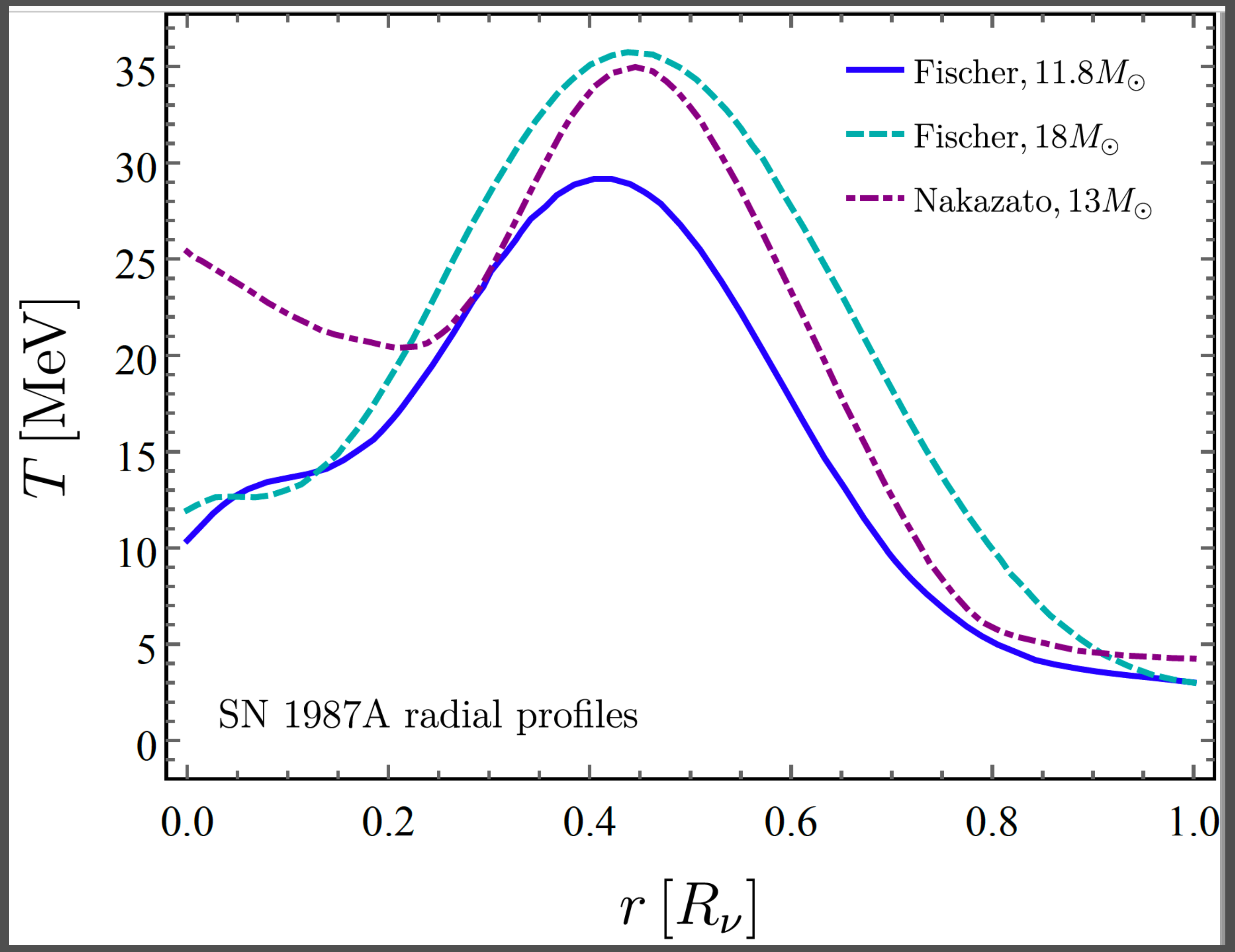

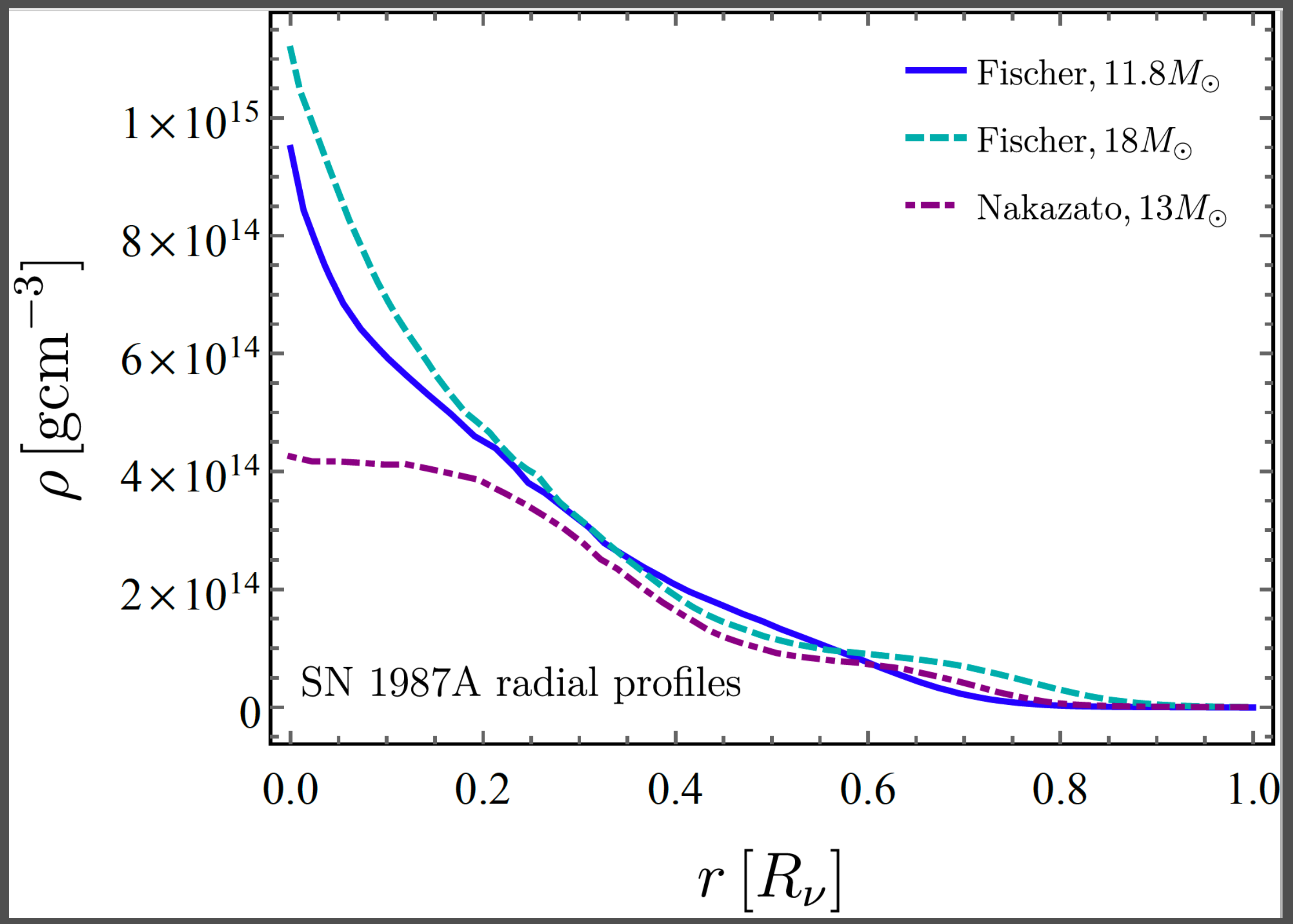

SN1987A RADIAL PROFILES

- We adopt the numerical profiles
  - ➡ Fischer $11.8\,M_\odot$
  - ➡ Fischer $18\,M_\odot$
  - ➡ Nakazato $13\,M_\odot$

Computed by solving the Boltzmann equation for neutrino transport with the AGILE-BOLTZTRAN code and an equation of state based on known nuclear isotopes and relativistic mean field models

Simulated with a 100 ms shock revival time inserted by hand

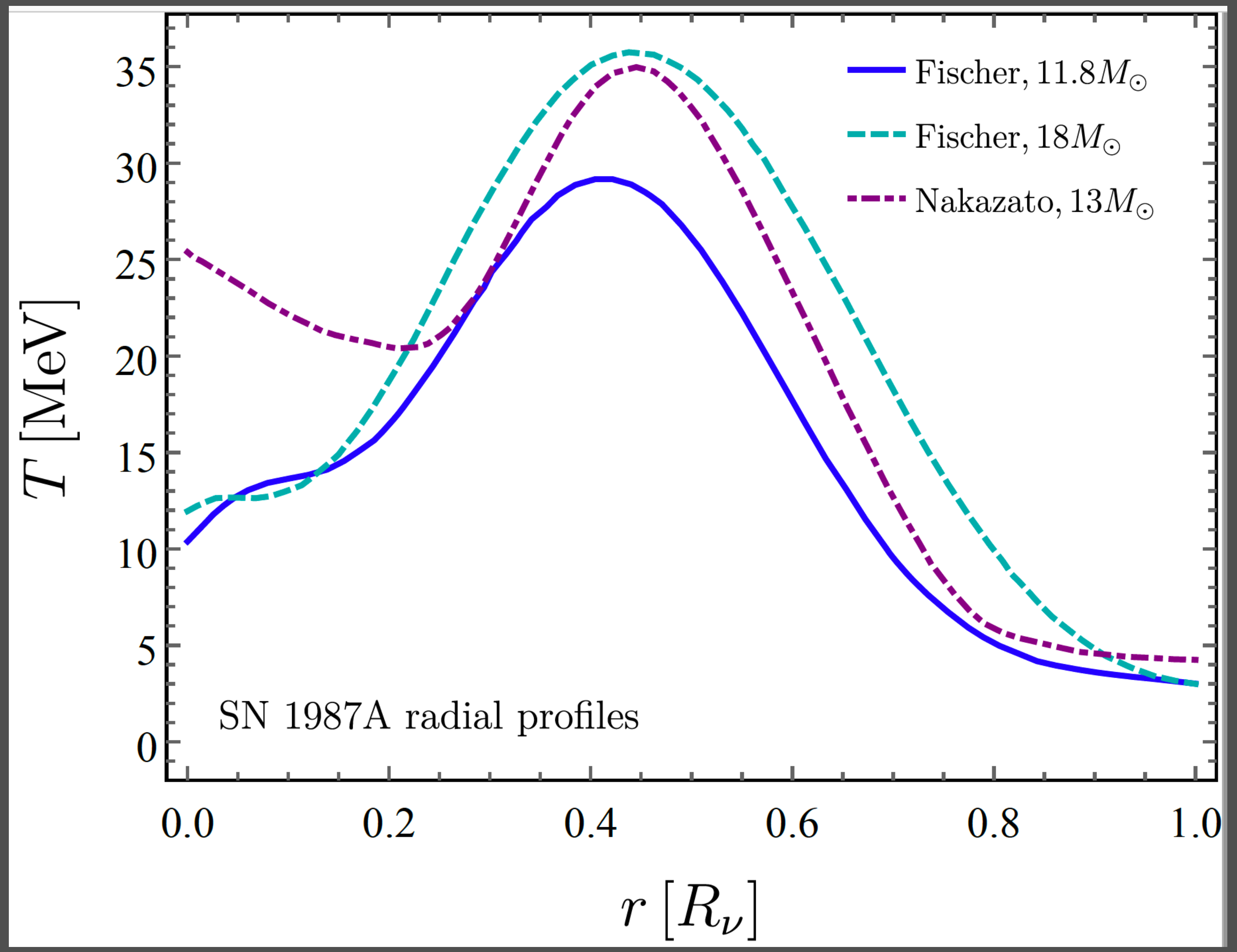

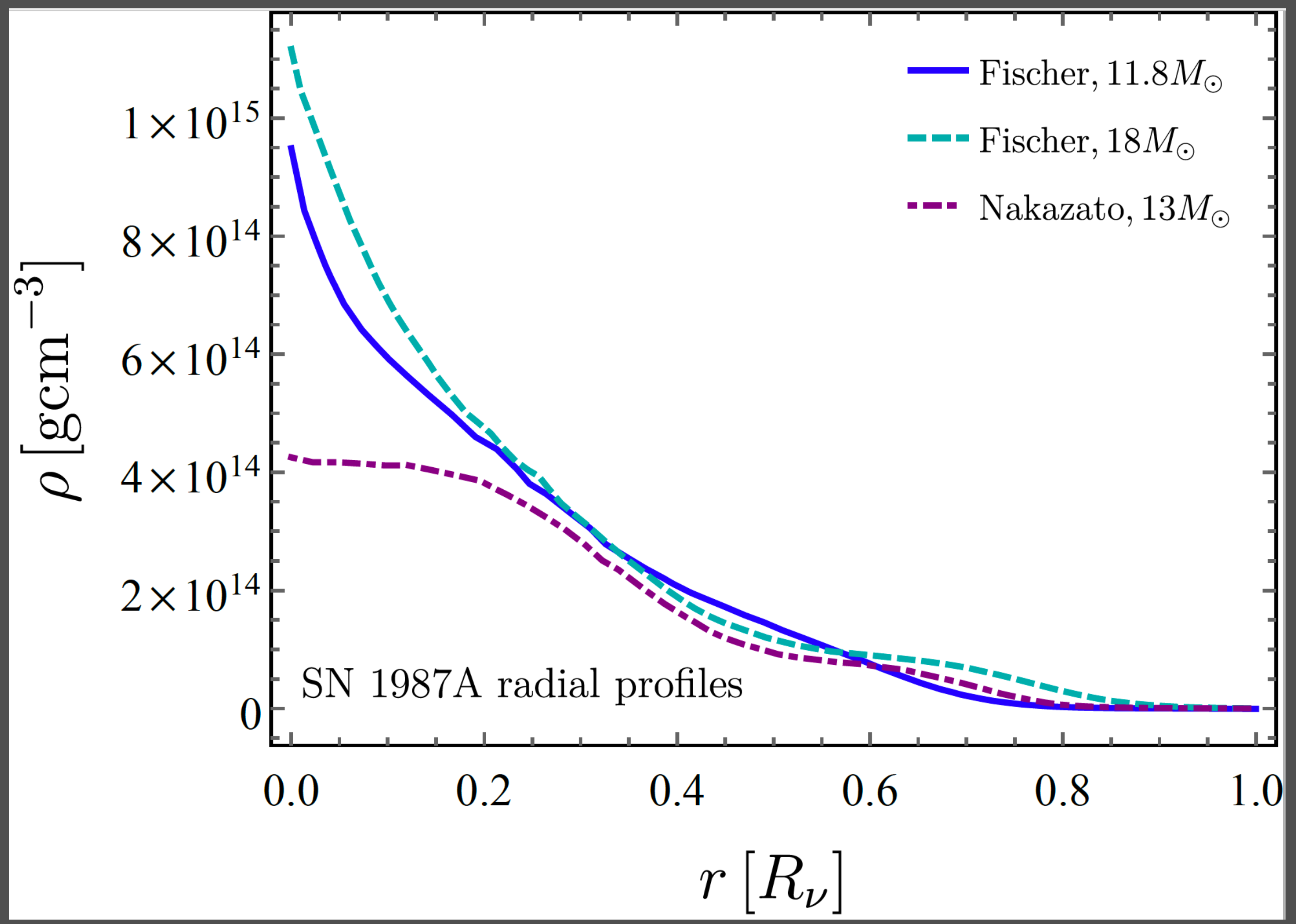

SN1987A RADIAL PROFILES

- We adopt the numerical profiles
  - ➡ Fischer $11.8\,M_\odot$
  - ➡ Fischer $18\,M_\odot$
  - ➡ Nakazato $13\,M_\odot$

Computed by solving the Boltzmann equation for neutrino transport with the AGILE-BOLTZTRAN code and an equation of state based on known nuclear isotopes and relativistic mean field models

Simulated with a 100 ms shock revival time inserted by hand

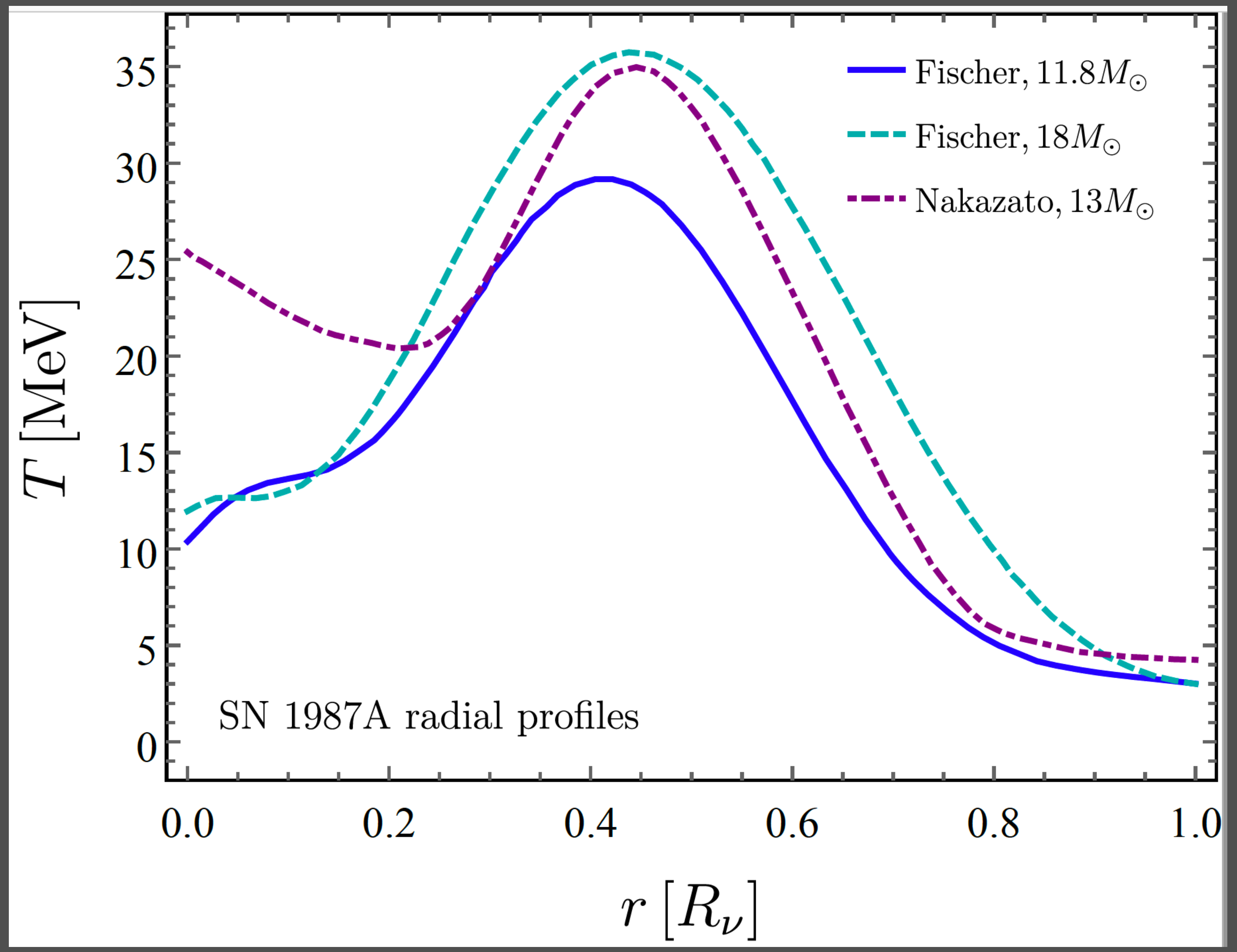

- These models can predict densities that vary by as much as an order of magnitude in certain regions of the proto-neutron star.

➡ currently not full control of subtleties resulting from the behaviour of the nuclear matter.

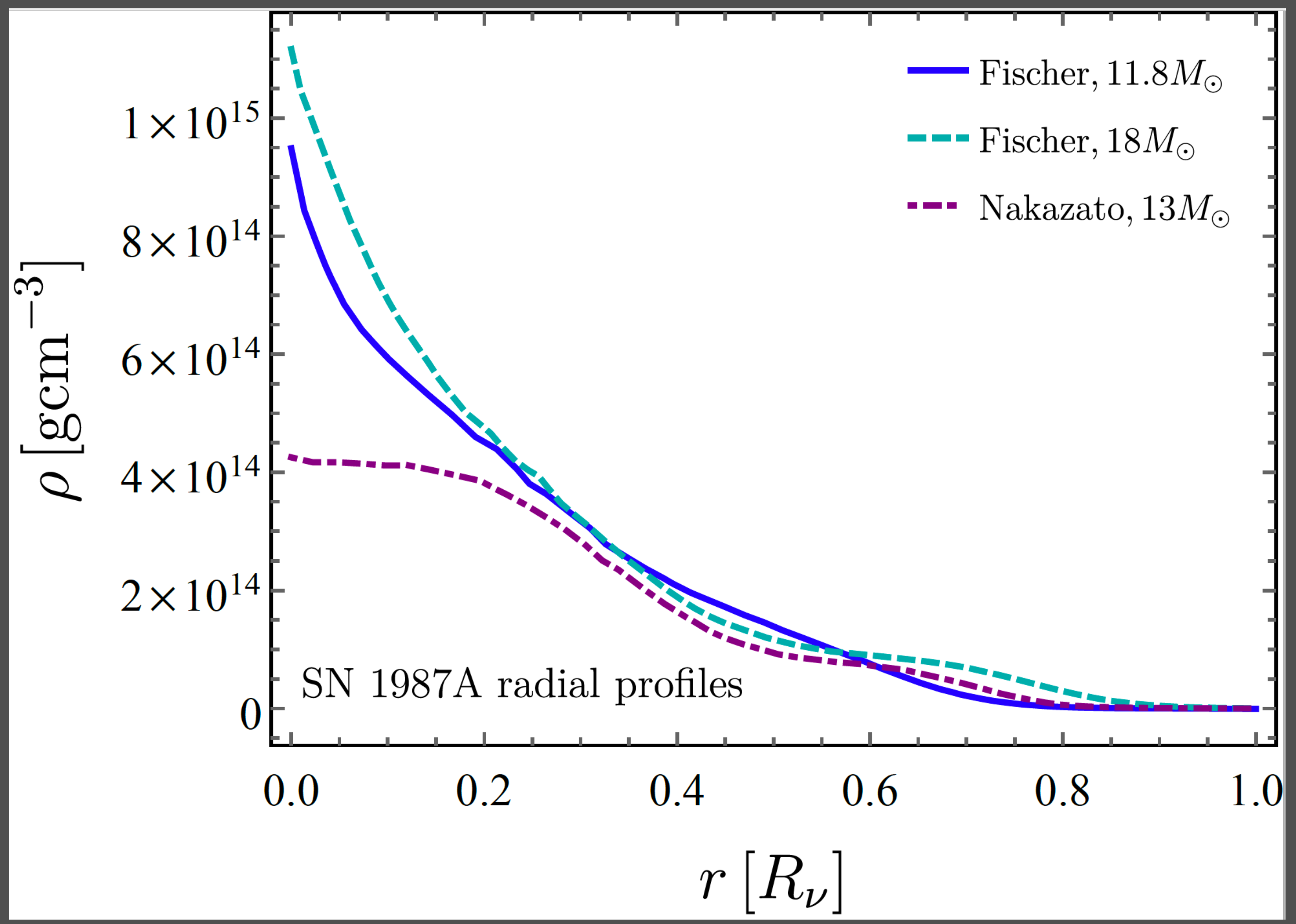

SN1987A RADIAL PROFILES

- We adopt the numerical profiles
  - ➡ Fischer $11.8\, M_\odot$
  - ➡ Fischer $18\, M_\odot$
  - ➡ Nakazato $13\, M_\odot$

Computed by solving the Boltzmann equation for neutrino transport with the AGILE-BOLTZTRAN code and an equation of state based on known nuclear isotopes and relativistic mean field models

Simulated with a 100 ms shock revival time inserted by hand

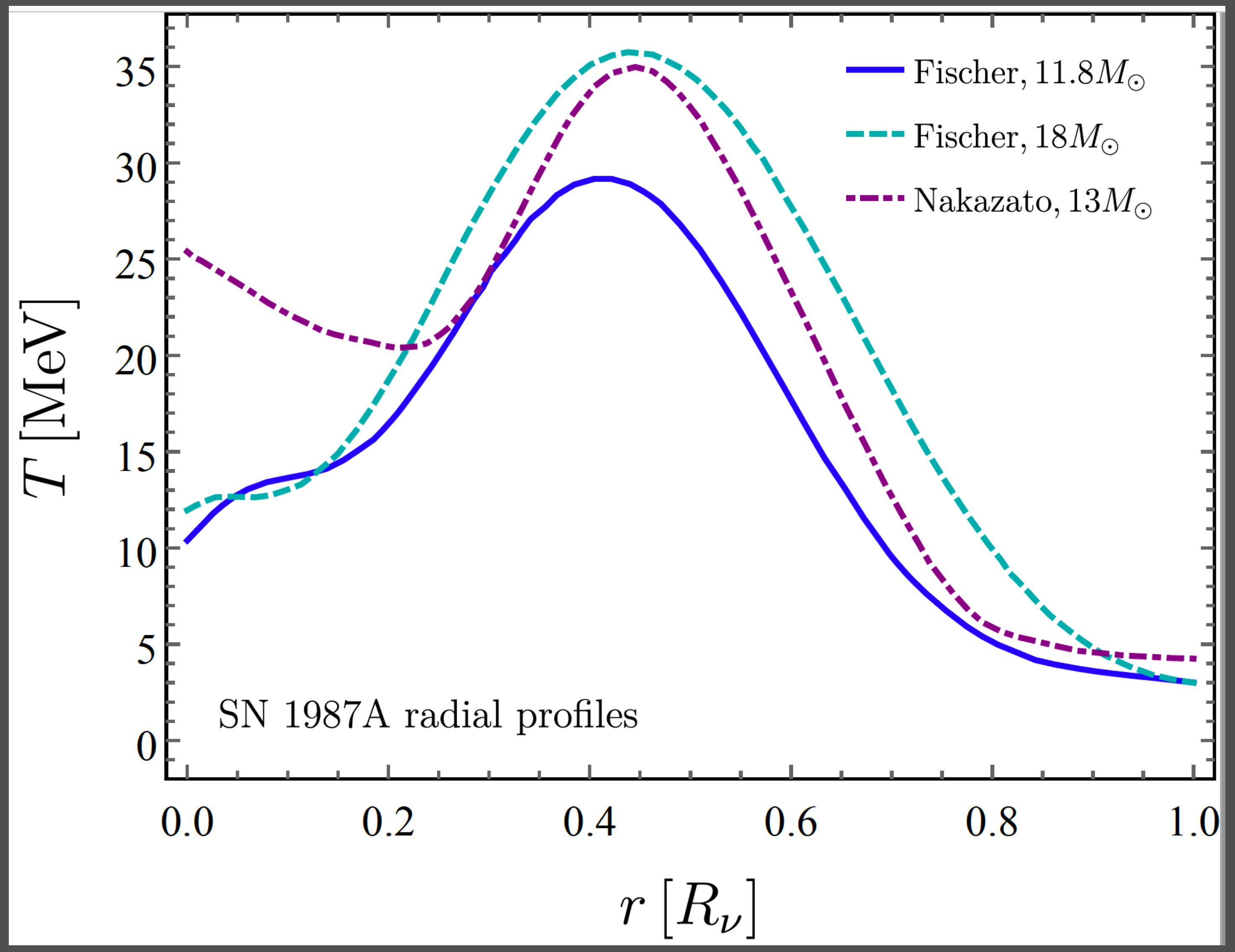

- These models can predict densities that vary by as much as an order of magnitude in certain regions of the proto-neutron star.

➡ currently not full control of subtleties resulting from the behaviour of the nuclear matter.

New physics constraints derived with any of the aforementioned profiles are necessarily approximate

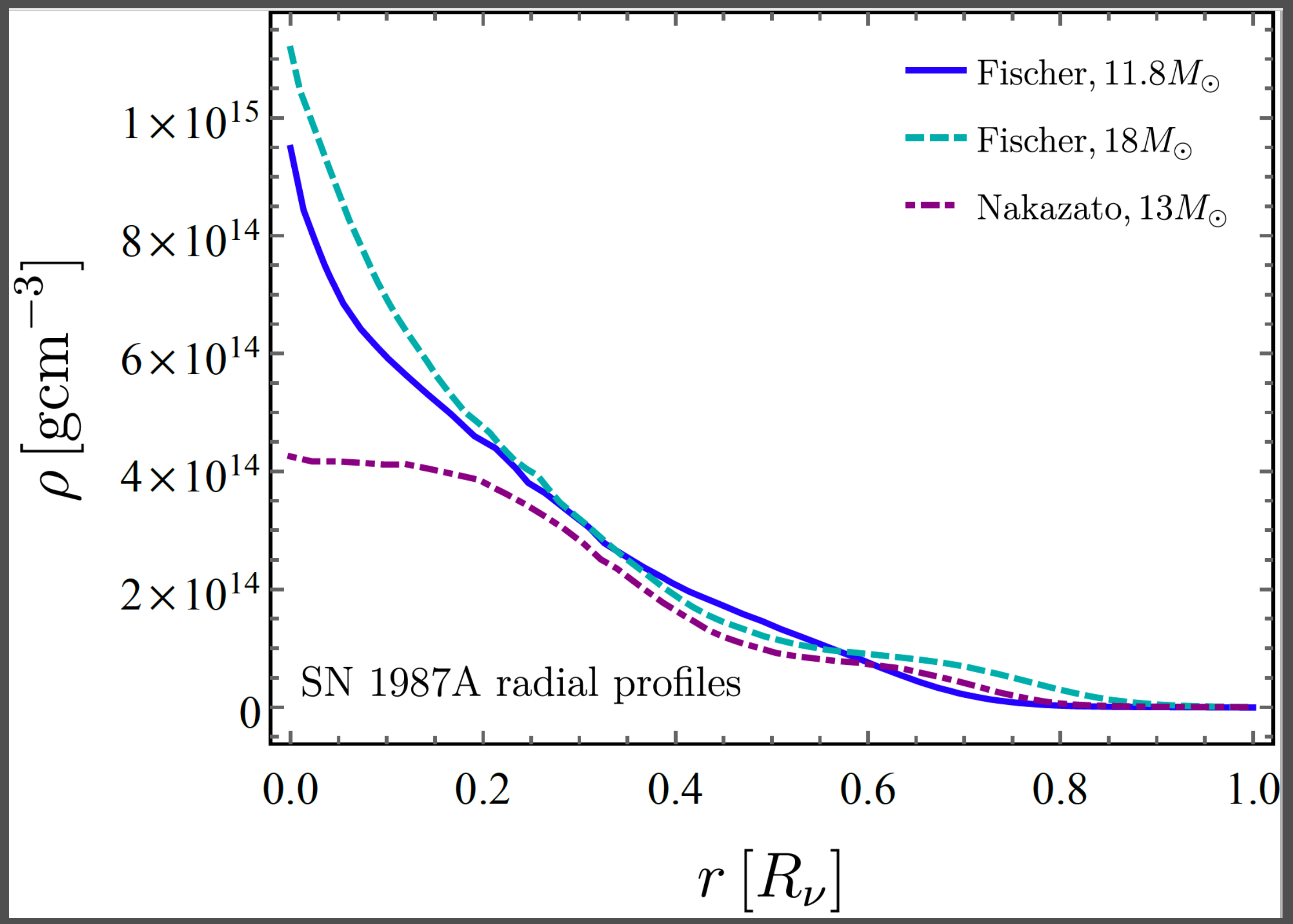

SN1987A RADIAL PROFILES

- We adopt the numerical profiles
  - ➡ Fischer $11.8\, M_{\odot}$
  - ➡ Fischer $18\, M_{\odot}$
  - ➡ Nakazato $13\, M_{\odot}$

Computed by solving the Boltzmann equation for neutrino transport with the AGILE-BOLTZTRAN code and an equation of state based on known nuclear isotopes and relativistic mean field models

Simulated with a 100 ms shock revival time inserted by hand

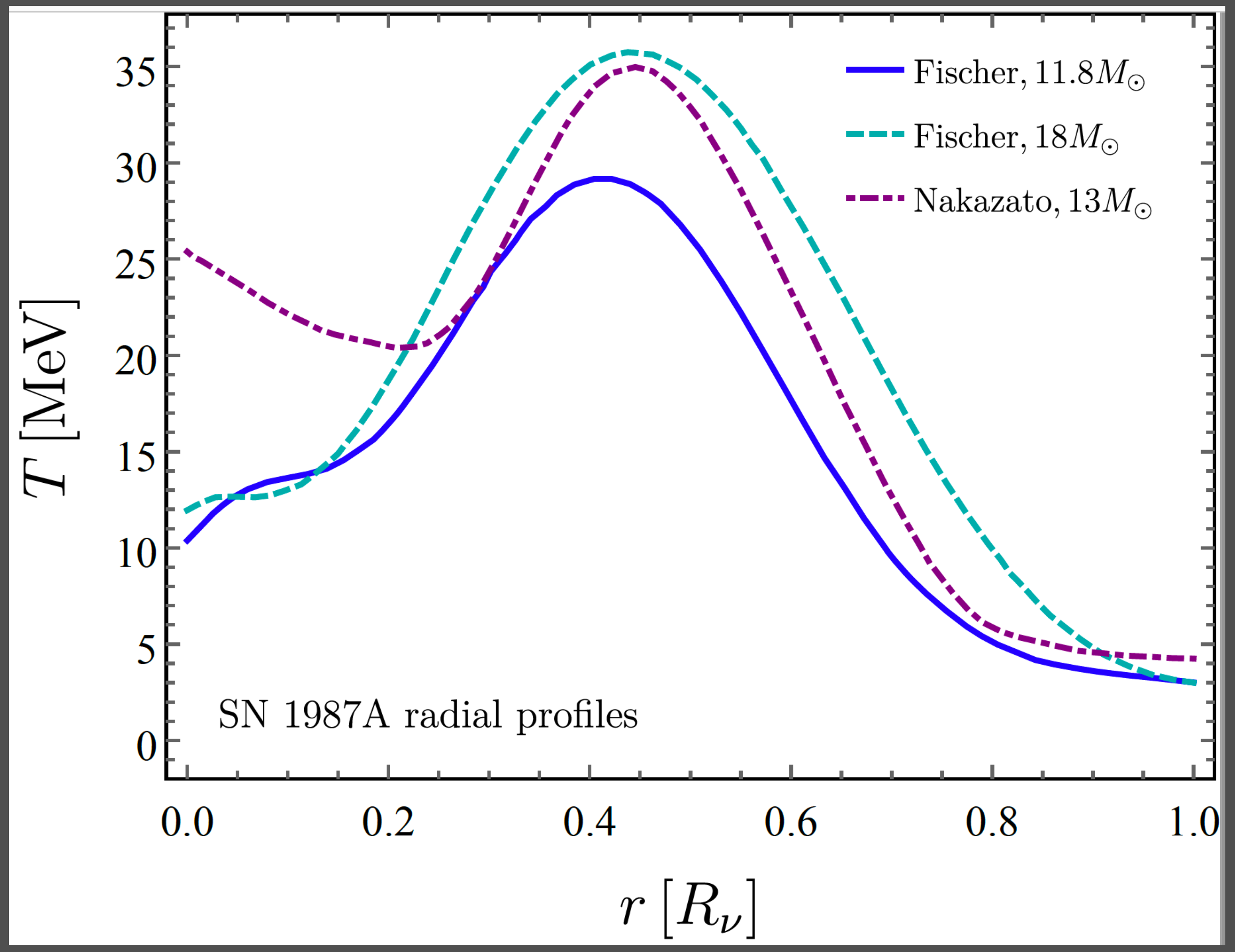

- These models can predict densities that vary by as much as an order of magnitude in certain regions of the proto-neutron star.

currently not full control of subtleties resulting from the behaviour of the nuclear matter.

New physics constraints derived with any of the aforementioned profiles are necessarily approximate

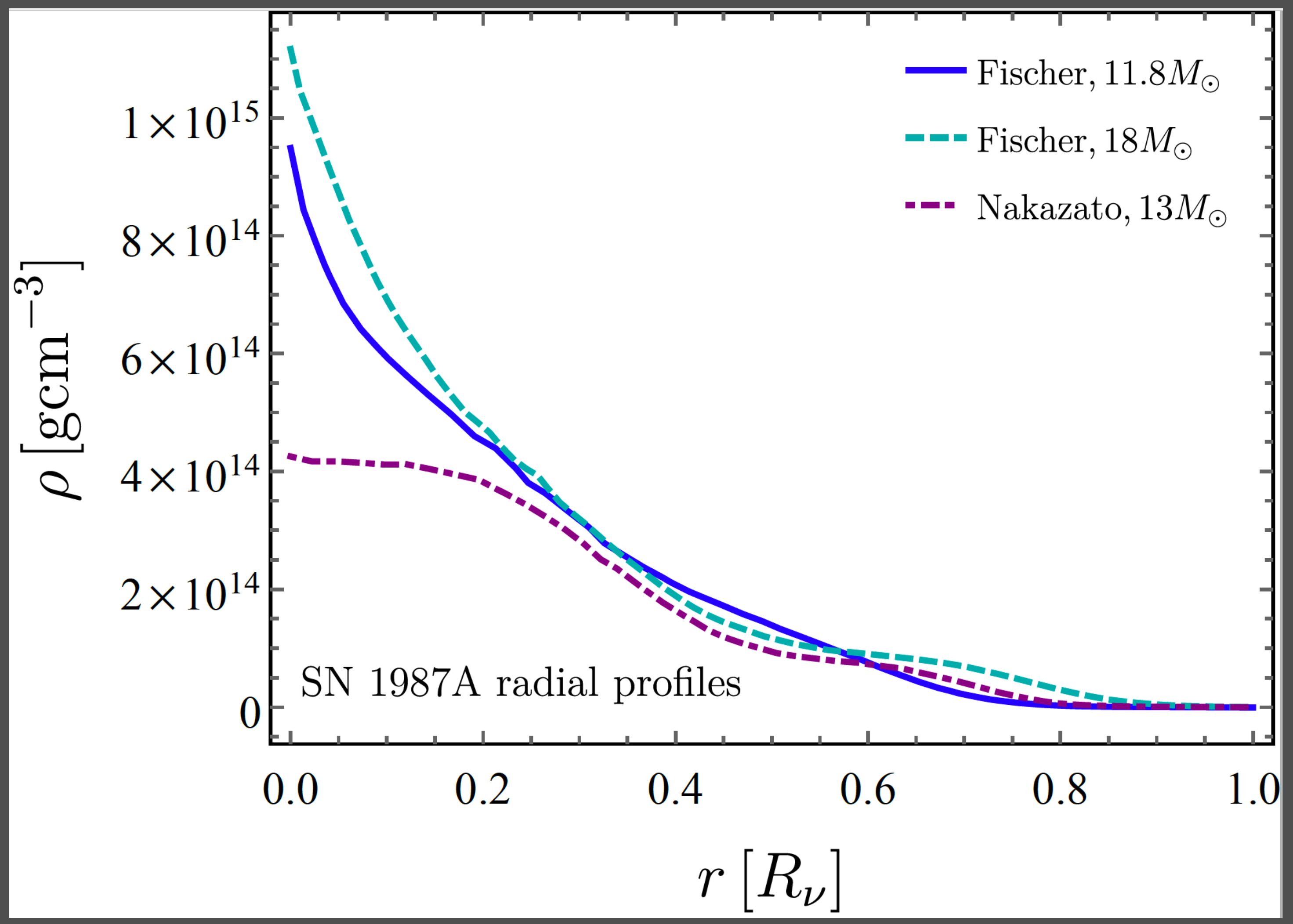

- Additional observations of core collapse could provide improved understanding of the nature of supernova cores in the future.

SN1987A RADIAL PROFILES

Neutrinosphere R_ν

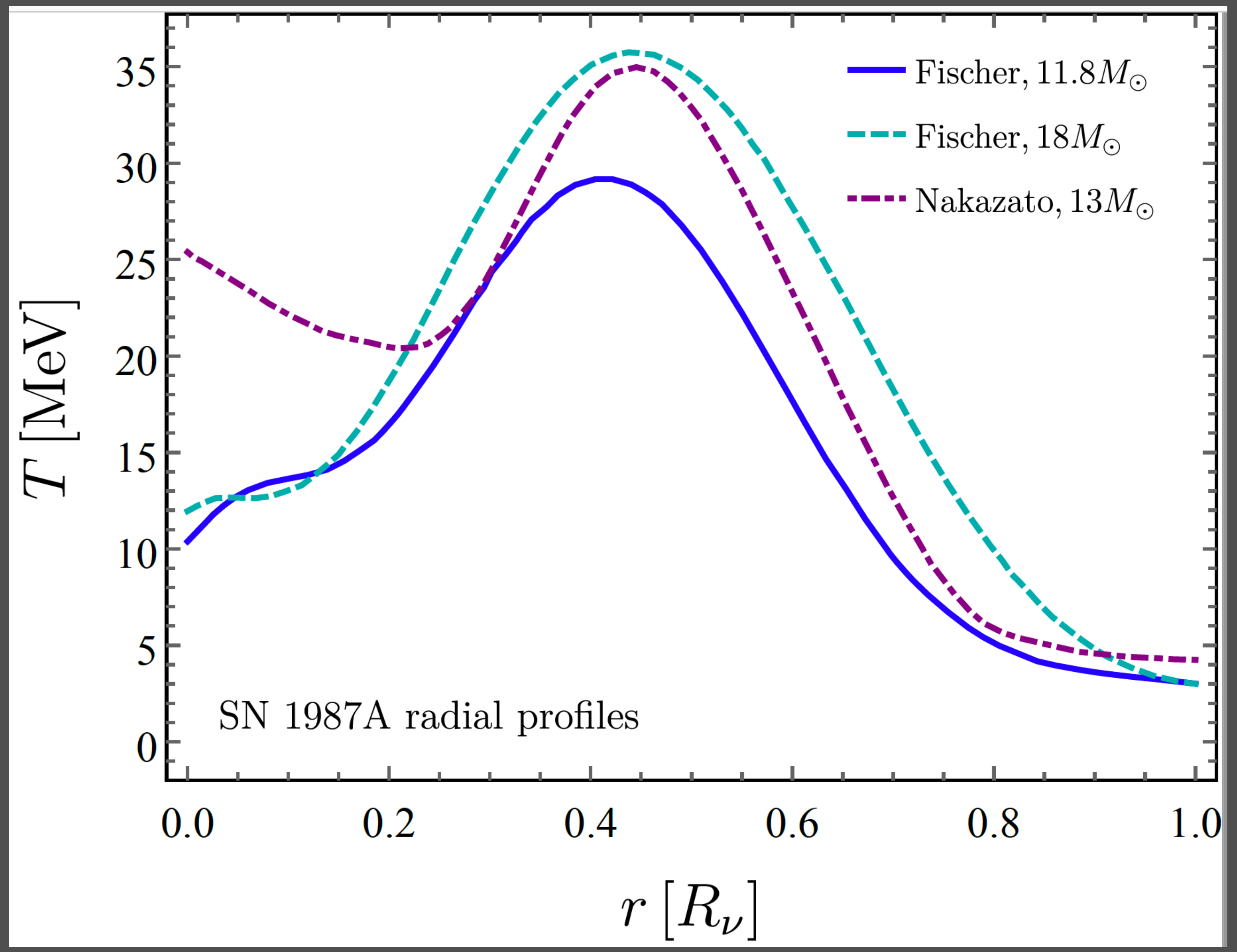

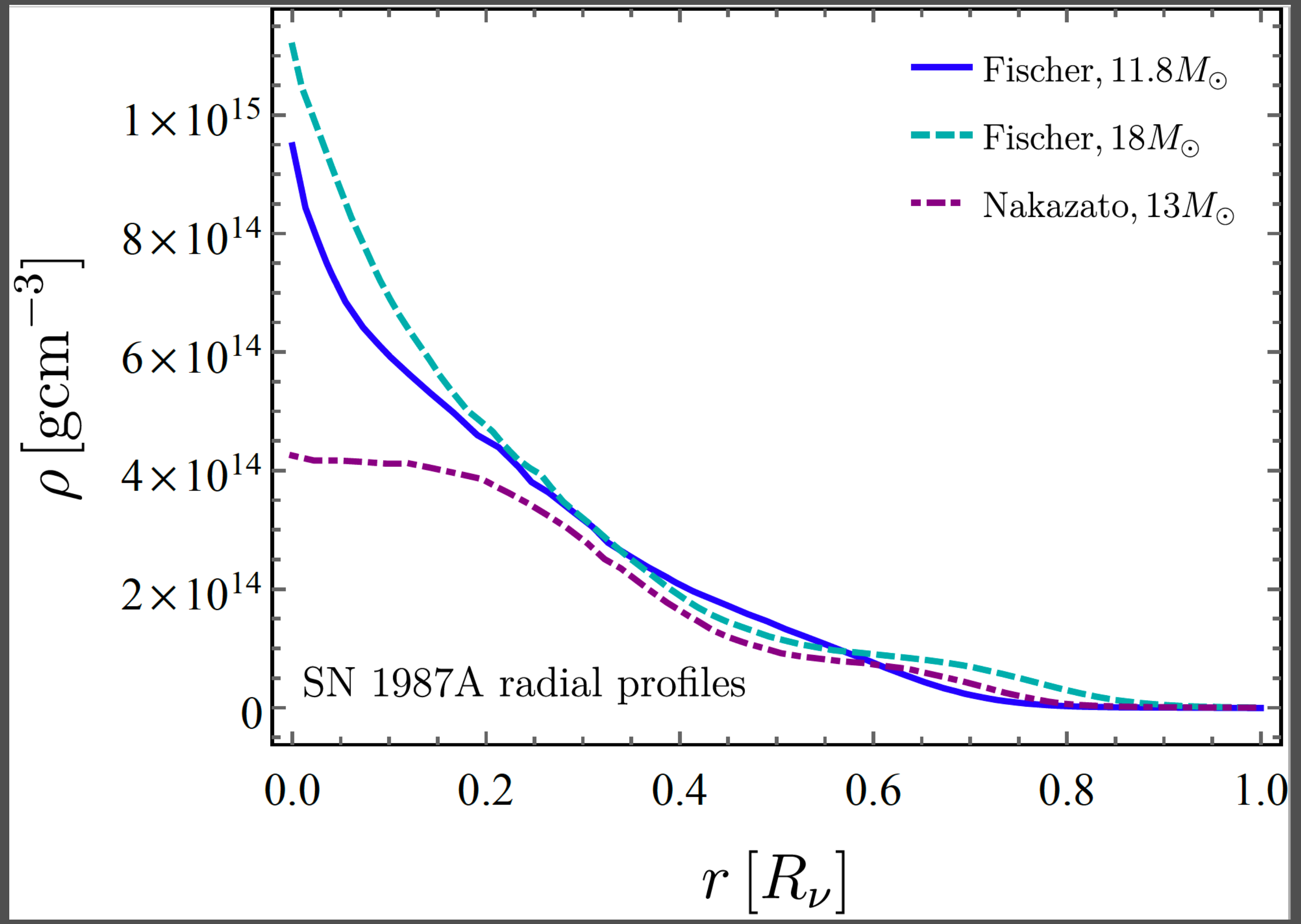

- The production and absorption of S in the supernova core depend both on the baryon density $\rho(r)$ and temperature $T(r)$

- We make the following assumptions

1. Neglect the production of S beyond the neutrinosphere R_ν
2. Assuming the scalar S can stream freely outside the neutrinosphere R_ν without being absorbed.
3. Treat protons and neutrons (nucleons) as being essentially the same

SN1987A RADIAL PROFILES

- 24.9 km (Fischer $11.8\,M_\odot$)

Neutrinosphere R_ν

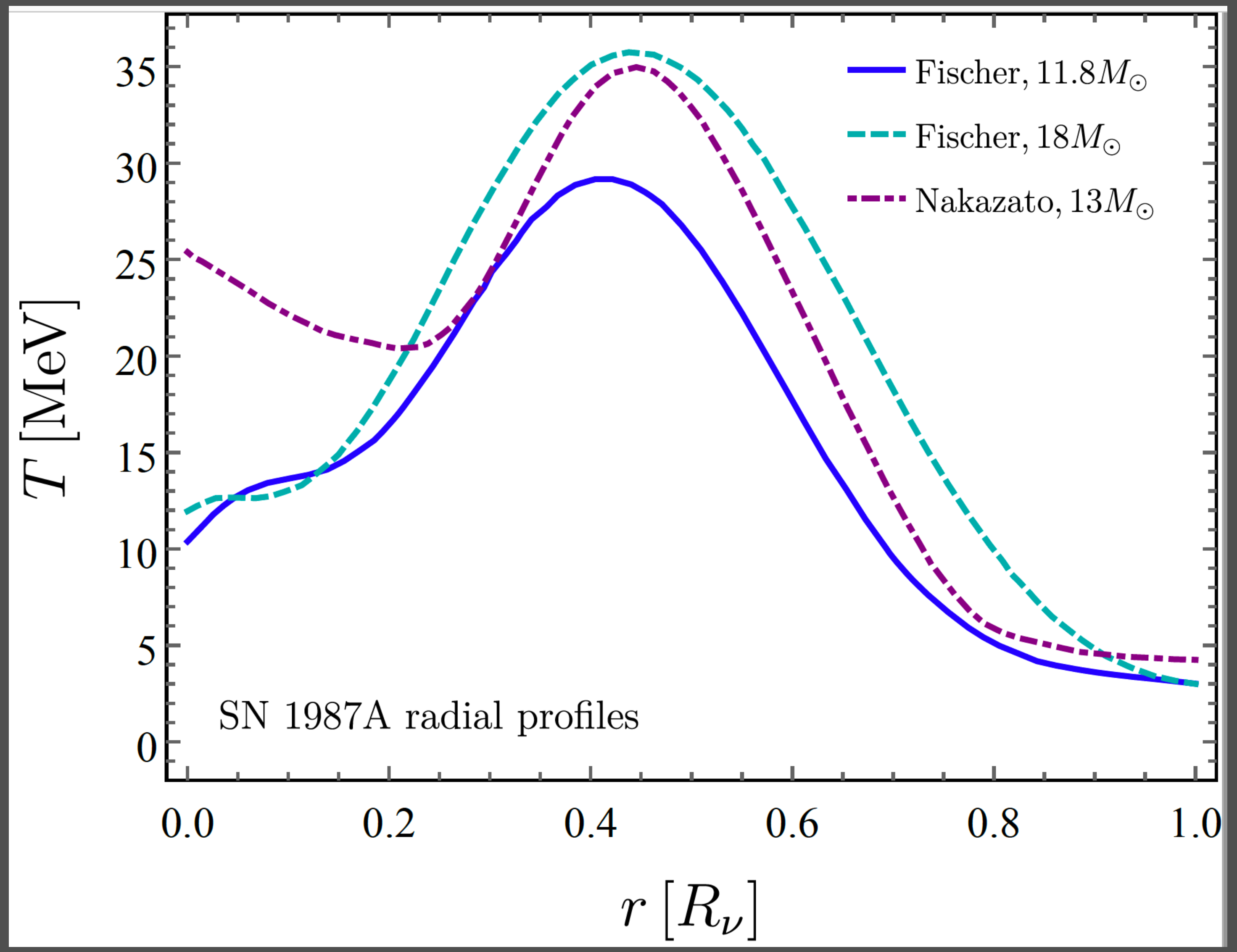

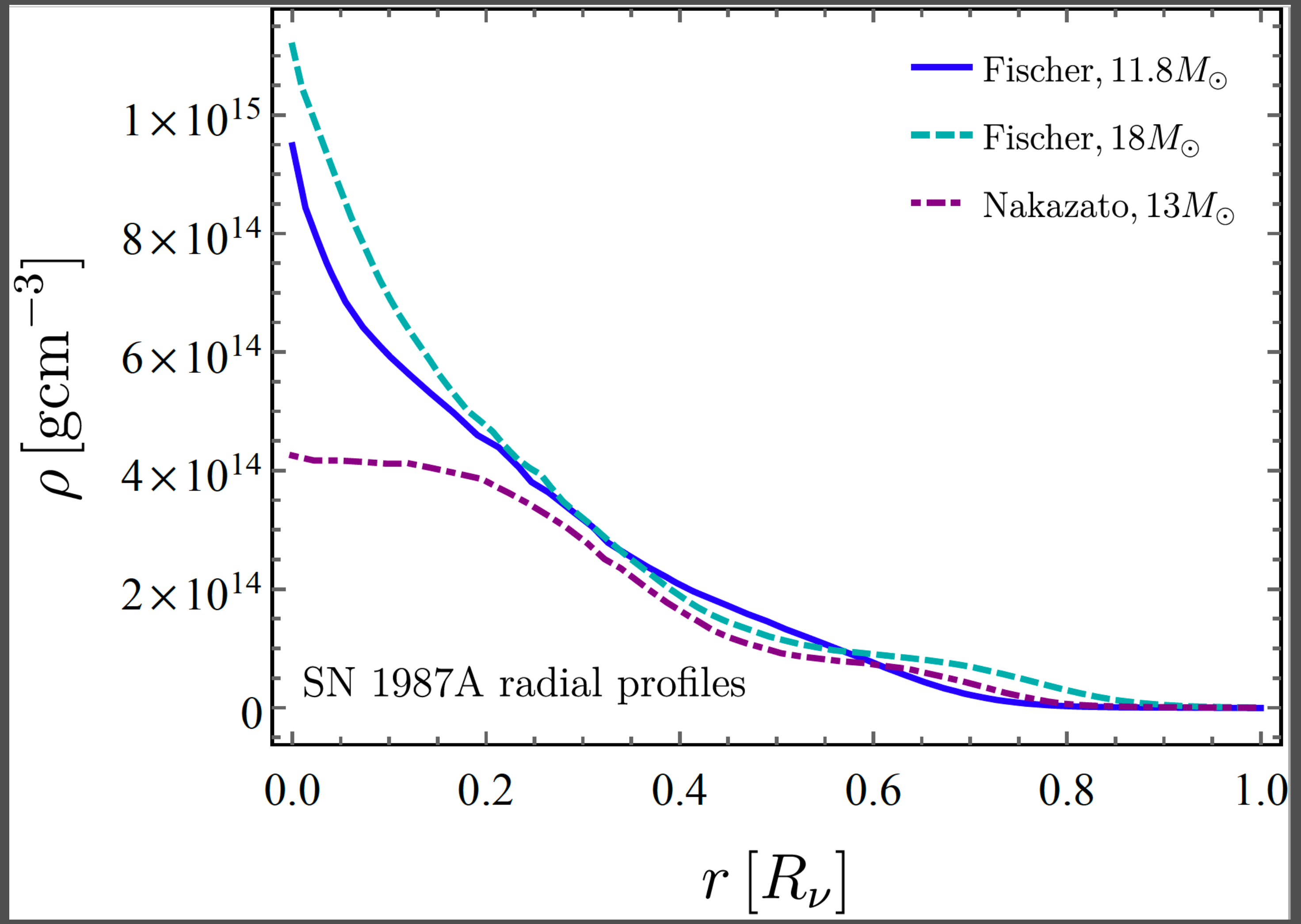

- The production and absorption of S in the supernova core depend both on the baryon density $\rho(r)$ and temperature $T(r)$

- We make the following assumptions

1. Neglect the production of S beyond the neutrinosphere R_ν
2. Assuming the scalar S can stream freely outside the neutrinosphere R_ν without being absorbed.
3. Treat protons and neutrons (nucleons) as being essentially the same

SN1987A RADIAL PROFILES

Neutrinosphere R_ν

- 24.9 km (Fischer $11.8\,M_\odot$)
- 23.6 km (Fischer $18\,M_\odot$)

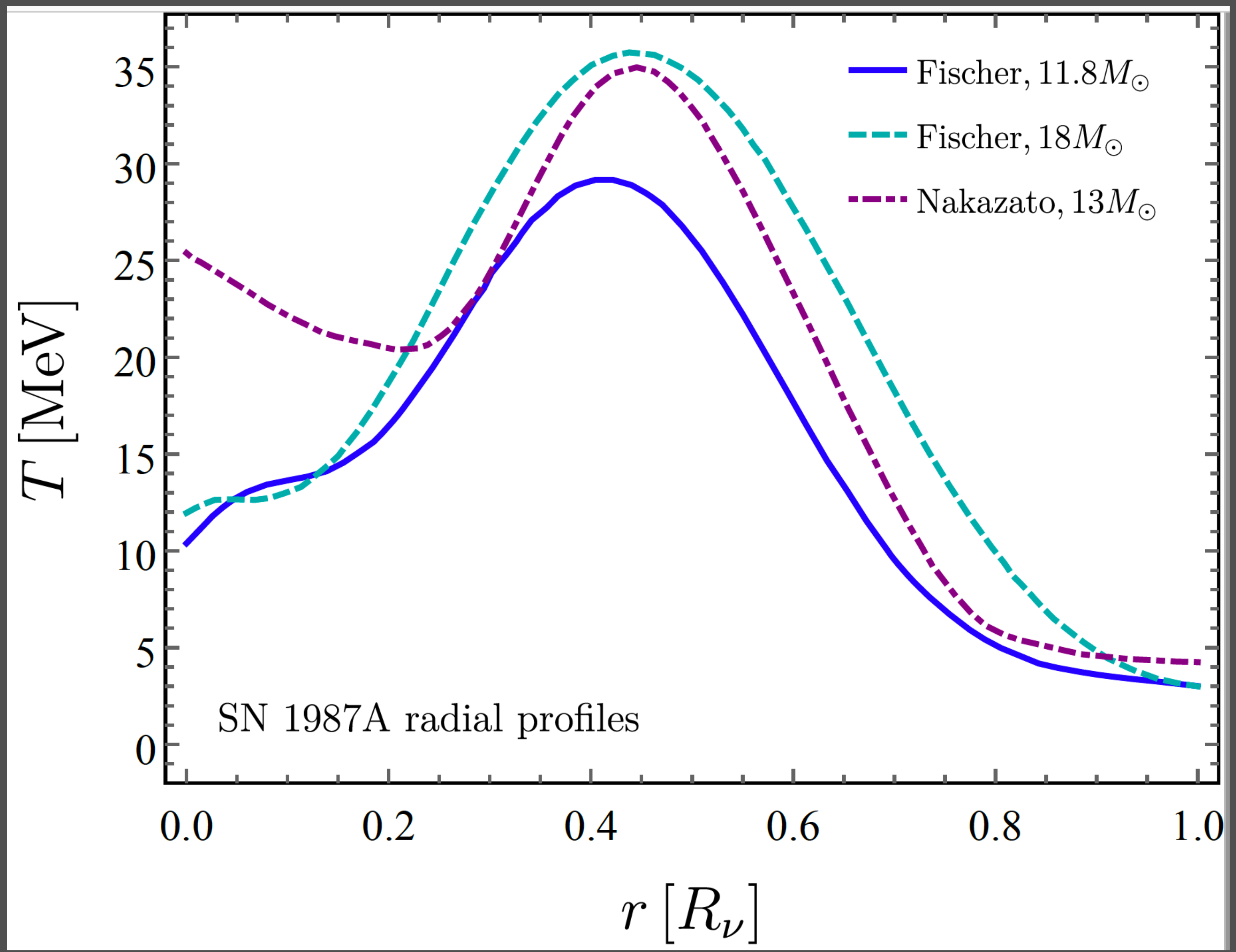

- The production and absorption of S in the supernova core depend both on the baryon density $\rho(r)$ and temperature $T(r)$

- We make the following assumptions

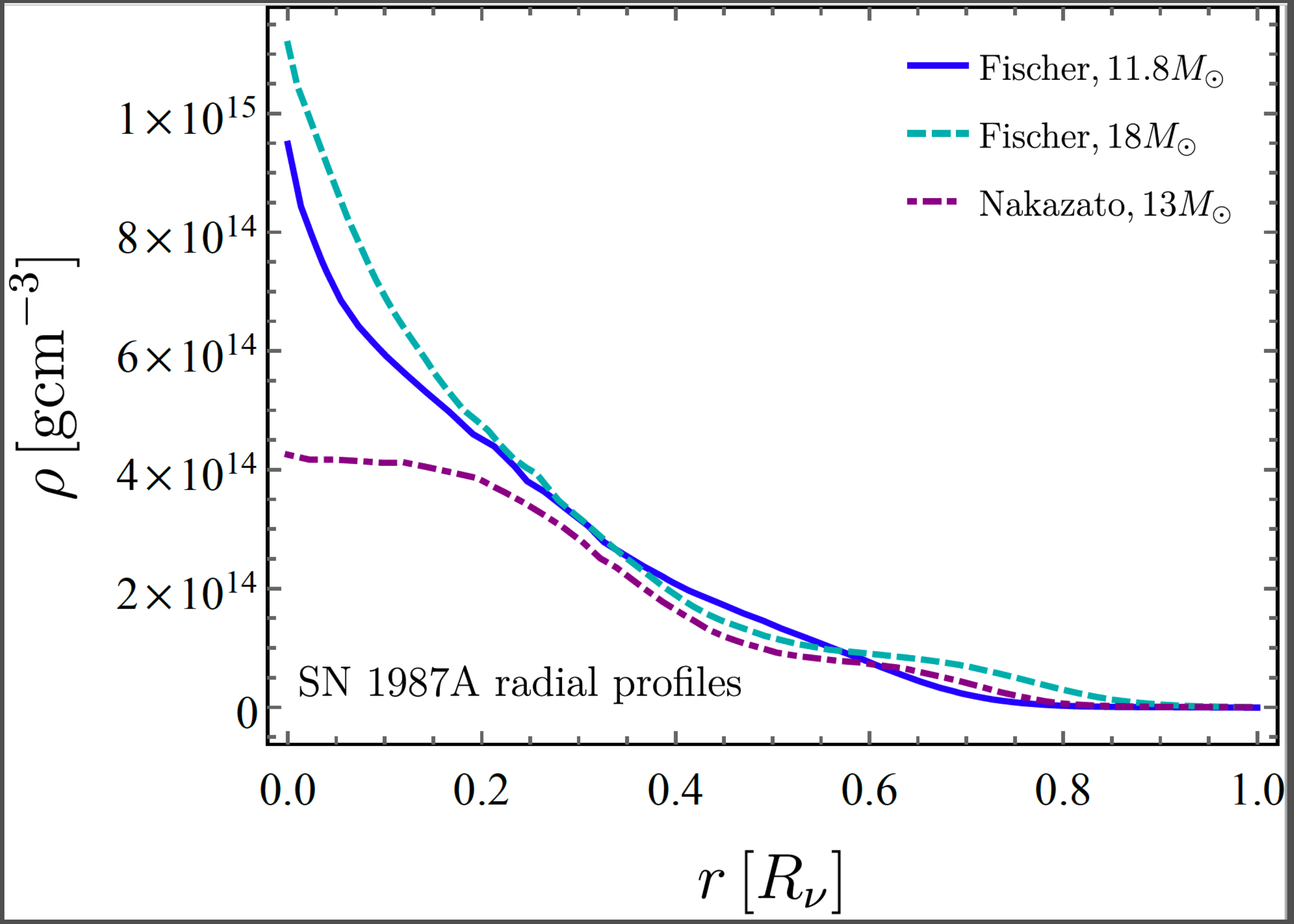

1. Neglect the production of S beyond the neutrinosphere R_ν
2. Assuming the scalar S can stream freely outside the neutrinosphere R_ν without being absorbed.
3. Treat protons and neutrons (nucleons) as being essentially the same

SN1987A RADIAL PROFILES

Neutrinosphere R_ν

- 24.9 km (Fischer $11.8\,M_\odot$)
- 23.6 km (Fischer $18\,M_\odot$)
- 25.6 km (Nakazato $13\,M_\odot$)

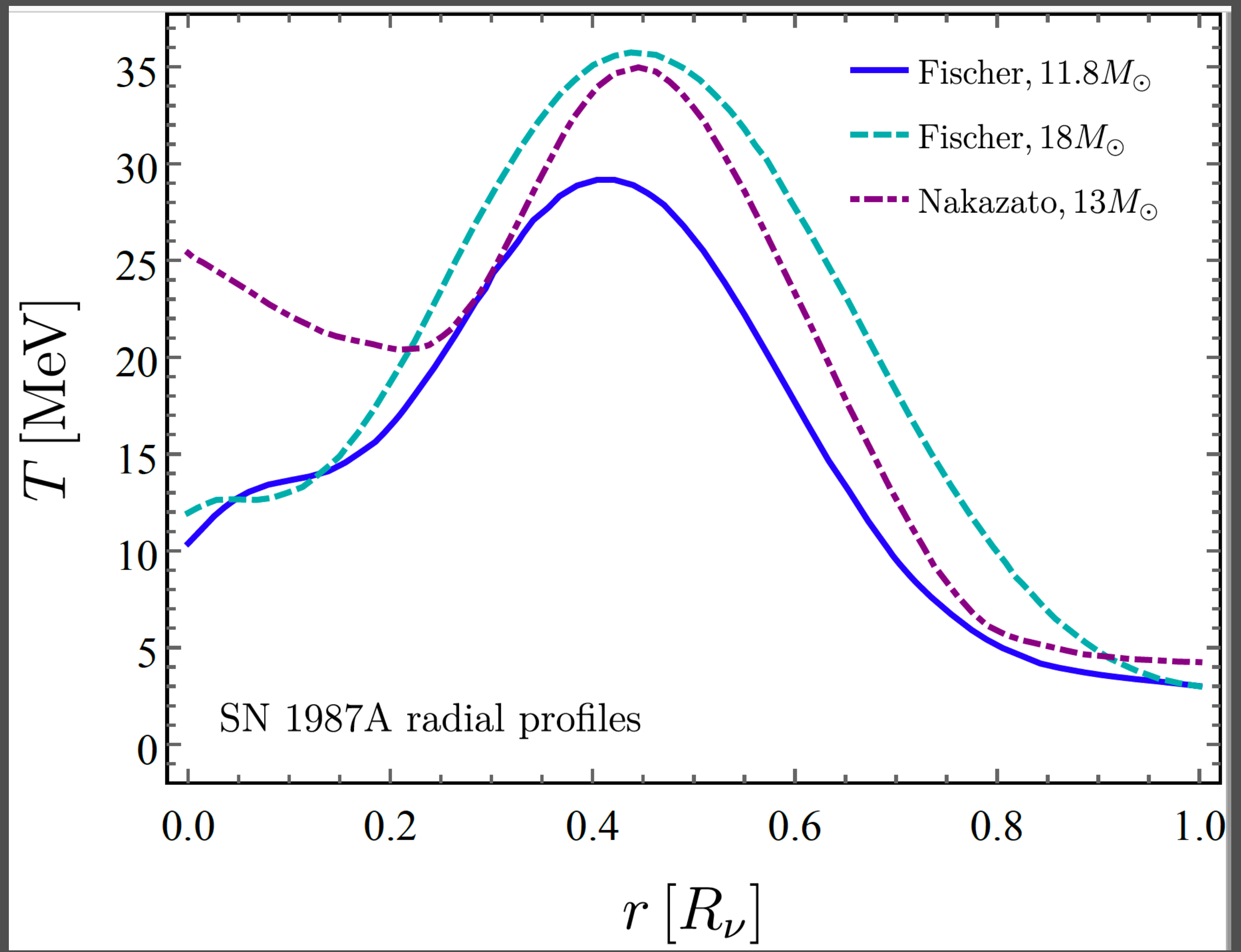

- The production and absorption of S in the supernova core depend both on the baryon density $\rho(r)$ and temperature $T(r)$

- We make the following assumptions

1. Neglect the production of S beyond the neutrinosphere R_ν
2. Assuming the scalar S can stream freely outside the neutrinosphere R_ν without being absorbed.
3. Treat protons and neutrons (nucleons) as being essentially the same

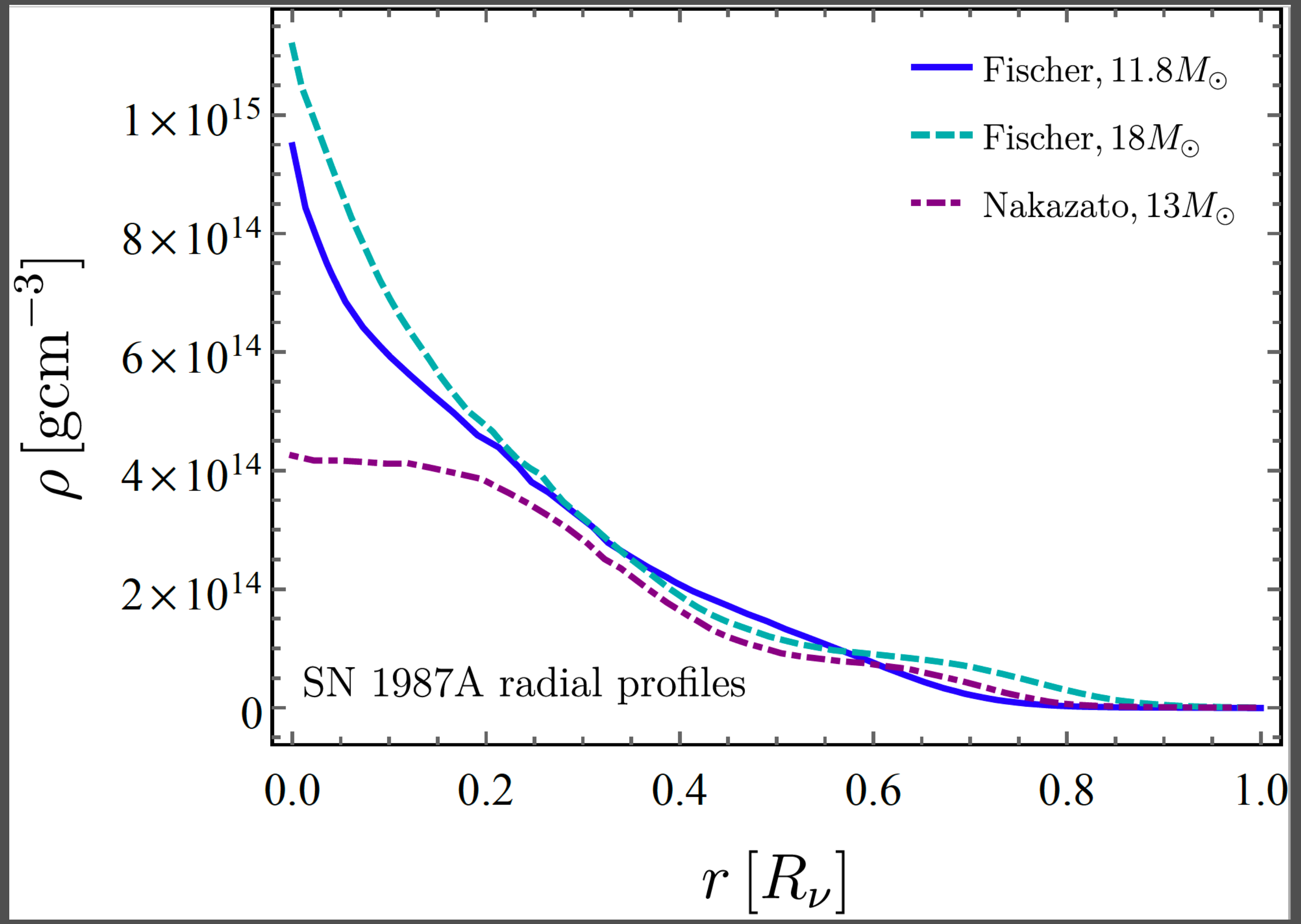

SN1987A RADIAL PROFILES

Neutrinosphere R_ν

- 24.9 km (Fischer $11.8\,M_\odot$)
- 23.6 km (Fischer $18\,M_\odot$)
- 25.6 km (Nakazato $13\,M_\odot$)

core radius R_c

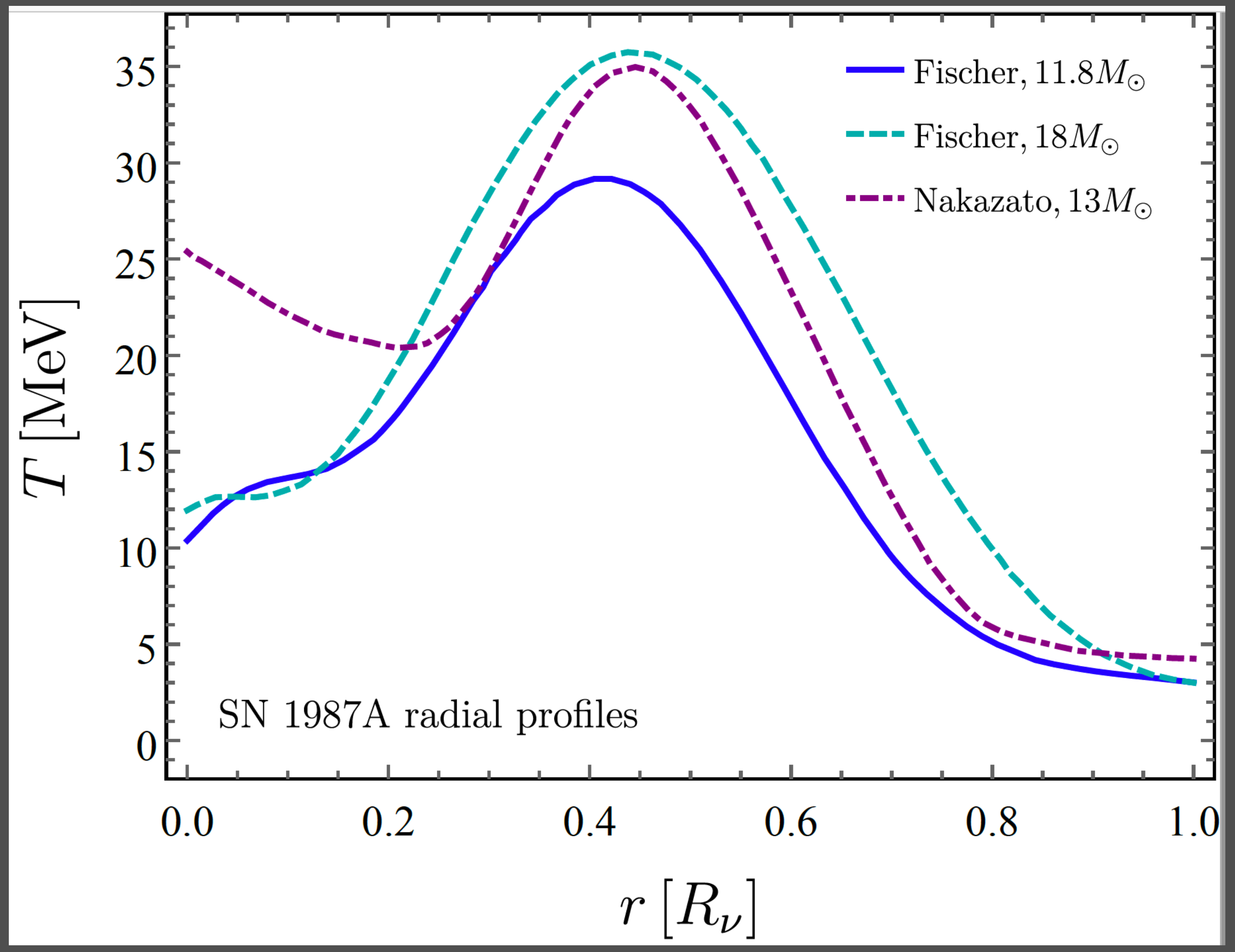

- The production and absorption of S in the supernova core depend both on the baryon density $\rho(r)$ and temperature $T(r)$

- We make the following assumptions

1. Neglect the production of S beyond the neutrinosphere R_ν
2. Assuming the scalar S can stream freely outside the neutrinosphere R_ν without being absorbed.
3. Treat protons and neutrons (nucleons) as being essentially the same

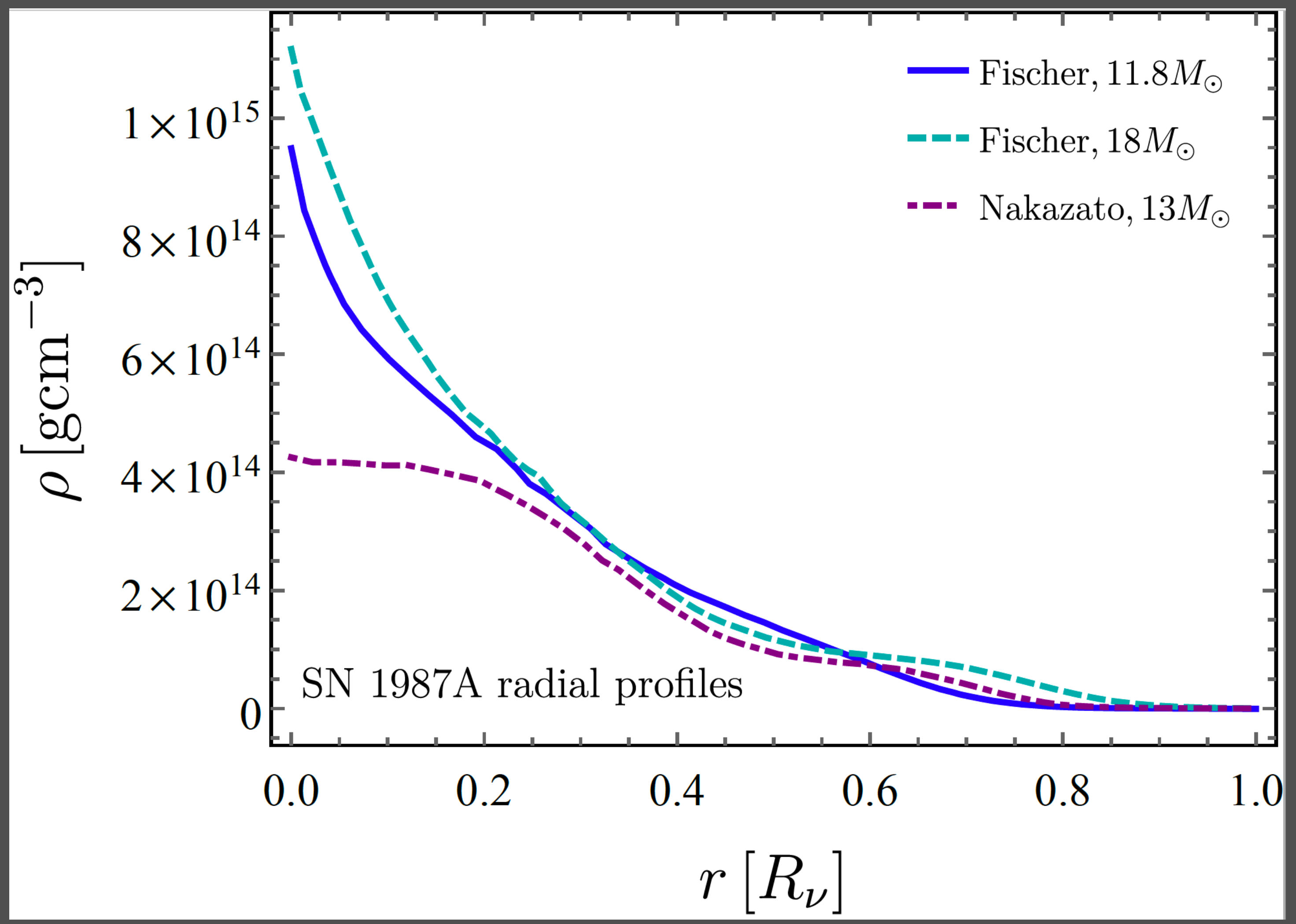

SN1987A RADIAL PROFILES

Neutrinosphere R_ν

- 24.9 km (Fischer $11.8\,M_\odot$)
- 23.6 km (Fischer $18\,M_\odot$)
- 25.6 km (Nakazato $13\,M_\odot$)

10 km

core radius R_c

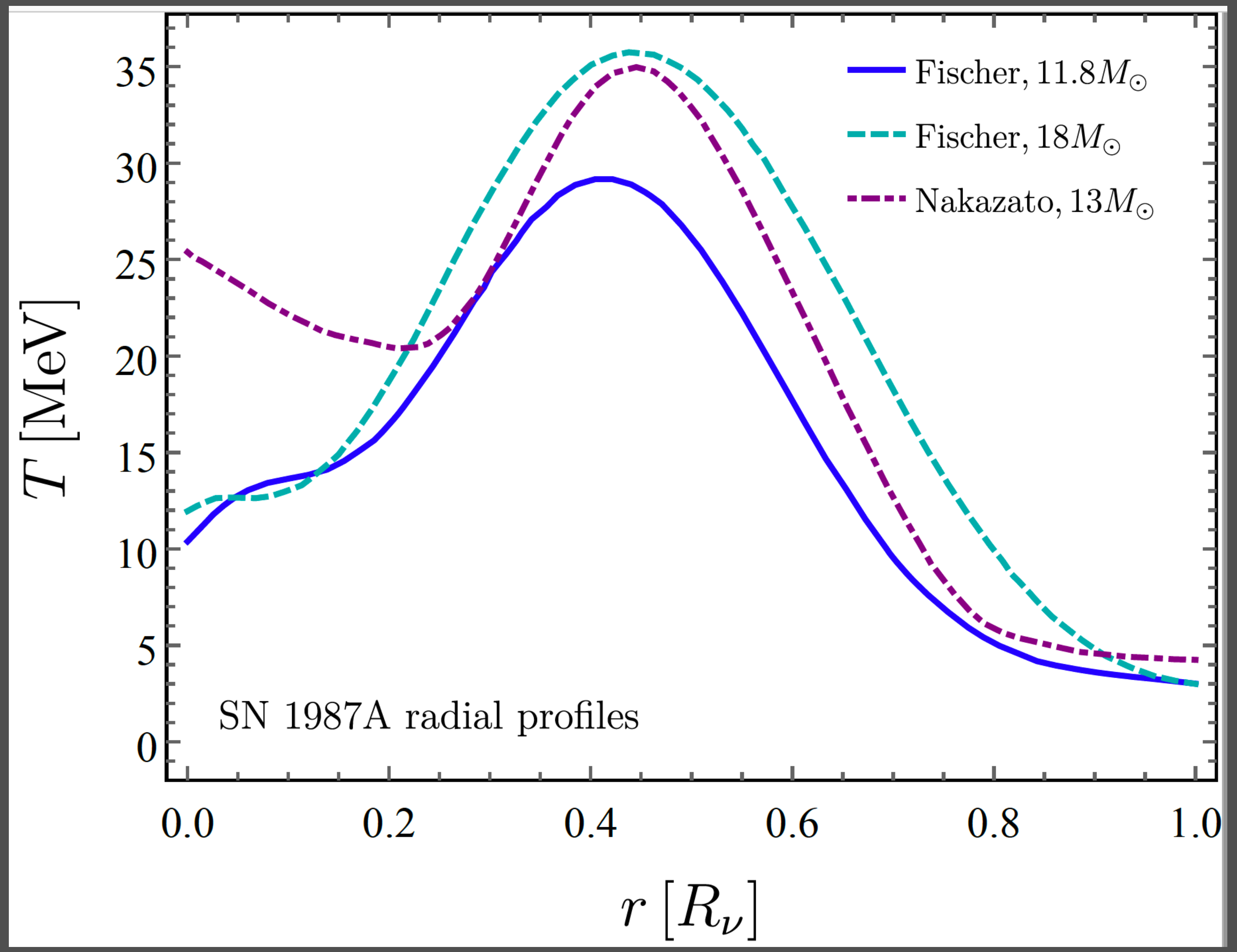

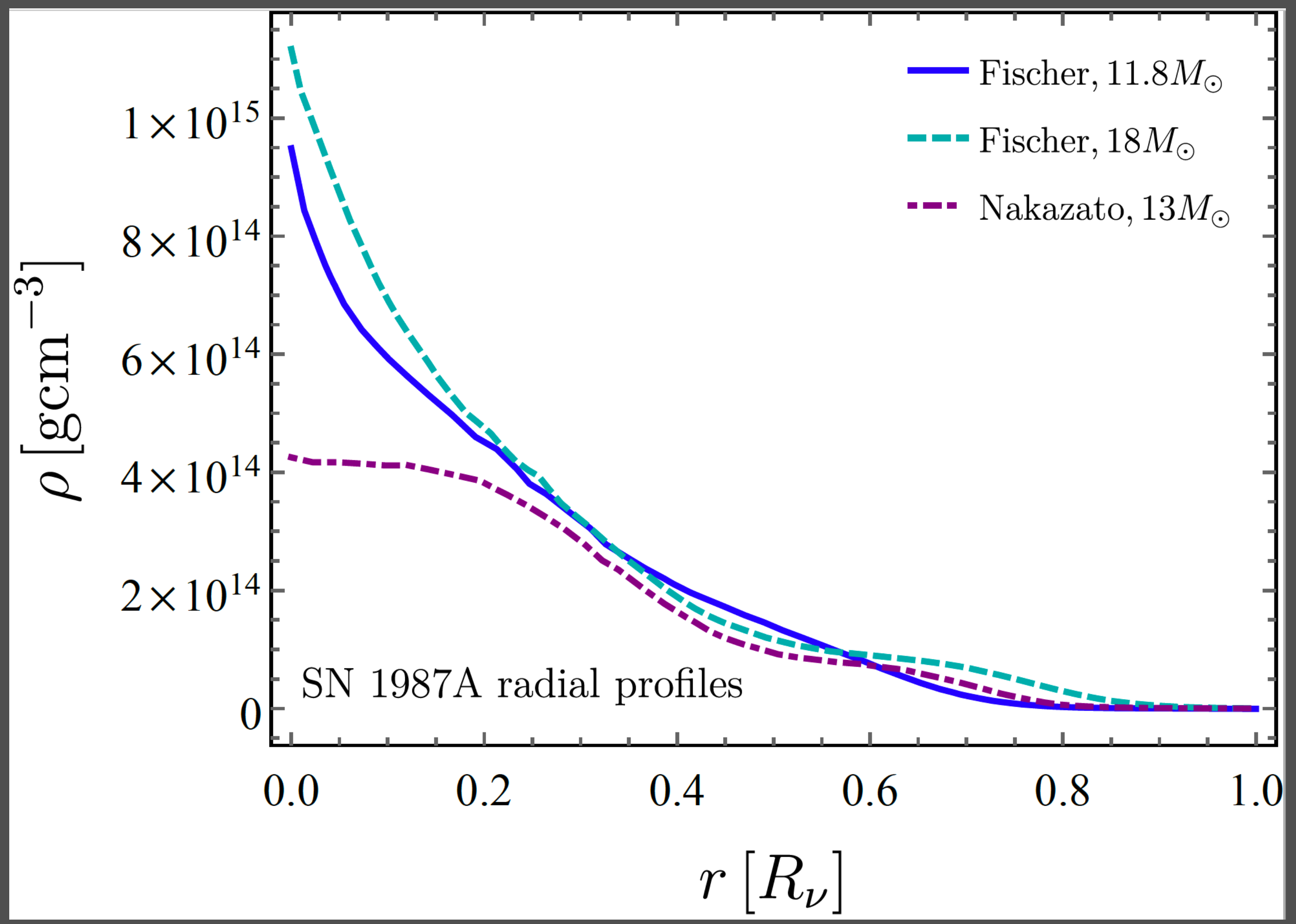

- The production and absorption of S in the supernova core depend both on the baryon density $\rho(r)$ and temperature $T(r)$
- We make the following assumptions

1. Neglect the production of S beyond the neutrinosphere R_ν
2. Assuming the scalar S can stream freely outside the neutrinosphere R_ν without being absorbed.
3. Treat protons and neutrons (nucleons) as being essentially the same

SN1987A RADIAL PROFILES

Neutrinosphere R_ν

- 24.9 km (Fischer $11.8\,M_\odot$) 10 km
- 23.6 km (Fischer $18\,M_\odot$) 11 km
- 25.6 km (Nakazato $13\,M_\odot$)

core radius R_c

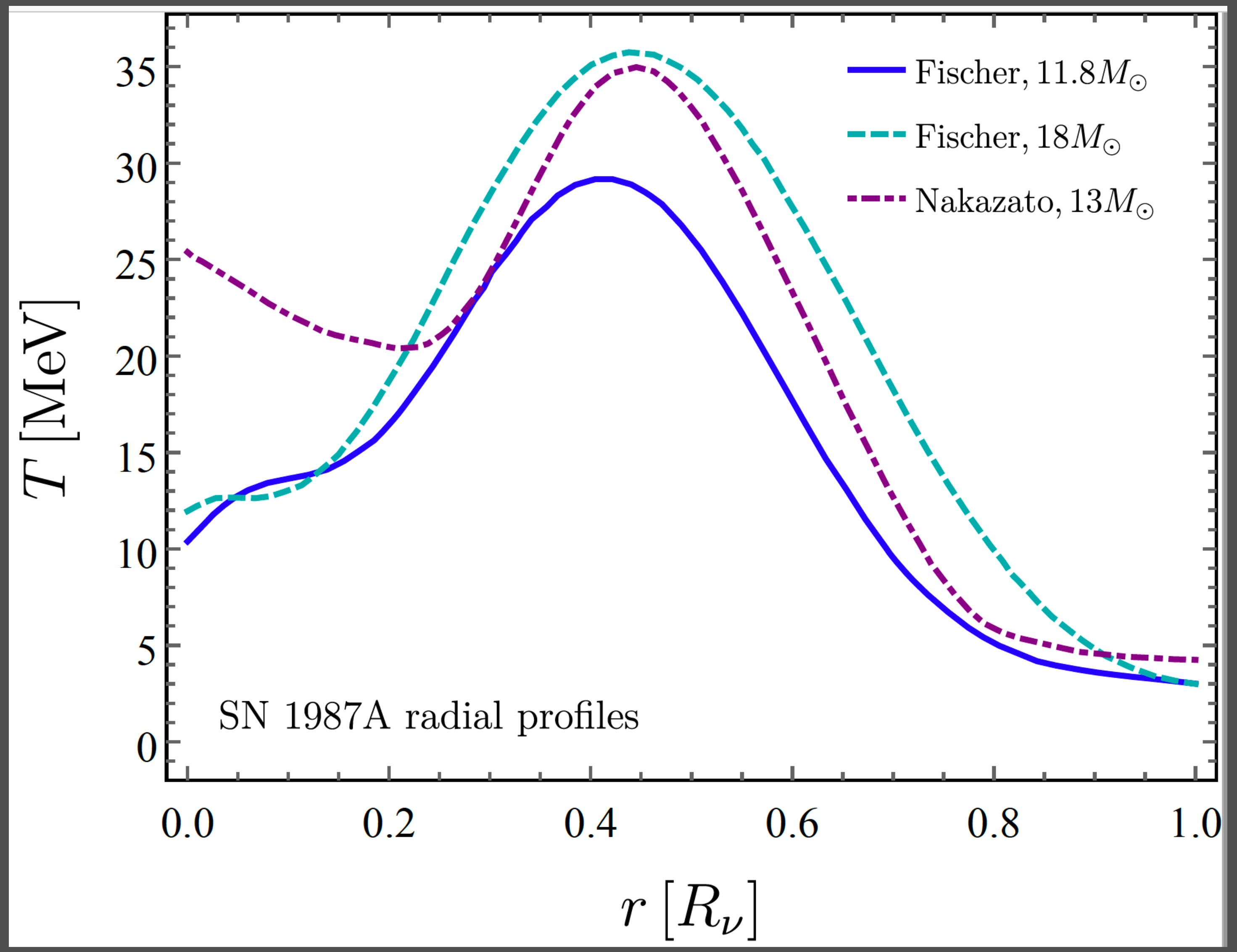

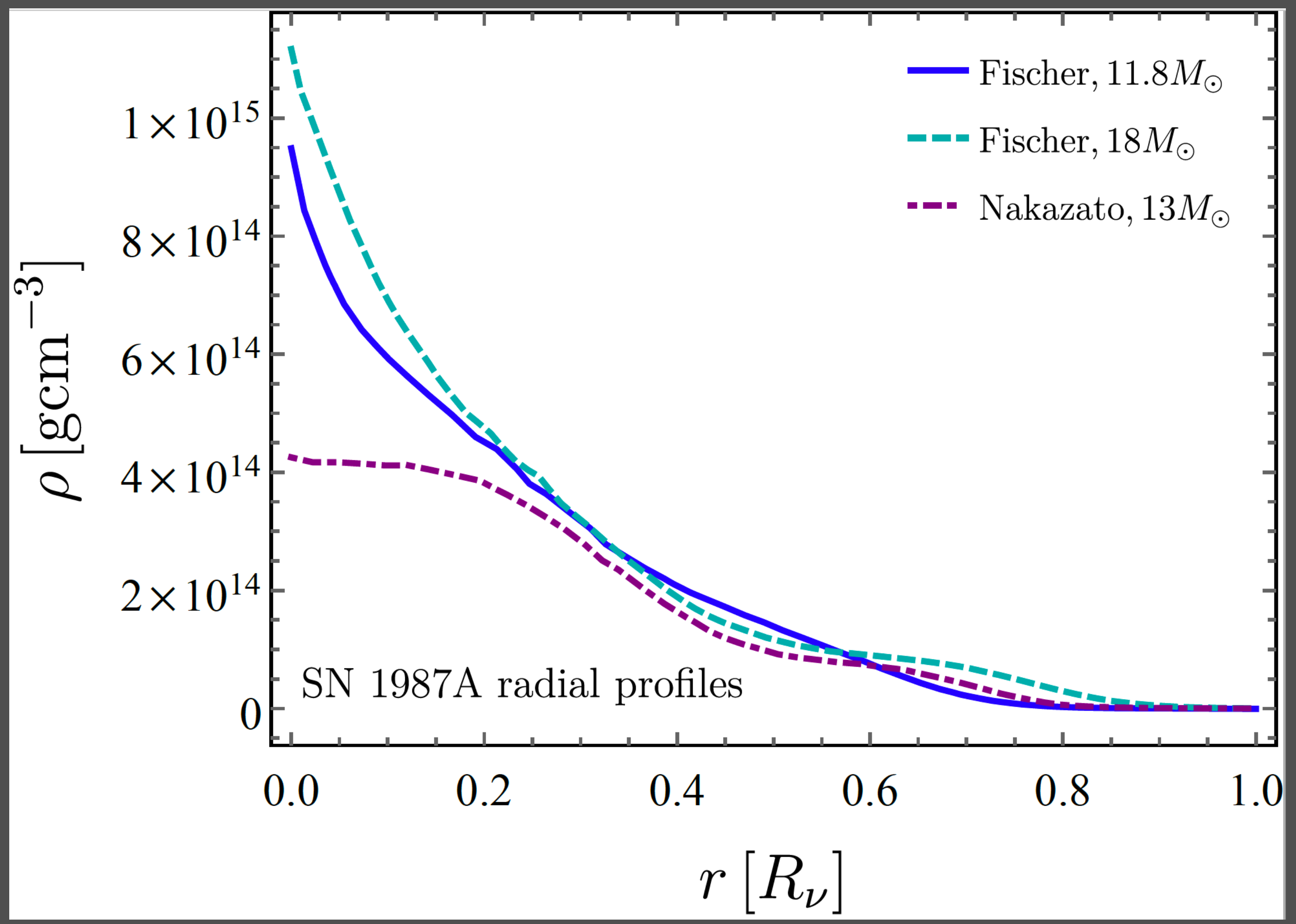

- The production and absorption of S in the supernova core depend both on the baryon density $\rho(r)$ and temperature $T(r)$
- We make the following assumptions

1. Neglect the production of S beyond the neutrinosphere R_ν
2. Assuming the scalar S can stream freely outside the neutrinosphere R_ν without being absorbed.
3. Treat protons and neutrons (nucleons) as being essentially the same

SN1987A RADIAL PROFILES

Neutrinosphere R_ν → core radius R_c

- 24.9 km (Fischer $11.8\,M_\odot$) — 10 km
- 23.6 km (Fischer $18\,M_\odot$) — 11 km
- 25.6 km (Nakazato $13\,M_\odot$) — 13 km

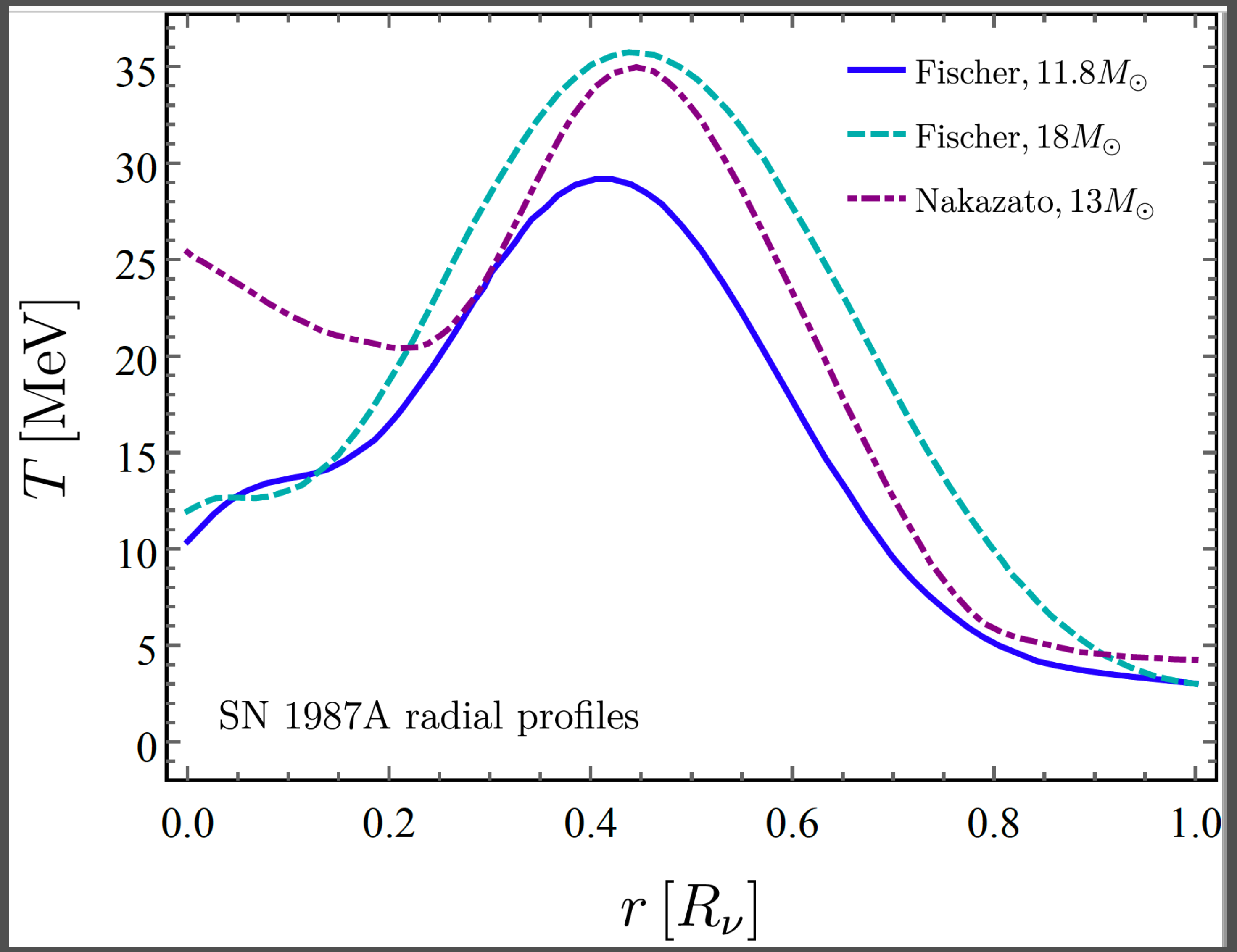

- The production and absorption of S in the supernova core depend both on the baryon density $\rho(r)$ and temperature $T(r)$

- We make the following assumptions

1. Neglect the production of S beyond the neutrinosphere R_ν
2. Assuming the scalar S can stream freely outside the neutrinosphere R_ν without being absorbed.
3. Treat protons and neutrons (nucleons) as being essentially the same

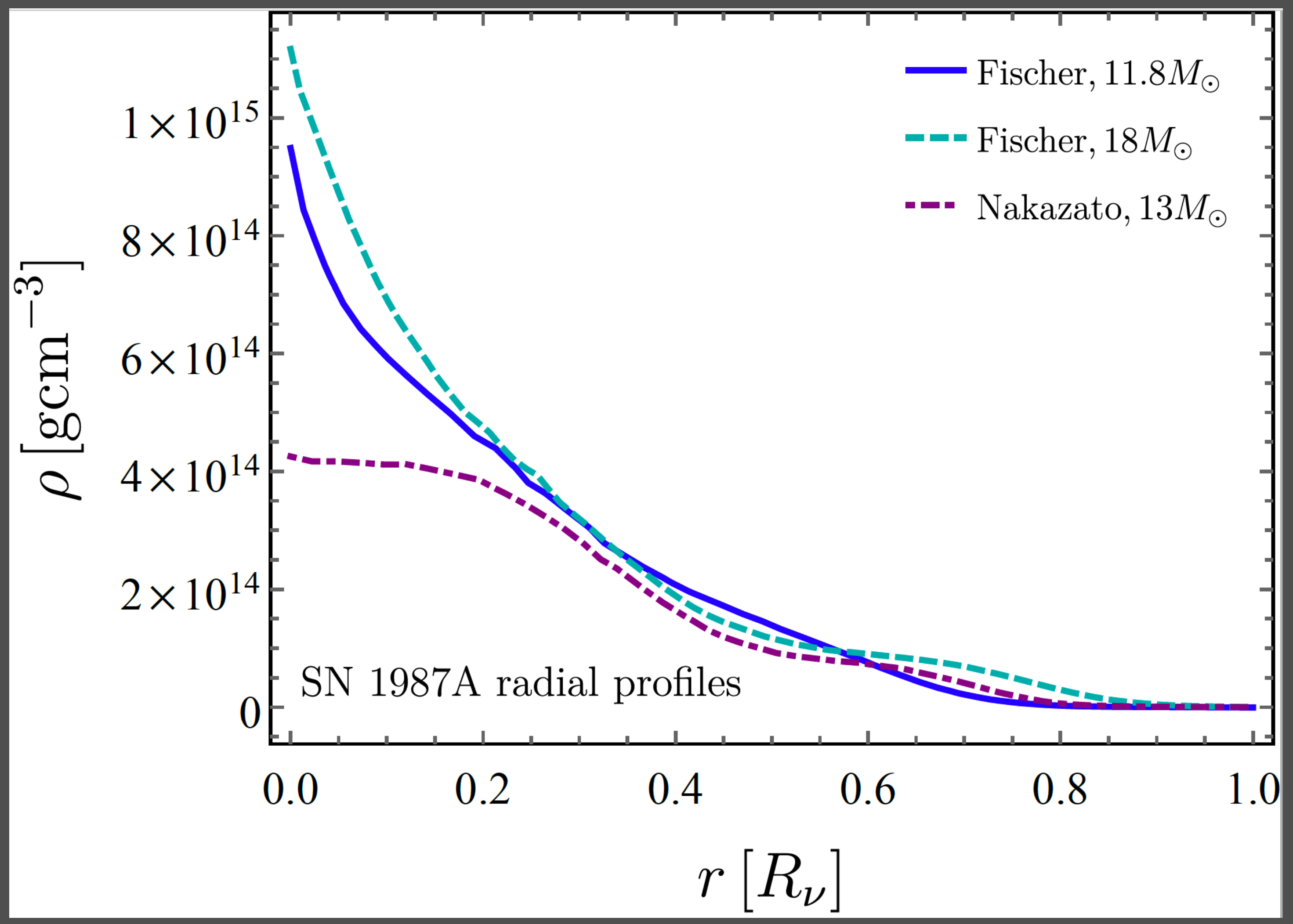

ENERGY LOSS DUE TO LIGHT SCALAR

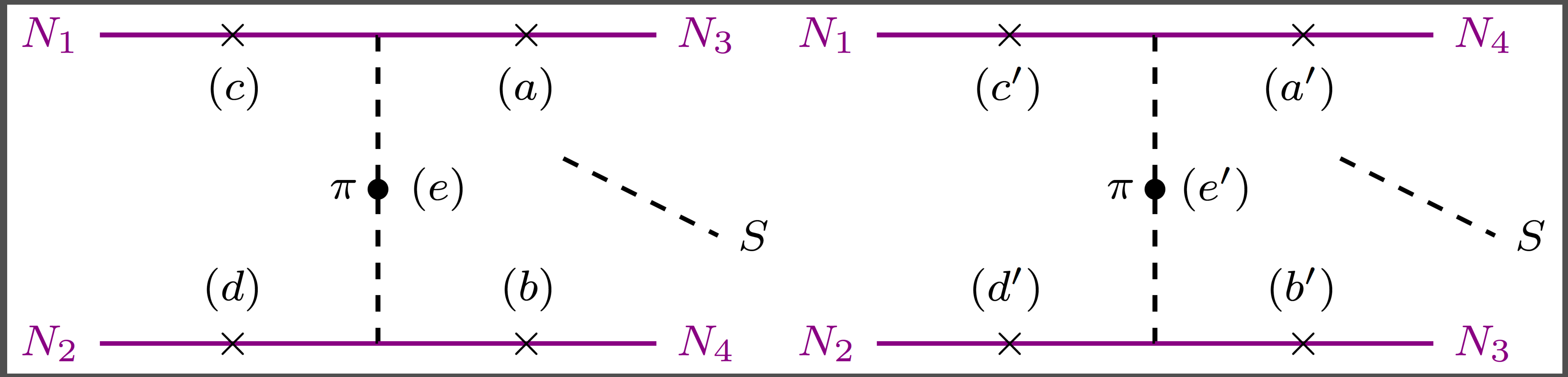

$$\mathcal{L} = \sin\theta S \left[y_{hNN}\overline{N}N + A_\pi(\pi^0\pi^0 + \pi^+\pi^-)\right]$$

ENERGY LOSS DUE TO LIGHT SCALAR

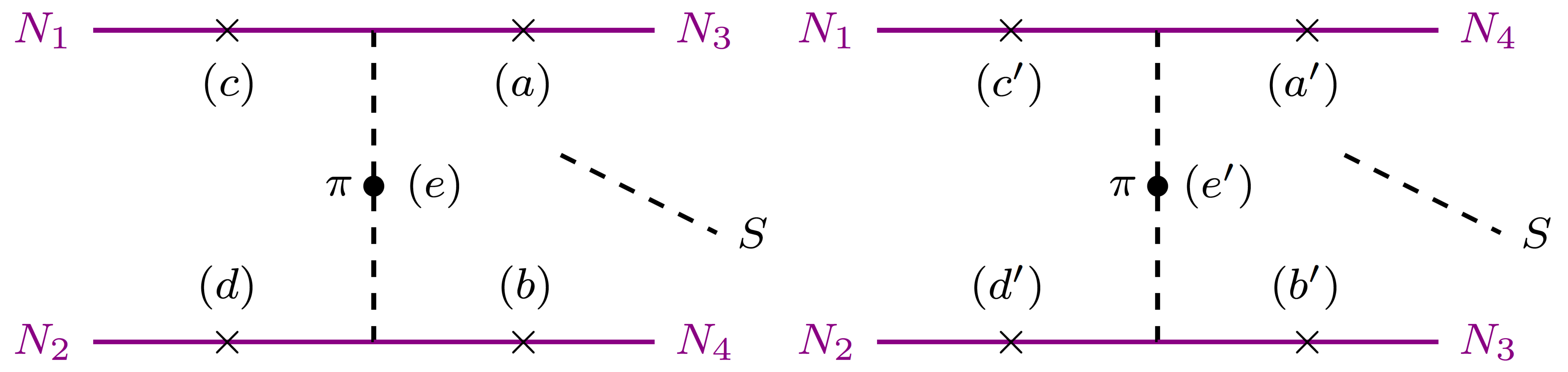

$$\mathcal{L} = \sin\theta S \left[\boxed{y_{hNN}} \overline{N} N + A_\pi (\pi^0\pi^0 + \pi^+\pi^-) \right]$$

effective coupling of
SM Higgs to nucleons
$\simeq 10^{-3}$

ENERGY LOSS DUE TO LIGHT SCALAR

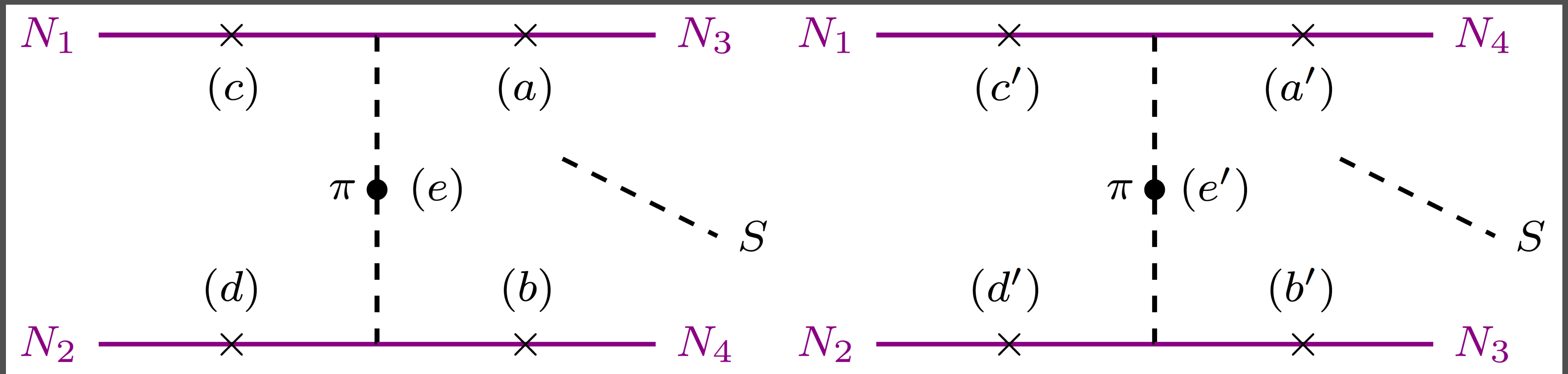

$$\mathcal{L} = \sin\theta S \left[y_{hNN} \overline{N} N + A_\pi (\pi^0 \pi^0 + \pi^+ \pi^-) \right]$$

effective coupling of
SM Higgs to nucleons
$\simeq 10^{-3}$

effective coupling of S to pions
from chiral perturbation theory

$$A_\pi = \frac{2}{9 v_{\rm EW}} \left(m_S^2 + \frac{11}{2} m_\pi^2 \right)$$

ENERGY LOSS DUE TO LIGHT SCALAR

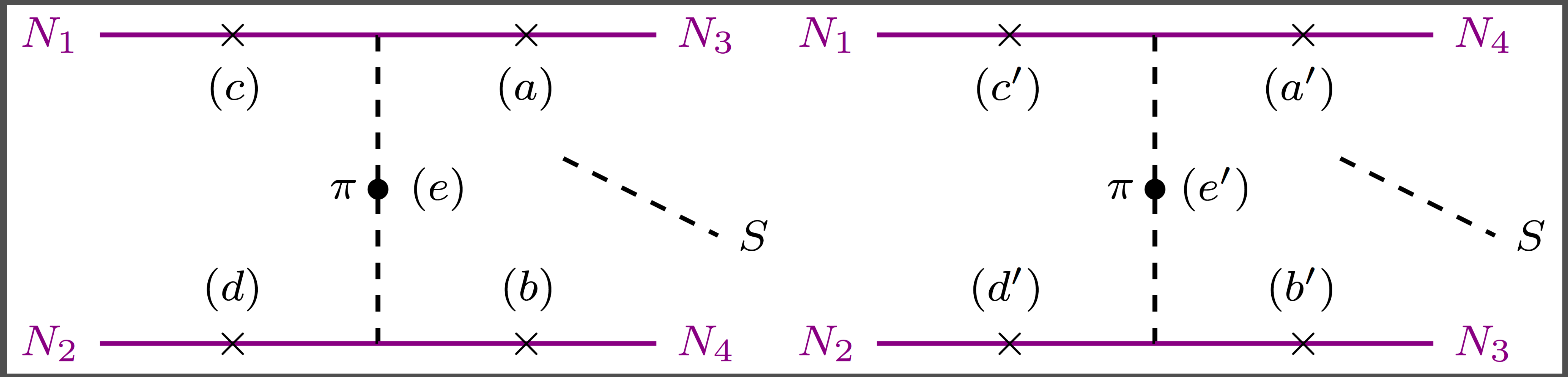

$$\mathcal{L} = \sin\theta S\left[y_{hNN}\overline{N}N + A_\pi(\pi^0\pi^0 + \pi^+\pi^-)\right]$$

effective coupling of SM Higgs to nucleons $\simeq 10^{-3}$

effective coupling of S to pions from chiral perturbation theory

$$A_\pi = \frac{2}{9v_{\mathrm{EW}}}\left(m_S^2 + \frac{11}{2}m_\pi^2\right)$$

In the supernova core, the production of scalar S is dominated by the nucleon bremsstrahlung process

$$N + N \to N + N + S$$

ENERGY LOSS DUE TO LIGHT SCALAR

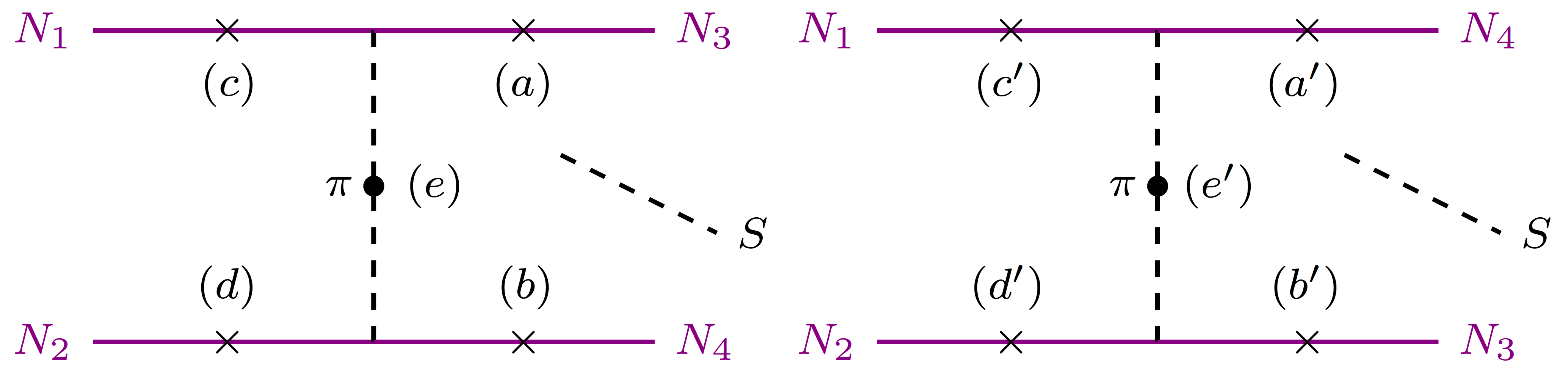

$$\mathcal{L} = \sin\theta S \left[y_{hNN}\overline{N}N + A_\pi(\pi^0\pi^0 + \pi^+\pi^-)\right]$$

effective coupling of SM Higgs to nucleons $\simeq 10^{-3}$

effective coupling of S to pions from chiral perturbation theory

$$\mathcal{A}_\pi = \frac{2}{9v_{\rm EW}}\left(m_S^2 + \frac{11}{2}m_\pi^2\right)$$

In the supernova core, the production of scalar S is dominated by the nucleon bremsstrahlung process

$$N + N \to N + N + S$$

Taking into account the couplings of S with both nucleons and the pion mediator, it is found that the contributions from the S-nucleon diagrams are partially canceled out. As a result, the matrix element for the process is dominated by the SNN and $S\pi\pi$ diagrams for the mass ranges of $m_S \gtrsim 10$ MeV and $m_S \lesssim 10$ MeV, respectively.

GEOMETRIC DEPENDENCE

The probability of S to decay and the probability of S to be absorbed before escaping the star depends on the geometry: where it is produced and which direction it takes through the stellar medium

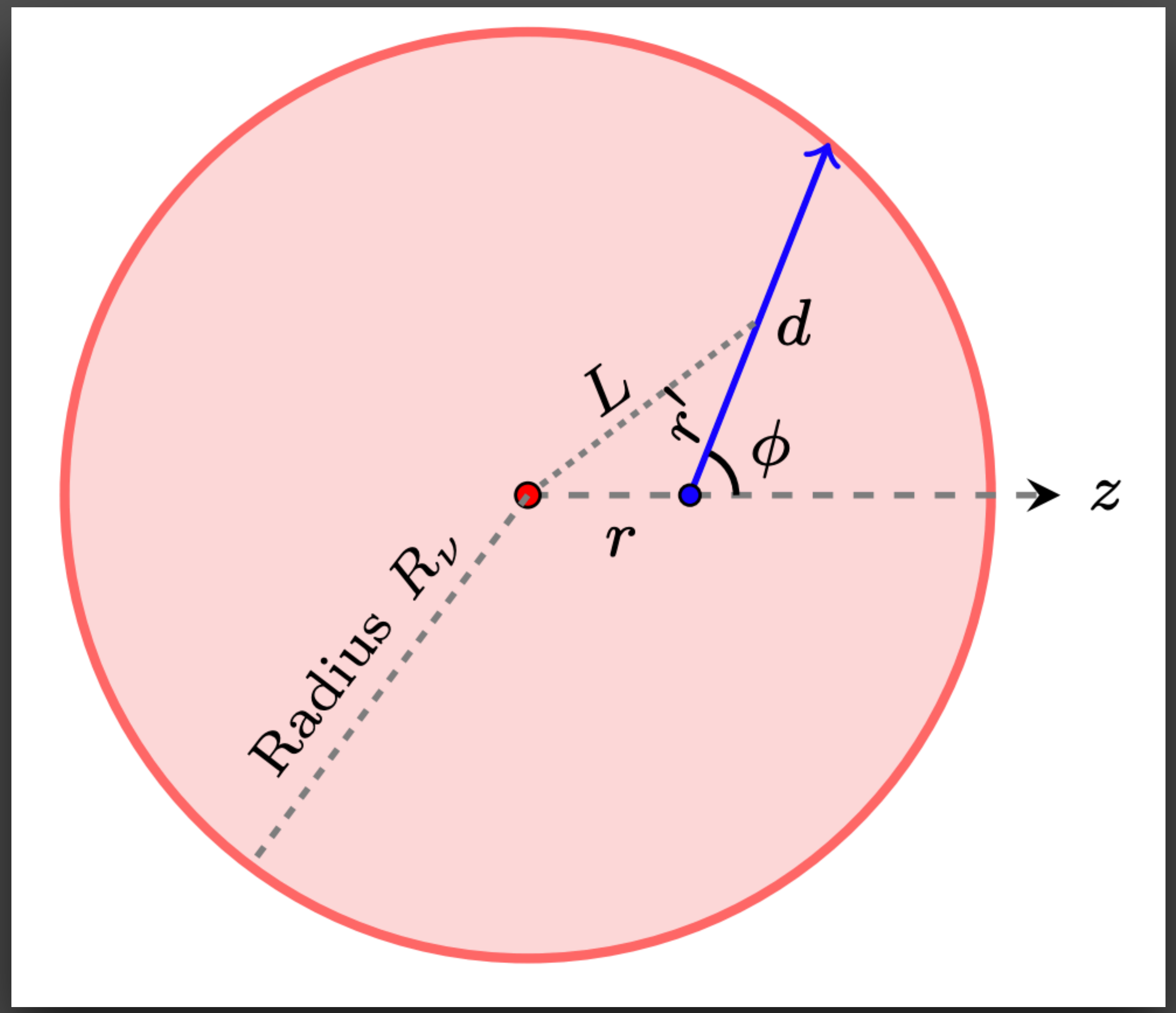

Spherical symmetry:

- The production site of S is determined by the distance r from the core
- Direction of the momentum of S is characterised by the polar angle ϕ

$$d(r,\phi) = \sqrt{R_\star^2 - r^2 \sin^2\phi} - r\cos\phi$$

$$L(r,\phi;r') = \sqrt{r^2 + r'^2 + 2rr'\cos\phi}$$

L varies when the auxiliary parameter r' changes from 0 to d.

We integrate over r' in between 0 to d.

ENERGY EMISSION RATE

$$\mathcal{Q}(r,\,\phi) \;=\; \int \mathrm{d}\Pi_5 \mathcal{S} \sum_{\text{spins}} |\mathcal{M}|^2 (2\pi)^4 \delta^4(p_1 + p_2 - p_3 - p_4 - k_S) E_S f_1 f_2 P_{\text{decay}} P_{\text{abs}}$$

ENERGY EMISSION RATE

$$\mathcal{Q}(r,\,\phi) \;=\; \int \mathrm{d}\Pi_5 \mathcal{S} \sum_{\text{spins}} |\mathcal{M}|^2 (2\pi)^4 \delta^4(p_1 + p_2 - p_3 - p_4 - k_S) E_S \boxed{f_1 f_2} P_{\text{decay}} P_{\text{abs}}$$

$$f_{1,\,2}(\mathbf{p};r) \;=\; \frac{\rho(r)}{2m_N}\left(\frac{2\pi}{m_N T(r)}\right)^{3/2} \mathrm{e}^{-\mathbf{p}^2/2m_N T(r)}$$

ENERGY EMISSION RATE

$$\mathcal{Q}(r,\,\phi) \;=\; \int \mathrm{d}\Pi_5 \mathcal{S} \sum_{\text{spins}} |\mathcal{M}|^2 (2\pi)^4 \delta^4(p_1+p_2-p_3-p_4-k_S) E_S \boxed{f_1 f_2} P_{\text{decay}} P_{\text{abs}}$$

$$P_{decay}(r,\phi) = \exp\left[-d(r,\phi)\,\Gamma_S\right]$$

decay probability

$$f_{1,\,2}(\mathbf{p};r) \;=\; \frac{\rho(r)}{2m_N}\left(\frac{2\pi}{m_N T(r)}\right)^{3/2} \mathrm{e}^{-\mathbf{p}^2/2m_N T(r)}$$

ENERGY EMISSION RATE

$$\mathcal{Q}(r,\,\phi) \;=\; \int \mathrm{d}\Pi_5 \mathcal{S} \sum_{\text{spins}} |\mathcal{M}|^2 (2\pi)^4 \delta^4(p_1 + p_2 - p_3 - p_4 - k_S) E_S f_1 f_2 P_{\text{decay}} P_{\text{abs}}$$

$$P_{decay}(r,\phi) = \exp\left[-d(r,\phi)\,\Gamma_S\right]$$

decay probability

$$f_{1,\,2}(\mathbf{p};r) \;=\; \frac{\rho(r)}{2m_N}\left(\frac{2\pi}{m_N T(r)}\right)^{3/2} \mathrm{e}^{-\mathbf{p}^2/2m_N T(r)}$$

$$\Gamma_S = \frac{m_S}{E_S}\Gamma_{0,S}$$

ENERGY EMISSION RATE

$$\mathcal{Q}(r,\,\phi) \;=\; \int \mathrm{d}\Pi_5 \mathcal{S} \sum_{\text{spins}} |\mathcal{M}|^2 (2\pi)^4 \delta^4(p_1+p_2-p_3-p_4-k_S) E_S f_1 f_2 P_{\text{decay}} P_{\text{abs}}$$

$$P_{decay}(r,\phi) = \exp\left[-d(r,\phi)\,\Gamma_S\right]$$

decay probability

$$f_{1,\,2}(\mathbf{p};r) \;=\; \frac{\rho(r)}{2m_N}\left(\frac{2\pi}{m_N T(r)}\right)^{3/2} \mathrm{e}^{-\mathbf{p}^2/2m_N T(r)}$$

$$\Gamma_S = \frac{m_S}{E_S}\Gamma_{0,S}$$

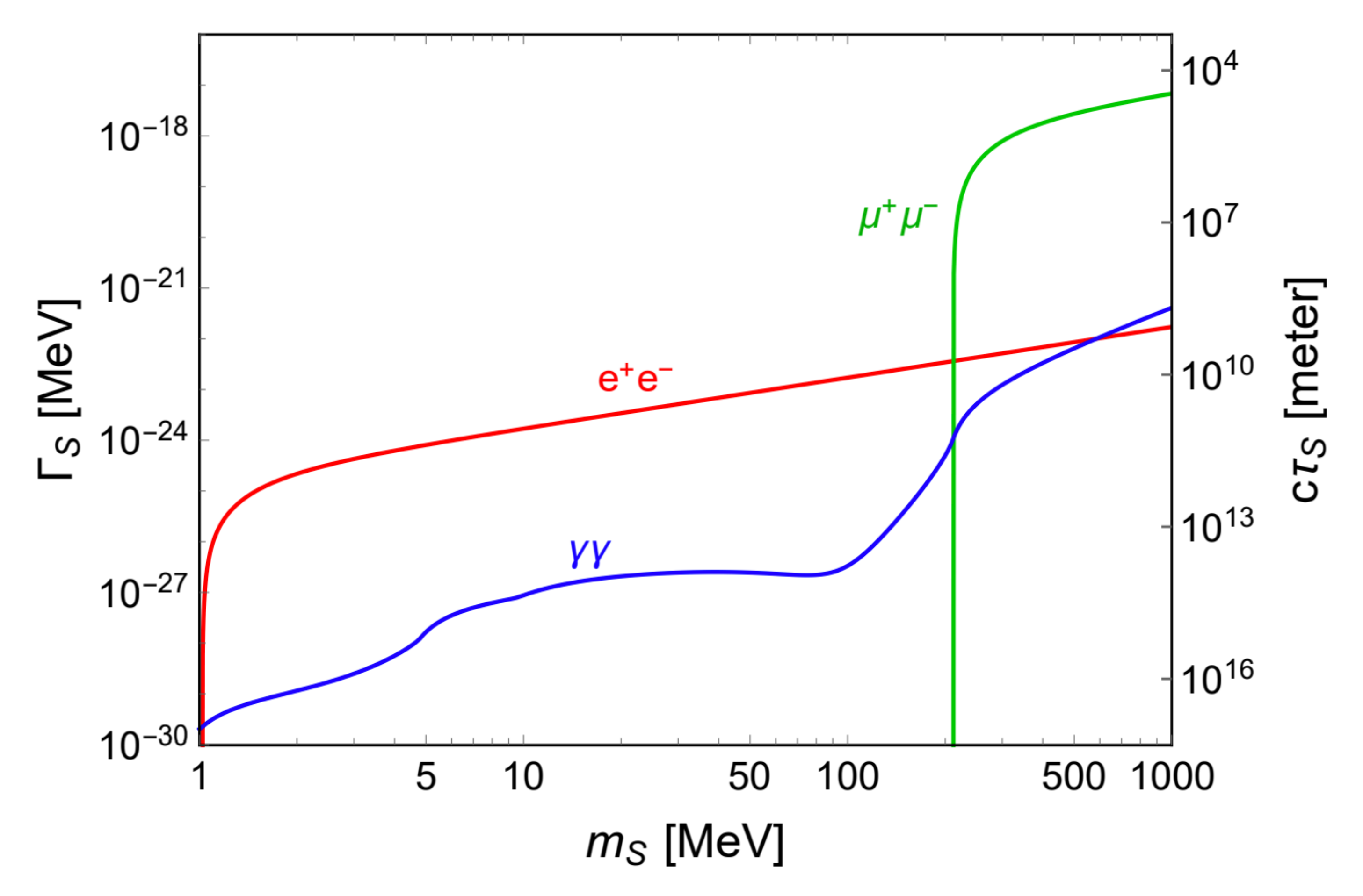

ENERGY EMISSION RATE

$$\mathcal{Q}(r,\,\phi) \;=\; \int \mathrm{d}\Pi_5 \mathcal{S} \sum_{\text{spins}} |\mathcal{M}|^2 (2\pi)^4 \delta^4(p_1 + p_2 - p_3 - p_4 - k_S) E_S \boxed{f_1 f_2} P_{\text{decay}} P_{\text{abs}}$$

$$P_{decay}(r,\phi) = \exp\left[-d(r,\phi)\,\Gamma_S\right]$$

decay probability

$$f_{1,\,2}(\mathbf{p};r) \;=\; \frac{\rho(r)}{2m_N}\left(\frac{2\pi}{m_N T(r)}\right)^{3/2} \mathrm{e}^{-\mathbf{p}^2/2m_N T(r)}$$

$$\Gamma_S = \frac{m_S}{E_S}\boxed{\Gamma_{0,S}}$$

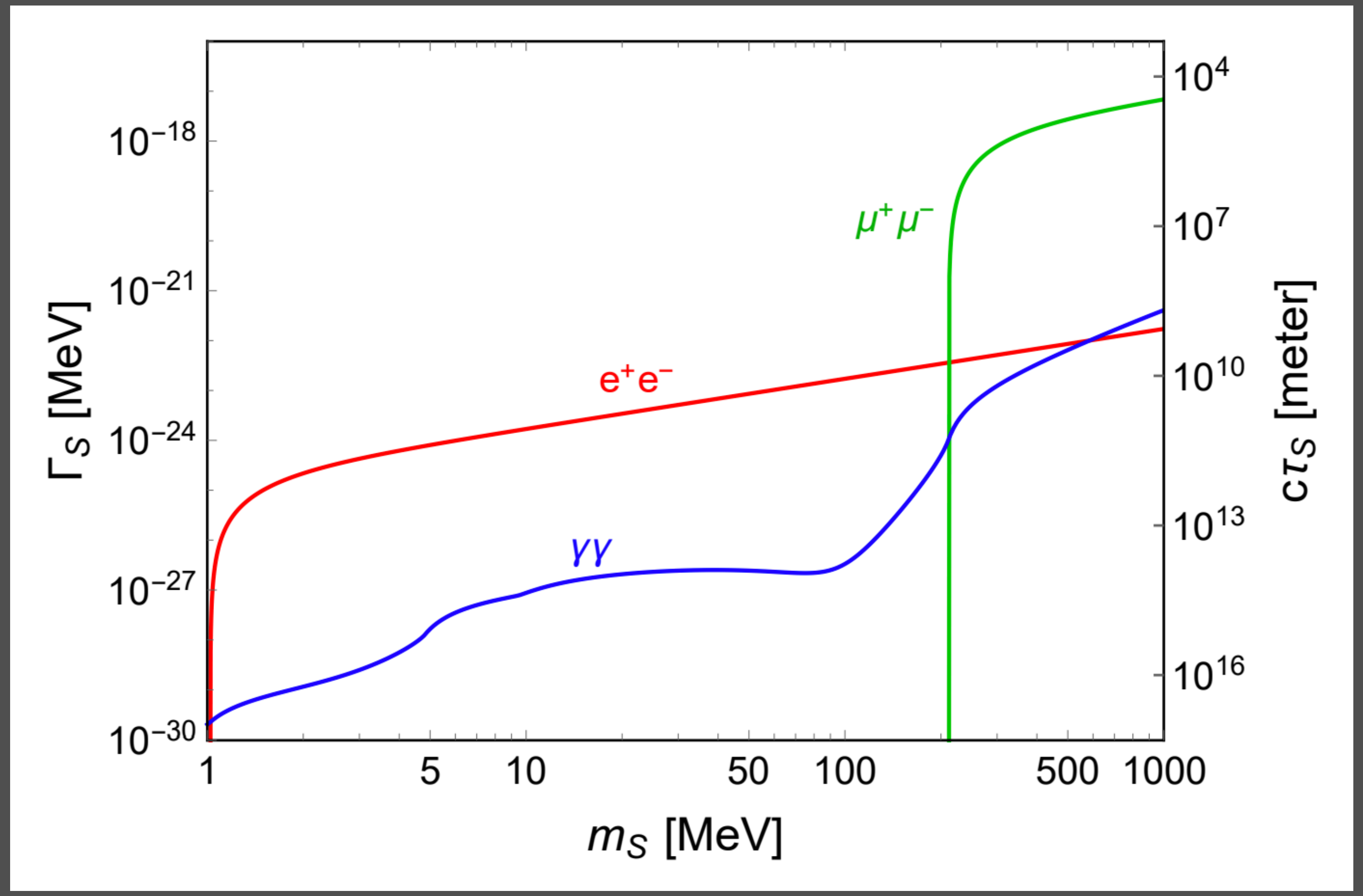

Absorption due to inverse BR

$$P_{abs}(r,\phi) = Exp\left[-\int_0^d \frac{dr'}{\lambda[L(r,\phi,r')]}\right]$$

$$N + N + S \to N + N$$

ENERGY EMISSION RATE

$$\mathcal{Q}(r,\,\phi) \;=\; \int \mathrm{d}\Pi_5 \mathcal{S} \sum_{\text{spins}} |\mathcal{M}|^2 (2\pi)^4 \delta^4(p_1 + p_2 - p_3 - p_4 - k_S) E_S \boxed{f_1 f_2} P_{\text{decay}} P_{\text{abs}}$$

$$P_{decay}(r,\phi) = \exp\left[-d(r,\phi)\,\Gamma_S\right]$$

decay probability

$$f_{1,\,2}(\mathbf{p};r) \;=\; \frac{\rho(r)}{2m_N}\left(\frac{2\pi}{m_N T(r)}\right)^{3/2} \mathrm{e}^{-\mathbf{p}^2/2m_N T(r)}$$

$$\Gamma_S = \frac{m_S}{E_S}\boxed{\Gamma_{0,S}}$$

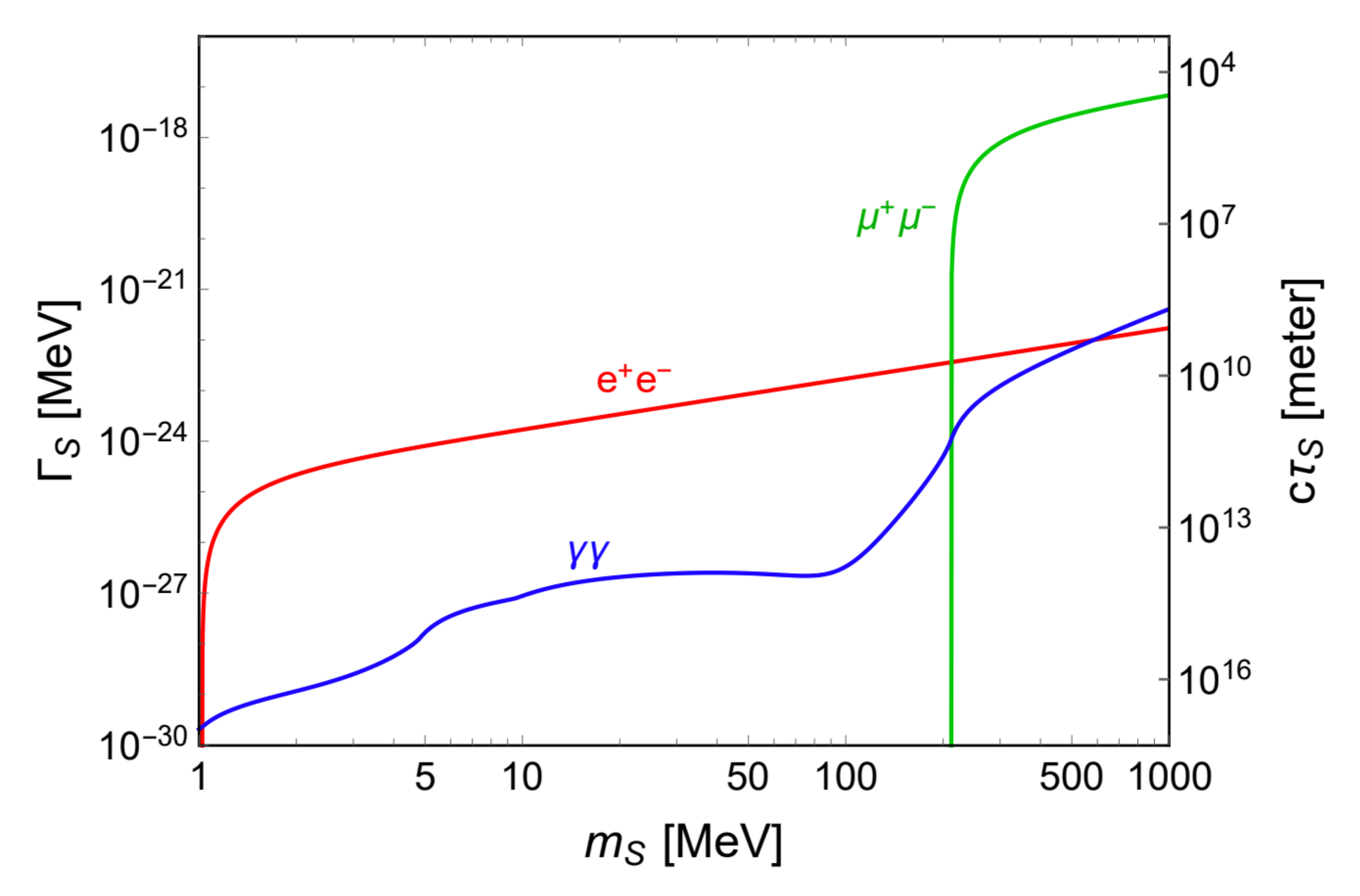

Absorption due to inverse BR

$$P_{abs}(r,\phi) = Exp\left[-\int_0^d \frac{dr'}{\lambda[L(r,\phi,r')]}\right]$$

$$N + N + S \rightarrow N + N$$

MFP depends on the
star density and temperature profiles

ENERGY EMISSION RATE

$$\mathcal{Q}(r,\,\phi) \;=\; \int \mathrm{d}\Pi_5 \mathcal{S} \sum_{\text{spins}} |\mathcal{M}|^2 (2\pi)^4 \delta^4(p_1+p_2-p_3-p_4-k_S) E_S \boxed{f_1 f_2} P_{\text{decay}} P_{\text{abs}}$$

$$P_{decay}(r,\phi) = \exp\left[-d(r,\phi)\,\Gamma_S\right]$$

decay probability

$$f_{1,\,2}(\mathbf{p};r) \;=\; \frac{\rho(r)}{2m_N}\left(\frac{2\pi}{m_N T(r)}\right)^{3/2} \mathrm{e}^{-\mathbf{p}^2/2m_N T(r)}$$

$$\Gamma_S = \frac{m_S}{E_S}\boxed{\Gamma_{0,S}}$$

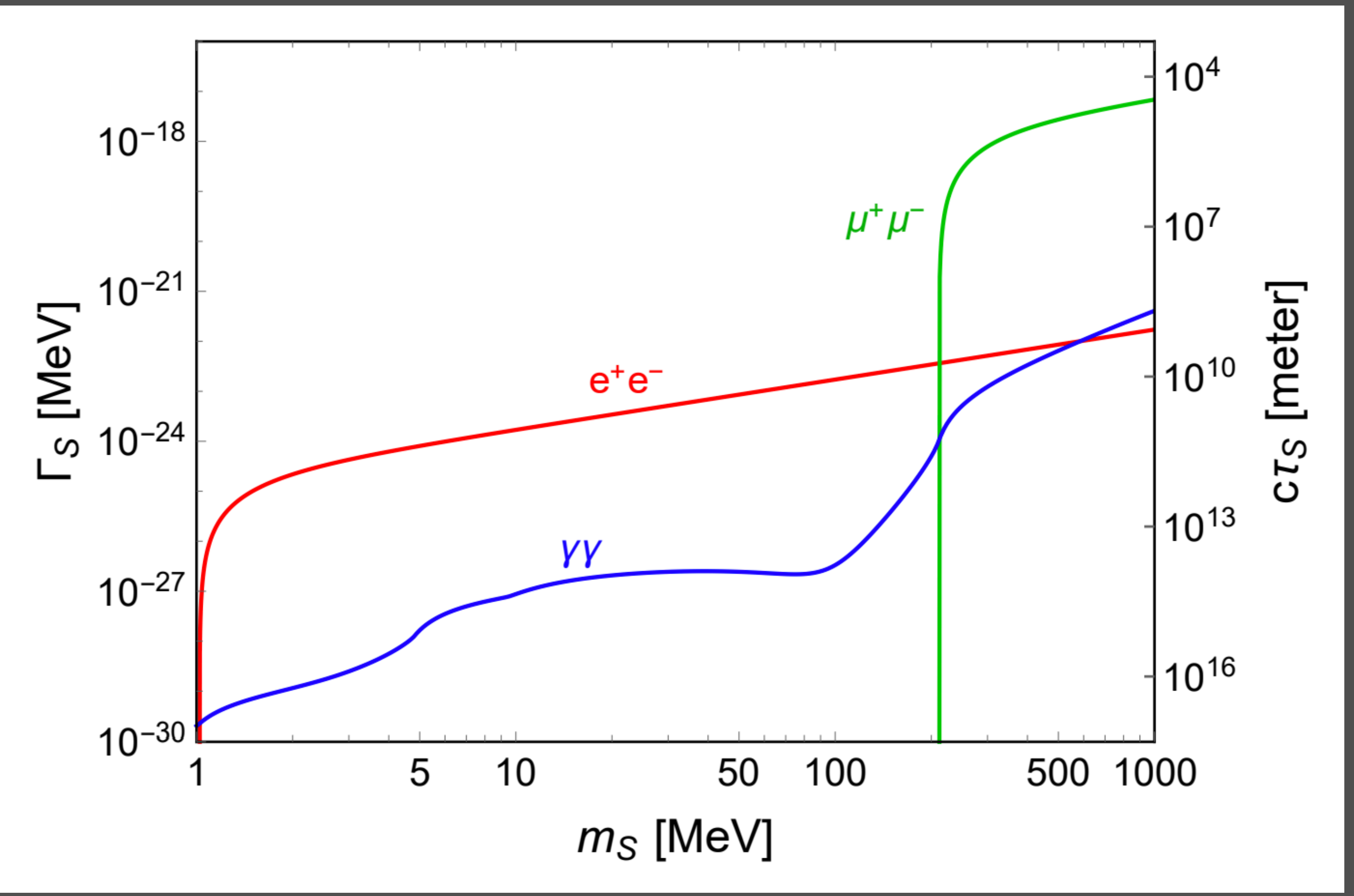

$$P_{abs}(r,\phi) = Exp\left[-\int_0^d \frac{dr'}{\lambda[L(r,\phi,r')]}\right]$$

Absorption due to inverse BR

$$N + N + S \rightarrow N + N$$

MFP depends on the
star density and temperature profiles

$$\lambda^{-1}(r;x) \;=\; \frac{1}{2E_S}\int \mathrm{d}\Pi_4 \mathcal{S} \sum_{\text{spins}} |\mathcal{M}|^2 (2\pi)^4 \delta^4(p_1+p_2-p_3-p_4+k_S) f_1 f_2$$

ENERGY EMISSION RATE

$$\mathcal{Q}(r,\,\phi) \;=\; \int \mathrm{d}\Pi_5 \mathcal{S} \sum_{\text{spins}} |\mathcal{M}|^2 (2\pi)^4 \delta^4(p_1+p_2-p_3-p_4-k_S) E_S f_1 f_2 P_{\text{decay}} P_{\text{abs}}$$

$$P_{decay}(r,\phi) = \exp\left[-d(r,\phi)\,\Gamma_S\right]$$

decay probability

$$f_{1,2}(\mathbf{p};r) \;=\; \frac{\rho(r)}{2m_N}\left(\frac{2\pi}{m_N T(r)}\right)^{3/2} \mathrm{e}^{-\mathbf{p}^2/2m_N T(r)}$$

$$\Gamma_S = \frac{m_S}{E_S}\Gamma_{0,S}$$

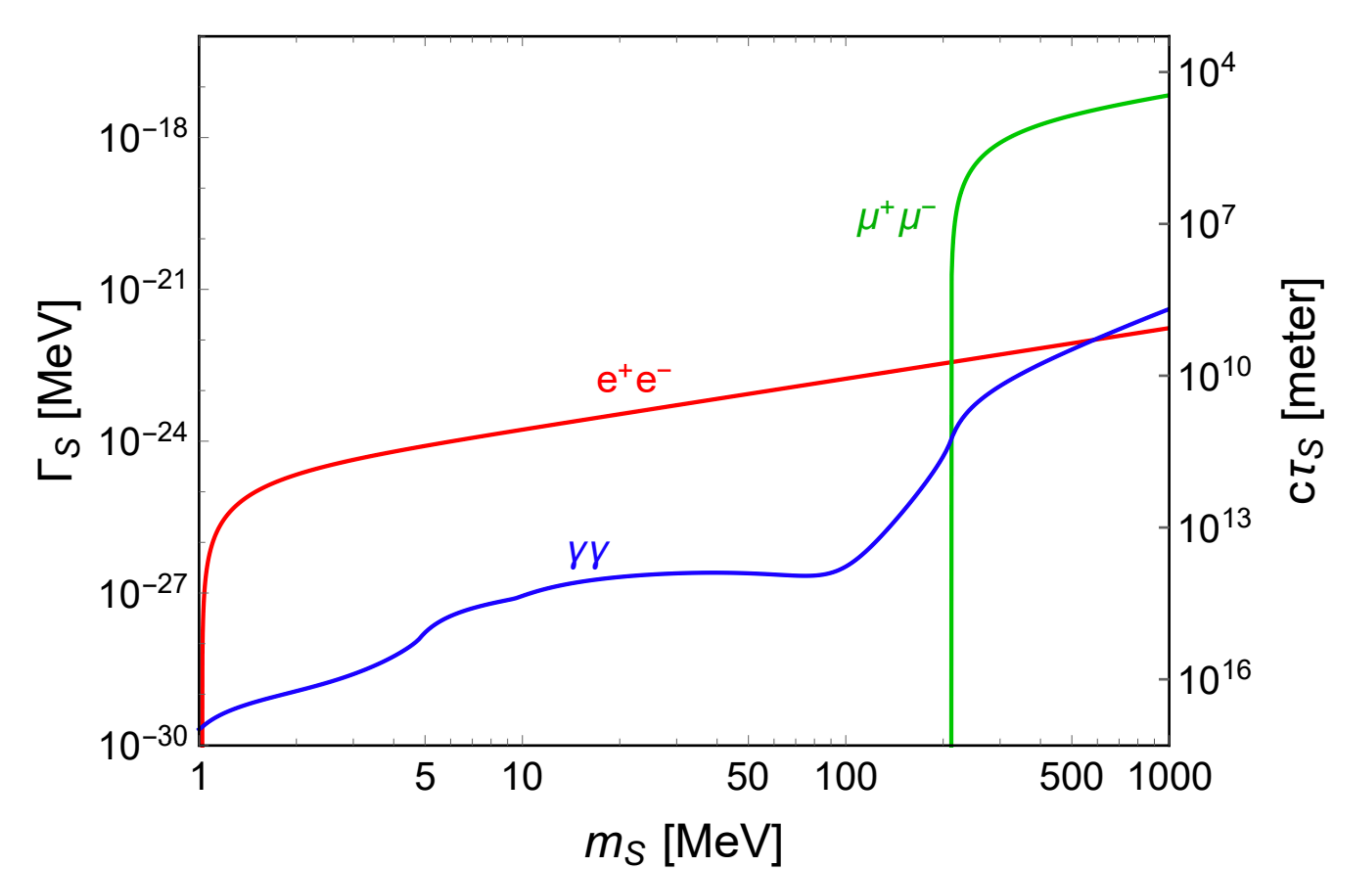

Absorption due to inverse BR

$$P_{abs}(r,\phi) = Exp\left[-\int_0^d \frac{dr'}{\lambda[L(r,\phi,r')]}\right]$$

$$N+N+S \rightarrow N+N$$

MFP depends on the
star density and temperature profiles

$$\lambda^{-1}(r;x) \;=\; \frac{1}{2E_S}\int \mathrm{d}\Pi_4 \mathcal{S} \sum_{\text{spins}} |\mathcal{M}|^2 (2\pi)^4 \delta^4(p_1+p_2-p_3-p_4+k_S) f_1 f_2$$

In the case of constant MFP λ, the absorption factor simply reduces to $\exp\{-d/\lambda\}$.

SN1987A LIMITS

- Integrating over the whole volume of SN1987A inside R_ν, we arrive at the luminosity due to the emission of the scalar S via the expression

$$\mathcal{L}_S = \int \mathcal{Q}(r,\phi)\mathrm{d}V = 2\pi \int_0^{R_\nu} \mathrm{d}r\, r^2 \int_0^{\pi} \mathrm{d}\phi \sin\phi\, \mathcal{Q}(r,\phi)\,.$$

- To set limits on the scalar mass m_S and the mixing angle $\sin\theta$, we conservatively require that the luminosity $\mathscr{L}_S$ is smaller than 10% of the measured neutrino luminosity $\mathscr{L}_\nu = \simeq 3 \times 10^{53}$erg/sec i.e. $\mathscr{L}_S < 3 \times 10^{52}$ erg/sec

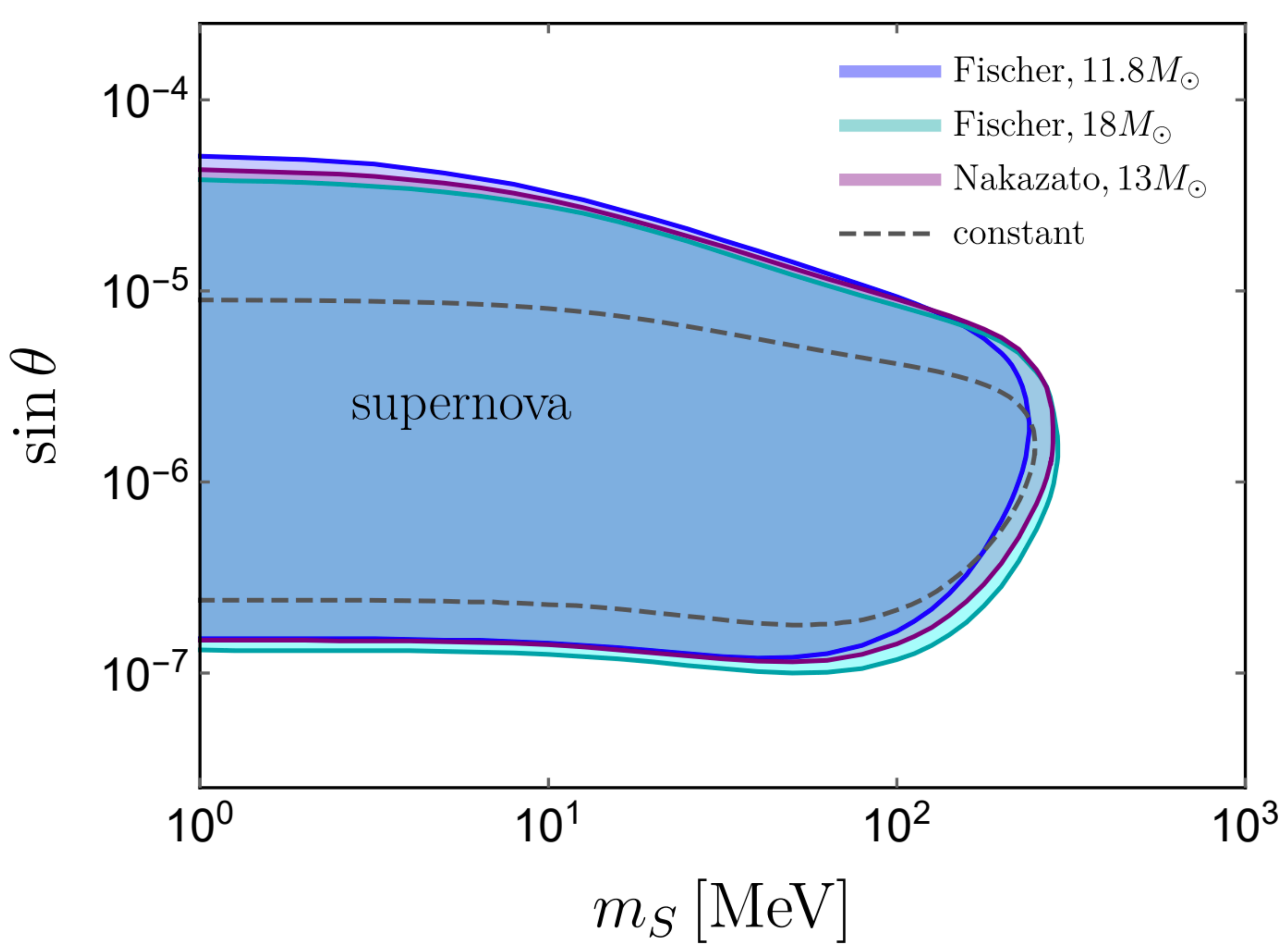

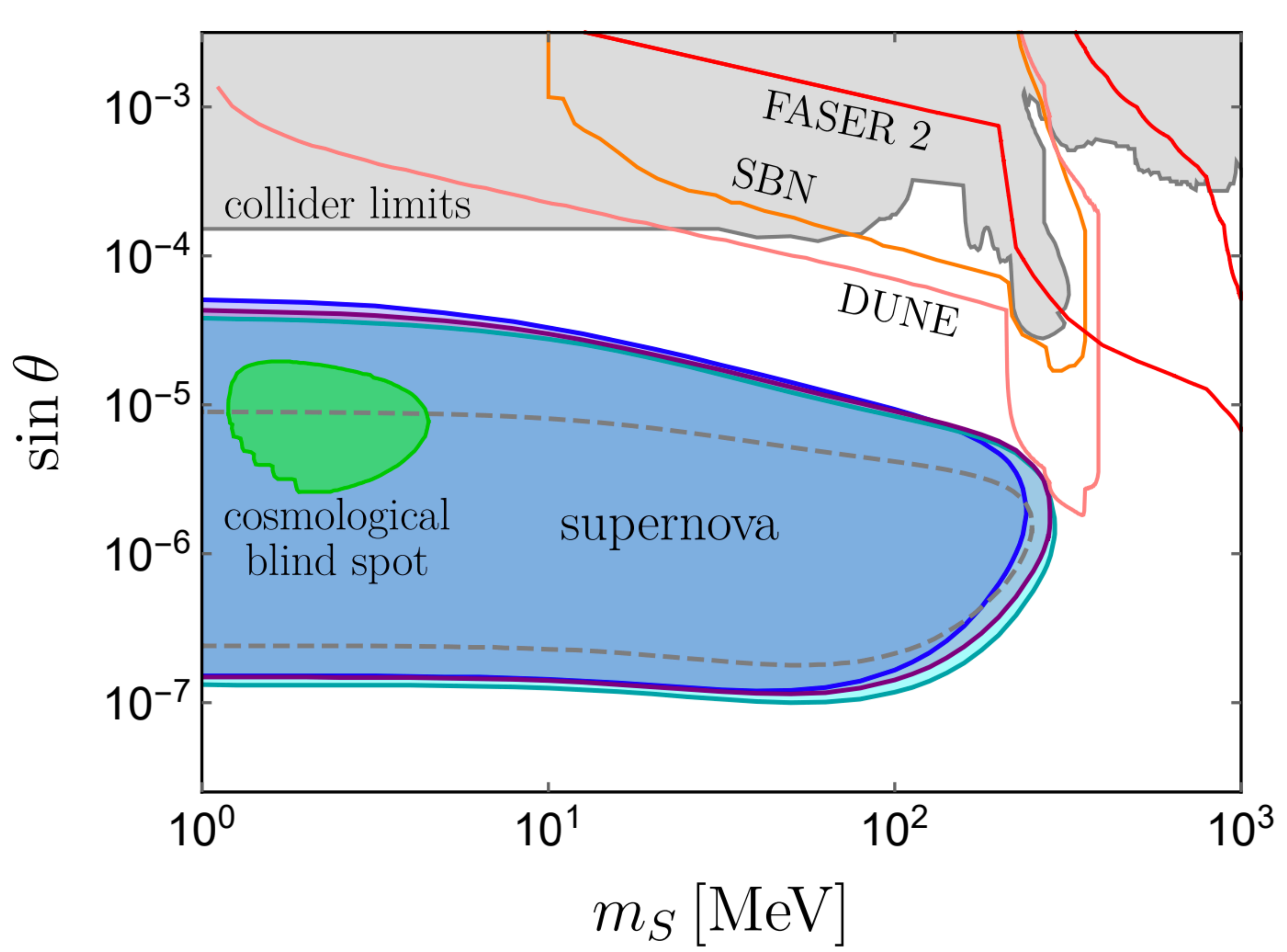

The dashed (constant case) is shown for constant temperature $T = 30$ MeV and baryon number density $n_B = 1.2 \times 10^{38}\,\mathrm{cm}^{-3}$.

SN1987A LIMITS CONTINUED

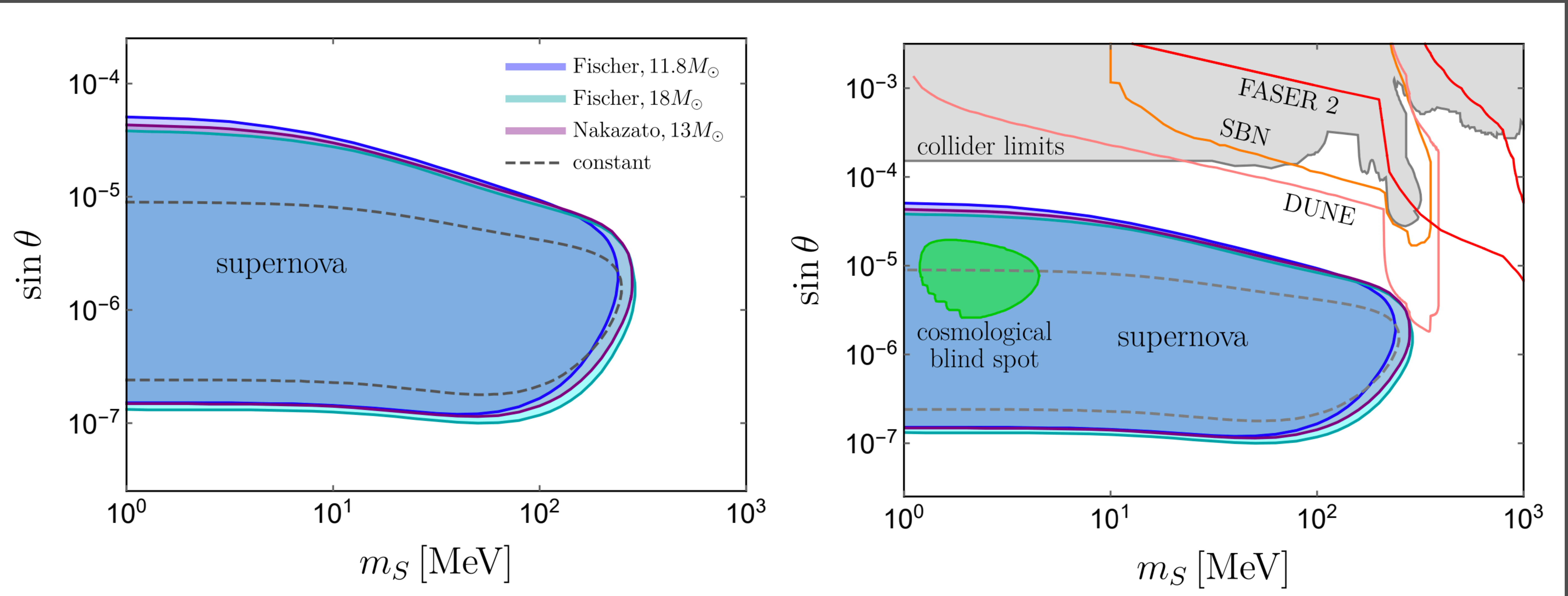

SN1987A LIMITS CONTINUED

- The supernova limits on S: largely complementary to those from collider searches, cosmological observations and other astrophysical limits

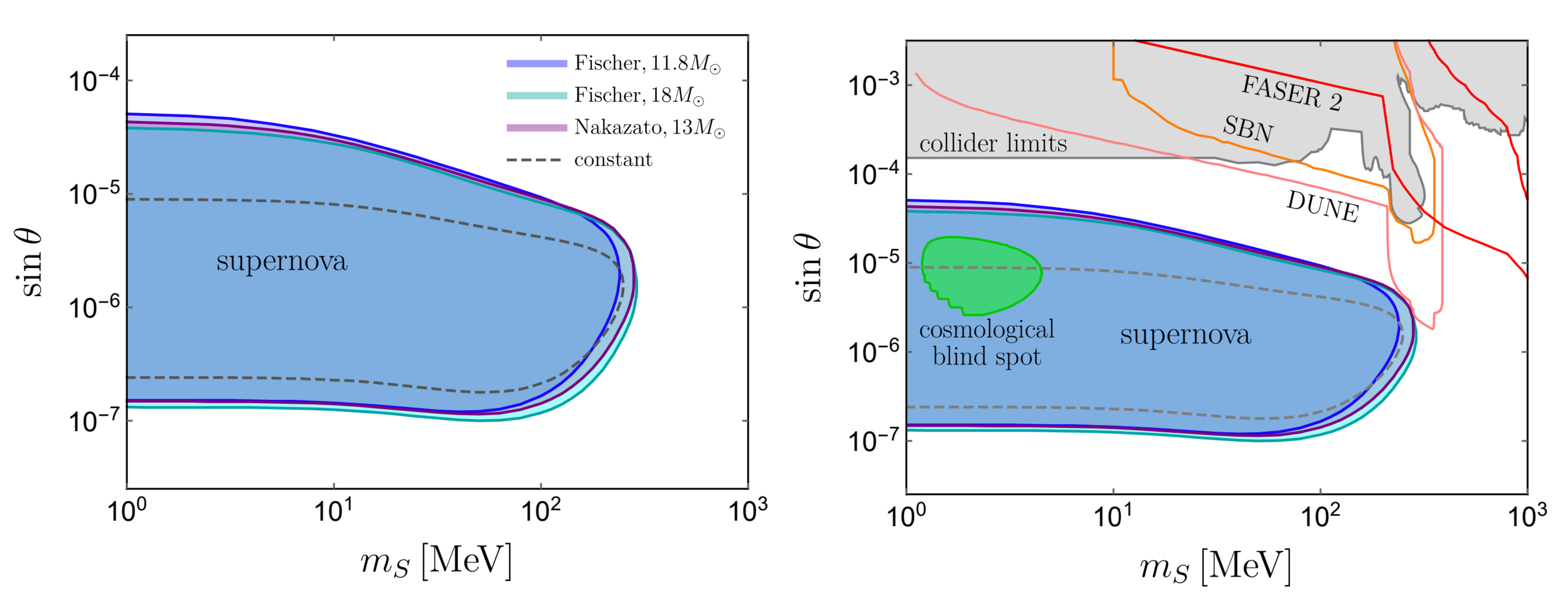

SN1987A LIMITS CONTINUED

- The supernova limits on S: largely complementary to those from collider searches, cosmological observations and other astrophysical limits

- Collider limits combined from NA48/2, KOTO, E949, NA62, KTeV, BaBar, Belle, LHCb and CHARM (gray) from FCNC S couplings to the SM quarks at the 1-loop level constrain $m_S \lesssim$ GeV can be produced from FCNC decays of SM mesons, e.g. $K, B \to \pi + S$ and $B \to K + S$.

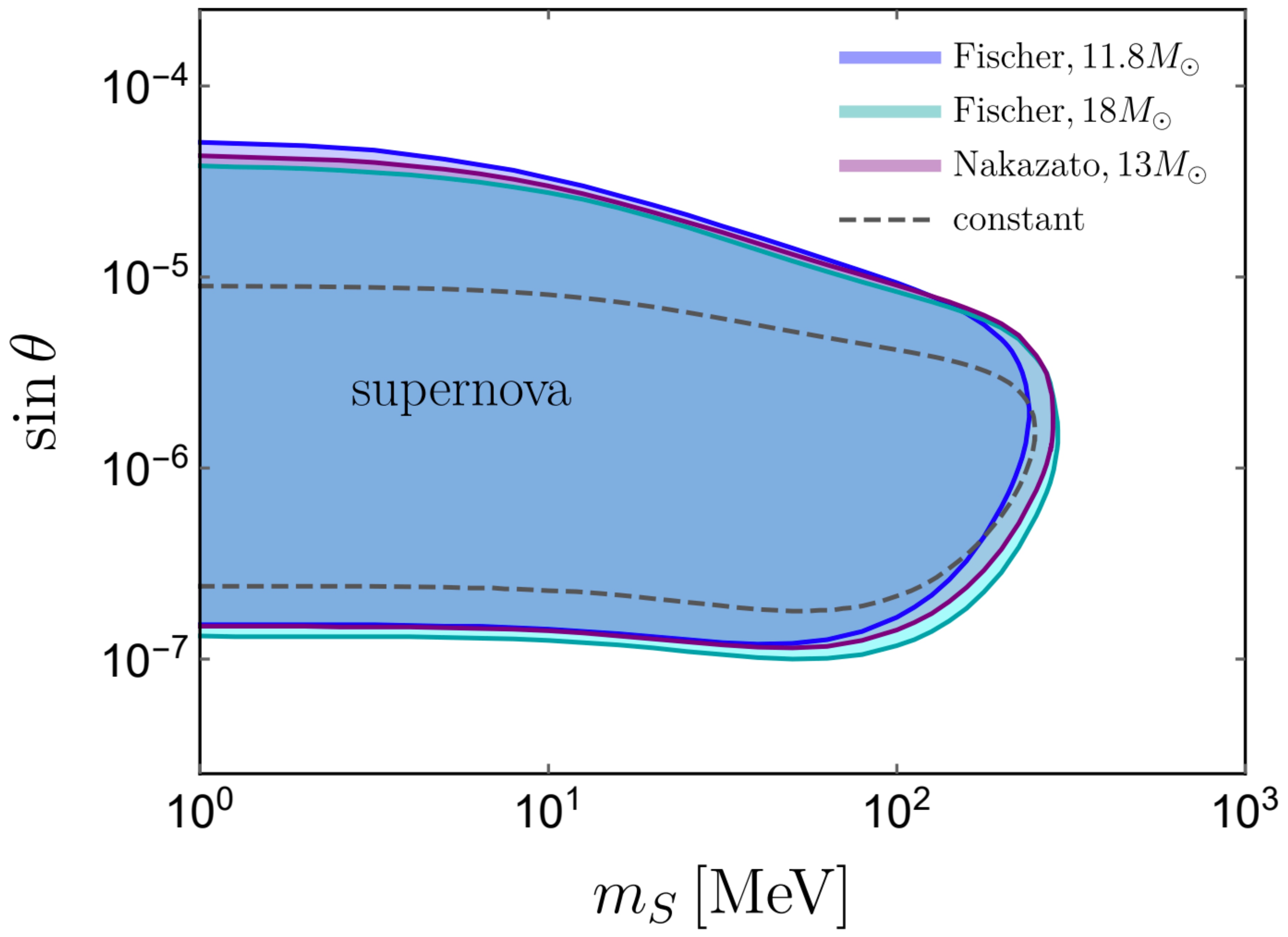

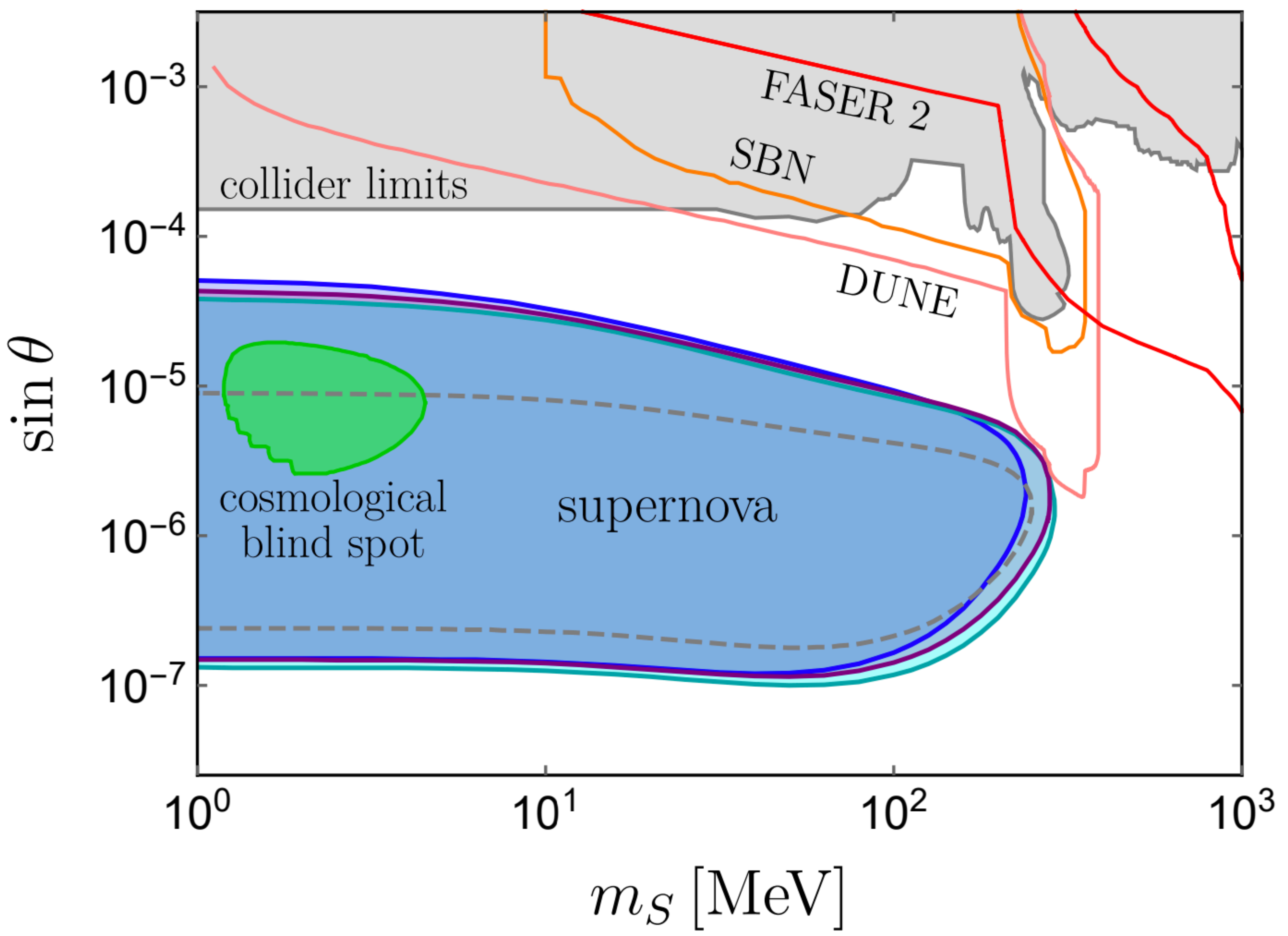

SN1987A LIMITS CONTINUED

- The supernova limits on S: largely complementary to those from collider searches, cosmological observations and other astrophysical limits

- Collider limits combined from NA48/2, KOTO, E949, NA62, KTeV, BaBar, Belle, LHCb and CHARM (gray) from FCNC S couplings to the SM quarks at the 1-loop level constrain $m_S \lesssim$ GeV can be produced from FCNC decays of SM mesons, e.g. $K, B \to \pi + S$ and $B \to K + S$.

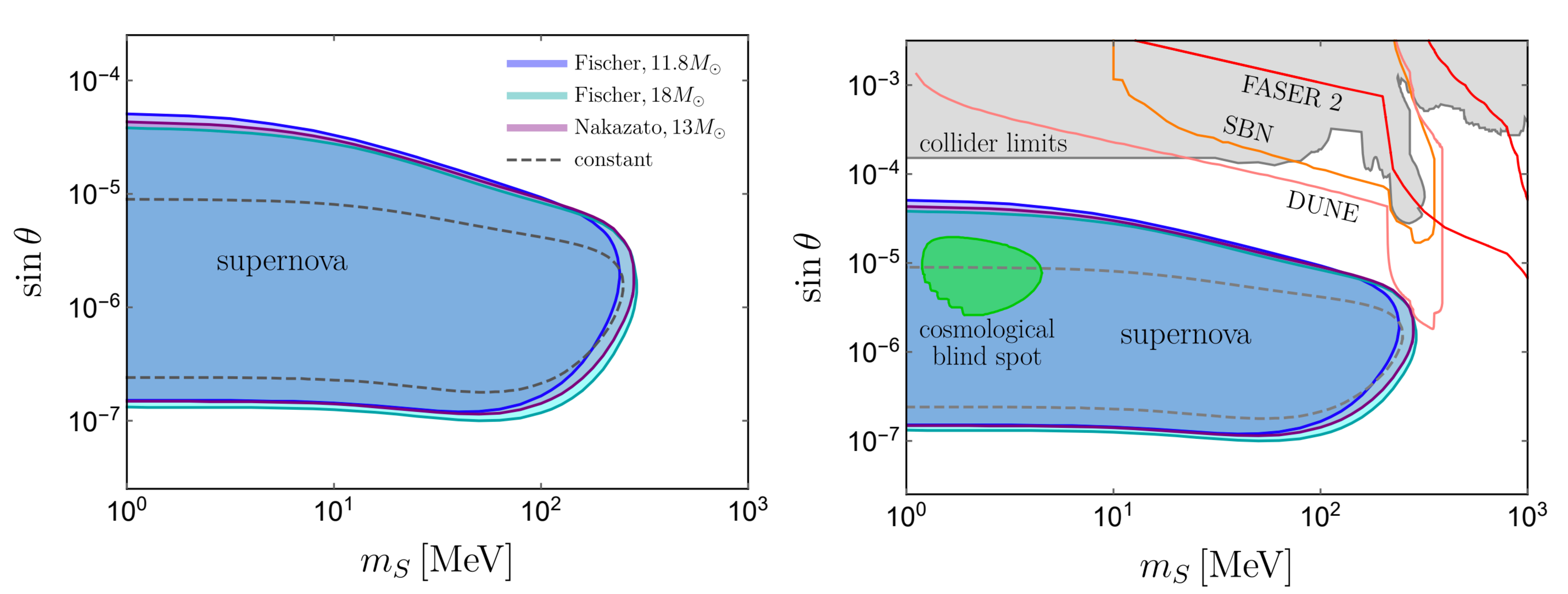

Projected sensitivities for DUNE, FASER 2 and SBN are also shown

SN1987A LIMITS CONTINUED

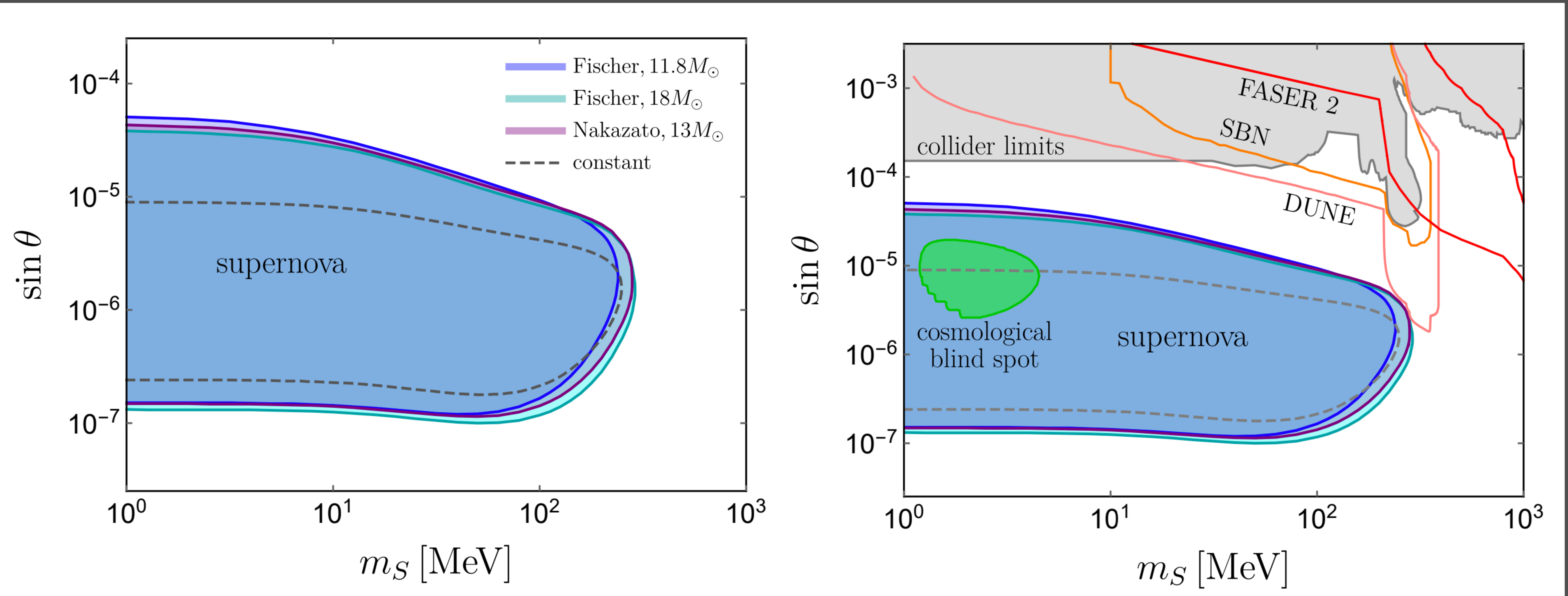

SN1987A LIMITS CONTINUED

- Early Universe: feeble S-SM couplings contributes to N_{eff} and spoils successful BBN, sensitive to reheating temperature T_R.

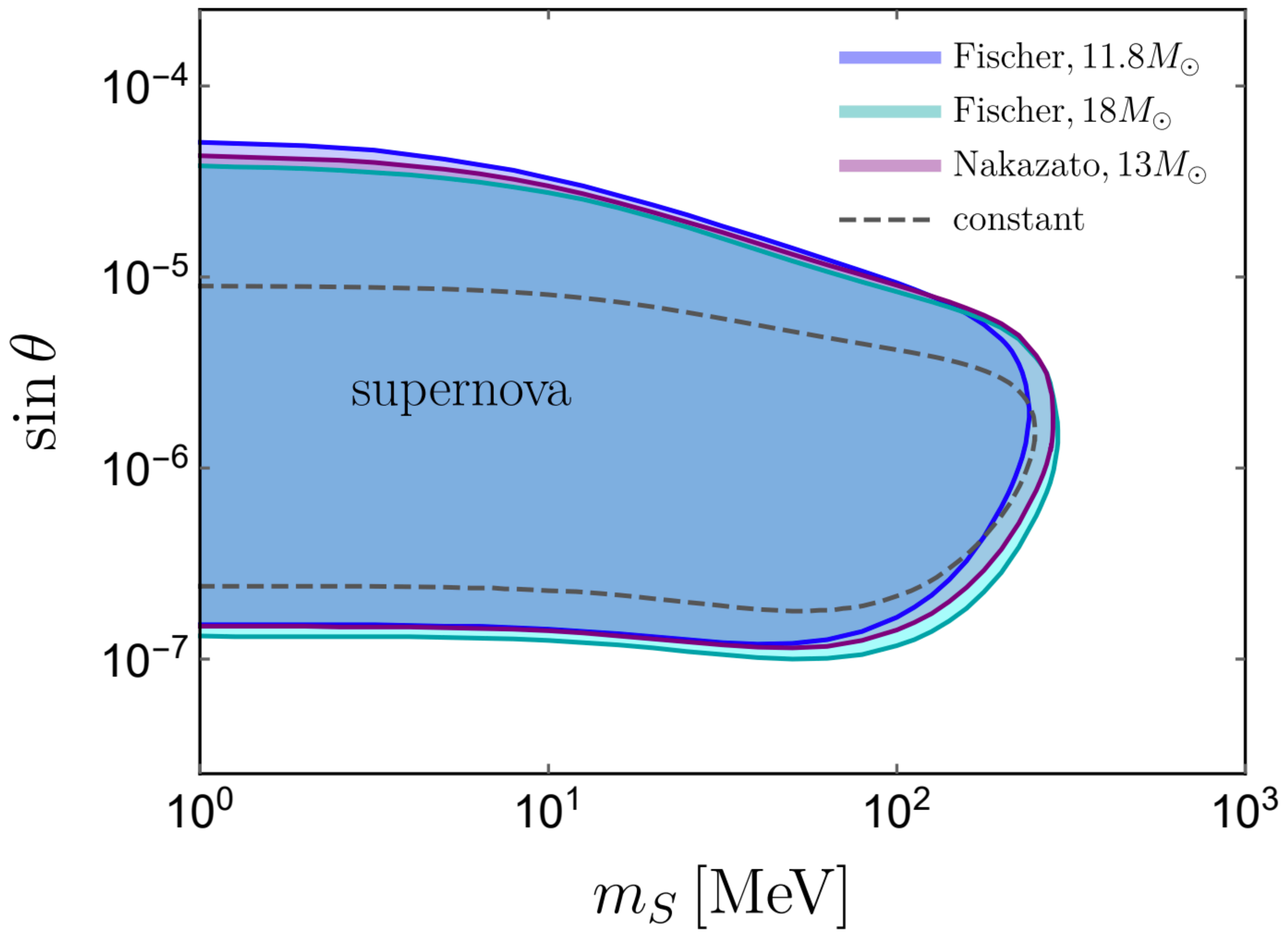

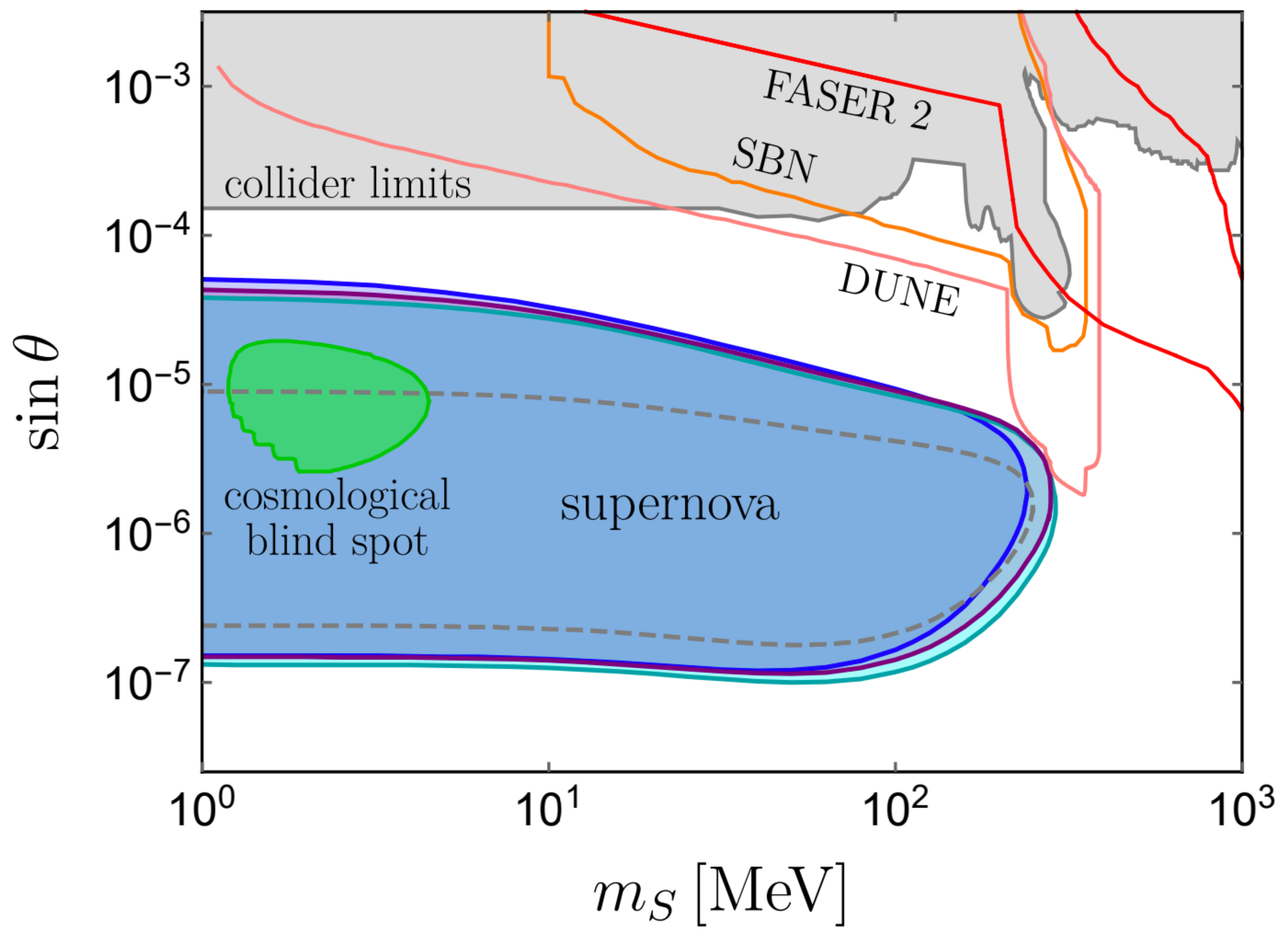

SN1987A LIMITS CONTINUED

- Early Universe: feeble S-SM couplings contributes to N_{eff} and spoils successful BBN, sensitive to reheating temperature T_R.

- There is a "blind spot'' left unconstrained (green region) that is consistent with CMB constraints on N_{eff}, μ and y distortions as well as post-recombination ionisation and X rays from S decays (see recent work by Ibe, Kobayashi, Nakayama and Shirai).

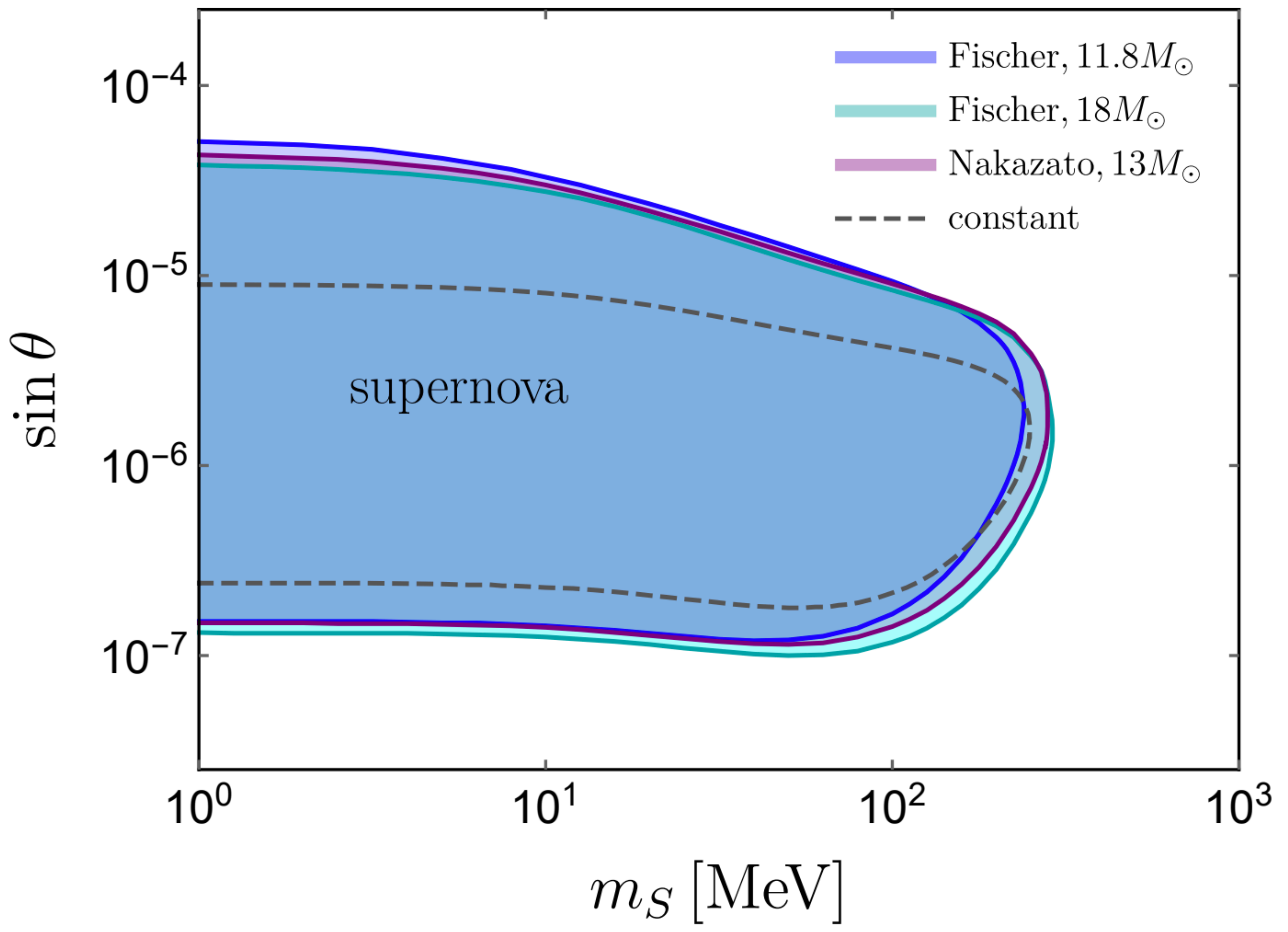

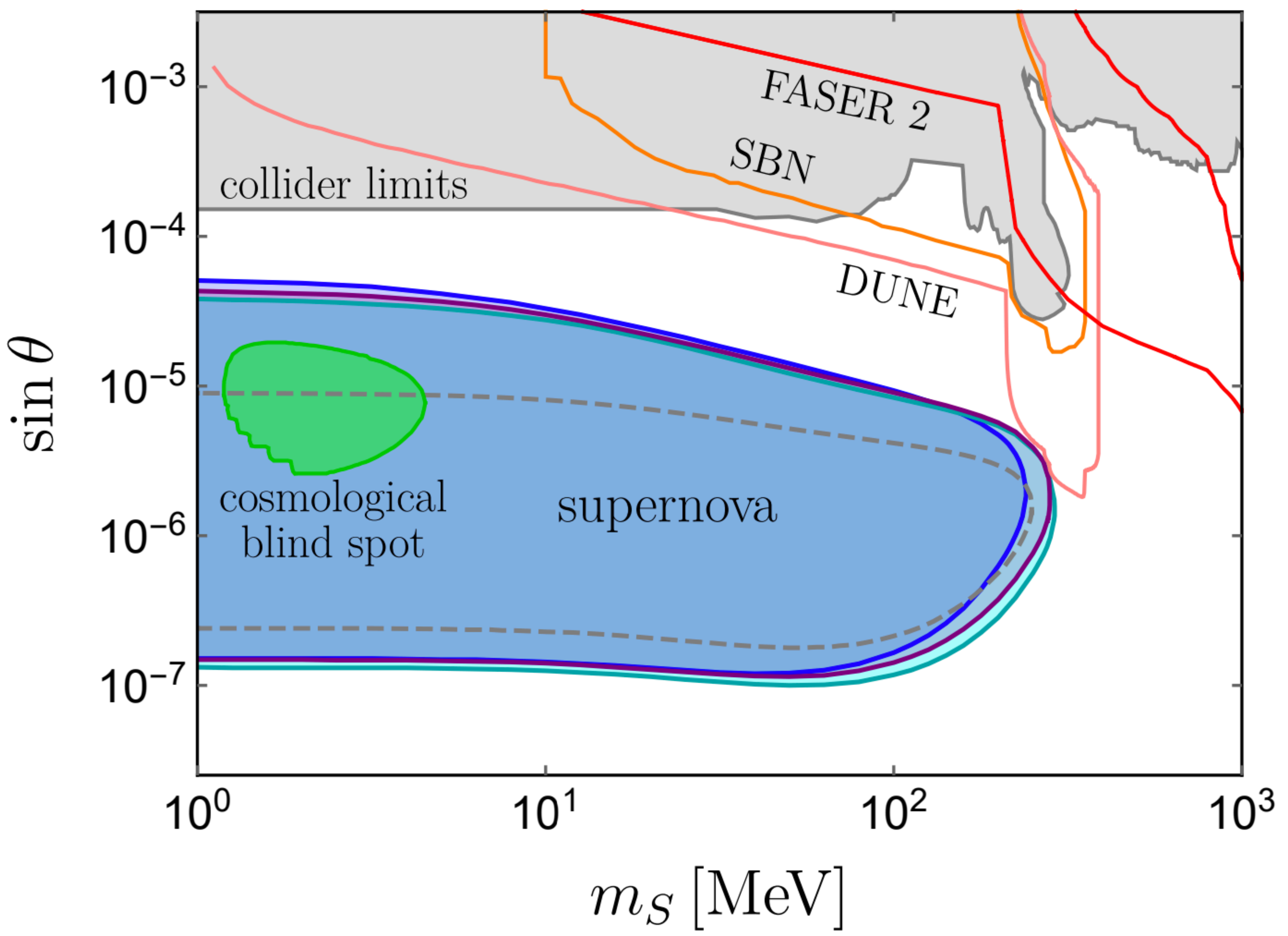

SN1987A LIMITS CONTINUED

- Early Universe: feeble S-SM couplings contributes to N_{eff} and spoils successful BBN, sensitive to reheating temperature T_R.

- There is a "blind spot'' left unconstrained (green region) that is consistent with CMB constraints on N_{eff}, μ and y distortions as well as post-recombination ionisation and X rays from S decays (see recent work by Ibe, Kobayashi, Nakayama and Shirai).

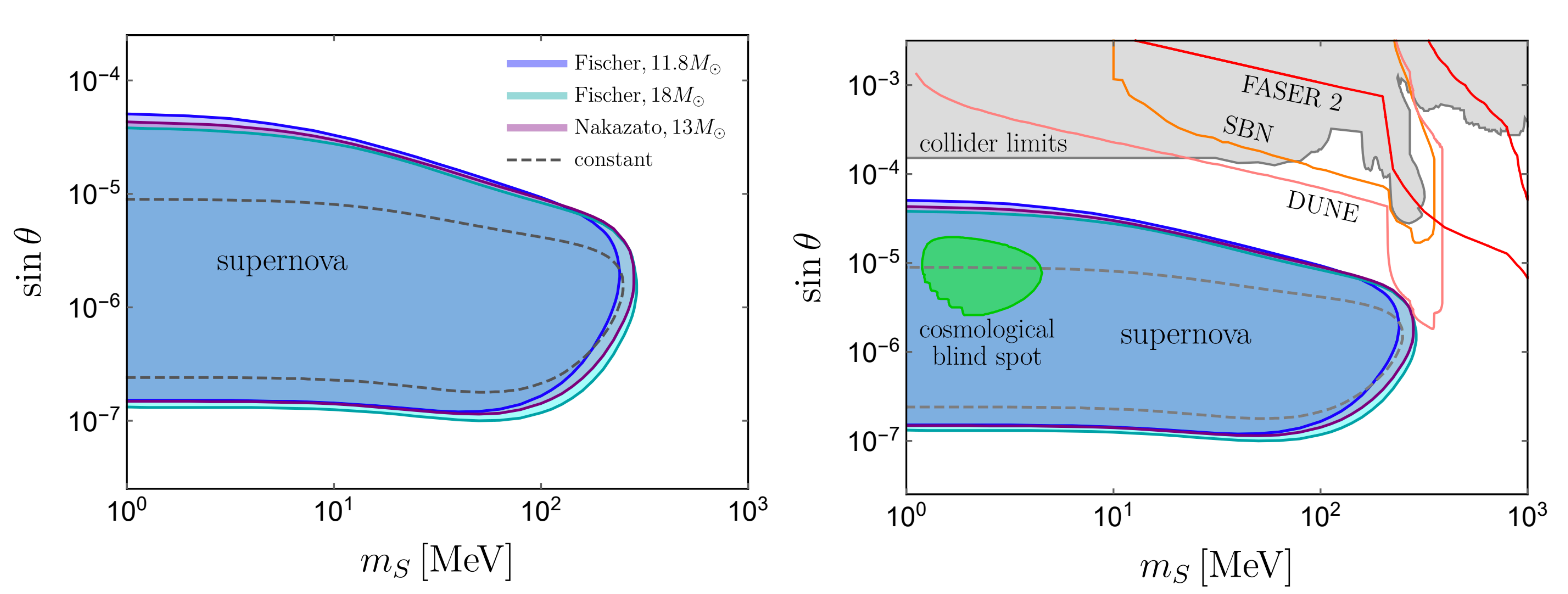

The cosmological "blind spot" is well excluded by the supernova limits with the three profiles adopted here. It is only partially excluded for the constant profile estimate.

SOLAR RADIAL PROFILES

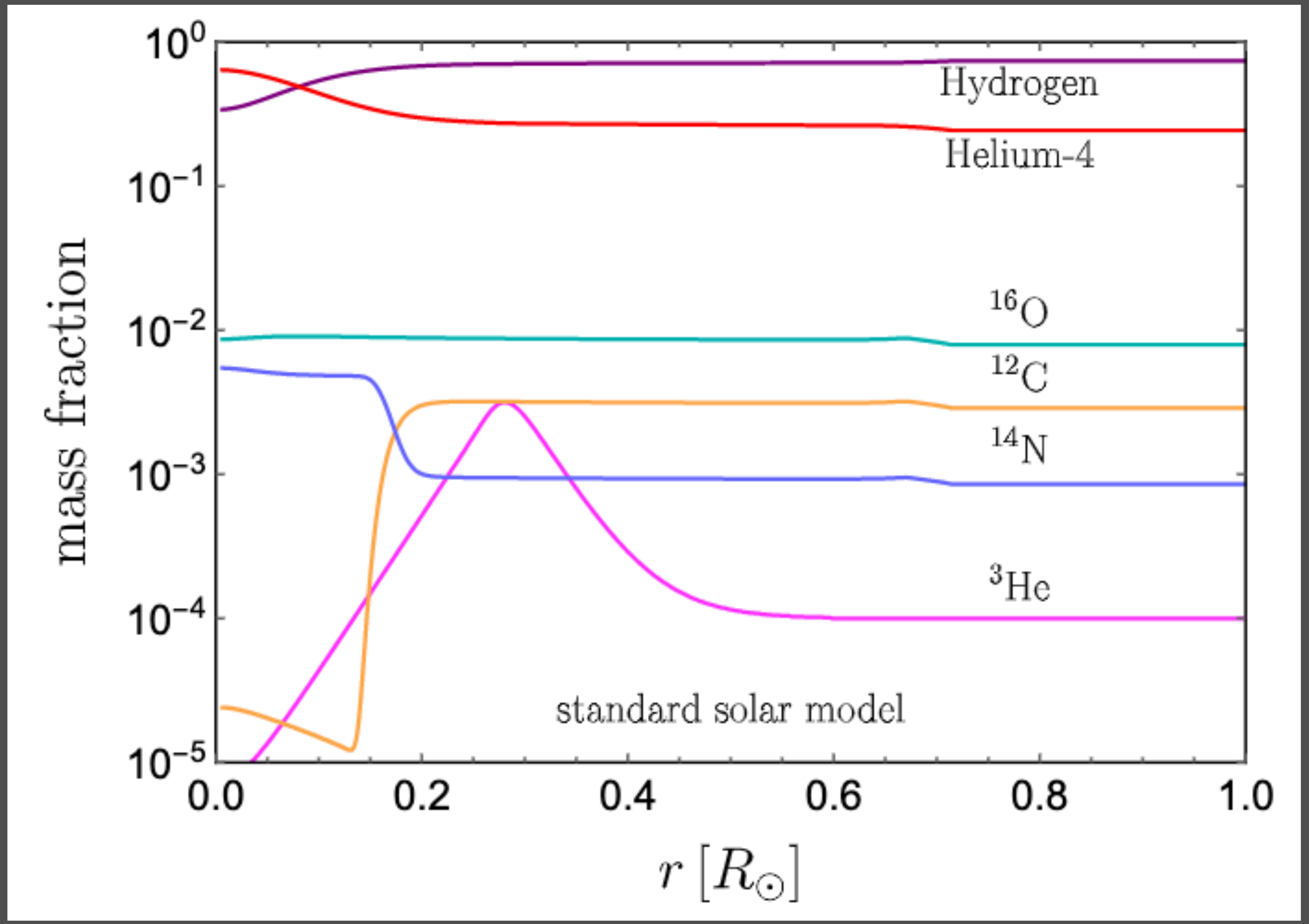

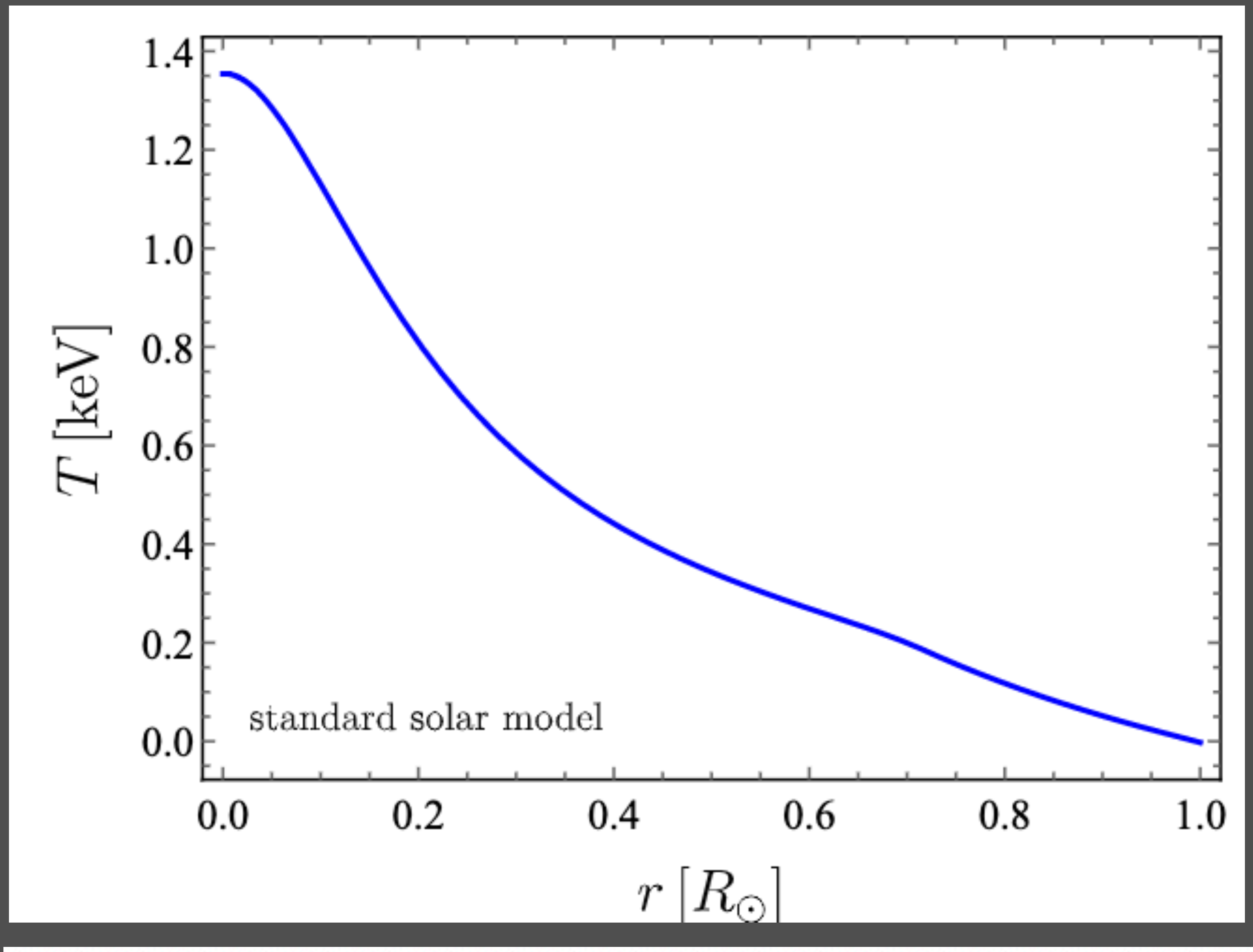

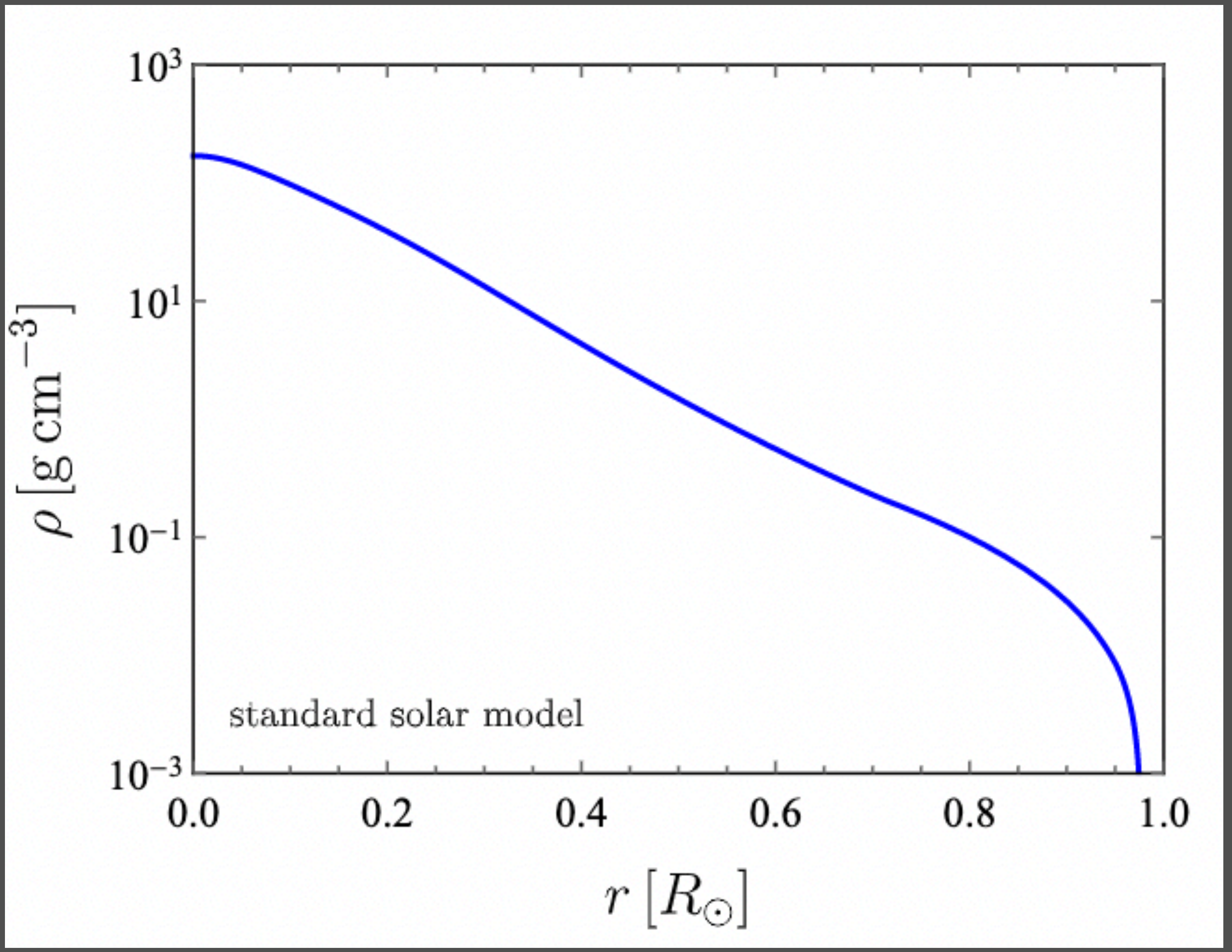

SOLAR RADIAL PROFILES

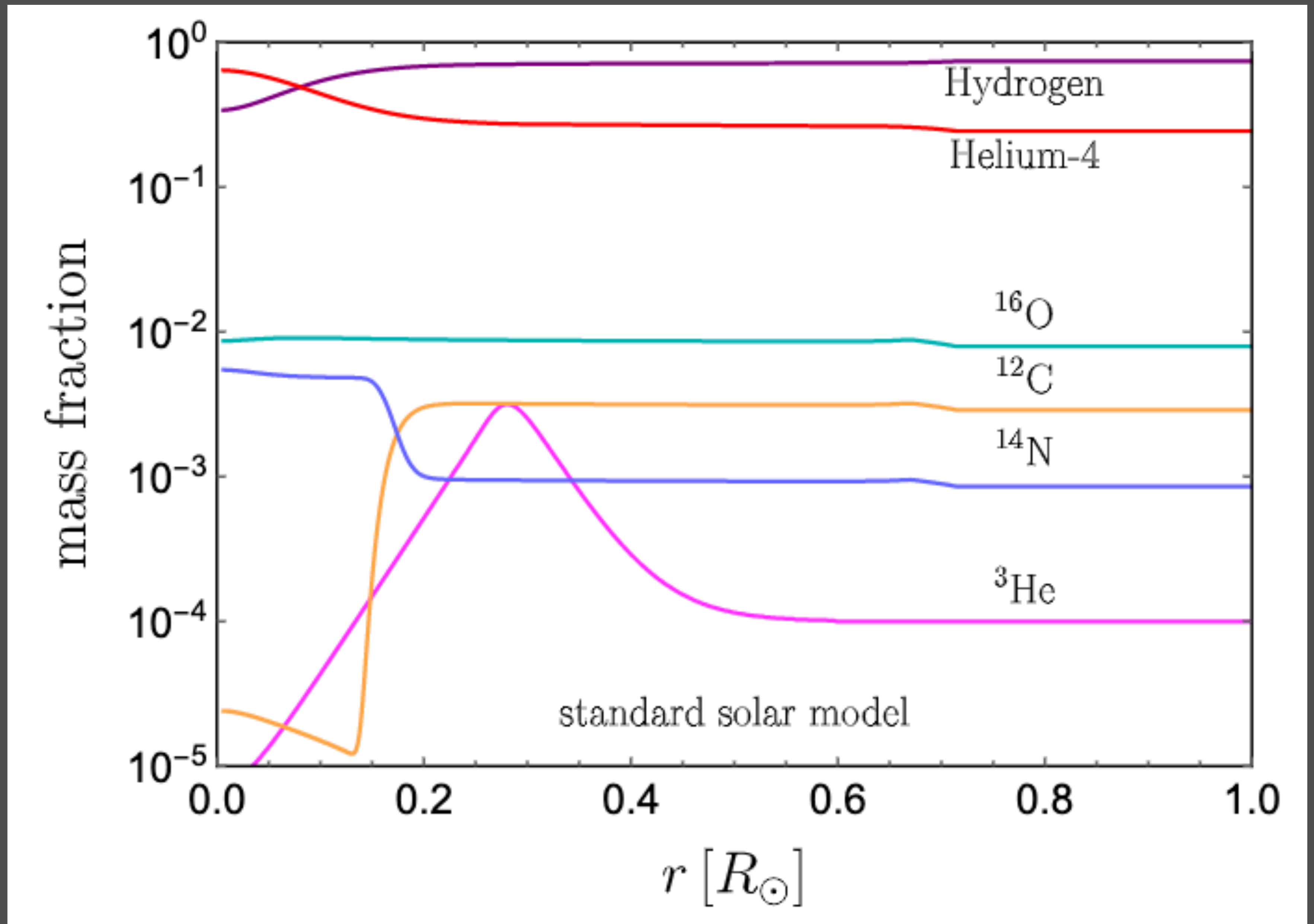

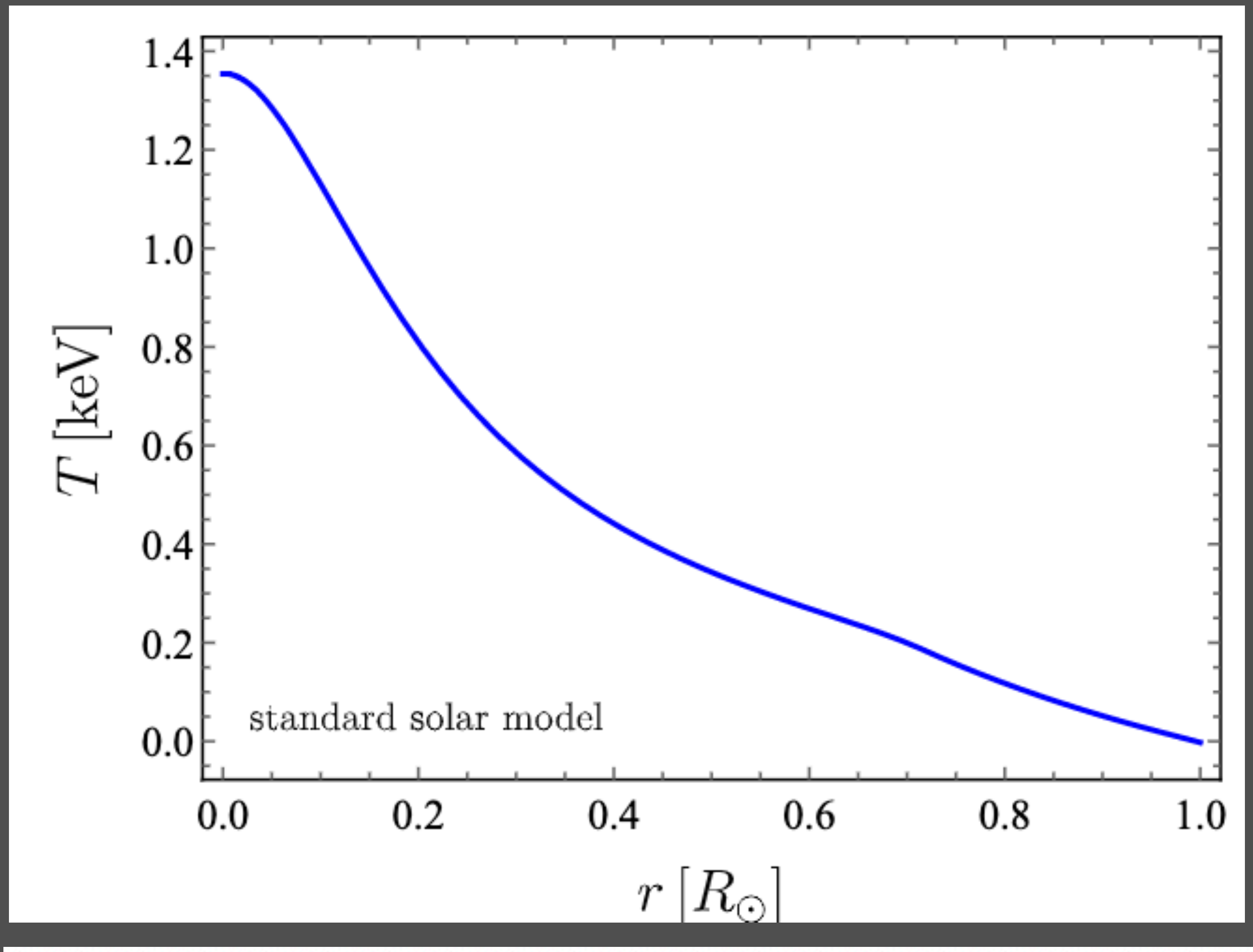

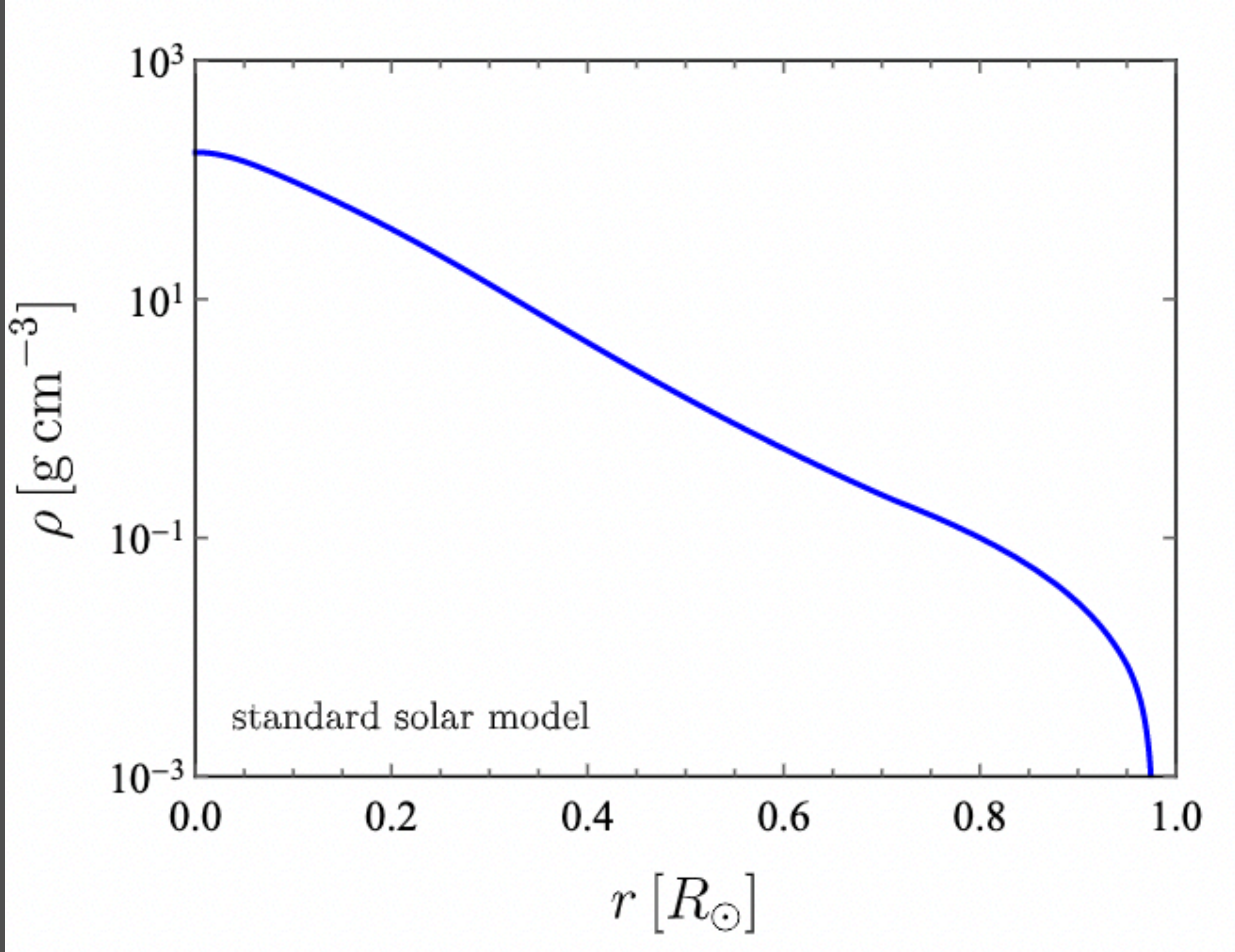

- The Sun is composed of mostly Hydrogen and Helium-4 ions, and their mass fractions are 34% and 64% at the solar core, changing smoothly to 74% and 24% at the solar surface. The remaining 2% mass fraction is Helium-3 and other heavy elements such as Carbon-12, Nitrogen-14 and Oxygen-16.

SOLAR RADIAL PROFILES

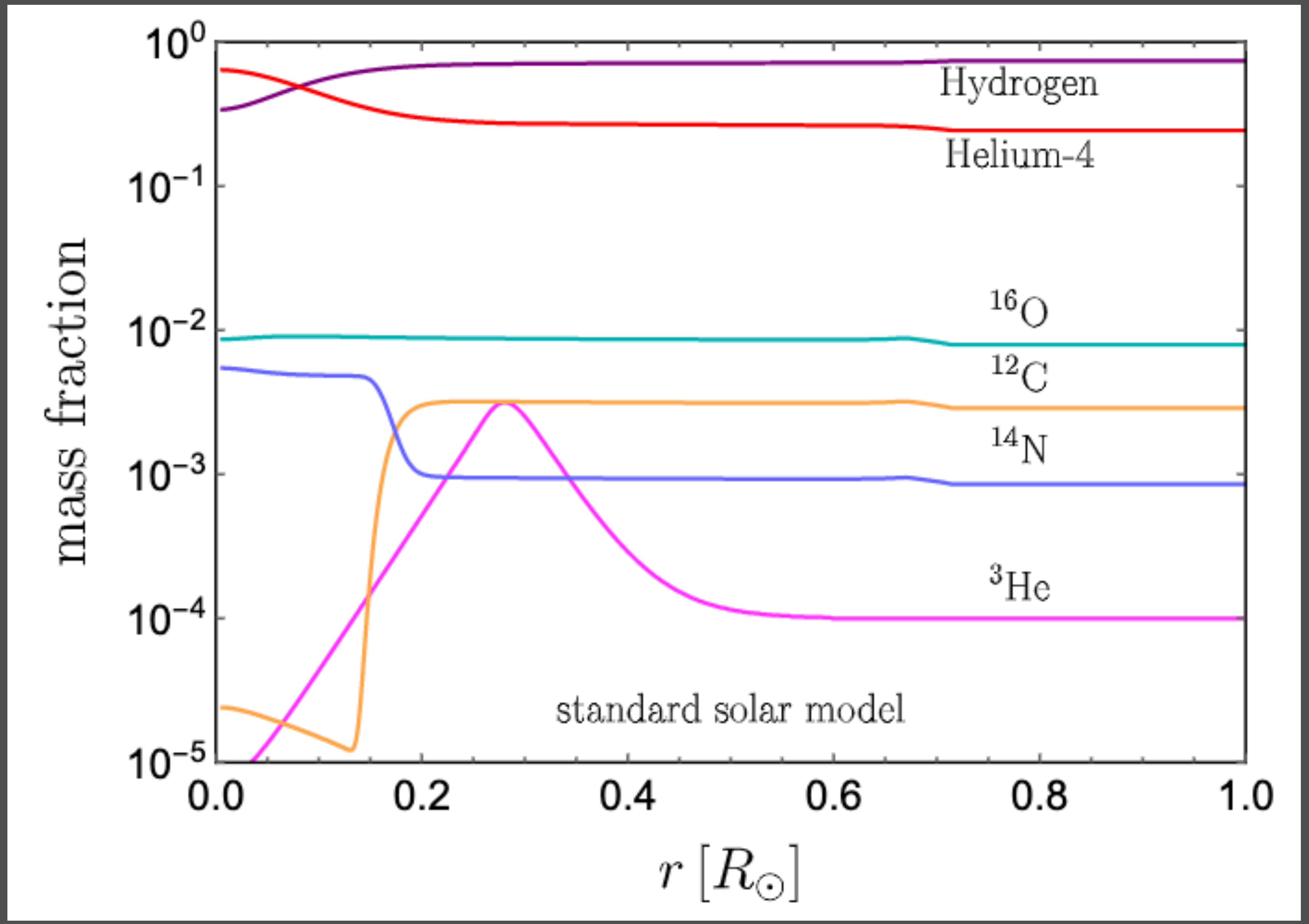

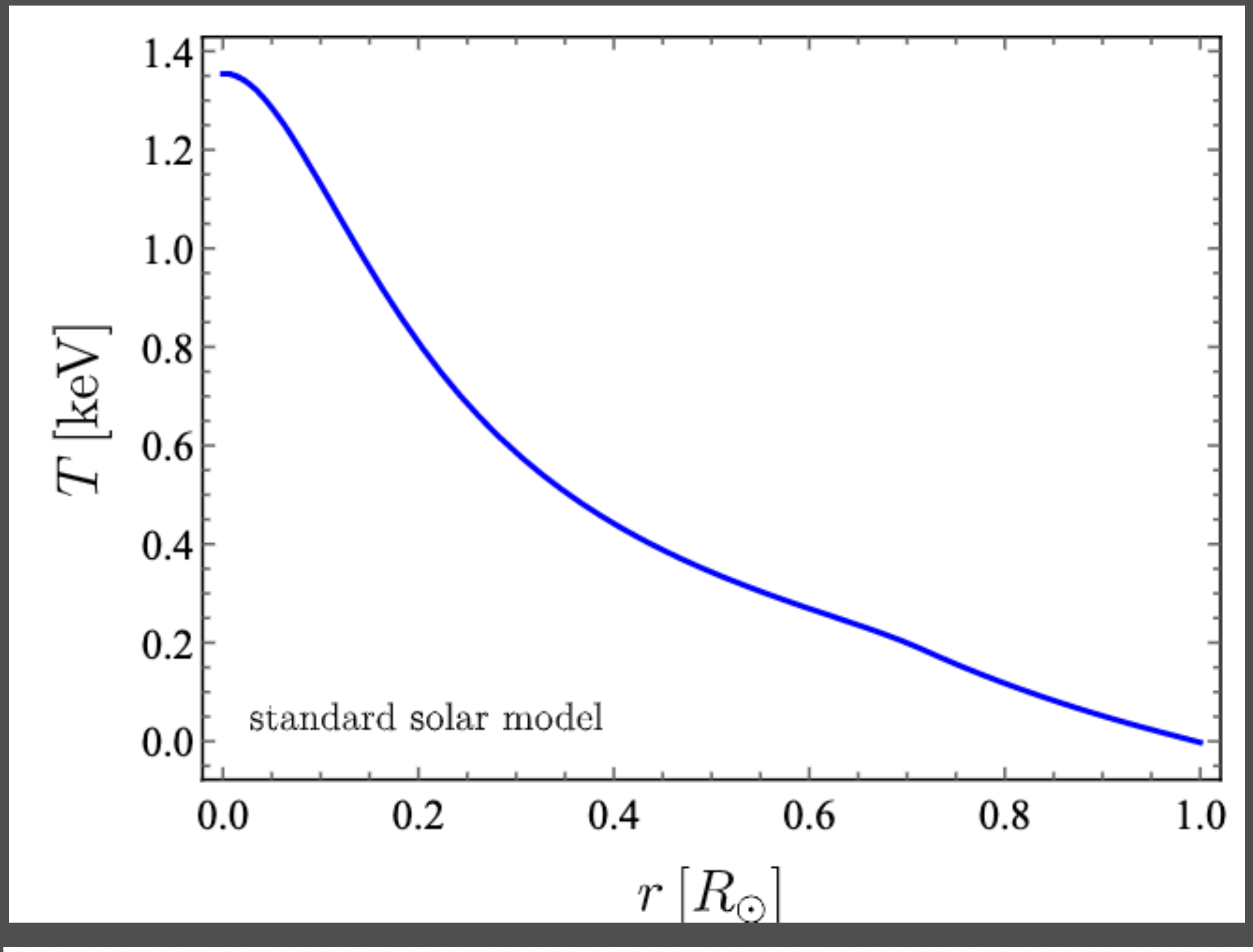

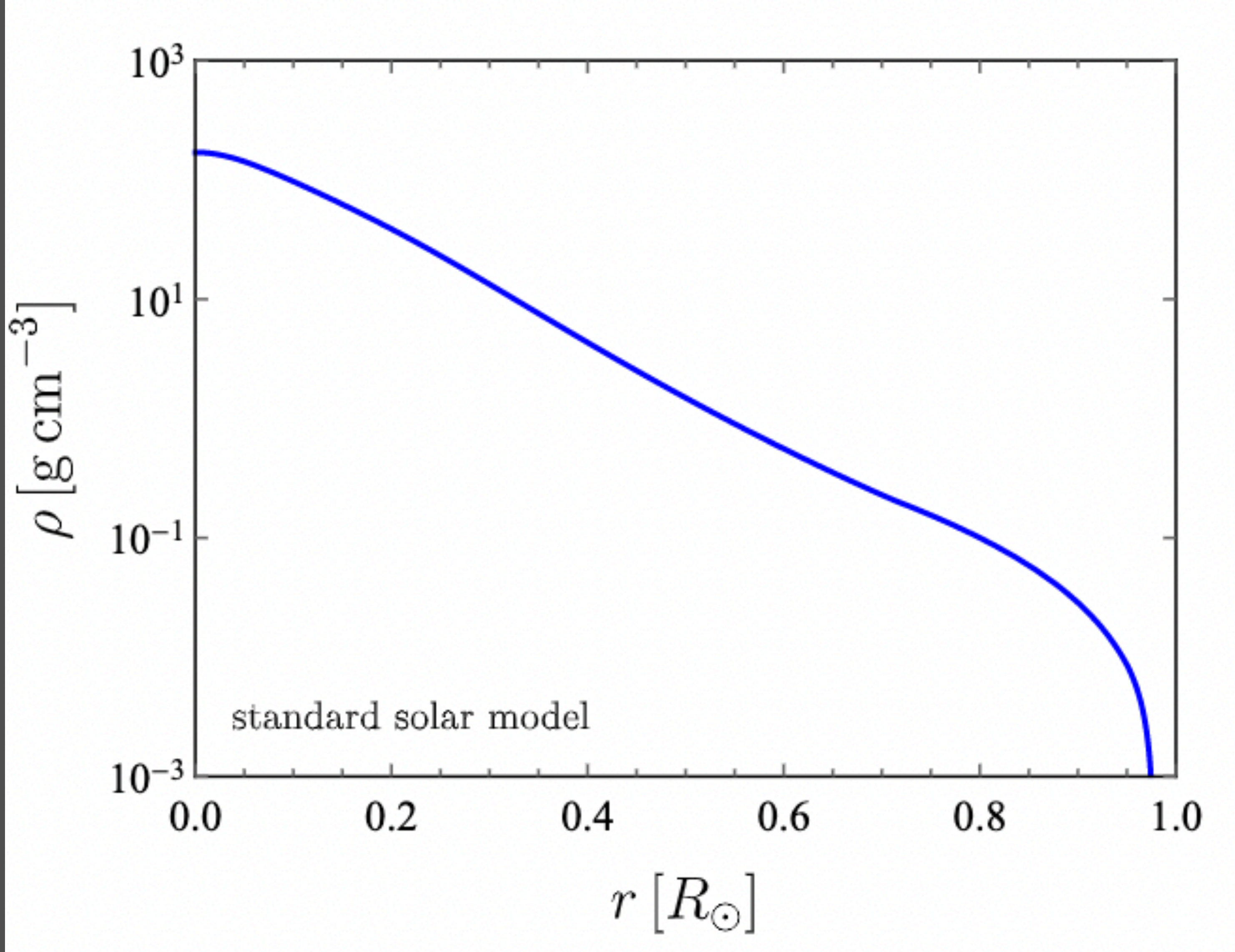

- The Sun is composed of mostly Hydrogen and Helium-4 ions, and their mass fractions are 34% and 64% at the solar core, changing smoothly to 74% and 24% at the solar surface. The remaining 2% mass fraction is Helium-3 and other heavy elements such as Carbon-12, Nitrogen-14 and Oxygen-16.
- In the solar center, the temperature can exceed 1.2 keV, and the density can reach up to $150\,\mathrm{g/cm^3}$

ENERGY EMISSION RATE

$$\mathcal{Q}(r,\phi) = \sum_i \int \mathrm{d}\Pi_5 \sum_{\text{spins}} |\mathcal{M}_i|^2 (2\pi)^4 \delta^4(p_1 + p_2 - p_3 - p_4 - k_S) E_S f_1^{(e)} f_2^{(N_i)} P_{\text{decay}} P_{\text{abs}}$$

ENERGY EMISSION RATE

$$\mathcal{Q}(r,\phi) = \sum_i \int \mathrm{d}\Pi_5 \sum_{\text{spins}} |\mathcal{M}_i|^2 (2\pi)^4 \delta^4(p_1 + p_2 - p_3 - p_4 - k_S) E_S \boxed{f_1^{(e)} f_2^{(N_i)}} P_{\text{decay}} P_{\text{abs}}$$

ENERGY EMISSION RATE

$$\mathcal{Q}(r,\phi) = \sum_i \int \mathrm{d}\Pi_5 \sum_{\text{spins}} |\mathcal{M}_i|^2 (2\pi)^4 \delta^4(p_1 + p_2 - p_3 - p_4 - k_S) E_S f_1^{(e)} f_2^{(N_i)} P_{\text{decay}} P_{\text{abs}}$$

In the solar core, the production of scalar is dominated by

$$e + N \rightarrow e + N + S$$

ENERGY EMISSION RATE

$$\mathcal{Q}(r,\phi) \;=\; \sum_i \int \mathrm{d}\Pi_5 \sum_{\text{spins}} |\mathcal{M}_i|^2 (2\pi)^4 \delta^4(p_1+p_2-p_3-p_4-k_S) E_S f_1^{(e)} f_2^{(N_i)} P_{\text{decay}} P_{\text{abs}}$$

In the solar core, the production of scalar is dominated by

$$e + N \to e + N + S$$

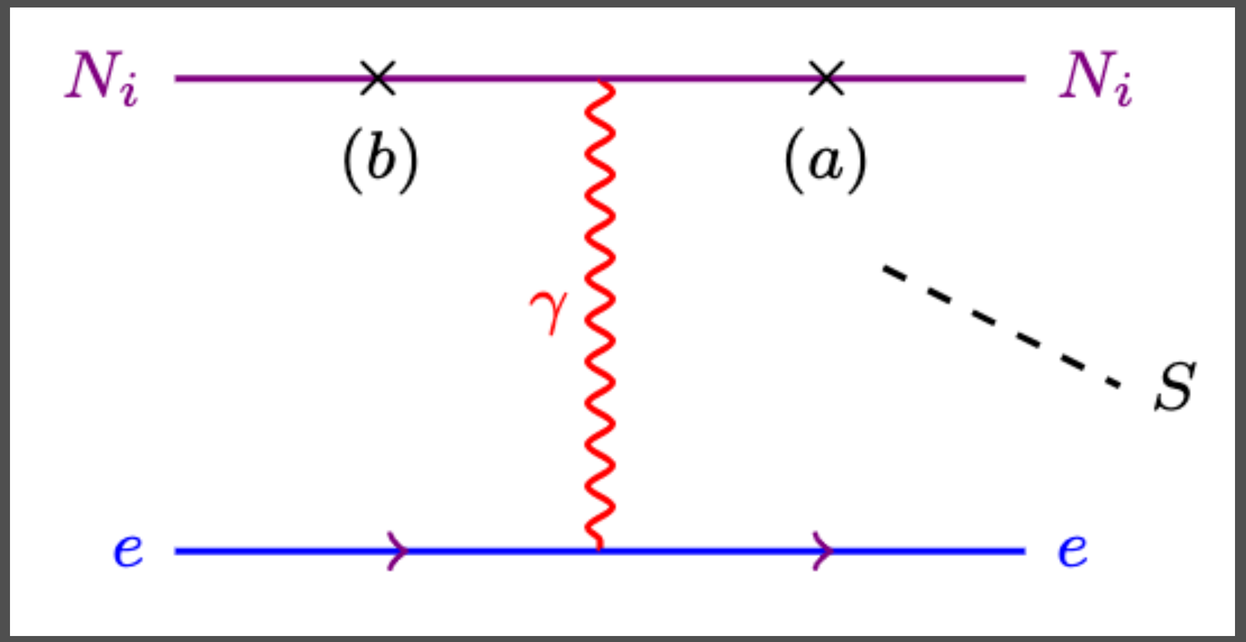

ENERGY EMISSION RATE

$$\mathcal{Q}(r,\phi) = \sum_i \int \mathrm{d}\Pi_5 \sum_{\text{spins}} |\mathcal{M}_i|^2 (2\pi)^4 \delta^4(p_1 + p_2 - p_3 - p_4 - k_S) E_S f_1^{(e)} f_2^{(N_i)} P_{\text{decay}} P_{\text{abs}}$$

$$P_{decay}(r,\phi) = \exp\left[-d(r,\phi)\,\Gamma_S\right]$$

decay probability

In the solar core, the production of scalar is dominated by

$$e + N \rightarrow e + N + S$$

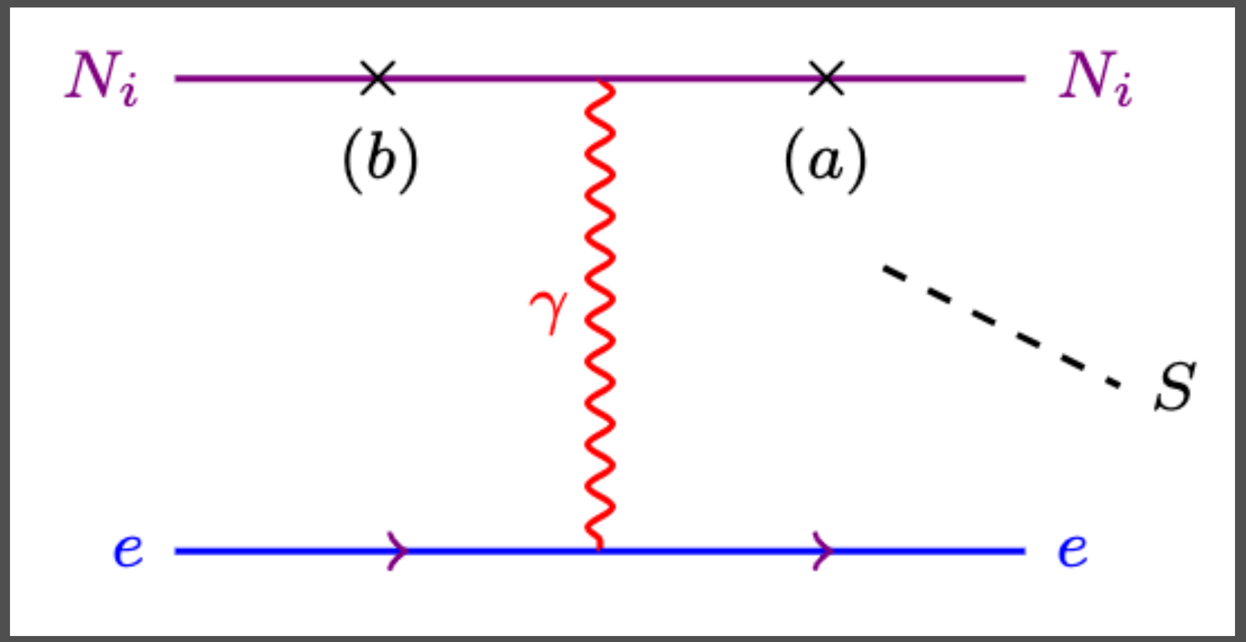

ENERGY EMISSION RATE

$$\mathcal{Q}(r,\phi) \quad = \quad \sum_i \int \mathrm{d}\Pi_5 \sum_{\text{spins}} |\mathcal{M}_i|^2 (2\pi)^4 \delta^4(p_1+p_2-p_3-p_4-k_S) E_S f_1^{(e)} f_2^{(N_i)} P_{\text{decay}} P_{\text{abs}}$$

$$P_{decay}(r,\phi) = \exp\left[-d(r,\phi)\,\Gamma_S\right]$$

decay probability

$$\Gamma_S = \frac{m_S}{E_S}\Gamma_{0,S}$$

$$\Gamma_0(S \to \gamma\gamma) = \frac{121}{9}\frac{\alpha^2 m_S^3 \sin^2\theta}{512\pi^3 v_{\text{EW}}^2}$$

In the solar core, the production of scalar is dominated by

$$e + N \to e + N + S$$

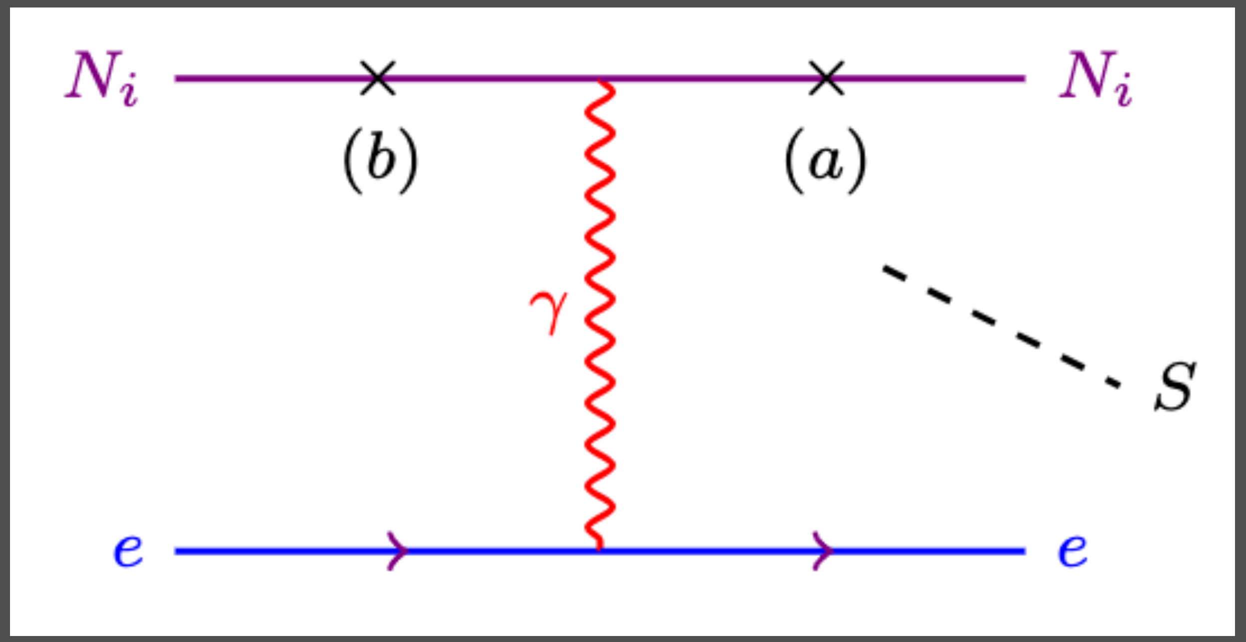

ENERGY EMISSION RATE

$$\mathcal{Q}(r,\phi) = \sum_i \int d\Pi_5 \sum_{\text{spins}} |\mathcal{M}_i|^2 (2\pi)^4 \delta^4(p_1+p_2-p_3-p_4-k_S) E_S \boxed{f_1^{(e)} f_2^{(N_i)}} P_{\text{decay}} P_{\text{abs}}$$

$$P_{decay}(r,\phi) = \exp\left[-d(r,\phi)\,\Gamma_S\right]$$

decay probability

$$\Gamma_S = \frac{m_S}{E_S}\boxed{\Gamma_{0,S}} \longrightarrow \Gamma_0(S\to\gamma\gamma) = \frac{121}{9}\frac{\alpha^2 m_S^3 \sin^2\theta}{512\pi^3 v_{\text{EW}}^2}$$

$$P_{abs}(r,\phi) = Exp\left[-\int_0^d \frac{dr'}{\lambda[L(r,\phi,r')]}\right]$$

Absorption due to inverse BR

$$e+N+S \to e+N$$

In the solar core, the production of scalar is dominated by

$$e+N \to e+N+S$$

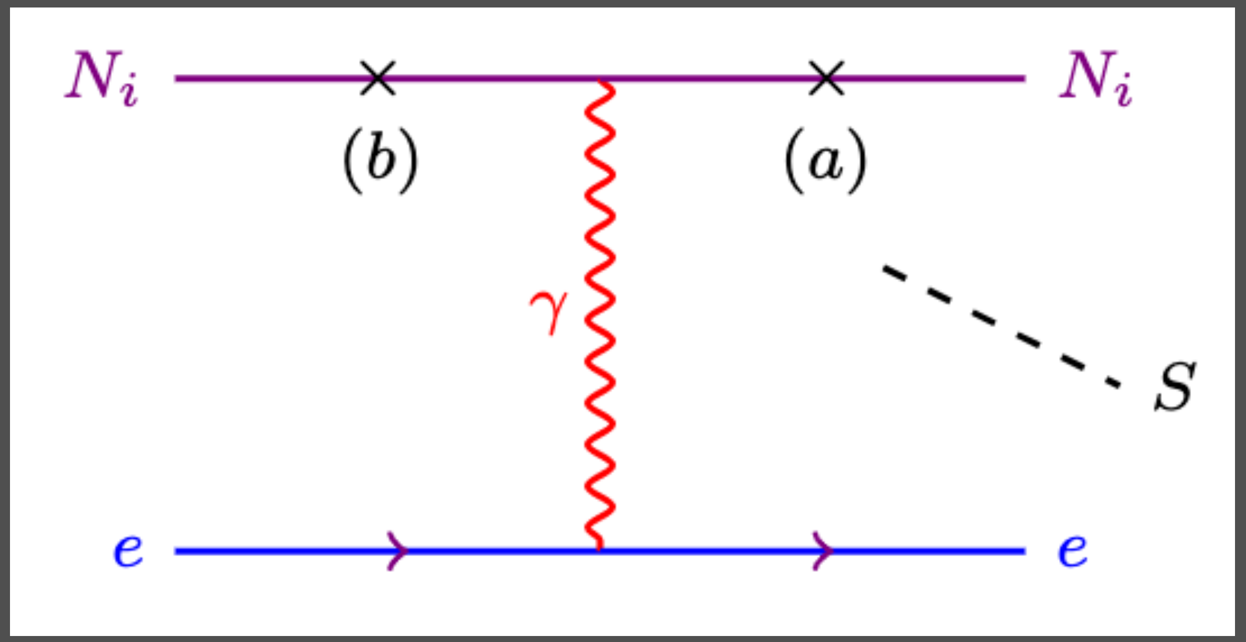

ENERGY EMISSION RATE

$$\mathcal{Q}(r,\phi) = \sum_i \int d\Pi_5 \sum_{\text{spins}} |\mathcal{M}_i|^2 (2\pi)^4 \delta^4(p_1+p_2-p_3-p_4-k_S) E_S f_1^{(e)} f_2^{(N_i)} P_{\text{decay}} P_{\text{abs}}$$

$$P_{decay}(r,\phi) = \exp\left[-d(r,\phi)\,\Gamma_S\right]$$

decay probability

$$\Gamma_S = \frac{m_S}{E_S}\Gamma_{0,S} \longrightarrow \Gamma_0(S\to\gamma\gamma) = \frac{121}{9}\frac{\alpha^2 m_S^3 \sin^2\theta}{512\pi^3 v_{\text{EW}}^2}$$

Absorption due to inverse BR

$$P_{abs}(r,\phi) = Exp\left[-\int_0^d \frac{dr'}{\lambda[L(r,\phi,r')]}\right]$$

$$e + N + S \to e + N$$

In the solar core, the production of scalar is dominated by

$$e + N \to e + N + S$$

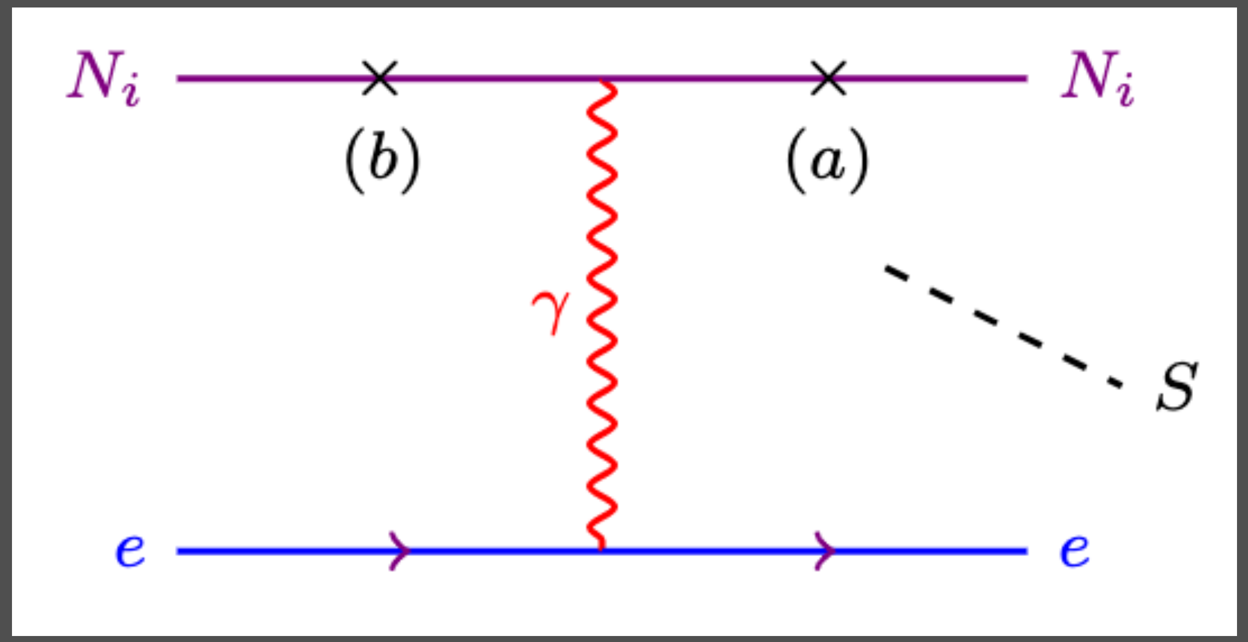

$$\frac{Q_{\text{B}}^{(NN)}}{Q_{\text{B}}^{(eN)}} \sim \frac{(2m_N/m_\pi)^4 A_N^4 f_{pp}^4}{e^4}\frac{m_e^2}{m_N^2}\frac{T^4}{m_\pi^4}\frac{m_S^2}{m_N^2} \ll 1\,.$$

ENERGY EMISSION RATE

$$\mathcal{Q}(r,\phi) = \sum_i \int d\Pi_5 \sum_{\text{spins}} |\mathcal{M}_i|^2 (2\pi)^4 \delta^4(p_1+p_2-p_3-p_4-k_S) E_S\, f_1^{(e)} f_2^{(N_i)} P_{\rm decay} P_{\rm abs}$$

$$P_{decay}(r,\phi) = \exp\left[-d(r,\phi)\,\Gamma_S\right]$$

decay probability

$$\Gamma_S = \frac{m_S}{E_S}\Gamma_{0,S} \longrightarrow \Gamma_0(S\to\gamma\gamma) = \frac{121}{9}\frac{\alpha^2 m_S^3 \sin^2\theta}{512\pi^3 v_{\rm EW}^2}$$

$$P_{abs}(r,\phi) = Exp\left[-\int_0^d \frac{dr'}{\lambda[L(r,\phi,r')]}\right]$$

MFP depends on the
star density and temperature profiles

Absorption due to inverse BR

$$e + N + S \to e + N$$

In the solar core, the production of scalar is dominated by

$$e + N \to e + N + S$$

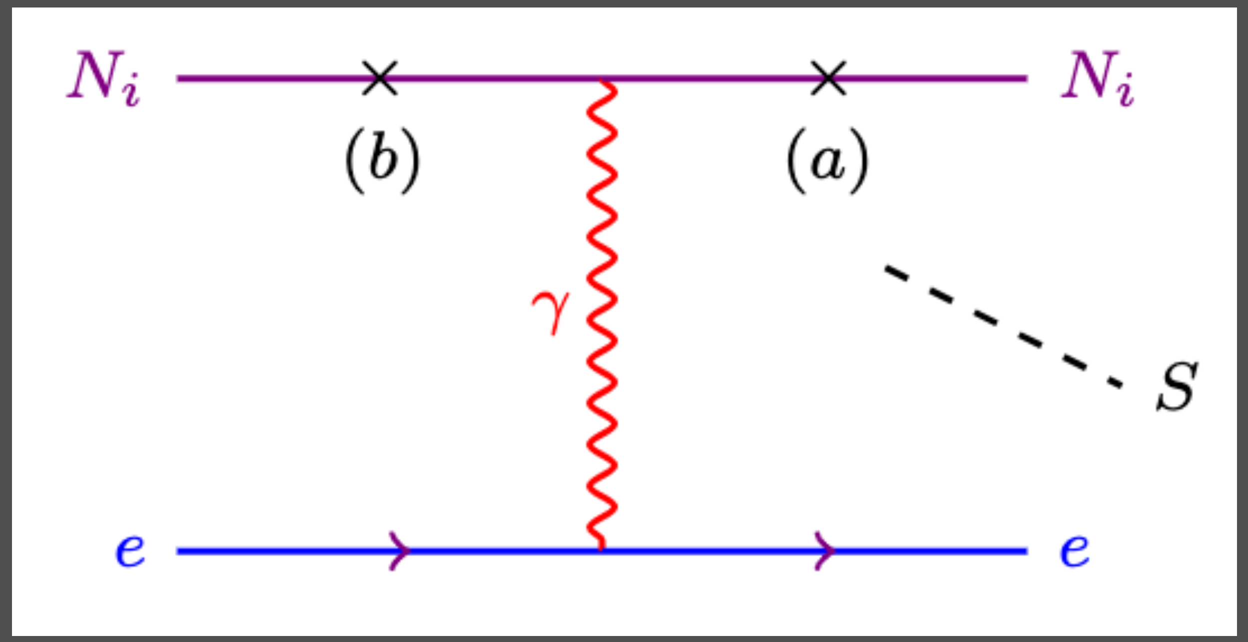

$$\frac{Q_{\rm B}^{(NN)}}{Q_{\rm B}^{(eN)}} \sim \frac{(2m_N/m_\pi)^4 A_N^4 f_{pp}^4}{e^4}\frac{m_e^2}{m_N^2}\frac{T^4}{m_\pi^4}\frac{m_S^2}{m_N^2} \ll 1\,.$$

ENERGY EMISSION RATE

$$\mathcal{Q}(r,\phi) \quad = \quad \sum_i \int d\Pi_5 \sum_{\text{spins}} |\mathcal{M}_i|^2 (2\pi)^4 \delta^4(p_1 + p_2 - p_3 - p_4 - k_S) E_S f_1^{(e)} f_2^{(N_i)} P_{\text{decay}} P_{\text{abs}}$$

In the solar core, the production of scalar is dominated by

$$e + N \to e + N + S$$

$$P_{decay}(r,\phi) = \exp\left[-d(r,\phi)\,\Gamma_S\right]$$

decay probability

$$\Gamma_S = \frac{m_S}{E_S}\Gamma_{0,S}$$

$$\Gamma_0(S \to \gamma\gamma) = \frac{121}{9}\,\frac{\alpha^2 m_S^3 \sin^2\theta}{512\pi^3 v_{\text{EW}}^2}$$

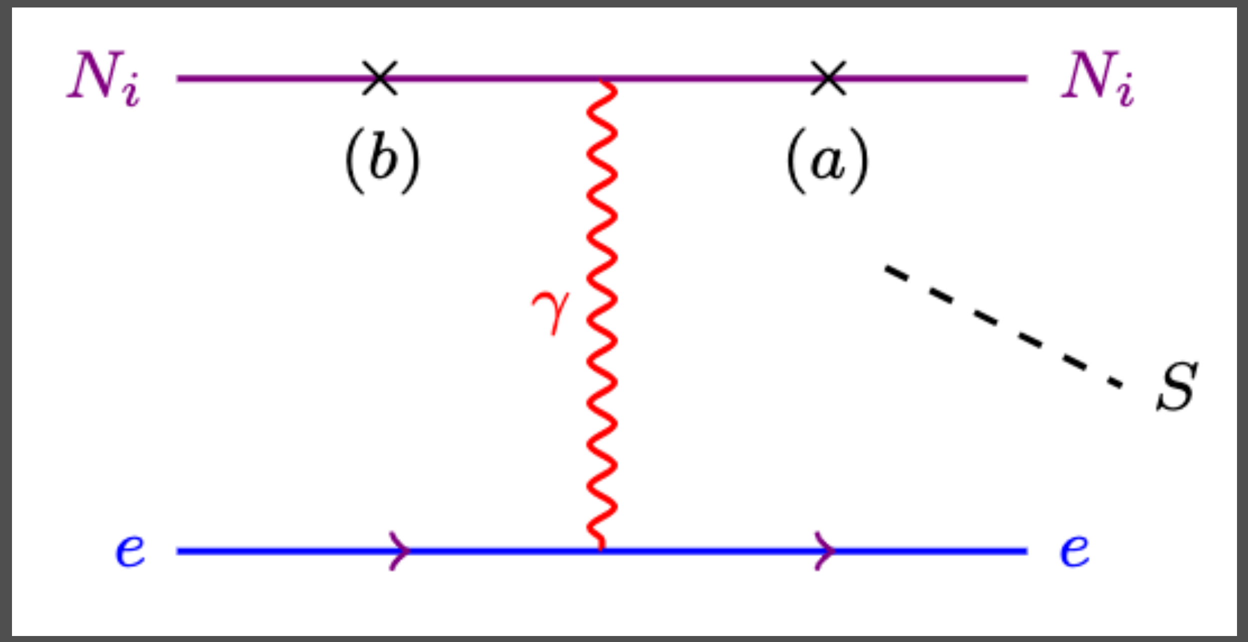

$$P_{abs}(r,\phi) = Exp\left[-\int_0^d \frac{dr'}{\lambda[L(r,\phi,r')]}\right]$$

Absorption due to inverse BR

$$e + N + S \to e + N$$

$$\frac{Q_{\text{B}}^{(NN)}}{Q_{\text{B}}^{(eN)}} \sim \frac{(2m_N/m_\pi)^4 A_N^4 f_{pp}^4}{e^4}\,\frac{m_e^2}{m_N^2}\,\frac{T^4}{m_\pi^4}\,\frac{m_S^2}{m_N^2} \ll 1\,.$$

MFP depends on the star density and temperature profiles

$$\lambda^{-1}(r;x) \quad = \quad \frac{1}{2E_S}\int d\Pi_4 \mathcal{S} \sum_{\text{spins}} |\mathcal{M}|^2 (2\pi)^4 \delta^4(p_1 + p_2 - p_3 - p_4 + k_S) f_1 f_2$$

ENERGY EMISSION RATE

$$\mathcal{Q}(r,\phi) \quad = \quad \sum_i \int \mathrm{d}\Pi_5 \sum_{\mathrm{spins}} |\mathcal{M}_i|^2 (2\pi)^4 \delta^4(p_1 + p_2 - p_3 - p_4 - k_S) E_S \, f_1^{(e)} f_2^{(N_i)} P_{\mathrm{decay}} P_{\mathrm{abs}}$$

$$P_{decay}(r,\phi) = \exp\left[-d(r,\phi)\,\Gamma_S\right]$$

decay probability

$$\Gamma_S = \frac{m_S}{E_S}\Gamma_{0,S}$$

$$\Gamma_0(S \to \gamma\gamma) = \frac{121}{9}\frac{\alpha^2 m_S^3 \sin^2\theta}{512\pi^3 v_{\mathrm{EW}}^2}$$

$$P_{abs}(r,\phi) = Exp\left[-\int_0^d \frac{dr'}{\lambda[L(r,\phi,r')]}\right]$$

Absorption due to inverse BR

$$e + N + S \to e + N$$

MFP depends on the
star density and temperature profiles

$$\lambda^{-1}(r;x) \quad = \quad \frac{1}{2E_S}\int \mathrm{d}\Pi_4 \mathcal{S} \sum_{\mathrm{spins}} |\mathcal{M}|^2 (2\pi)^4 \delta^4(p_1 + p_2 - p_3 - p_4 + k_S) f_1 f_2$$

In the solar core, the production of scalar is dominated by

$$e + N \to e + N + S$$

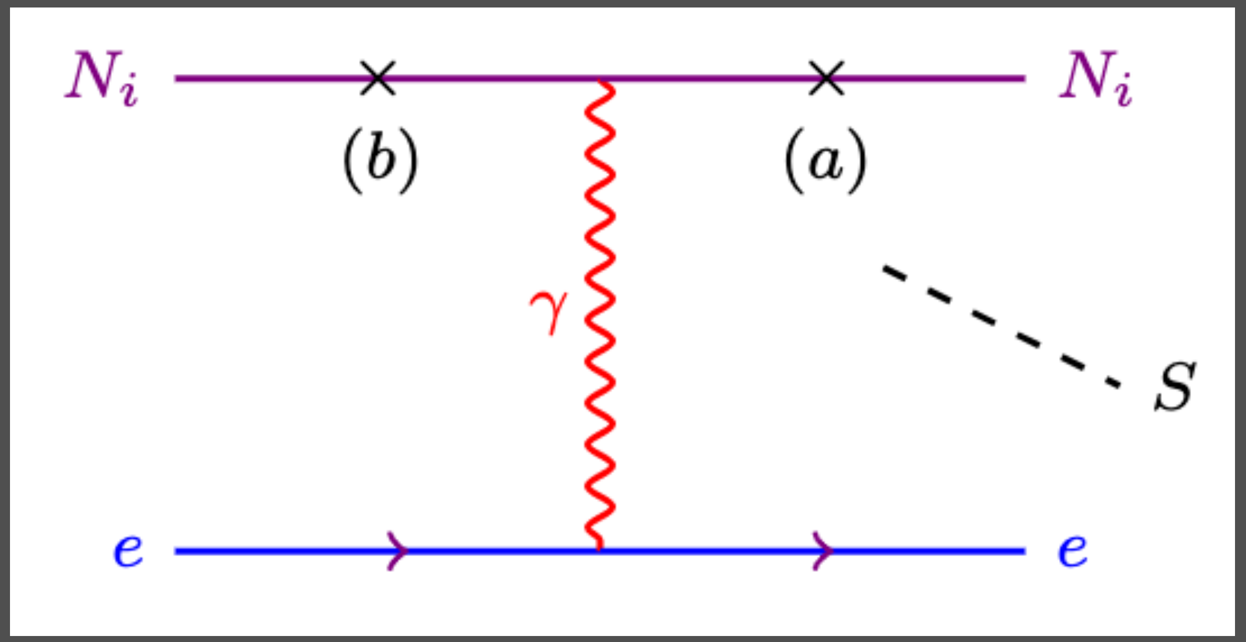

$$\frac{Q_{\mathrm{B}}^{(NN)}}{Q_{\mathrm{B}}^{(eN)}} \sim \frac{(2m_N/m_\pi)^4 A_N^4 f_{pp}^4}{e^4}\frac{m_e^2}{m_N^2}\frac{T^4}{m_\pi^4}\frac{m_S^2}{m_N^2} \ll 1\,.$$

In the case of constant MFP λ, the absorption factor simply reduces to $\exp\{-d/\lambda\}$.

SUN LIMITS

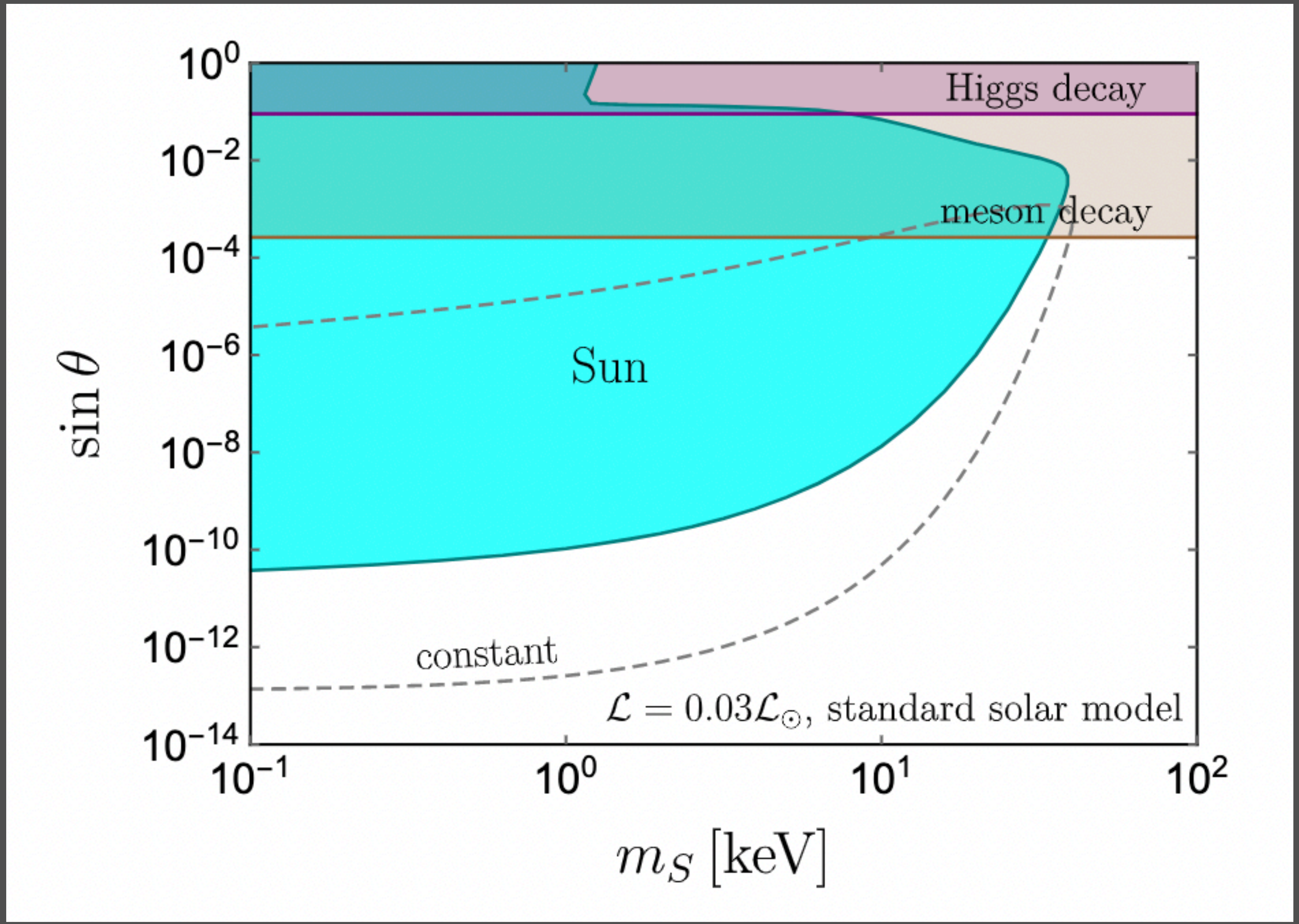

Higgs decay
meson decay
Sun
constant
$\mathcal{L} = 0.03\mathcal{L}_\odot$, standard solar model
$\sin\theta$
m_S [keV]
10^{0}
10^{-2}
10^{-4}
10^{-6}
10^{-8}
10^{-10}
10^{-12}
10^{-14}
10^{-1}
10^{0}
10^{1}
10^{2}

SUN LIMITS

- To set limits on the scalar mass m_S and the mixing angle $\sin\theta$, we conservatively require that the luminosity $\mathscr{L}_S$ is smaller than 3% of the measured neutrino luminosity i.e. $\mathscr{L}_S < 1.2 \times 10^{32}\ \mathrm{erg/sec}$

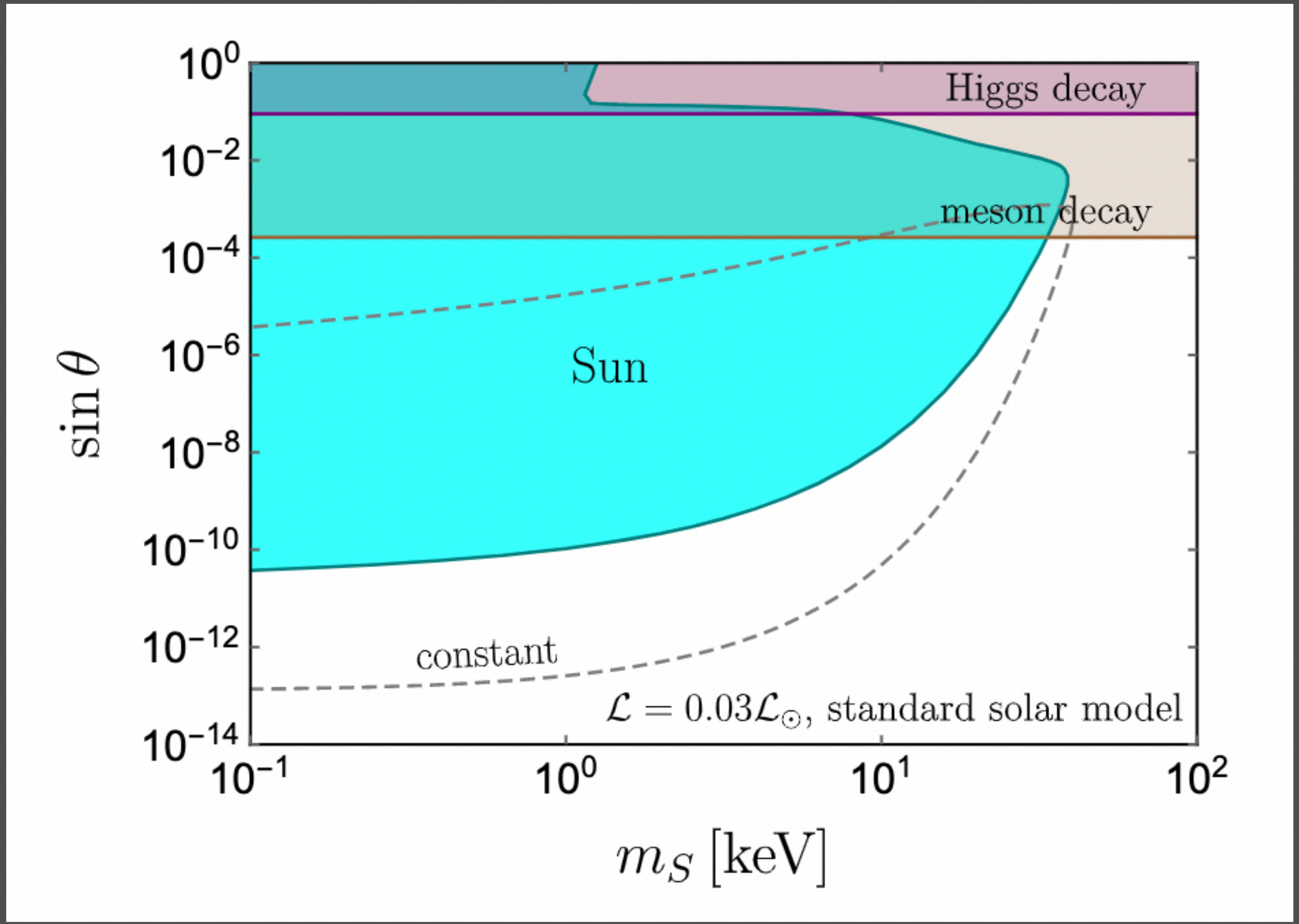

SUN LIMITS

- To set limits on the scalar mass m_S and the mixing angle $\sin\theta$, we conservatively require that the luminosity $\mathscr{L}_S$ is smaller than 3% of the measured neutrino luminosity i.e. $\mathscr{L}_S < 1.2 \times 10^{32}$ erg/sec

- The complimentary collider limits from: Higgs to invisible and meson decays are also shown

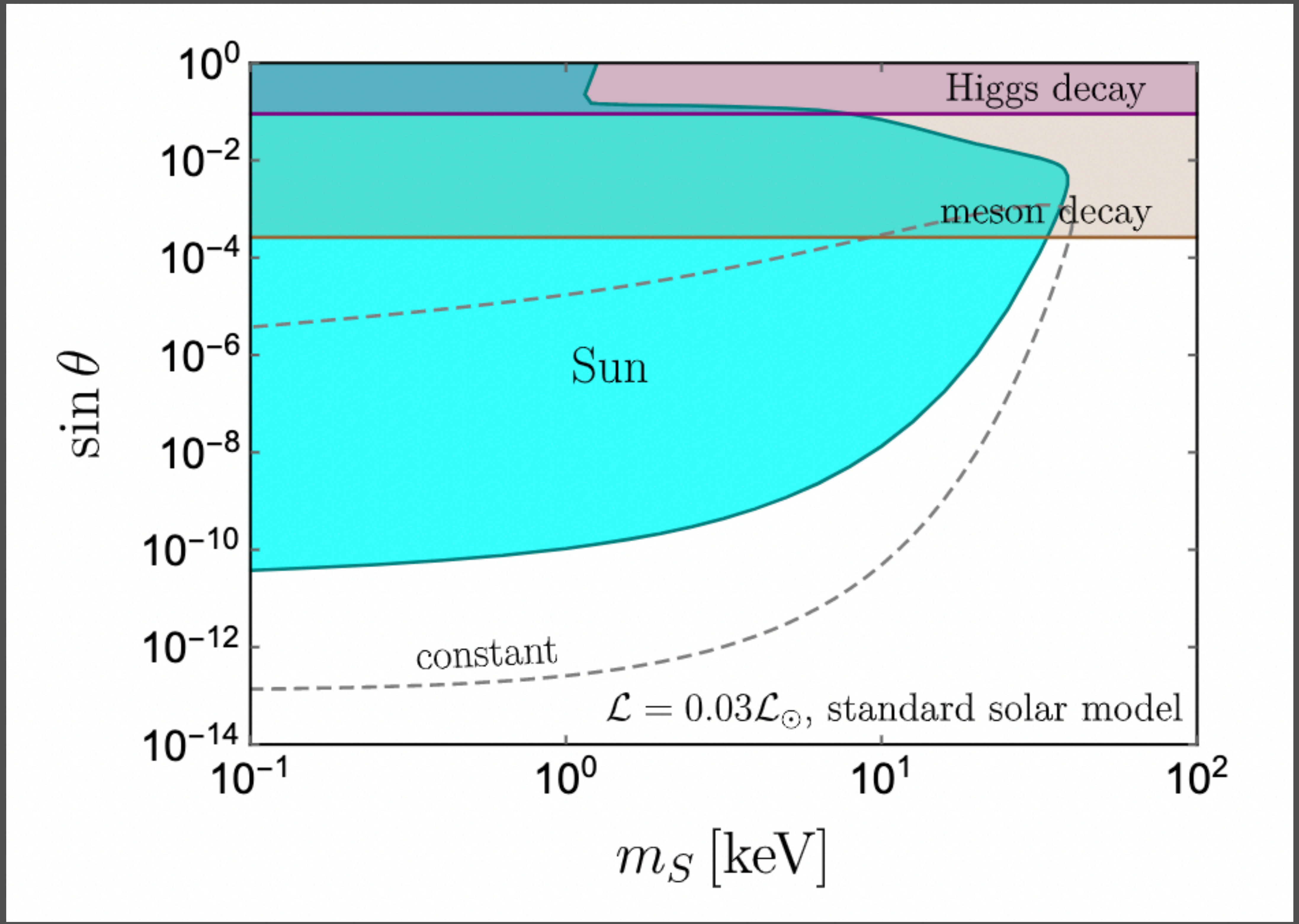

SUN LIMITS

- To set limits on the scalar mass m_S and the mixing angle $\sin\theta$, we conservatively require that the luminosity $\mathscr{L}_S$ is smaller than 3% of the measured neutrino luminosity i.e. $\mathscr{L}_S < 1.2 \times 10^{32}$ erg/sec

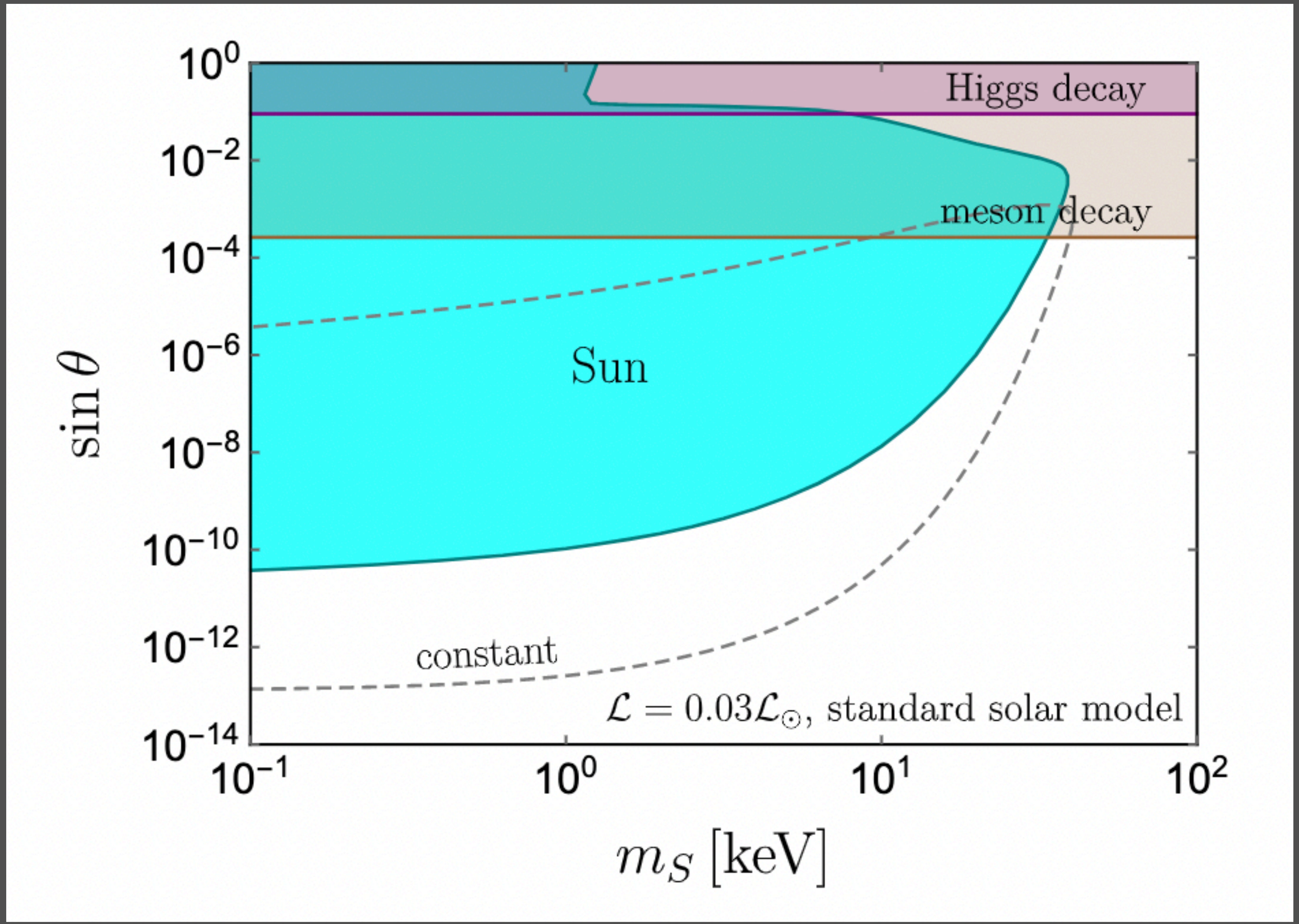

- The complimentary collider limits from: Higgs to invisible and meson decays are also shown

- The dashed (constant case) is shown for constant temperature $T = 1$ keV and electron number density $n_e = 1.2 \times 10^{26}\,\mathrm{cm}^{-3}$.

WHITE DWARF AND RED GIANT LIMITS

Star	Core composition	T [keV]	n_e [cm^{-3}]	R [cm]	$\mathcal{L}/\mathcal{L}_\odot$
RGs [130, 131]	^{4}He	10	3×10^{27}	6×10^8	2.8
WDs [4, 132–134]	50% ^{12}C 50% ^{16}O	6	10^{30}	10^9	10^{-5}

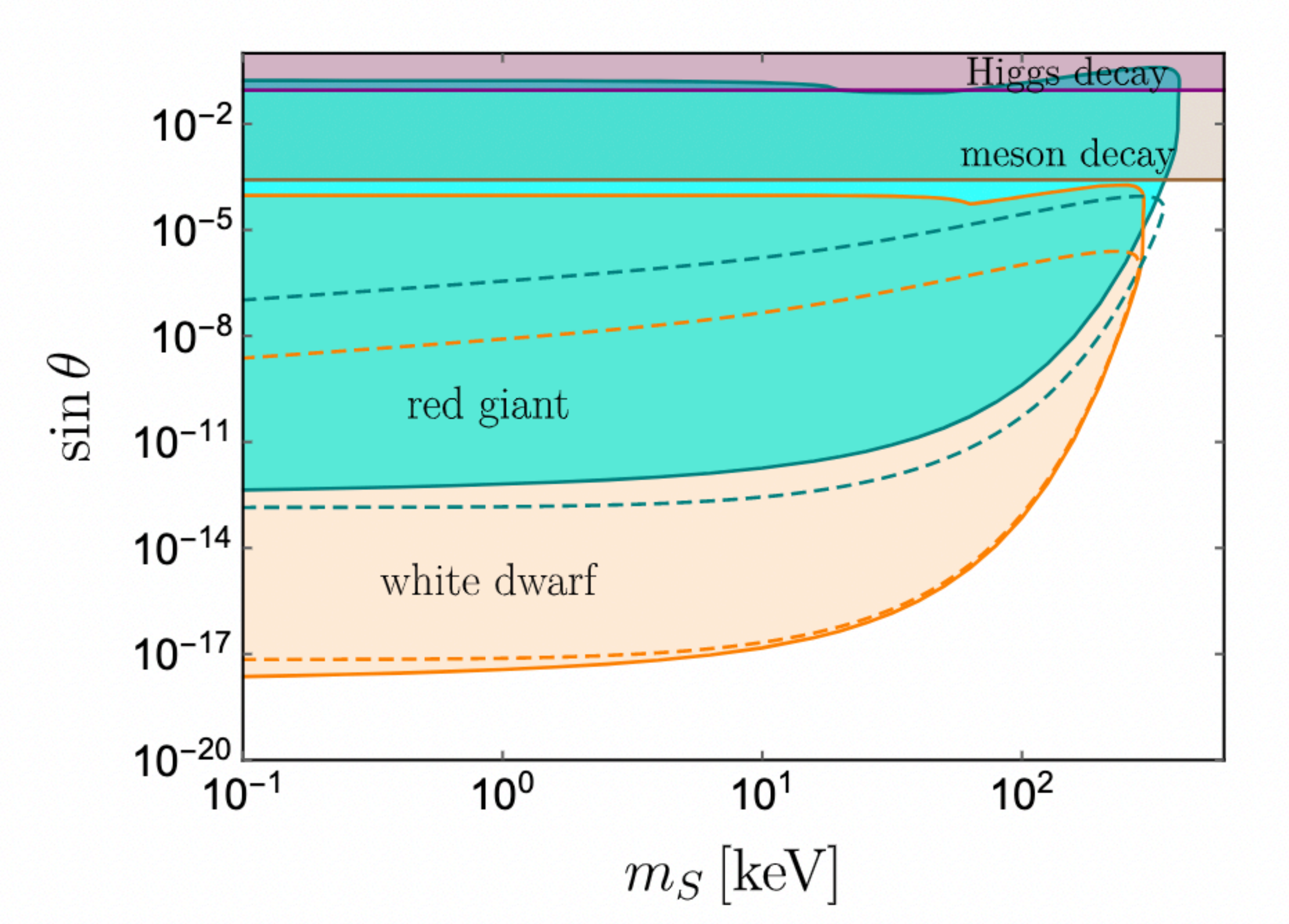

WHITE DWARF AND RED GIANT LIMITS

- The limits derived from SN1987A and the Sun with radial stellar profiles computed from the equation-of-state can also be applied to other stars, notably WDs and RGs. However, the profiles of these stars suffer from much larger uncertainties.

Star	Core composition	T [keV]	n_e [cm^{-3}]	R [cm]	$\mathcal{L}/\mathcal{L}_\odot$
RGs [130, 131]	^{4}He	10	3×10^{27}	6×10^8	2.8
WDs [4, 132–134]	50% ^{12}C 50% ^{16}O	6	10^{30}	10^9	10^{-5}

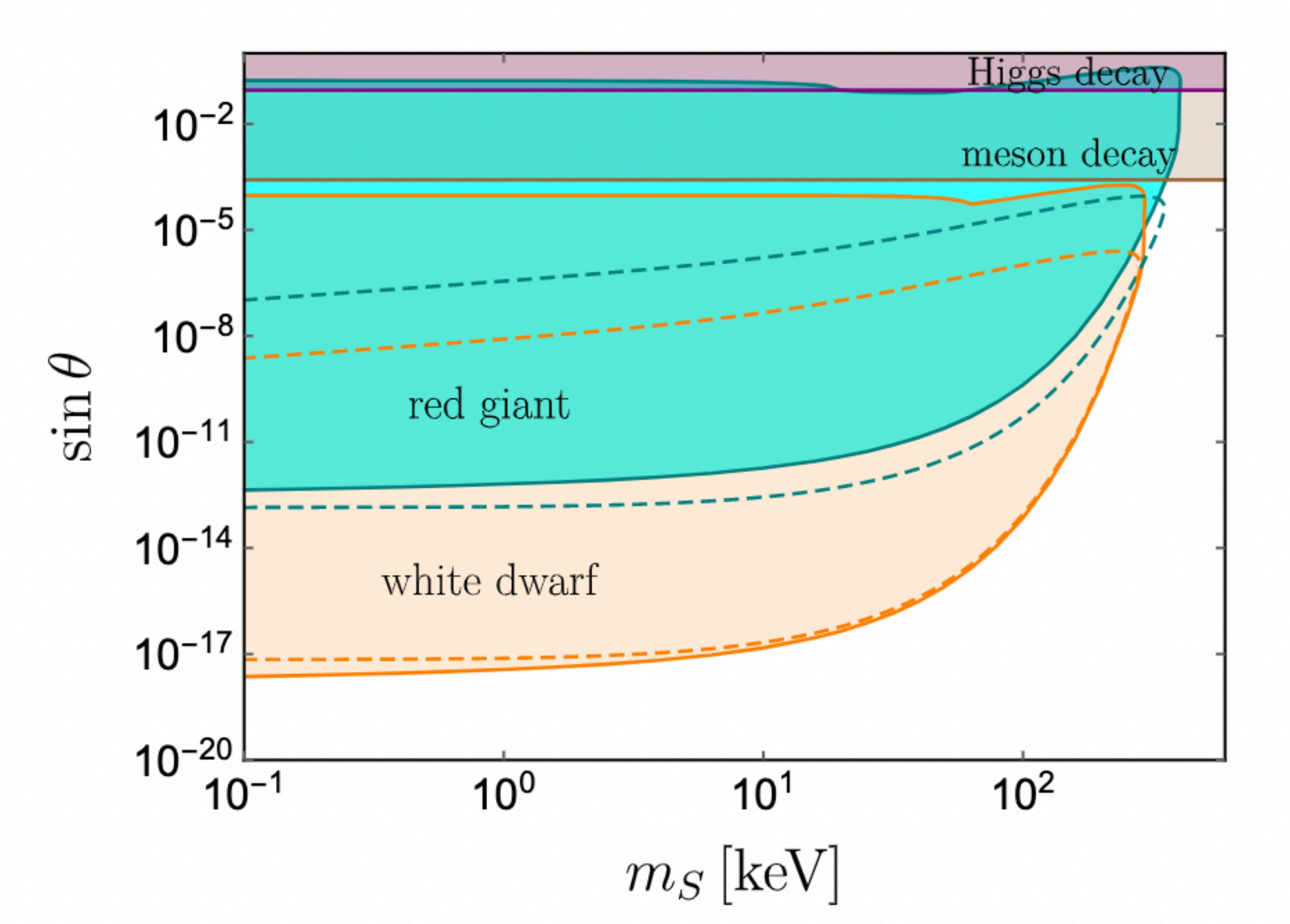

WHITE DWARF AND RED GIANT LIMITS

- The limits derived from SN1987A and the Sun with radial stellar profiles computed from the equation-of-state can also be applied to other stars, notably WDs and RGs. However, the profiles of these stars suffer from much larger uncertainties.

- Therefore, we will assume the baryon densities in these stars are constant. However, we will consider the dependence of the decay and absorption factors on the geometric parameters r and ϕ.

Star	Core composition	T [keV]	n_e [cm^{-3}]	R [cm]	$\mathcal{L}/\mathcal{L}_\odot$
RGs [130, 131]	^{4}He	10	3×10^{27}	6×10^8	2.8
WDs [4, 132–134]	50% ^{12}C 50% ^{16}O	6	10^{30}	10^9	10^{-5}

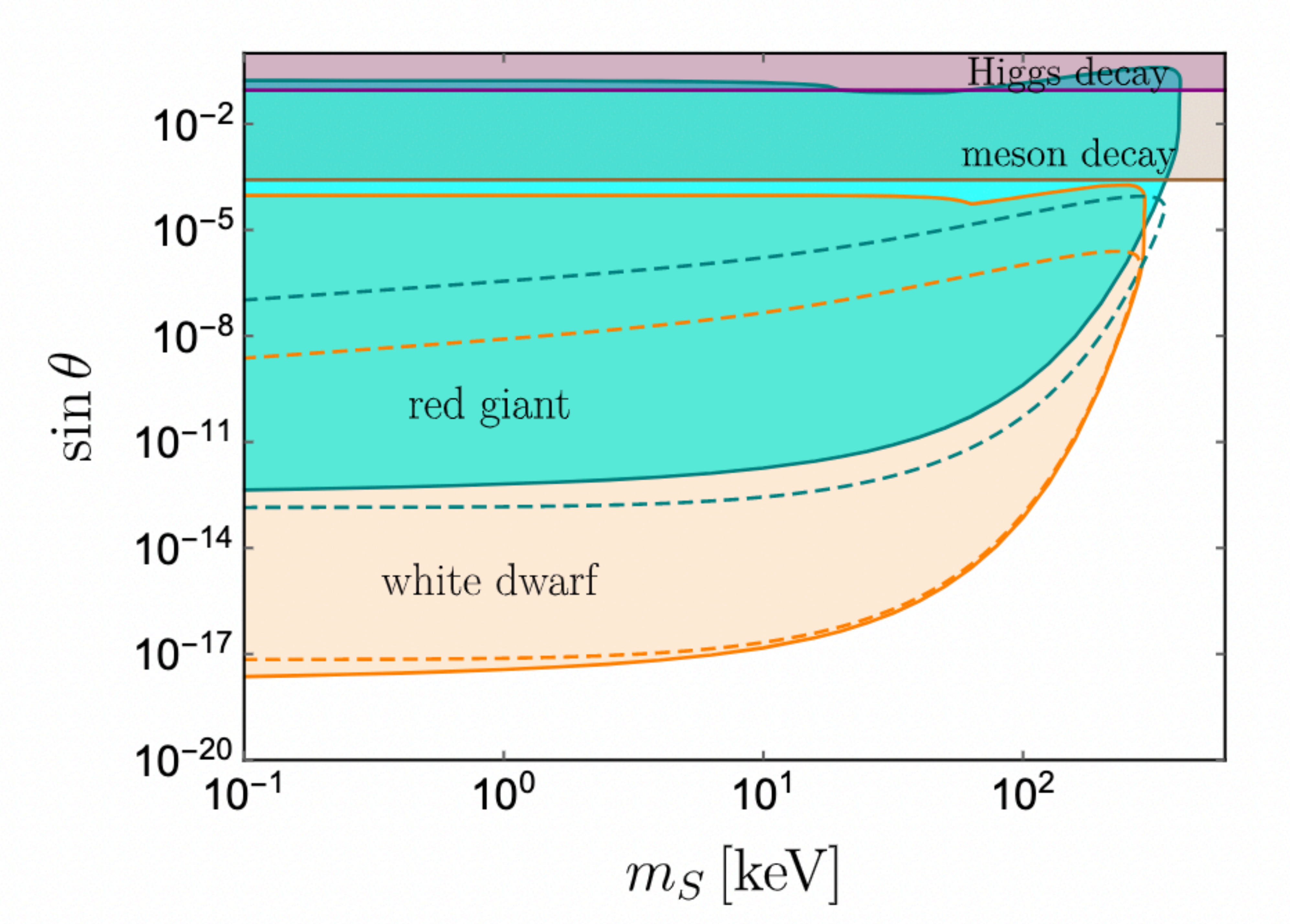

WHITE DWARF AND RED GIANT LIMITS

- The limits derived from SN1987A and the Sun with radial stellar profiles computed from the equation-of-state can also be applied to other stars, notably WDs and RGs. However, the profiles of these stars suffer from much larger uncertainties.

- Therefore, we will assume the baryon densities in these stars are constant. However, we will consider the dependence of the decay and absorption factors on the geometric parameters r and ϕ.

Star	Core composition	T [keV]	n_e [cm^{-3}]	R [cm]	$\mathcal{L}/\mathcal{L}_\odot$
RGs [130, 131]	^{4}He	10	3×10^{27}	6×10^8	2.8
WDs [4, 132–134]	50% ^{12}C 50% ^{16}O	6	10^{30}	10^9	10^{-5}

- Stellar parameters for the RGs and WDs: the dominant elements in the core and their mass fractions, core temperatures T, electron number densities n_e, sizes R, and the luminosity limits in unit of the solar luminosity of $\mathscr{L}_\odot = 4 \times 10^{33}$ erg/sec.

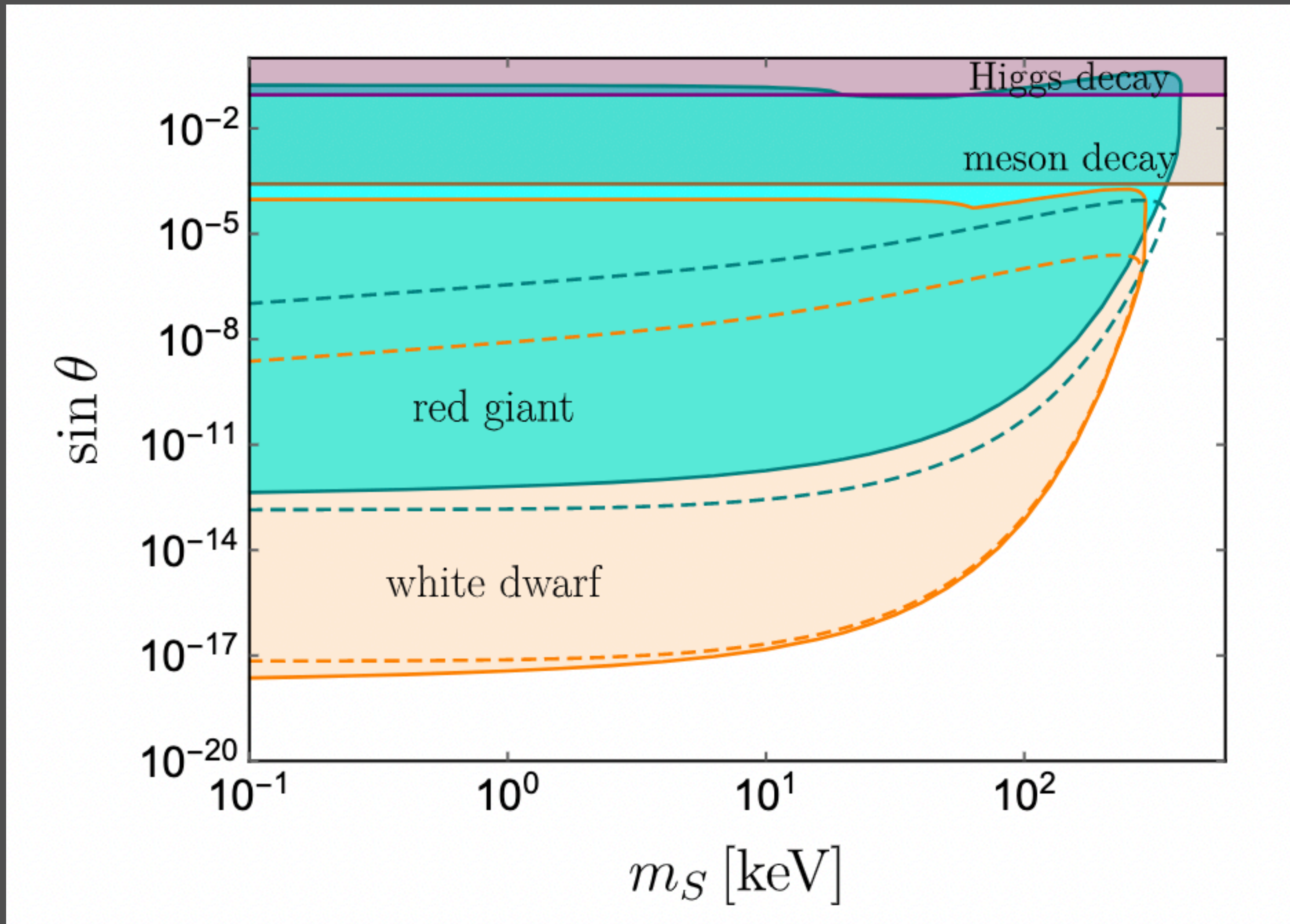

SUMMARY OF ASTROPHYSICAL LIMITS

Star	Profile	Geometry	$\sin\theta$ range	m_S range
SN1987A	–	–	$2.4 \times 10^{-7} - 9.0 \times 10^{-6}$	< 249 MeV
	Fischer $11.8 M_\odot$	✓	$1.2 \times 10^{-7} - 6.4 \times 10^{-5}$	< 204 MeV
	Fischer $18 M_\odot$	✓	$1.0 \times 10^{-7} - 4.7 \times 10^{-5}$	< 238 MeV
	Nakazato $13 M_\odot$	✓	$1.1 \times 10^{-7} - 5.4 \times 10^{-5}$	< 224 MeV
Sun	–	–	$1.4 \times 10^{-13} - 1.2 \times 10^{-3}$	< 40 keV
	standard solar model	✓	$3.8 \times 10^{-11} - 1$	< 39 keV
RGs	–	–	$1.4 \times 10^{-13} - 1.0 \times 10^{-7}$	< 350 keV
	–	✓	$4.4 \times 10^{-13} - 0.4$	< 404 keV
WDs	–	–	$7.0 \times 10^{-18} - 2.4 \times 10^{-9}$	< 282 keV
	–	✓	$2.3 \times 10^{-18} - 1.9 \times 10^{-4}$	< 294 keV

SUMMARY OF ASTROPHYSICAL LIMITS

We may summarise the limits from the objects considered as shown below

Star	Profile	Geometry	$\sin\theta$ range	m_S range
SN1987A	–	–	$2.4 \times 10^{-7} - 9.0 \times 10^{-6}$	< 249 MeV
	Fischer $11.8 M_\odot$	✓	$1.2 \times 10^{-7} - 6.4 \times 10^{-5}$	< 204 MeV
	Fischer $18 M_\odot$	✓	$1.0 \times 10^{-7} - 4.7 \times 10^{-5}$	< 238 MeV
	Nakazato $13 M_\odot$	✓	$1.1 \times 10^{-7} - 5.4 \times 10^{-5}$	< 224 MeV
Sun	–	–	$1.4 \times 10^{-13} - 1.2 \times 10^{-3}$	< 40 keV
	standard solar model	✓	$3.8 \times 10^{-11} - 1$	< 39 keV
RGs	–	–	$1.4 \times 10^{-13} - 1.0 \times 10^{-7}$	< 350 keV
	–	✓	$4.4 \times 10^{-13} - 0.4$	< 404 keV
WDs	–	–	$7.0 \times 10^{-18} - 2.4 \times 10^{-9}$	< 282 keV
	–	✓	$2.3 \times 10^{-18} - 1.9 \times 10^{-4}$	< 294 keV

SUMMARY OF ASTROPHYSICAL LIMITS

We may summarise the limits from the objects considered as shown below

Star	Profile	Geometry	$\sin\theta$ range	m_S range
SN1987A	–	–	$2.4\times10^{-7} - 9.0\times10^{-6}$	< 249 MeV
	Fischer $11.8M_\odot$	✓	$1.2\times10^{-7} - 6.4\times10^{-5}$	< 204 MeV
	Fischer $18M_\odot$	✓	$1.0\times10^{-7} - 4.7\times10^{-5}$	< 238 MeV
	Nakazato $13M_\odot$	✓	$1.1\times10^{-7} - 5.4\times10^{-5}$	< 224 MeV
Sun	–	–	$1.4\times10^{-13} - 1.2\times10^{-3}$	< 40 keV
	standard solar model	✓	$3.8\times10^{-11} - 1$	< 39 keV
RGs	–	–	$1.4\times10^{-13} - 1.0\times10^{-7}$	< 350 keV
	–	✓	$4.4\times10^{-13} - 0.4$	< 404 keV
WDs	–	–	$7.0\times10^{-18} - 2.4\times10^{-9}$	< 282 keV
	–	✓	$2.3\times10^{-18} - 1.9\times10^{-4}$	< 294 keV

Limits on light CP-even scalar S from SN1987A, the Sun, RGs and WDs obtained in this paper including the geometric factor and stellar profiles to those with constant temperature, density and mass fractions. The second and third columns indicate the stellar profile adopted and whether geometry is included, respectively. The fourth and fifth columns are the excluded ranges of $\sin\theta$ and m_S, respectively.

CONCLUSION

CONCLUSION

- Compact astrophysical objects such as the supernova cores and stars such as the Sun, RGs and WDs offer some of the densest environments in the Universe

CONCLUSION

- Compact astrophysical objects such as the supernova cores and stars such as the Sun, RGs and WDs offer some of the densest environments in the Universe
    - Provide some of the primary high-intensity facilities in nature to search for the feeble interactions of light BSM particles, such as ALPs and light CP-even scalars

CONCLUSION

- Compact astrophysical objects such as the supernova cores and stars such as the Sun, RGs and WDs offer some of the densest environments in the Universe
    - Provide some of the primary high-intensity facilities in nature to search for the feeble interactions of light BSM particles, such as ALPs and light CP-even scalars

- Considered a generic CP-even scalar S mixing with the SM Higgs, so that we have only two free parameters, i.e. the scalar mass m_S and the mixing angle $\sin\theta$

CONCLUSION

- Compact astrophysical objects such as the supernova cores and stars such as the Sun, RGs and WDs offer some of the densest environments in the Universe
    - Provide some of the primary high-intensity facilities in nature to search for the feeble interactions of light BSM particles, such as ALPs and light CP-even scalars

- Considered a generic CP-even scalar S mixing with the SM Higgs, so that we have only two free parameters, i.e. the scalar mass m_S and the mixing angle $\sin\theta$

- Most recent and precise stellar limits on the S mass and mixing from

CONCLUSION

- Compact astrophysical objects such as the supernova cores and stars such as the Sun, RGs and WDs offer some of the densest environments in the Universe
  - Provide some of the primary high-intensity facilities in nature to search for the feeble interactions of light BSM particles, such as ALPs and light CP-even scalars

- Considered a generic CP-even scalar S mixing with the SM Higgs, so that we have only two free parameters, i.e. the scalar mass m_S and the mixing angle $\sin\theta$

- Most recent and precise stellar limits on the S mass and mixing from
  - SN1987A,

CONCLUSION

- Compact astrophysical objects such as the supernova cores and stars such as the Sun, RGs and WDs offer some of the densest environments in the Universe
  - Provide some of the primary high-intensity facilities in nature to search for the feeble interactions of light BSM particles, such as ALPs and light CP-even scalars

- Considered a generic CP-even scalar S mixing with the SM Higgs, so that we have only two free parameters, i.e. the scalar mass m_S and the mixing angle $\sin\theta$

- Most recent and precise stellar limits on the S mass and mixing from
  - SN1987A,
  - the Sun,

CONCLUSION

- Compact astrophysical objects such as the supernova cores and stars such as the Sun, RGs and WDs offer some of the densest environments in the Universe
    - Provide some of the primary high-intensity facilities in nature to search for the feeble interactions of light BSM particles, such as ALPs and light CP-even scalars

- Considered a generic CP-even scalar S mixing with the SM Higgs, so that we have only two free parameters, i.e. the scalar mass m_S and the mixing angle $\sin\theta$

- Most recent and precise stellar limits on the S mass and mixing from
    - SN1987A,
    - the Sun,
    - RGs

CONCLUSION

- Compact astrophysical objects such as the supernova cores and stars such as the Sun, RGs and WDs offer some of the densest environments in the Universe
  - Provide some of the primary high-intensity facilities in nature to search for the feeble interactions of light BSM particles, such as ALPs and light CP-even scalars

- Considered a generic CP-even scalar S mixing with the SM Higgs, so that we have only two free parameters, i.e. the scalar mass m_S and the mixing angle $\sin\theta$

- Most recent and precise stellar limits on the S mass and mixing from
  - SN1987A,
  - the Sun,
  - RGs
  - WDs

CONCLUSION

- Compact astrophysical objects such as the supernova cores and stars such as the Sun, RGs and WDs offer some of the densest environments in the Universe
  - Provide some of the primary high-intensity facilities in nature to search for the feeble interactions of light BSM particles, such as ALPs and light CP-even scalars

- Considered a generic CP-even scalar S mixing with the SM Higgs, so that we have only two free parameters, i.e. the scalar mass m_S and the mixing angle $\sin\theta$

- Most recent and precise stellar limits on the S mass and mixing from
  - SN1987A,
  - the Sun,
  - RGs
  - WDs

Radial

CONCLUSION

- Compact astrophysical objects such as the supernova cores and stars such as the Sun, RGs and WDs offer some of the densest environments in the Universe
  - Provide some of the primary high-intensity facilities in nature to search for the feeble interactions of light BSM particles, such as ALPs and light CP-even scalars

- Considered a generic CP-even scalar S mixing with the SM Higgs, so that we have only two free parameters, i.e. the scalar mass m_S and the mixing angle $\sin\theta$

- Most recent and precise stellar limits on the S mass and mixing from
  - SN1987A,
  - the Sun,
  - RGs
  - WDs

Radial

Geometric effects for the decay and absorption S

CONCLUSION

- Compact astrophysical objects such as the supernova cores and stars such as the Sun, RGs and WDs offer some of the densest environments in the Universe
    - Provide some of the primary high-intensity facilities in nature to search for the feeble interactions of light BSM particles, such as ALPs and light CP-even scalars

- Considered a generic CP-even scalar S mixing with the SM Higgs, so that we have only two free parameters, i.e. the scalar mass m_S and the mixing angle $\sin\theta$

- Most recent and precise stellar limits on the S mass and mixing from
    - SN1987A,
    - the Sun,
    - RGs
    - WDs

  Radial

  Geometric effects for the decay and absorption S

- The procedure for calculating stellar limits on the light scalar S in this paper can be applied to other astrophysical systems such as neutron star mergers, as well as to other BSM particles such as the dark photon, Z' boson, ALPs and axions

CONCLUSION

- Compact astrophysical objects such as the supernova cores and stars such as the Sun, RGs and WDs offer some of the densest environments in the Universe
  - Provide some of the primary high-intensity facilities in nature to search for the feeble interactions of light BSM particles, such as ALPs and light CP-even scalars

- Considered a generic CP-even scalar S mixing with the SM Higgs, so that we have only two free parameters, i.e. the scalar mass m_S and the mixing angle $\sin\theta$

- Most recent and precise stellar limits on the S mass and mixing from
  - SN1987A,
  - the Sun,
  - RGs
  - WDs

Radial

Geometric effects for the decay and absorption S

- The procedure for calculating stellar limits on the light scalar S in this paper can be applied to other astrophysical systems such as neutron star mergers, as well as to other BSM particles such as the dark photon, Z' boson, ALPs and axions

- We have limited ourselves only to the luminosity considerations to derive the limits; depending on the mass and coupling of the BSM particles, their decay outside the stars could generate γ-rays or x-rays

BACK UP

VARIABLE DEFINITIONS

Where we utilised the following dimensionless variables

$$u \equiv \frac{\mathbf{p}_i^2}{m_N T}\,, \qquad v \equiv \frac{\mathbf{p}_f^2}{m_N T}\,, \qquad x \equiv \frac{E_S}{T}\,, \qquad q \equiv \frac{m_S}{T}\,, \qquad y \equiv \frac{m_\pi^2}{m_N T}\,.$$

Denoting $\mathbf{p}_i$ (with $i = 1, 2, 3, 4$) as the three-momenta for the two nucleons in the initial state of the nucleon bremsstrahlung process and the two nucleons in the final state, we define

$$\mathbf{p}_1 \equiv \mathbf{P} + \mathbf{p}_i\,, \quad \mathbf{p}_2 \equiv \mathbf{P} - \mathbf{p}_i\,, \quad \mathbf{p}_3 \equiv \mathbf{P} + \mathbf{p}_f\,, \quad \mathbf{p}_4 \equiv \mathbf{P} - \mathbf{p}_f\,,$$

The dimensionless function $\mathcal{I}_{\text{tot}}$ is given given in the Appendix in terms of dimensionless variables u, x, y and z

N-N BREMSSTRAHLUNG EMISSION

After many simplifications, we arrive at the following expressions for the emission rate

N-N BREMSSTRAHLUNG EMISSION

After many simplifications, we arrive at the following expressions for the emission rate

$$\boxed{\mathcal{Q}(r,\,\phi) \quad = \quad \frac{\alpha_\pi^2 f_{pp}^4 \sin^2\theta T^{7/2}(r)\rho^2(r)}{8\pi^{3/2} m_N^{13/2}} \int_q^\infty \mathrm{d}u \int_0^\infty \mathrm{d}v \int_{-1}^1 \mathrm{d}z \int_q^\infty \mathrm{d}x\ \delta(u-v-x)\sqrt{uv}e^{-u} x\sqrt{x^2-q^2} P_{\mathrm{decay}} P_{\mathrm{abs}} \mathcal{I}_{\mathrm{tot}}}$$

N-N BREMSSTRAHLUNG EMISSION

After many simplifications, we arrive at the following expressions for the emission rate

$$\boxed{\mathcal{Q}(r,\,\phi) \quad = \quad \frac{\alpha_\pi^2 f_{pp}^4 \sin^2\theta T^{7/2}(r)\rho^2(r)}{8\pi^{3/2} m_N^{13/2}} \int_q^\infty \mathrm{d}u \int_0^\infty \mathrm{d}v \int_{-1}^1 \mathrm{d}z \int_q^\infty \mathrm{d}x\ \delta(u-v-x)\sqrt{uv}e^{-u}x\sqrt{x^2-q^2}P_{\rm decay}P_{\rm abs}\mathcal{I}_{\rm tot}}$$

$$\alpha_\pi \equiv (2m_N/m_\pi)^2/4\pi \simeq 15$$

N-N BREMSSTRAHLUNG EMISSION

After many simplifications, we arrive at the following expressions for the emission rate

$$\mathcal{Q}(r,\,\phi) \quad = \quad \frac{\alpha_\pi^2 f_{pp}^4 \sin^2\theta T^{7/2}(r)\rho^2(r)}{8\pi^{3/2} m_N^{13/2}} \int_q^\infty \mathrm{d}u \int_0^\infty \mathrm{d}v \int_{-1}^1 \mathrm{d}z \int_q^\infty \mathrm{d}x\ \delta(u-v-x)\sqrt{uv}e^{-u}x\sqrt{x^2-q^2}P_{\mathrm{decay}}P_{\mathrm{abs}}\mathcal{I}_{\mathrm{tot}}$$

$$\alpha_\pi \equiv (2m_N/m_\pi)^2/4\pi \simeq 15$$

where $f_{pp} = 1$. The above contains within P_{abs} the inverse mean free path

N-N BREMSSTRAHLUNG EMISSION

After many simplifications, we arrive at the following expressions for the emission rate

$$\boxed{\mathcal{Q}(r,\,\phi) \quad = \quad \frac{\alpha_\pi^2 f_{pp}^4 \sin^2\theta T^{7/2}(r)\rho^2(r)}{8\pi^{3/2} m_N^{13/2}} \int_q^\infty \mathrm{d}u \int_0^\infty \mathrm{d}v \int_{-1}^1 \mathrm{d}z \int_q^\infty \mathrm{d}x\ \delta(u-v-x)\sqrt{uv}e^{-u}x\sqrt{x^2-q^2}P_{\mathrm{decay}}P_{\mathrm{abs}}\mathcal{I}_{\mathrm{tot}}}$$

$$\alpha_\pi \equiv (2m_N/m_\pi)^2/4\pi \simeq 15$$

where $f_{pp} = 1$. The above contains within P_{abs} the inverse mean free path

$$\boxed{\lambda^{-1}(r;x) \quad = \quad \frac{\pi^{1/2}\alpha_\pi^2 f_{pp}^4 \sin^2\theta\rho^2(r)}{4m_N^{13/2}T^{1/2}(r)}\frac{1}{x}\int_0^\infty \mathrm{d}u \int_q^\infty \mathrm{d}v \int_{-1}^1 \mathrm{d}z\sqrt{uv}e^{-u}\delta(u-v+x)\mathcal{I}_{\mathrm{tot}}}$$

N-N BREMSSTRAHLUNG EMISSION

After many simplifications, we arrive at the following expressions for the emission rate

$$\mathcal{Q}(r,\,\phi) \quad = \quad \frac{\alpha_\pi^2 f_{pp}^4 \sin^2\theta T^{7/2}(r)\rho^2(r)}{8\pi^{3/2} m_N^{13/2}} \int_q^\infty \mathrm{d}u \int_0^\infty \mathrm{d}v \int_{-1}^1 \mathrm{d}z \int_q^\infty \mathrm{d}x \; \delta(u-v-x)\sqrt{uv}e^{-u} x\sqrt{x^2-q^2} P_{\mathrm{decay}} P_{\mathrm{abs}} \mathcal{I}_{\mathrm{tot}}$$

$$\alpha_\pi \equiv (2m_N/m_\pi)^2/4\pi \simeq 15$$

where $f_{pp} = 1$. The above contains within P_{abs} the inverse mean free path

$$\lambda^{-1}(r;x) \;=\; \frac{\pi^{1/2}\alpha_\pi^2 f_{pp}^4 \sin^2\theta\rho^2(r)}{4m_N^{13/2}T^{1/2}(r)} \frac{1}{x} \int_0^\infty \mathrm{d}u \int_q^\infty \mathrm{d}v \int_{-1}^1 \mathrm{d}z \sqrt{uv}e^{-u}\delta(u-v+x)\mathcal{I}_{\mathrm{tot}}$$

From here we may numerically solve for the luminosity due to light scalar emission

ENERGY AVERAGED MEAN FREE PATH

$$\langle\lambda^{-1}\rangle(r) \equiv \frac{\int \mathrm{d}E_S \frac{E_S^3}{e^{E_S/T}-1}\lambda^{-1}(E_S;r)}{\int \mathrm{d}E_S \frac{E_S^3}{e^{E_S/T}-1}} = \frac{\int \mathrm{d}x \frac{x^3}{e^x-1}\lambda^{-1}(x;r)}{\int \mathrm{d}x \frac{x^3}{e^x-1}}.$$

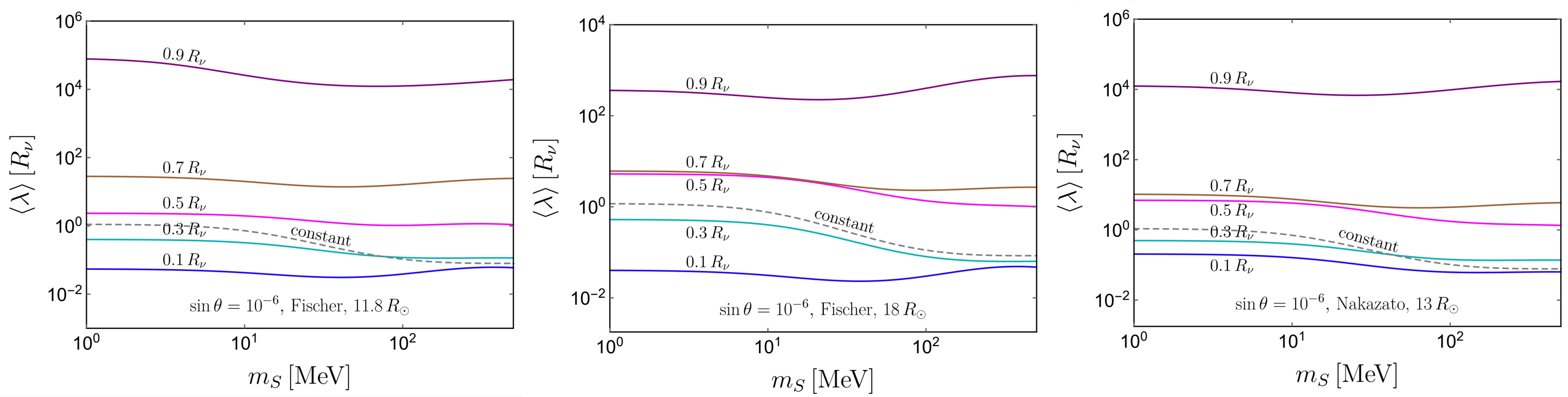

The dashed lines are the corresponding MFPs for constant temperature $T = 30$ MeV and baryon number density $n_B = 1.2 \times 10^{38}\,\mathrm{cm}^{-3}$.
The mixing angle is fixed to $\sin\theta = 10^{-6}$

SOLAR RADIAL PROFILES

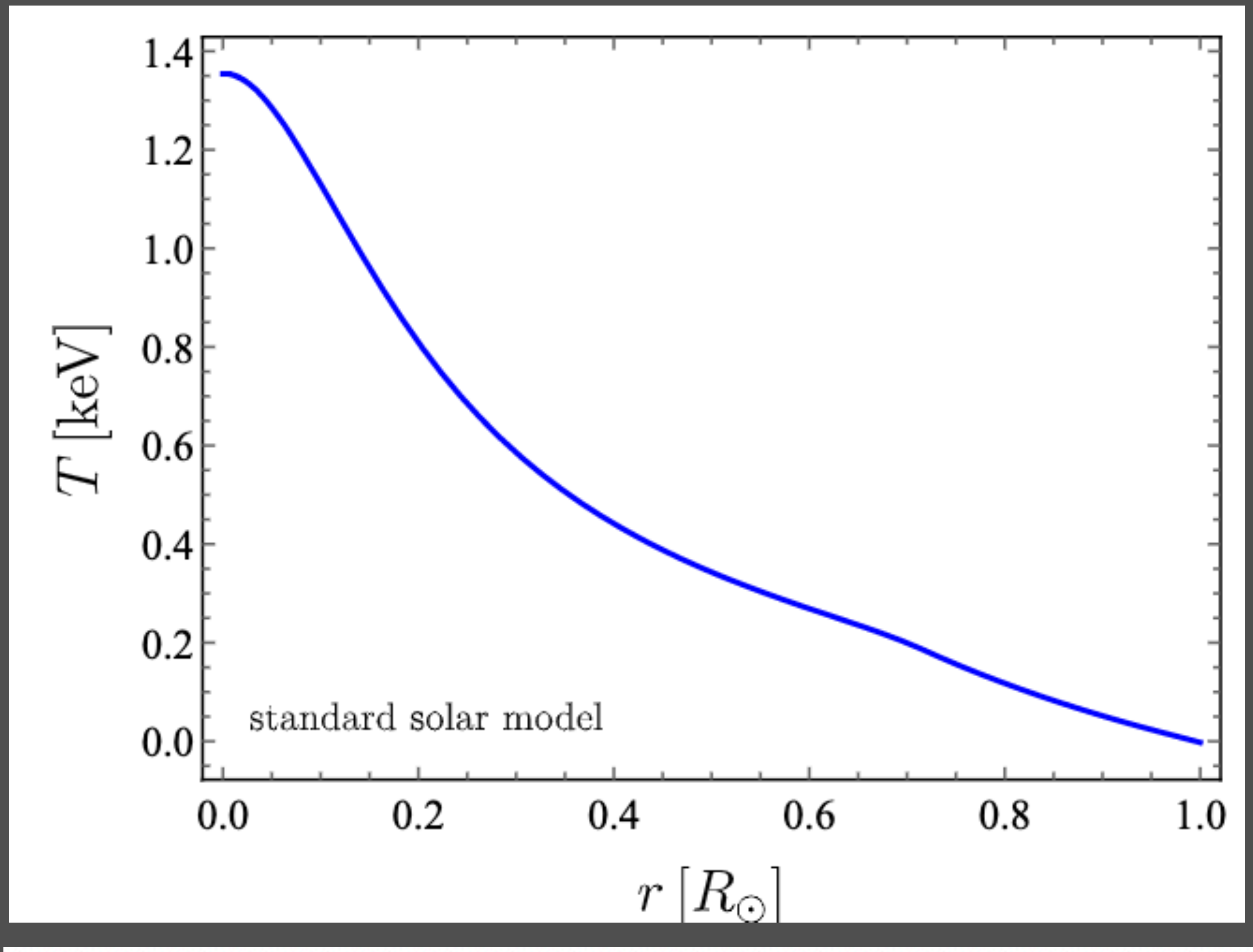

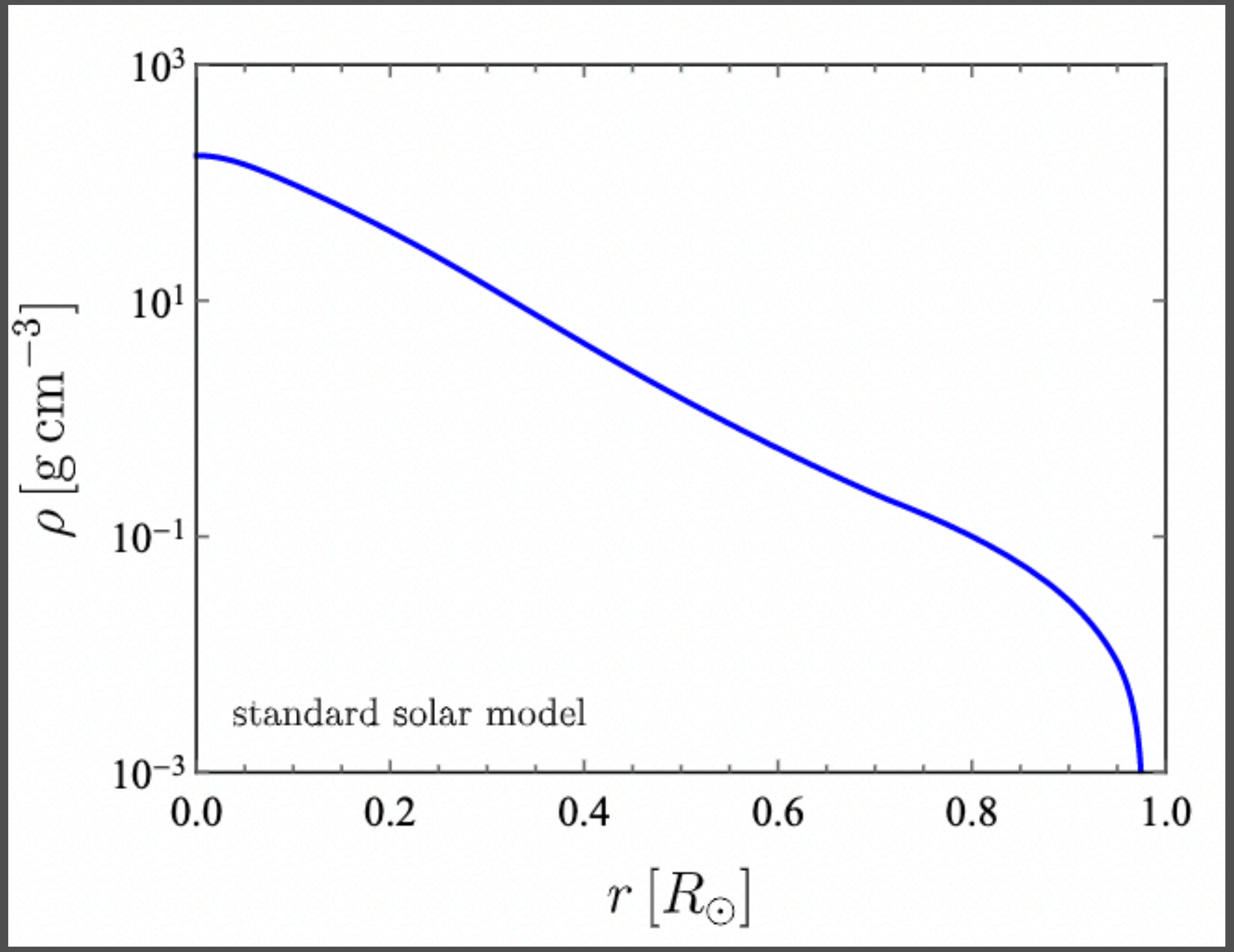

SOLAR RADIAL PROFILES

- The Sun can also be used to constrain light new physics because of how well its internal physics is understood

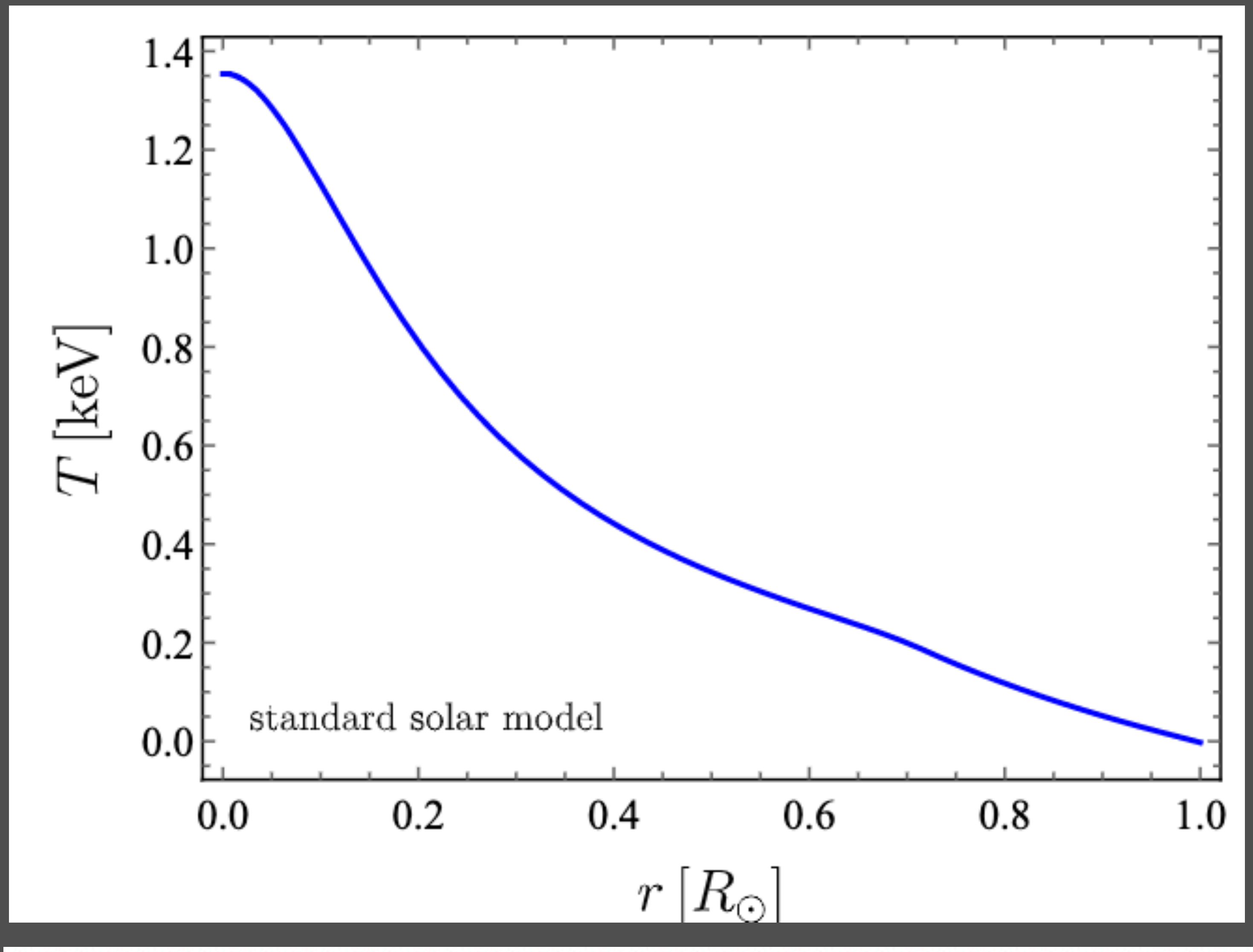

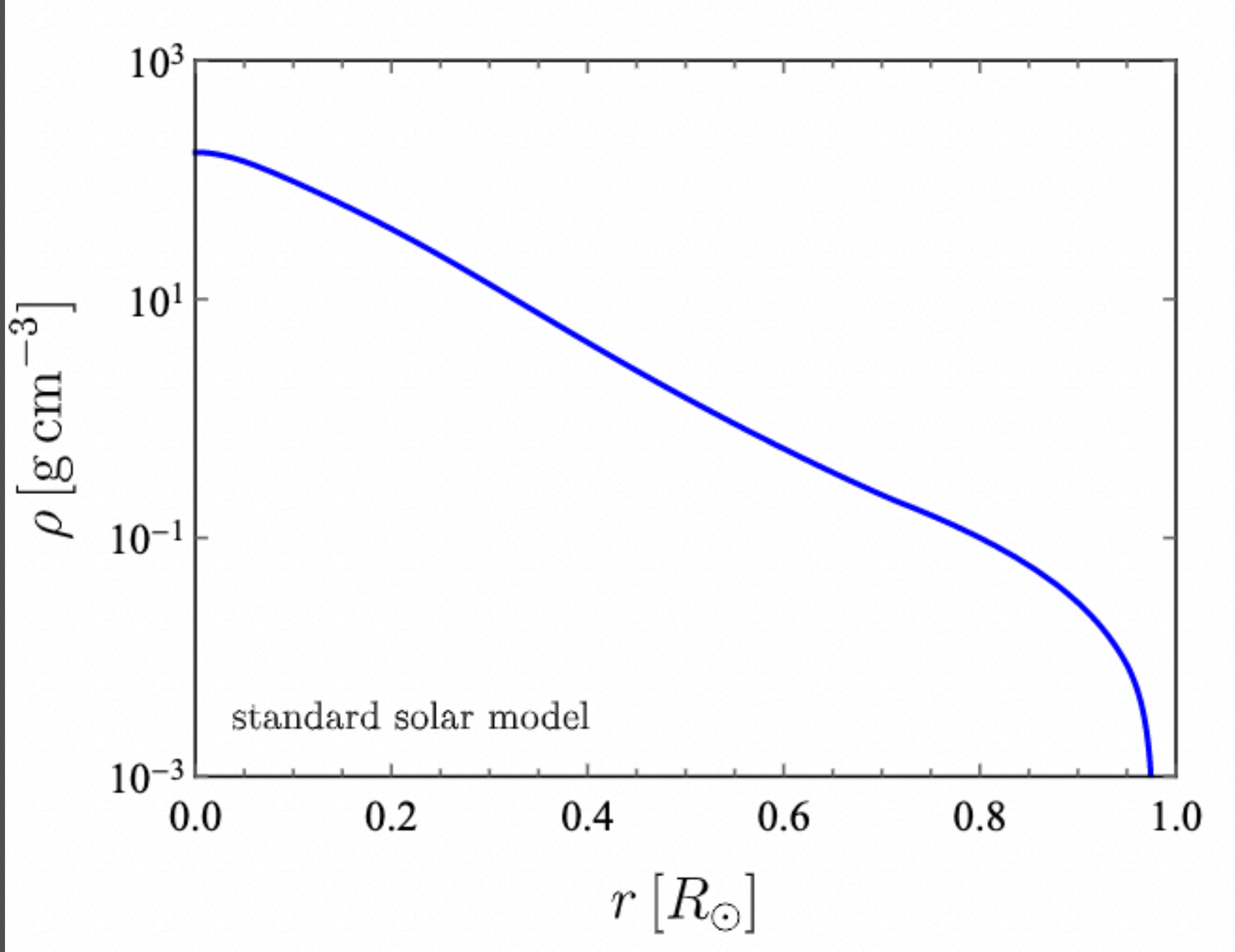

SOLAR RADIAL PROFILES

- The Sun can also be used to constrain light new physics because of how well its internal physics is understood

- Use the standard solar model where the Sun is modelled as a spherically symmetric quasi-static star.

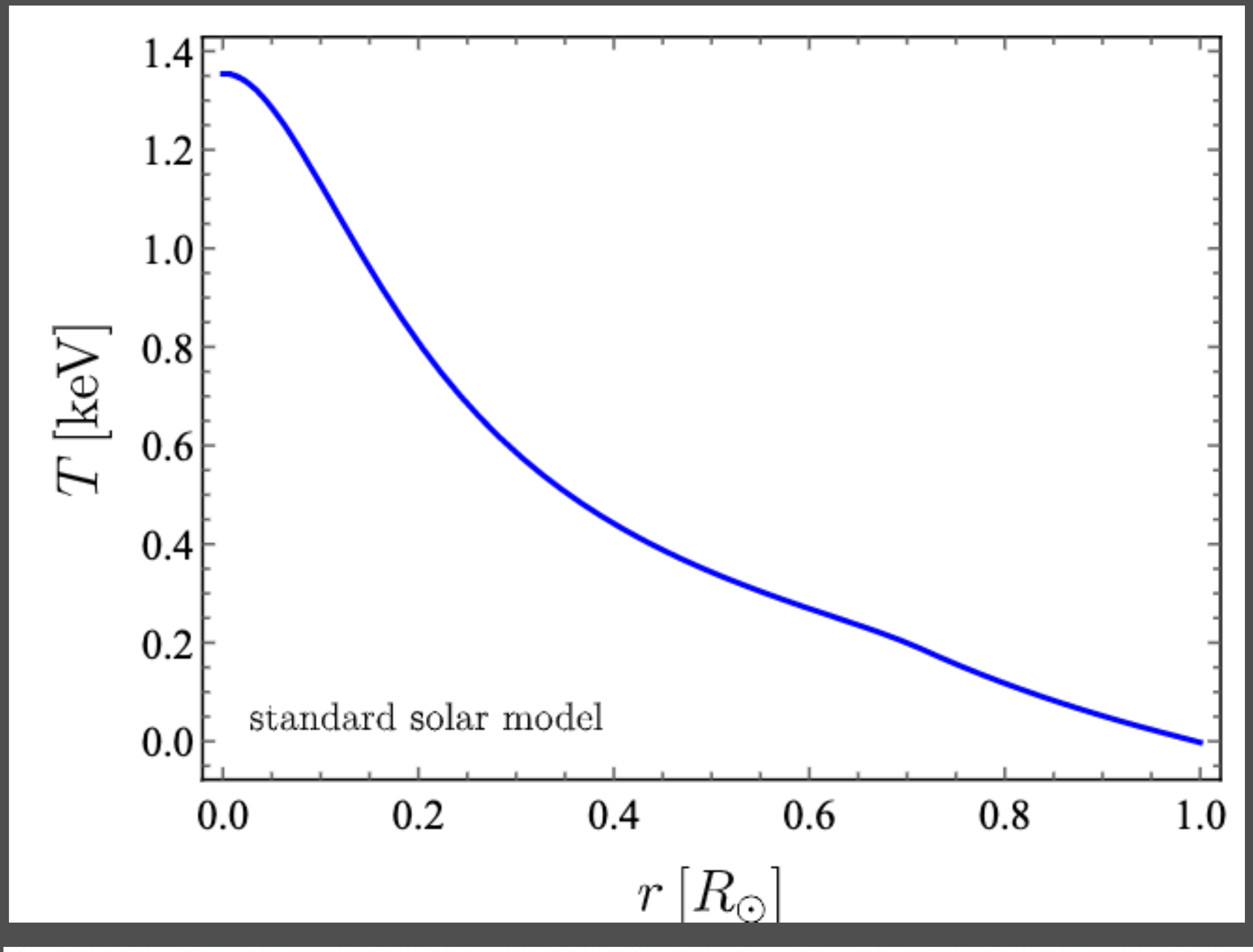

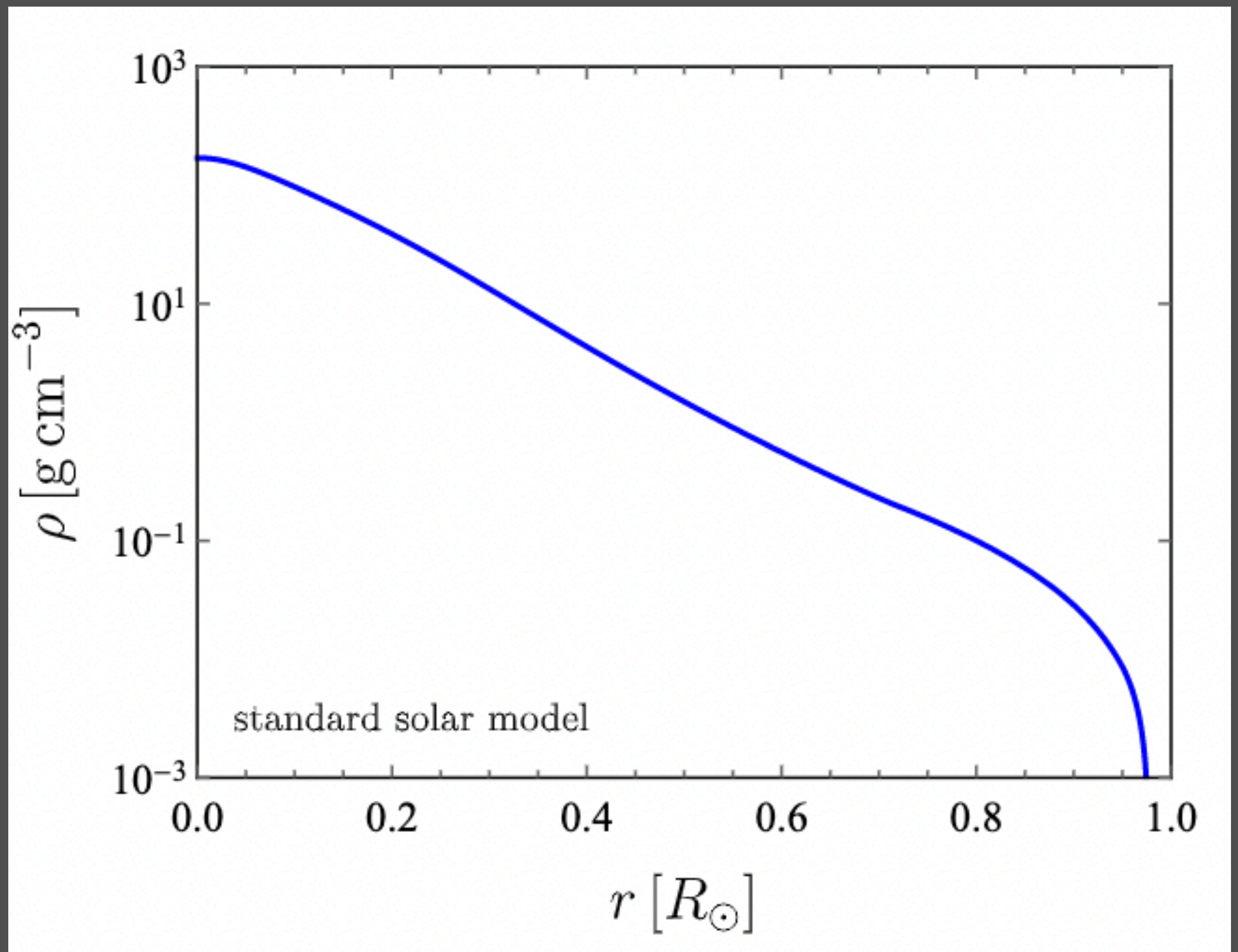

SOLAR RADIAL PROFILES

- The Sun can also be used to constrain light new physics because of how well its internal physics is understood

- Use the standard solar model where the Sun is modelled as a spherically symmetric quasi-static star.

- The differential equations involve pressure, opacity and the energy generation rate written in terms of the density, temperature and composition.

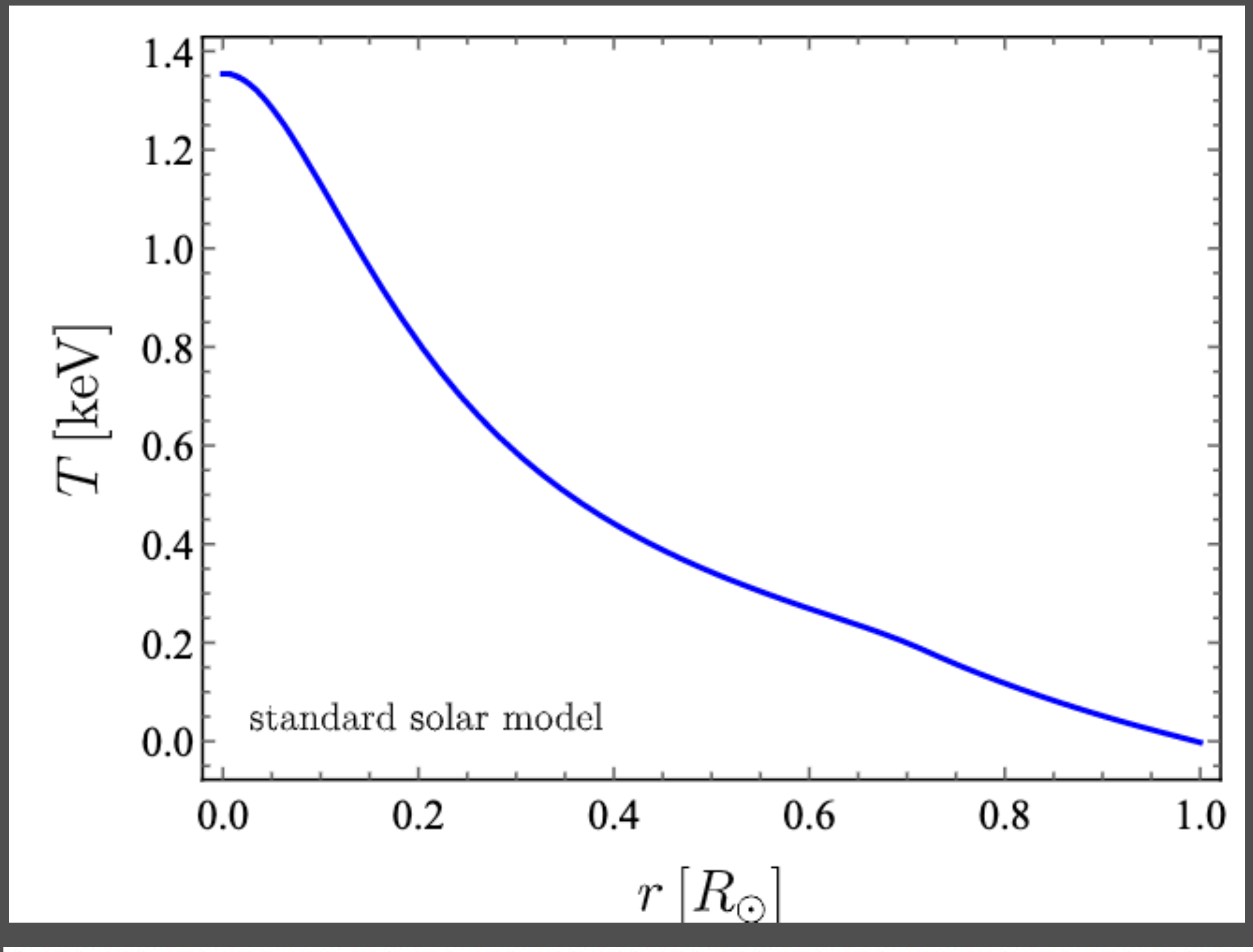

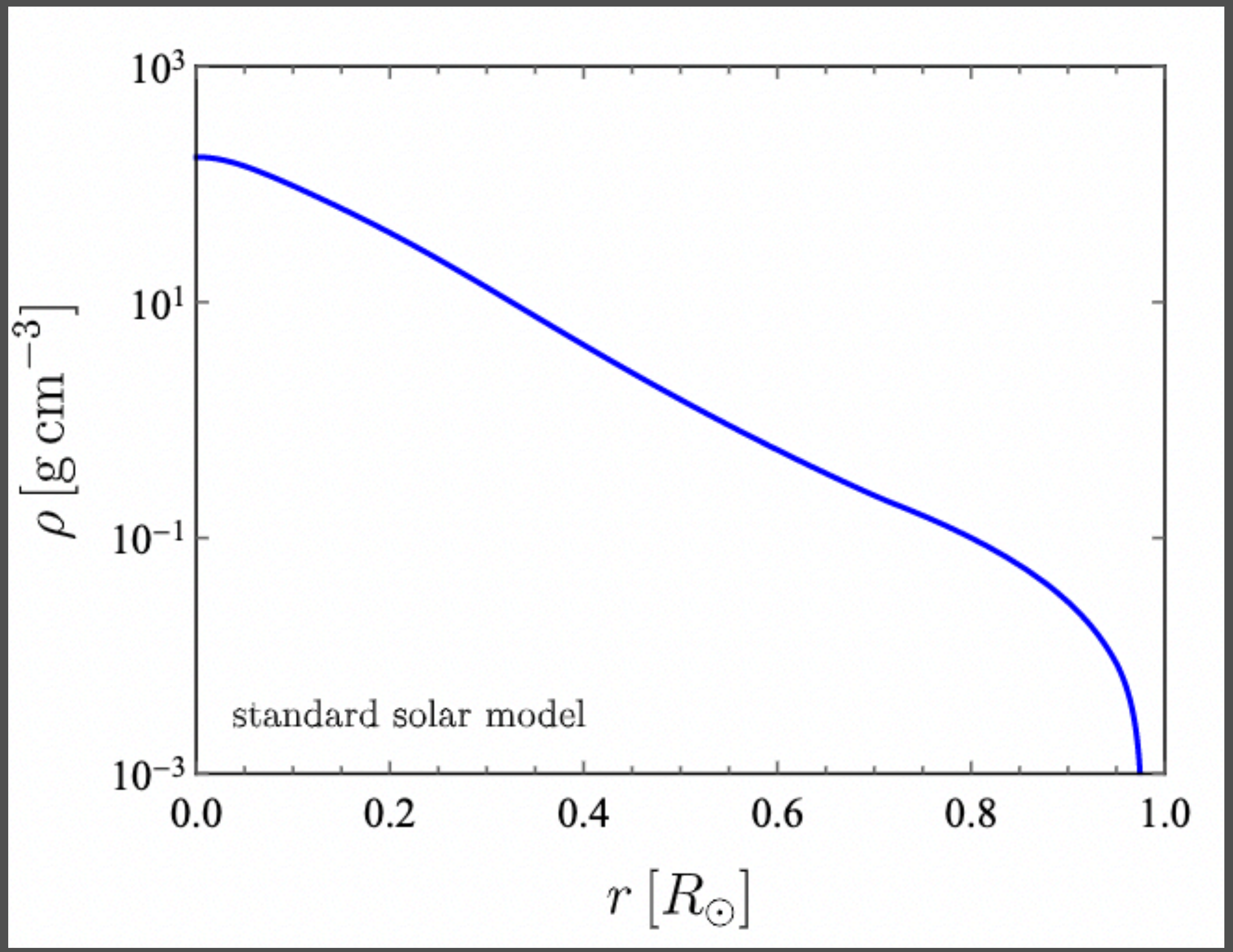

SOLAR RADIAL PROFILES

- The Sun can also be used to constrain light new physics because of how well its internal physics is understood

- Use the standard solar model where the Sun is modelled as a spherically symmetric quasi-static star.

- The differential equations involve pressure, opacity and the energy generation rate written in terms of the density, temperature and composition.

- The stellar structure is described completely by a set of differential equations and boundary conditions for the luminosity, radius, age and composition of the Sun:

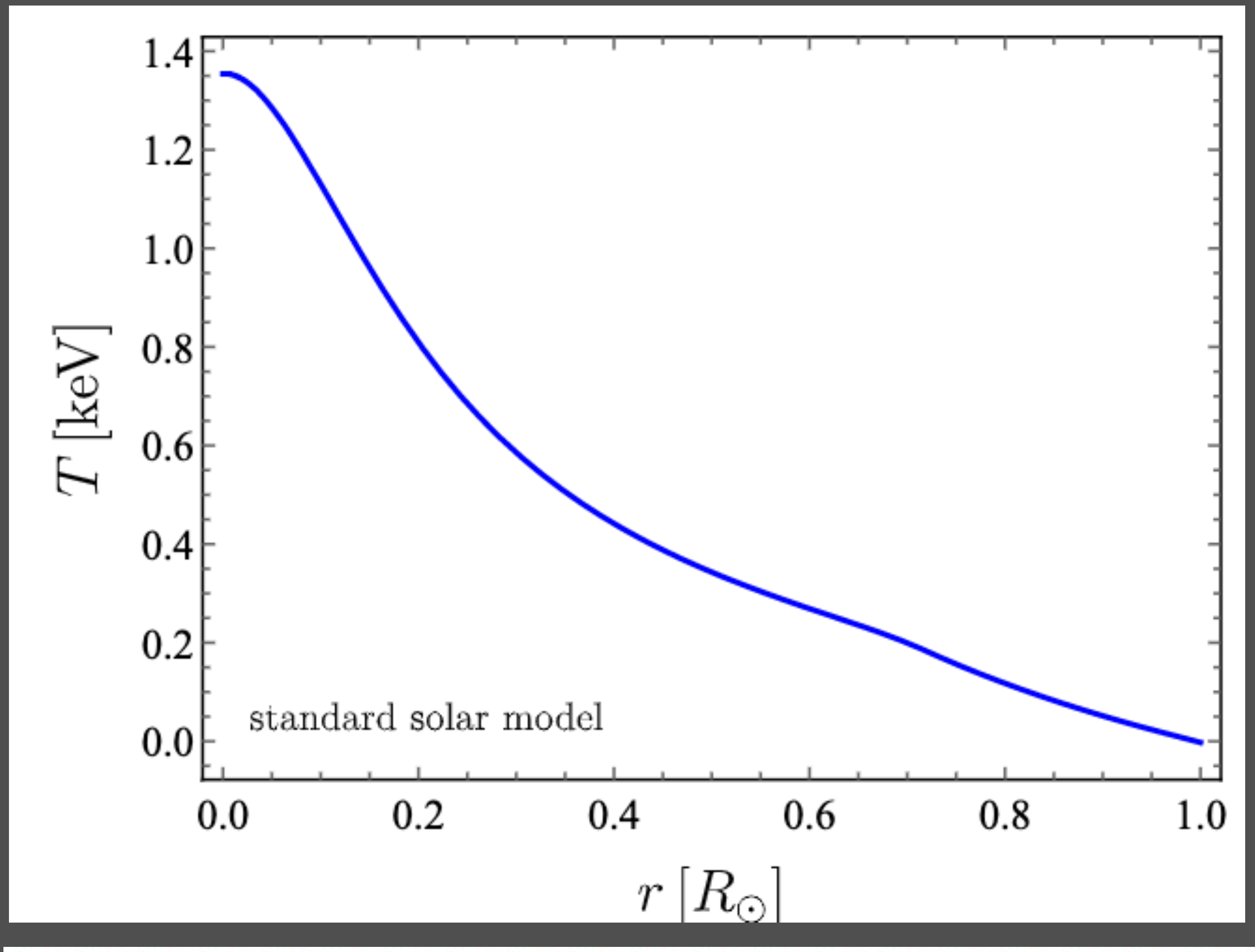

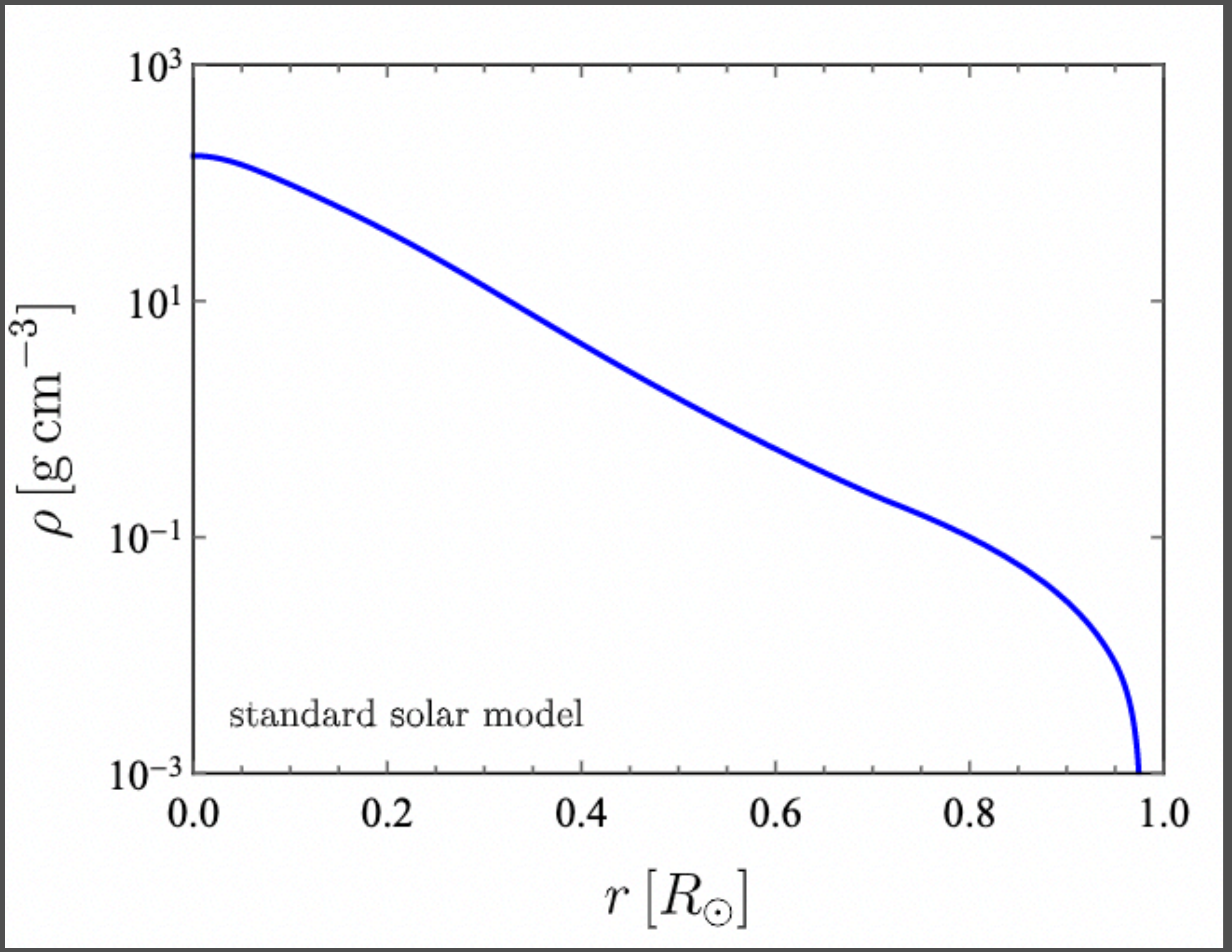

SOLAR RADIAL PROFILES

- The Sun can also be used to constrain light new physics because of how well its internal physics is understood

- Use the standard solar model where the Sun is modelled as a spherically symmetric quasi-static star.

- The differential equations involve pressure, opacity and the energy generation rate written in terms of the density, temperature and composition.

- The stellar structure is described completely by a set of differential equations and boundary conditions for the luminosity, radius, age and composition of the Sun:

    - pressure

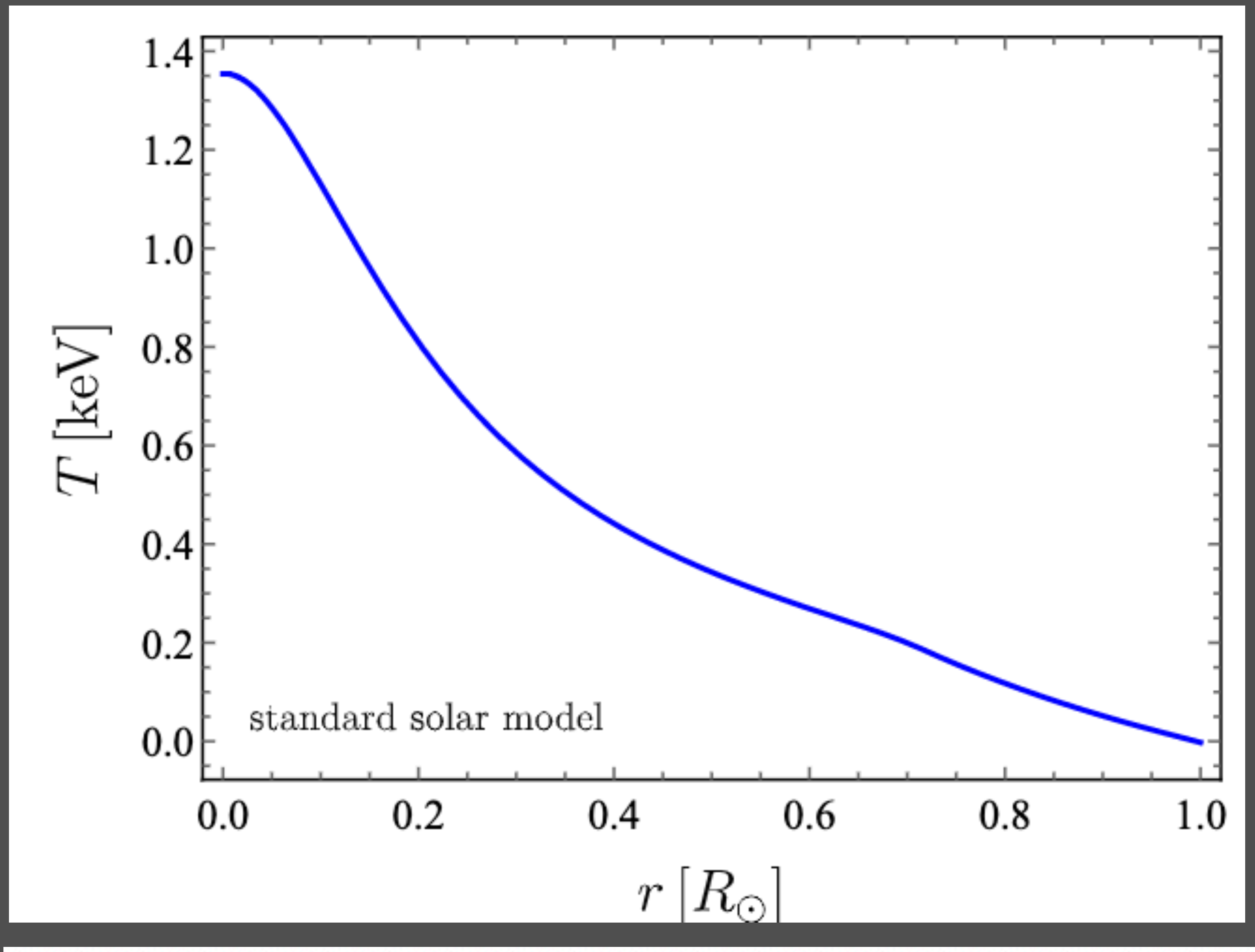

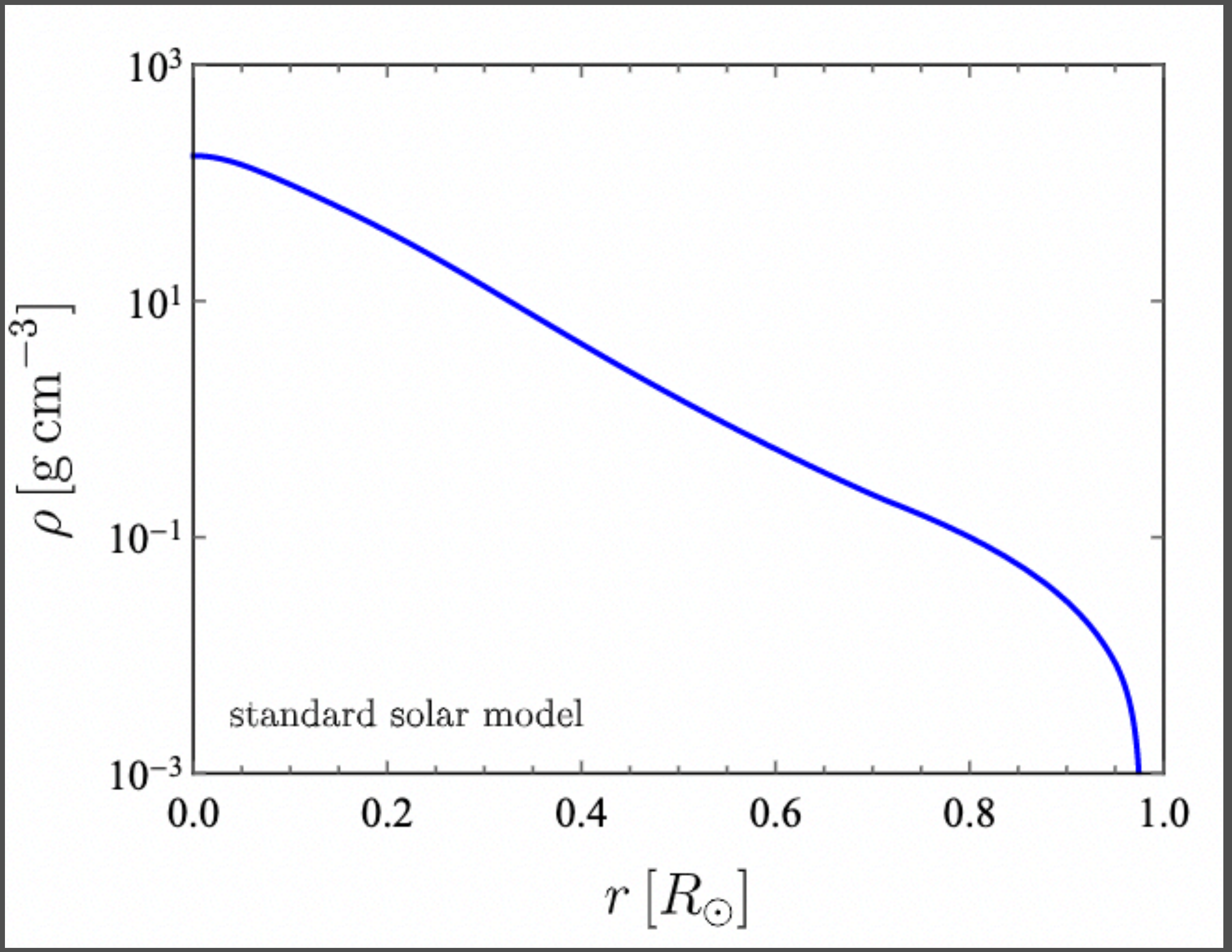

SOLAR RADIAL PROFILES

- The Sun can also be used to constrain light new physics because of how well its internal physics is understood

- Use the standard solar model where the Sun is modelled as a spherically symmetric quasi-static star.

- The differential equations involve pressure, opacity and the energy generation rate written in terms of the density, temperature and composition.

- The stellar structure is described completely by a set of differential equations and boundary conditions for the luminosity, radius, age and composition of the Sun:

  - pressure
  - opacity

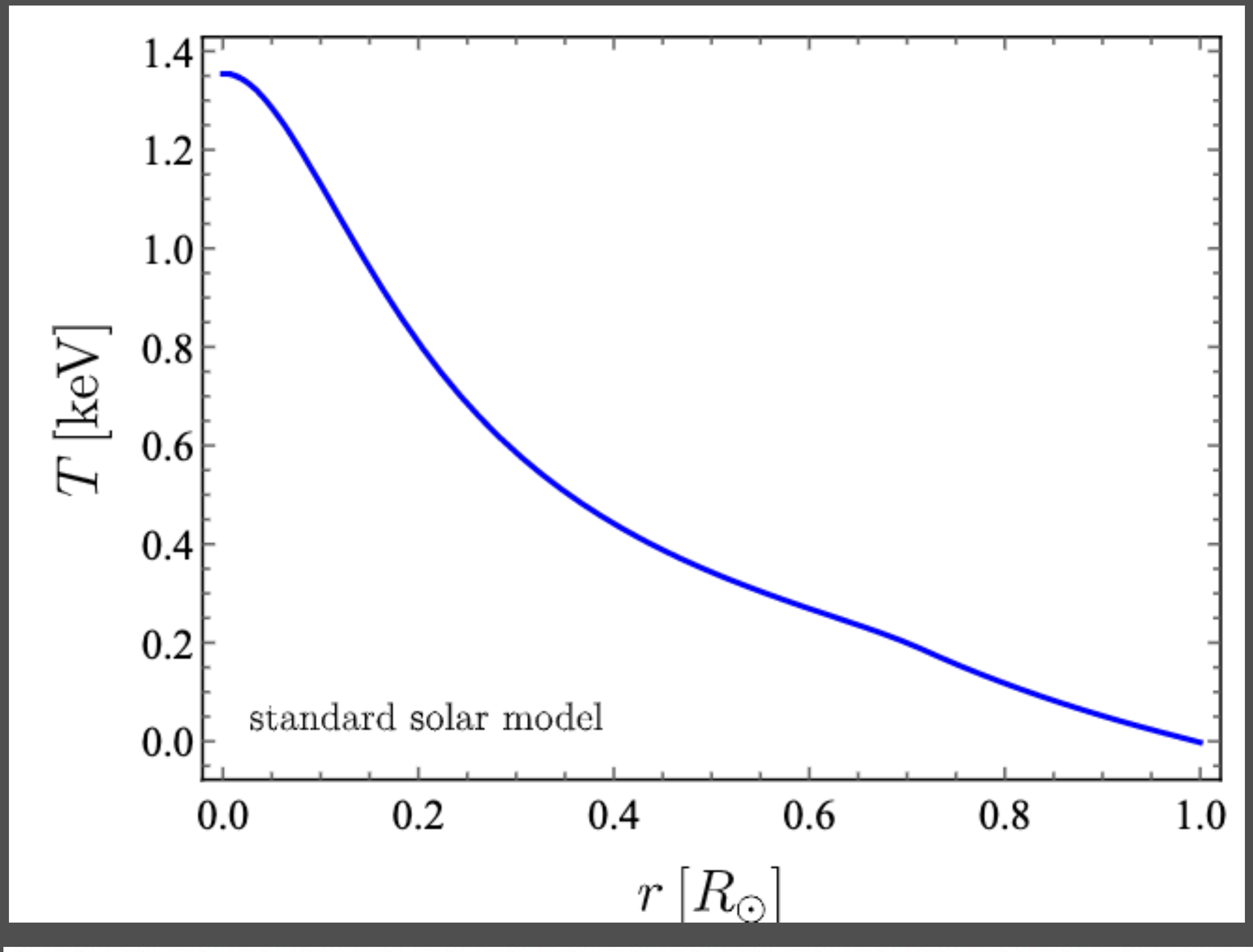

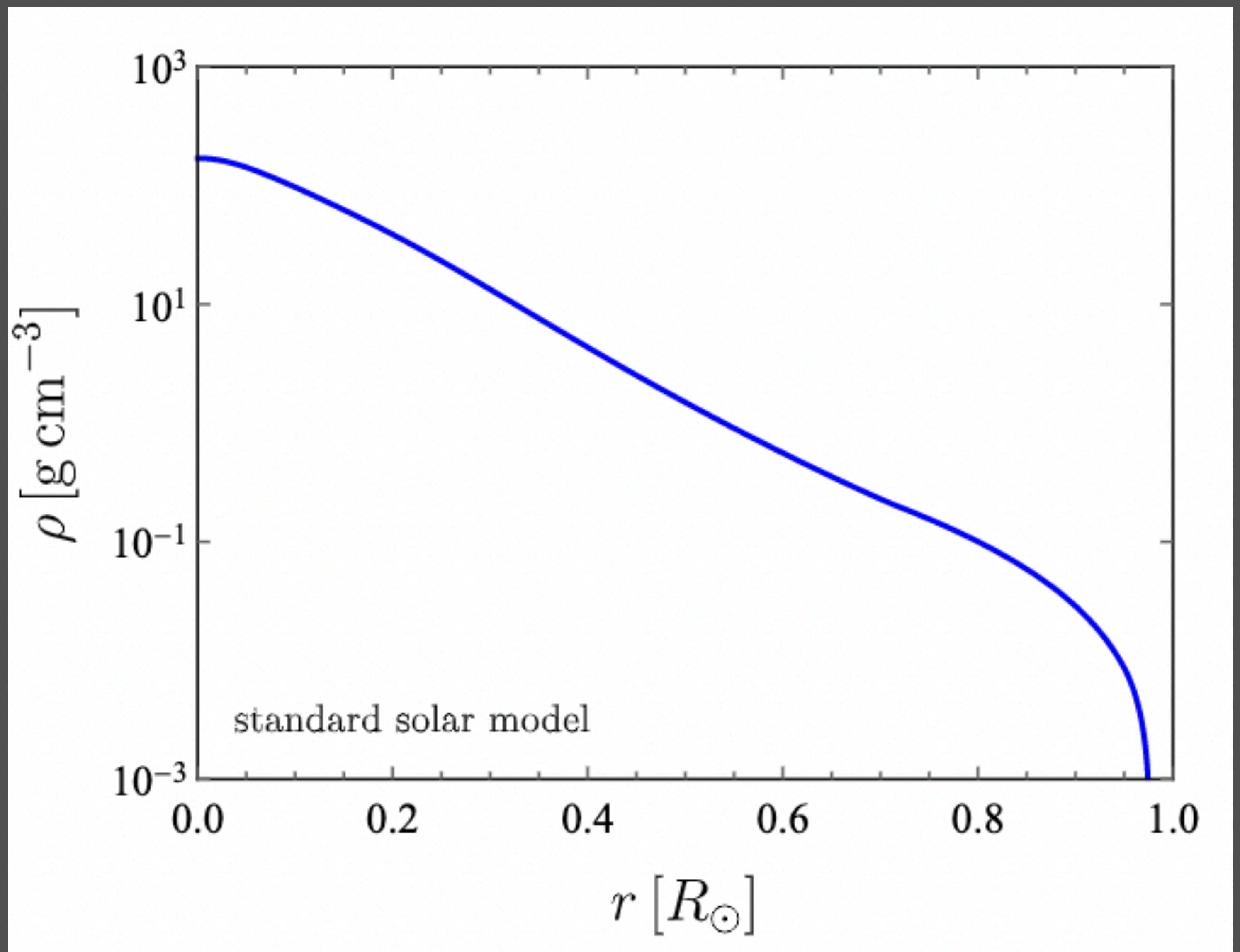

SOLAR RADIAL PROFILES

- The Sun can also be used to constrain light new physics because of how well its internal physics is understood

- Use the standard solar model where the Sun is modelled as a spherically symmetric quasi-static star.

- The differential equations involve pressure, opacity and the energy generation rate written in terms of the density, temperature and composition.

- The stellar structure is described completely by a set of differential equations and boundary conditions for the luminosity, radius, age and composition of the Sun:

- pressure
- opacity
- the energy generation rate: written in terms of density and temperature

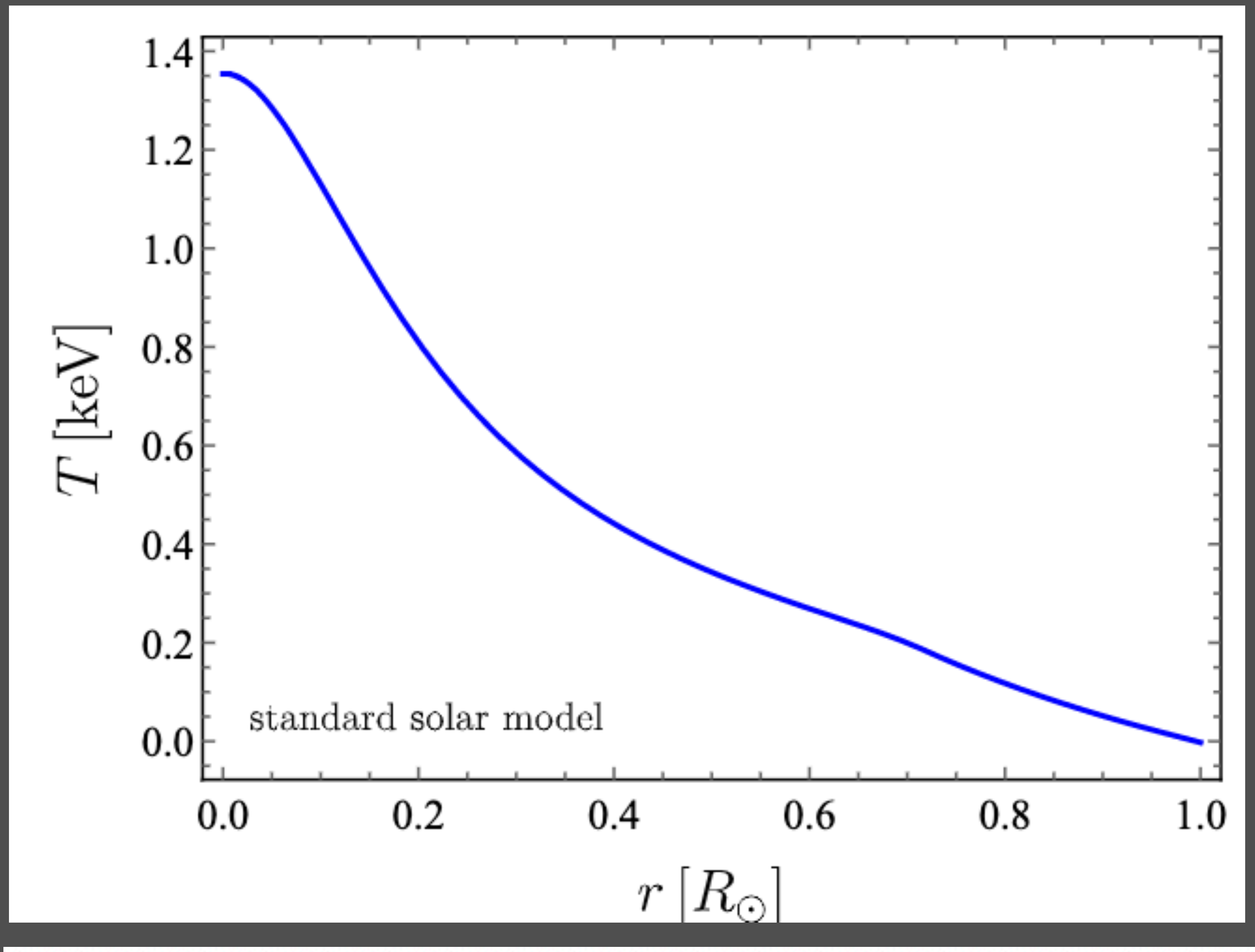

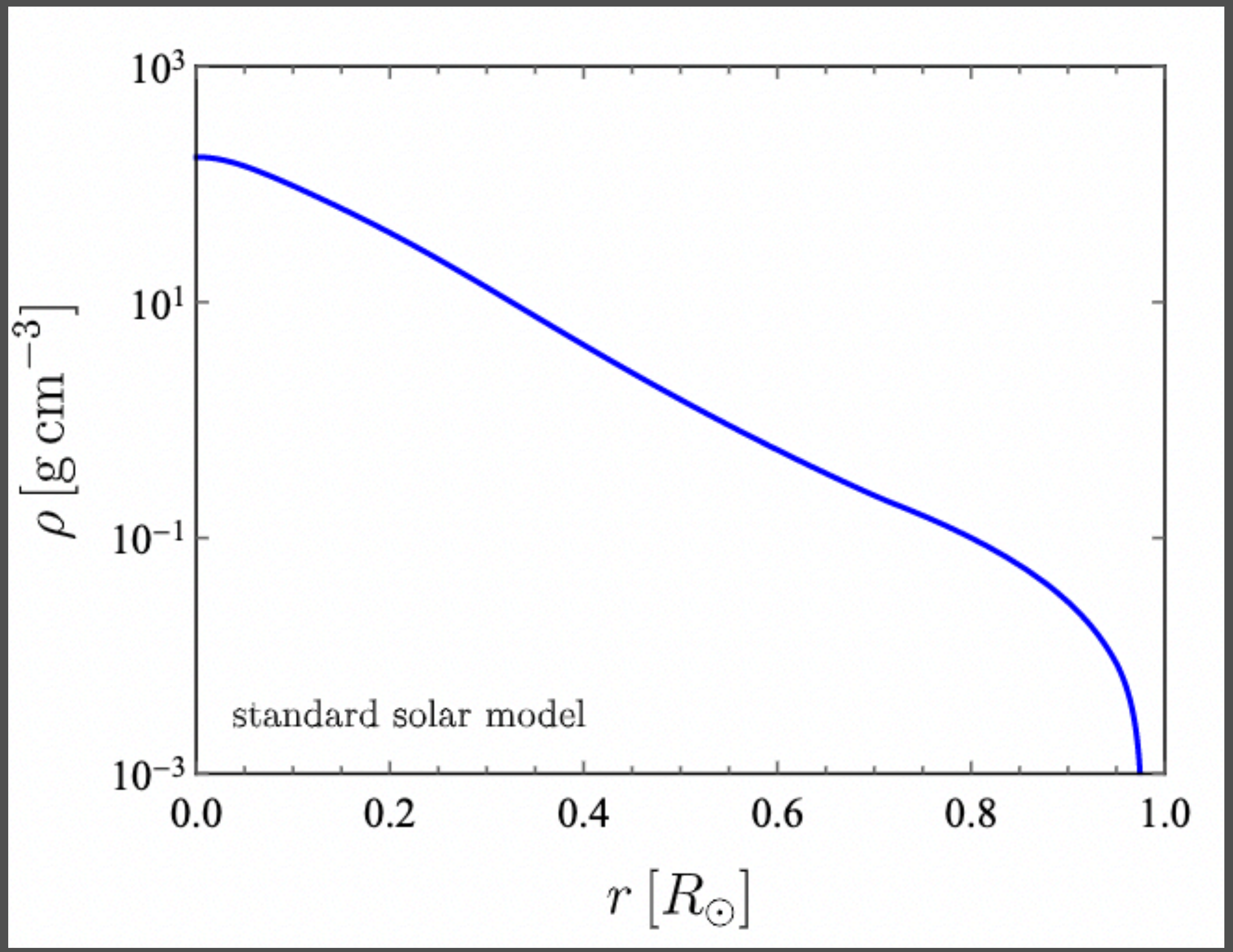

E-N BREMSSTRAHLUNG EMISSION

After many simplifications, we arrive at the following expressions for the emission rate

E-N BREMSSTRAHLUNG EMISSION

After many simplifications, we arrive at the following expressions for the emission rate

$$\mathcal{Q}(r,\phi) \quad = \quad \left(\sum_i Z_{N_i}^2 A_{N_i}^2 n_{N_i}(r)\right) \frac{\alpha^2 y_N^2 \sin^2\theta T^{1/2}(r) n_e(r)}{\pi^{3/2} m_e^{3/2}} \int_q^\infty \mathrm{d}u \int_0^\infty \mathrm{d}v \int_q^\infty \mathrm{d}x \int_{-1}^1 \mathrm{d}z \sqrt{uv} e^{-u} \sqrt{x^2-q^2} \frac{\delta(u-v-x)}{(u+v-2\sqrt{uv}z)^2} P_{\mathrm{decay}} P_{\mathrm{abs}}$$

E-N BREMSSTRAHLUNG EMISSION

After many simplifications, we arrive at the following expressions for the emission rate

$$\mathcal{Q}(r,\phi) = \left(\sum_i Z_{N_i}^2 A_{N_i}^2 n_{N_i}(r)\right) \frac{\alpha^2 y_N^2 \sin^2\theta T^{1/2}(r) n_e(r)}{\pi^{3/2} m_e^{3/2}} \int_q^\infty \mathrm{d}u \int_0^\infty \mathrm{d}v \int_q^\infty \mathrm{d}x \int_{-1}^1 \mathrm{d}z \sqrt{uv} e^{-u} \sqrt{x^2-q^2} \frac{\delta(u-v-x)}{(u+v-2\sqrt{uv}z)^2} P_{\mathrm{decay}} P_{\mathrm{abs}}$$

$$n_{N_i}(r) \simeq \frac{\rho(r) Y_{N_i}(r)}{A_{N_i} m_N}$$

E-N BREMSSTRAHLUNG EMISSION

After many simplifications, we arrive at the following expressions for the emission rate

$$\mathcal{Q}(r,\phi) = \left(\sum_i Z_{N_i}^2 A_{N_i}^2 n_{N_i}(r)\right) \frac{\alpha^2 y_N^2 \sin^2\theta T^{1/2}(r) n_e(r)}{\pi^{3/2} m_e^{3/2}} \int_q^\infty \mathrm{d}u \int_0^\infty \mathrm{d}v \int_q^\infty \mathrm{d}x \int_{-1}^{1} \mathrm{d}z \sqrt{uv} e^{-u} \sqrt{x^2-q^2} \frac{\delta(u-v-x)}{(u+v-2\sqrt{uv}z)^2} P_{\mathrm{decay}} P_{\mathrm{abs}}$$

$$n_{N_i}(r) \simeq \frac{\rho(r) Y_{N_i}(r)}{A_{N_i} m_N}$$

$$n_e(r) = \sum_i Z_{N_i} n_{N_i}(r)$$

E-N BREMSSTRAHLUNG EMISSION

After many simplifications, we arrive at the following expressions for the emission rate

$$\mathcal{Q}(r,\phi) = \Big(\sum_i Z_{N_i}^2 A_{N_i}^2 n_{N_i}(r)\Big)\frac{\alpha^2 y_N^2 \sin^2\theta T^{1/2}(r) n_e(r)}{\pi^{3/2} m_e^{3/2}} \int_q^\infty \mathrm{d}u \int_0^\infty \mathrm{d}v \int_q^\infty \mathrm{d}x \int_{-1}^1 \mathrm{d}z \sqrt{uv} e^{-u} \sqrt{x^2 - q^2} \frac{\delta(u-v-x)}{(u+v-2\sqrt{uv}z)^2} P_{\mathrm{decay}} P_{\mathrm{abs}}$$

$$n_{N_i}(r) \simeq \frac{\rho(r) Y_{N_i}(r)}{A_{N_i} m_N}$$

$$n_e(r) = \sum_i Z_{N_i} n_{N_i}(r)$$

The above contains within P_{abs} the inverse mean free path

E-N BREMSSTRAHLUNG EMISSION

After many simplifications, we arrive at the following expressions for the emission rate

$$\mathcal{Q}(r,\phi) = \left(\sum_i Z_{N_i}^2 A_{N_i}^2 n_{N_i}(r)\right) \frac{\alpha^2 y_N^2 \sin^2\theta T^{1/2}(r) n_e(r)}{\pi^{3/2} m_e^{3/2}} \int_q^\infty \mathrm{d}u \int_0^\infty \mathrm{d}v \int_q^\infty \mathrm{d}x \int_{-1}^1 \mathrm{d}z \sqrt{uv} e^{-u} \sqrt{x^2-q^2} \frac{\delta(u-v-x)}{(u+v-2\sqrt{uv}z)^2} P_{\mathrm{decay}} P_{\mathrm{abs}}$$

$$n_{N_i}(r) \simeq \frac{\rho(r) Y_{N_i}(r)}{A_{N_i} m_N} \qquad n_e(r) = \sum_i Z_{N_i} n_{N_i}(r)$$

The above contains within P_{abs} the inverse mean free path

$$\lambda^{-1}(r;x) = \left(\sum_i Z_{N_i}^2 A_{N_i}^2 n_{N_i}(r)\right) \frac{1}{x^2} \frac{2\pi^{1/2}\alpha^2 y_N^2 \sin^2\theta n_e(r)}{m_e^{3/2} T^{7/2}(r)} \int_0^\infty \mathrm{d}u \int_q^\infty \mathrm{d}v \int_{-1}^1 \mathrm{d}z \sqrt{uv} e^{-u} \frac{\delta(u-v+x)}{(u+v-2\sqrt{uv}z)^2}$$

E-N BREMSSTRAHLUNG EMISSION

After many simplifications, we arrive at the following expressions for the emission rate

$$\mathcal{Q}(r,\phi) \quad = \quad \left(\sum_i Z_{N_i}^2 A_{N_i}^2 n_{N_i}(r)\right) \frac{\alpha^2 y_N^2 \sin^2\theta T^{1/2}(r) n_e(r)}{\pi^{3/2} m_e^{3/2}} \int_q^\infty \mathrm{d}u \int_0^\infty \mathrm{d}v \int_q^\infty \mathrm{d}x \int_{-1}^1 \mathrm{d}z \sqrt{uv} e^{-u} \sqrt{x^2-q^2} \frac{\delta(u-v-x)}{(u+v-2\sqrt{uv}z)^2} P_{\mathrm{decay}} P_{\mathrm{abs}}$$

$$n_{N_i}(r) \simeq \frac{\rho(r) Y_{N_i}(r)}{A_{N_i} m_N} \qquad\qquad n_e(r) = \sum_i Z_{N_i} n_{N_i}(r)$$

The above contains within P_{abs} the inverse mean free path

$$\lambda^{-1}(r;x) \quad = \quad \left(\sum_i Z_{N_i}^2 A_{N_i}^2 n_{N_i}(r)\right) \frac{1}{x^2} \frac{2\pi^{1/2}\alpha^2 y_N^2 \sin^2\theta n_e(r)}{m_e^{3/2} T^{7/2}(r)} \int_0^\infty \mathrm{d}u \int_q^\infty \mathrm{d}v \int_{-1}^1 \mathrm{d}z \sqrt{uv} e^{-u} \frac{\delta(u-v+x)}{(u+v-2\sqrt{uv}z)^2}$$

From here we may once again numerically solve for the luminosity due to light scalar emission

ENERGY AVERAGED MEAN FREE PATH

$$\langle\lambda^{-1}\rangle(r) \equiv \frac{\int \mathrm{d}E_S \frac{E_S^3}{e^{E_S/T}-1}\lambda^{-1}(E_S;r)}{\int \mathrm{d}E_S \frac{E_S^3}{e^{E_S/T}-1}} = \frac{\int \mathrm{d}x \frac{x^3}{e^x-1}\lambda^{-1}(x;r)}{\int \mathrm{d}x \frac{x^3}{e^x-1}}.$$

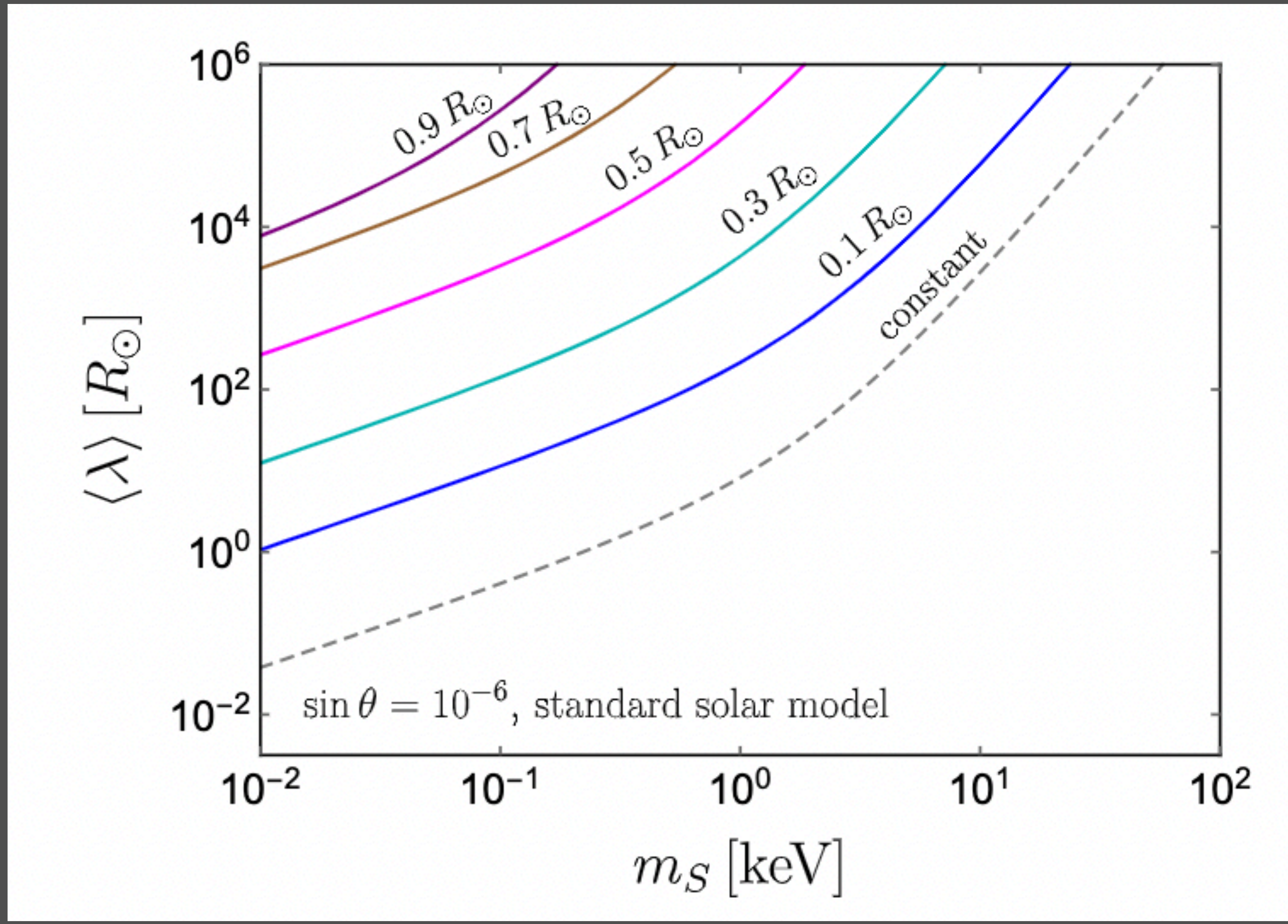

The dashed lines are the corresponding MFPs for constant temperature $T = 1$ keV and the electron number density $n_e = 10^{26}\,\mathrm{cm}^{-3}$. The mixing angle is fixed to $\sin\theta = 10^{-6}$

DIFFERENT CHANNELS